

The effects of melatonin supplementation on vascular tissue during first line ART: an *in vivo*, *ex vivo* and *in vitro* study

by
Jordyn Rawstorne

Thesis presented in fulfilment of the requirements for the degree of Master of Science in the Faculty of Health Science at Stellenbosch University



UNIVERSITEIT
iYUNIVESITHI
STELLENBOSCH
UNIVERSITY

100
1918 · 2018

Supervisor: Dr Ingrid Webster
Co-supervisor: Prof Hans Strijdom

March 2018

Declaration

By submitting this thesis electronically, I declare that the entirety of the work contained therein is my own, original work, that I am the sole author thereof (save to the extent explicitly otherwise stated), that reproduction and publication thereof by Stellenbosch University will not infringe any third party rights and that I have not previously in its entirety or in part submitted it for obtaining any qualification.

March 2018

Copyright © 2018 Stellenbosch University

All rights reserved

Abstract

Introduction: Although Antiretroviral therapy (ART) has dramatically reduced HIV-associated morbidity and mortality, non-HIV-related conditions and comorbidities continue to rise in this population. Cardiovascular disease (CVD) has been reported to be the leading cause of death in the HIV-positive population receiving ART. ART is thought to impair vascular endothelial function through increased reactive oxygen species (ROS) and reactive nitrogen species (RNS) production. In this study, we aim to assess the effects of melatonin - a potent antioxidant -supplementation during ART on specific intracellular products of rat Aortic Endothelial Cells (AECs) as well as on the vascular reactivity of rat aortas.

Methods: Cells were serum starved and treated with three different melatonin (1nM; 1uM; 10uM) or ART (**Low:** EFV: 5µM; FTC: 5µM; TDF: 80nM; **Mid:** EFV: 8µM; FTC: 7.5µM; TDF: 400nM; **High:** EFV: 12µM; FTC: 10µM; TDF: 1µM) concentrations for up to 24 hours. Nitric oxide (NO), RNS and necrosis were measured with a platereader (control expressed as 100%). The concentration that resulted in the greatest differences, compared to untreated cells, was selected for co-treatment studies and protein investigations, where the same parameters were measured. The effects of acute melatonin and ART administration on vascular reactivity was measured by aortic ring isometric tension studies in aortas extracted from control male Wistar rats. The endothelium-dependent and independent vascular reactivity was measured by isometric tension studies on aortas harvested from male Wistar rats that were treated for 8 weeks with melatonin (10mg/kg/day) and/or ART (EFV: 51.6 mg/kg; FTC: 17.4 mg/kg; TDF: 25.8 mg/kg). Signalling proteins involved in these changes were measured by western blot analyses.

Results (Mean±SEM): Dose Response Studies: 1nM melatonin decreased necrosis [92.56±3.11%;p=0.0004] compared to untreated controls [100.00±1.04%; p=0.0004]. High-concentration ART lead to increased NO production [112.70±2.17%; Control:100.00±2.22%;p=0.0015], RNS production [108.80±2.20%; Control:100±0.79%;p=0.0152] and necrosis [107.30±1.34%; Control: 100.00±0.86%;p=0.0251], compared to untreated controls.

Main Studies: 1nM melatonin decreased necrosis [92.43±3.75%;p=0.0002], while High-concentration ART increased necrosis [121.30±9.11%;p=0.0002] compared to untreated cells [100.00±1.07%;p=0.0002]. When combined, 1nM melatonin + High-concentration ART decreased necrosis [94.17±5.08%;p=0.0002] compared to ART alone.

Western blot analyses (arbitrary units) showed that ART increased nitrotyrosine levels [2.31 ± 0.34 ; Control: 1.00 ± 0.18 ; $p=0.0486$], but decreased p22 PHOX [0.20 ± 0.043 ; Control: 1.00 ± 0.15 ; $p < 0.0001$], and cleaved caspase-3 [0.25 ± 0.038 ; Control: 1.00 ± 0.18 ; $p=0.0005$], expression.

In acute aortic ring experiments, ART exposure elicited a burst of contraction during the treatment period, followed by a significant attenuation in accumulative contraction compared to all other groups. In endothelium-dependent and independent contraction studies on aortas from treated rats, all groups showed a pro-contractile response compared to the control. Western blot analyses showed that ART decreased cleaved caspase-3 [0.27 ± 0.08 ; $p=0.0055$] expression.

Conclusion: Decreased necrosis in AECs treated with combined melatonin and ART, compared to AECs treated with ART alone shows the protective effect of melatonin. Further specific protein investigations are needed to elucidate this mechanism. Western blots showed that ART induced anti-apoptotic effects and increased RNS production, but not NADPH-oxidase activity. The initial contractile burst following acute ART exposure may precondition the aortas, resulting in the decreased accumulative contractile capacity. Chronic ART treatment studies showed that ART treatment does not seem to affect vasorelaxation. Blot data reconfirmed that ART is also anti-apoptotic *in vivo*.

Abstrak

Inleiding: Alhoewel antiretrovirale terapie HIV verwante morbiditeit en mortaliteit dramaties verminder het, styg nie-HIV-verwante toestande in hierdie populasie. Kardiovaskulêre siektes word beskou as die hoof oorsaak van sterftes in die HIV positiewe populasie wat antiretrovirale terapie (ART) ontvang. ART kan die vaskulêre endoteelfunksie benadeel deur verhoogde reaktiewe suurstof spesies (ROS) en reaktiewe stikstof spesies (RNS) produksie. In hierdie studie was die effekte van melatonien (kragtige antioksidant) aanvulling gedurende ART ondersoek, met spesifieke verwysing na intrasellulêre afskeidingsprodukte van rot aorta endoteelselle, asook in die konteks van rot aorta vaskulêre reaktiwiteit.

Metodes: Selle was onderwerp aan serum weerhouding en behandel met drie verskillende melatonien (1nM; 1uM; 10uM) of ART (**Laag:** EFV: 5µM; FTC: 5µM; TDF: 80nM; **Medium:** EFV: 8µM; FTC: 7.5µM; TDF: 400nM; **Hoog:** EFV: 12µM; FTC: 10µM; TDF: 1µM) konsentrasies vir tot 24uur. Stikstofoksied (NO), RNS and nekrose is gemeet met 'n plaatleser (kontrole uitgedruk as 100%). Die konsentrasie wat gelei het tot die grootste verskille, in vergelyking met die onbehandelde selle, was gekies vir ko-behandeling studies en proteïen ontledings, waar dieselfde veranderlikes gemeet was. Die effekte van akute melatonien en ART toediening op vaskulêre reaktiwiteit is gemeet d.m.v. aortiese ring isometriese spanningstudies in aortas afkomstig van gesonde manlike Wistar rotte. Die endoteel-afhanklike en onafhanklike vaskulêre reaktiwiteit is gemeet d.m.v. isometriese spanningstudies in aortas afkomstig van manlike Wistar rotte wat vir 8 weke behandel was met melatonien (10mg/kg/day) en/of ART (EFV: 51.6 mg/kg; FTC: 17.4 mg/kg; TDF: 25.8 mg/kg). Seinproteïne in hierdie weefsel is gemeet deur Western blot analises.

Resultate (Mean±SEM): Dosis-reaksie Ondersoeke: 1nM melatonien het nekrose [92.56±3.11%;p=0.0004] laat verminder in vergelyking met onbehandelde kontrole [100.00±1.04%;p=0.0004]. Hoë-konsentrasie ART het tot verhoogde NO produksie [112.70±2.17%; kontrole:100.00±2.22%;p=0.0015], RNS produksie [108.80±2.20%; kontrole:100.00±0.79%;p=0.0152] en nekrose [107.30±1.34%; kontrole: 100.00±0.86%; p=0.0251] gelei, in vergelyking met onbehandelde kontrole.

Hoof Ondersoeke: 1nM melatonien nekrose [92.43±3.75%;p=0.0002] laat toeneem, terwyl hoë-konsentrasie ART nekrose [121.30±9.11%;p=0.0002] in vergelyking met onbehandelde selle [100.00±1.07%;p=0.0002] verhoog. Tydens gekombineerde

behandeling, het 1nM melatonien + Hoë-konsentrasie ART nekrose [$94.17 \pm 5.08\%$; $p=0.0002$] verlaag teenoor ART alleen. Western blot analyses (arbitrêre eenhede) het getoon dat ART nitrotirosien vlakke vermeerder het [2.31 ± 0.34 ; kontrole: 1.00 ± 0.18 ; $p=0.0486$], maar p22 PHOX [0.20 ± 0.04 ; kontrole: 1.00 ± 0.15 ; $p < 0.0001$], en gekliefde kaspase-3 [0.25 ± 0.038 ; kontrole: 1.00 ± 0.18 ; $p=0.0005$] uitdrukking verlaag het. In akute aorta ring eksperimente, het ART blootstelling 'n skielike en kortstondige kontraksie gedurende die behandelings periode veroorsaak, gevolg deur 'n beduidende verswakking in akkumulatiewe kontraksie teenoor al die ander groepe. In endoteel-afhanklike en onafhanklike kontraksie studies op aortas van behandelde rotte, het alle groepe 'n pro-kontraktiele reaksie getoon in vergelyking met die kontrole. Western blot analyses het getoon dat ART v gekliefde kaspase-3 uitdrukking verlaag het [0.27 ± 0.08 ; $p=0.0055$].

Gevolgtrekking: Die verlaagde nekrose wat in aorta endoteelselle (AECs), behandel met gekombineerde melatonien en ART, waargeneem is teenoor AECs wat slegs ART ontvang het, is 'n bewys van die beskermde effekte van melatonien. Toekomstige studies wat spesifieke proteïene ondersoek is nodig om die meganisme verder te verklaar. Western blots ondersoek het gewys dat ART anti-apoptotiese effekte en vermeerde RNS produksie veroorsaak, maar geen effekte op NADPH-oksidasie aktiwiteit toon nie. Die aanvanklike kontraktiele respons tydens akute ART blootstelling kan die aortas vooraf kondisioneer wat 'n verlaagde akkumulatiewe kontraktiele kapasiteit veroorsaak het. Chroniese ART behandeling studies het getoon dat die behandeling nie die bloedvatverslapping beïnvloed nie. Die Western blot resultate van die *in vivo* studies het die anti-apoptotiese effekte van ART herbevestig.

Acknowledgements

- To my former supervisor, Dr Corli Westcott, I would like to express my sincerest appreciation for all the help, guidance and kind words she shared with me over the years. I thank her for sharing her passion and commitment with me, as well as for her continued help and guidance, no matter where in the world she was.
- I would like to thank Dr Ingrid Webster for all her help and support with the animal work and for always being positive, no matter what the situation.
- To Prof Hans Strijdom, I express my greatest gratitude for his unparalleled commitment and work ethic. Without his excellent guidance, fast feedback and extreme patience and understanding, I would not have completed this thesis.
- I would like to thank the NRF Thuthuka Fund and the Harry Crossley Foundation for their financial support throughout my Masters degree.
- Thank you to my dear friend Natalie who so graciously helped me translate my abstract.
- Thank you to my amazing parents for providing me with the opportunity to further myself without limit. I am eternally grateful.
- To my sister who was always willing to lend a helping hand or provide encouragement.
- Lastly I would like to thank my wonderful husband, who always inspires me to work harder and pushes me to do better. Thank you for taking such good care of me while I was on the home stretch., and for being so understanding when I worked over our entire mini-moon. I could not have done it without you.

Table of Contents

DECLARATION	II
ABSTRACT	III
ABSTRAK	V
ACKNOWLEDGEMENTS.....	VII
TABLE OF CONTENTS	VIII
LIST OF ABBREVIATIONS	XII
LIST OF FIGURES	XIX
LIST OF TABLES.....	XXIII
1 - LITERATURE REVIEW.....	1
1.1 GENERAL INTRODUCTION.....	1
1.2 THE VASCULAR ENDOTHELIUM	1
1.2.1 Localisation and Structure	2
1.2.2 Function.....	3
1.3 ENDOTHELIAL DYSFUNCTION	9
1.3.1 Pathophysiology	11
1.3.2 Aetiology and Mechanisms of ED.....	11
1.3.3 Consequences of ED.....	16
1.3.4 Prevention and Treatment of ED.....	18
1.4 HIV/AIDS & ART.....	19
1.4.1 Epidemiology.....	20
1.4.2 Virus Structure, Targets and Life-cycle.....	20
1.4.4 Antiretroviral therapy (ART)	23
1.4.5 HIV & ART in a South African Context.....	25
1.5 HIV, ART AND ED/CVD.....	28
1.5.1 ART induced ED/CVD.....	29
1.6 MELATONIN	32
1.6.1 Antioxidant Actions.....	33
1.6.2 Melatonin in ART induced ED.....	38
1.7 CONCLUSION	39
1.8 PROBLEM IDENTIFICATION AND STUDY AIMS.....	40
1.8.1 Problem Identification.....	40
1.8.2 Main Study Aim.....	40
2 - MATERIALS AND METHODS: IN VITRO STUDIES	42

2.1	AORTIC ENDOTHELIAL CELL CULTURE	42
2.1.1	<i>Materials</i>	42
2.1.2	<i>Passaging</i>	42
2.2	EXPERIMENTAL GROUPS AND PROTOCOLS.....	45
2.2.1	<i>Melatonin and Vehicle</i>	45
2.2.2	<i>ART and Vehicle</i>	46
2.2.3	<i>Combined drugs and Vehicles</i>	49
2.3	PLATE READER ANALYSES	49
2.3.1	<i>Materials</i>	49
2.3.2	<i>Methods</i>	49
2.4	SIGNALLING INVESTIGATIONS – WESTERN BLOT ANALYSES.....	57
2.4.1	<i>Materials</i>	57
2.4.2	<i>Methods</i>	58
2.5	ORAC ASSAY	62
2.6	STATISTICAL ANALYSES	62
3	- MATERIALS AND METHODS: EX VIVO AND IN VIVO STUDIES	63
3.1	MATERIALS.....	63
3.2	ETHICS CLEARANCE AND ANIMAL CARE	63
3.3	EXPERIMENTAL PROTOCOLS AND STUDY DESIGN.....	64
3.3.1	<i>Excision and Mounting of Aortic Rings</i>	64
3.3.2	<i>Ex Vivo Studies</i>	66
3.3.3	<i>In Vivo Studies</i>	68
3.4	SIGNALLING INVESTIGATIONS – WESTERN BLOT ANALYSES.....	76
3.4.1	<i>Materials</i>	76
3.4.2	<i>Methods</i>	76
3.5	ORAC ASSAY	76
3.6	STATISTICAL ANALYSES	77
4	- RESULTS: IN VITRO STUDIES	78
4.1	PLATE READER ANALYSES	78
4.1.1	<i>Melatonin Dose-Response Studies</i>	78
4.1.2	<i>ART Dose-Response Studies</i>	85
4.1.3	<i>Combination Studies</i>	89
4.2	WESTERN BLOT ANALYSES.....	92
4.2.1	<i>NO & RNS Signalling</i>	92
4.2.2	<i>ROS Signalling</i>	95
4.2.3	<i>Cell Viability Signalling</i>	95

4.3	ANTIOXIDANT CAPACITY ANALYSES.....	96
4.3.1	ORAC Assay.....	96
5	- RESULTS: EX VIVO AND IN VIVO STUDIES.....	98
5.1	EX VIVO STUDIES.....	98
5.1.1	Phe-contraction / Ach-relaxation.....	98
5.2	IN VIVO STUDIES.....	100
5.2.1	Endothelium-dependent aortic ring investigations.....	100
5.2.2	Endothelium-independent aortic ring investigations.....	106
5.2.3	Western Blot Analyses.....	108
5.2.4	Antioxidant Capacity Studies.....	114
6	- DISCUSSION: IN VITRO STUDIES.....	115
6.1	MELATONIN DOSE-RESPONSE.....	115
6.2	ART DOSE-RESPONSE.....	118
6.3	EFFECTS OF MELATONIN AND ART TREATMENT ON NO PRODUCTION, RNS PRODUCTION AND CELL VIABILITY IN AECs.....	120
6.4	WESTERN BLOT ANALYSES.....	121
6.4.1	NO & RNS Signalling.....	121
6.4.2	ROS Signalling.....	123
6.4.3	Cell Viability Signalling.....	124
6.5	ANTIOXIDANT CAPACITY ANALYSES.....	125
6.6	CONCLUDING REMARKS.....	125
7	- DISCUSSION: EX VIVO AND IN VIVO STUDIES.....	127
7.1	EX VIVO STUDIES.....	127
7.2	IN VIVO STUDIES.....	129
7.2.1	Endothelium-dependent Aortic Ring Investigations.....	129
7.2.2	Endothelium-independent Aortic Ring Investigations.....	131
7.2.3	Western Blot Analyses.....	132
7.2.4	Antioxidant Capacity Studies.....	133
7.3	CONCLUDING REMARKS.....	133
8	- OVERALL CONCLUSIONS.....	135
8.1	ADVANTAGES, LIMITATIONS AND FUTURE DIRECTIONS.....	137
8.2	SPECIFIC ROLES IN THE STUDY.....	137
8.3	RESEARCH OUTPUTS ASSOCIATED WITH THE STUDY.....	138
	APPENDIX A: IN VITRO MELATONIN AND VEHICLE CONCENTRATION CALCULATIONS.....	139
	APPENDIX B: IN VITRO ART AND VEHICLE CONCENTRATION CALCULATIONS.....	140

APPENDIX C: WESTERN BLOT AND ORAC 1 NM MELATONIN, HIGH CONCENTRATION ART AND VEHICLE CONCENTRATION CALCULATIONS (COMBINED VEHICLES)	143
APPENDIX D: WESTERN BLOT RAW DATA NORMALISATION	144
EXAMPLE DATA:.....	144
APPENDIX E: <i>EX VIVO</i> 10 μ M MELATONIN, HIGH CONCENTRATION ART AND VEHICLE CONCENTRATION CALCULATIONS (COMBINED VEHICLES)	147
APPENDIX F: <i>IN VITRO</i> MELATONIN STOCK PREPARATION	149
APPENDIX G: <i>IN VITRO</i> ART STOCK PREPARATION.....	151
APPENDIX H: <i>SNP CONCENTRATION CALCULATIONS</i>	154
APPENDIX I: <i>MALE WISTAR RAT BIOMETRIC DATA</i>	155
REFERENCES.....	156

List of Abbreviations

+C	Positive control
3TC	Lamivudine
5-HT	Serotonin
AA-NAT	Arylakylamine N-acetyltransferase
ABC	Abacavir
AC	Absolute control
ACE	Angiotensin-converting enzyme
Ach	Acetylcholine
ADP	Adenosine di-phosphate
ADR	Adverse drug reaction
AECs	Aortic endothelial cells
AFMK	<i>N1-acetyl-N2-formyl-5-methoxykynuramine</i>
ALLINIs	Allosteric integrase inhibitors
Ang II	Angiotensin II
APV	Amprenavir
ART	Antiretroviral therapy
ARV	Antiretroviral
AT-I	Angiotensin receptor type I
AT-II	Angiotensin receptor type II
ATP	Adenosine tri-phosphate
AZT	Zidovudine
AZV	Atazanavir
BH₃	Trihydrobiopterin
BH₄	Tetrahydrobiopterin
BK	Bradykinin

C	Control
Ca²⁺	Calcium ions
cAMP	Cyclic adenosine monophosphate
CAT	Catalase
Cav-1	Caveolin
CCR5	C-C chemokine receptor type 5
CD₄	Cluster of differentiation 4
cGMP	Cyclic guanosine-3', 5-monophosphate
CHD	Coronary heart disease
CO₂	Carbon dioxide
COX	Cyclooxygenase
COX-1	Cyclooxygenase-1
COX-2	Cyclooxygenase-2
CREB-ATF	Camp responsive element binding protein and activating transcription factor
CRP	C-reactive protein
CV	Cardiovascular
CXCR4	C-X-C chemokine receptor type 4
cyt. P450	Cytochrome P450 monooxygenases
d4T	Stavudine
DAD	Data Collection on Adverse Events of Anti-HIV Drugs
DAF-2/DA	4,5-diaminofluorescein-2/diacetate
DAG	Diacylglycerol
ddC	Zalcitabine
Ddl	Didanosine
DEA	Diethylamine nonoate diethylammonium salt
dH₂O	Distilled water

DHR-123	Dihydrorhodamine-1,2
DLV	Delavordine
DMSO	Dimethyl sulfoxide
ECE	Endothelin converting enzyme
ECL	Enhanced chemiluminescence
ECs	Endothelial cells
ED	Endothelial dysfunction
EDCF	Endothelium-derived contracting factors
EDHF	Endothelium-derived hyperpolarising factor
EFV	Efavirenz
EGM-2	Endothelial cell growth medium
eNOS	Endothelial Nitric Oxide Synthase
Env	Envelope
ENV	T-20 efuvirtide
ER	Endoplasmic reticulum
ERK	Extracellular signal–regulated kinases
ET-1	Endothelin-1
ETA	Endothelin A receptor
ETB	Endothelin B receptor
FAD	Flavin adenine dinucleotide
FBS	Foetal bovine serum
FDC	Fixed dose combination
FMD	Flow-mediated dialation
FTC	Emtricitabine
Gag	Group-specific antigen
Gp	Glycoprotein

GP	Glutathione peroxynitrite
GPx	Glutathione peroxidase
GRd	Glutathione reductase
GSH	Tripeptide glutathione
GSH-Px	Glutathione peroxidase
GSSG	Glutathione disulfide
GTP	Guanosine triphosphate
H₂O	Water
H₂O₂	Hydrogen peroxide
HAART	Highly active antiretroviral therapy
HIV	Human immunodeficiency virus
HRP	Horseradish peroxidase
IDV	Indinavir
iNOS	Inducible Nitric Oxide Synthase
InSTIs	Integrase strand transfer inhibitors
IP	Intraperitoneal
IP₃	Inositol triphosphate
KHB	Krebs Henseleit buffer
L-Arg	L-arginine
L-Cit	L-citrulline
L-NAME	N ω -Nitro-L-arginine methyl ester
LOX	Lipoxygenases
M	Muscarinic receptor
MeOH	Methanol
MI	Myocardial infarction
MLCK	Myosin light chain kinase

mRNA	Messenger-ribonucleic acid
mtPTP	Mitochondrial permeability transition pore
NADPH	Nicotinamide adenine dinucleotide phosphate
NFV	Nelfinavir
nNOS	Neuronal Nitric Oxide Synthase
NNRTIs	Non-Nucleoside reverse transcriptase inhibitors
NO	Nitric oxide
NO₂⁻	Nitrite
NOS	Nitric oxide synthase
NOX	Nicotinamide adenine dinucleotide phosphate oxidase
NRTIs	Nucleoside reverse transcriptase inhibitors
NtRTIs	Nucleotide reverse transcriptase inhibitors
NVP	Nevirapine
O₂	Oxygen
O₂⁻	Superoxide anion
OH⁻	Hydroxyl
ONOO⁻	Peroxynitrite
ONOOCO₂⁻	Nitroso-peroxocarboxylate
ONOOH	Peroxynitrous acid
ORAC	Oxygen radical absorbance capacity
PAOD	Peripheral arterial occlusive disease
PBS	Phosphate-buffered saline
PGH₂	Prostaglandin H ₂
PGI₂	Prostaglandin I ₂
Phe	Phenylephrine
PI	Propidium iodide

PIs	Protease inhibitors
PKA	Protein kinase A
PKC	Protein kinase C
R3-IGF-1	Long chain human insulin-like growth factor
rhEGF	Recombinant human epidermal growth factor
rhFGF-B	Recombinant human fibroblastic growth factor B
rLPV	Lopinavir/ritonavir
RNS	Reactive nitrogen species
ROS	Reactive oxygen species
RPM	Revolutions per minute
RT	Reverse transcriptase
RTV	Ritonavir
S1B	Serotonin receptor
SA	South africa
SABS	South African Bureau of Standards
SDS	Sodium dodecyl sylphate
SEM	Standard error of the mean
sGC	Soluble guanylyl cyclase
SMART	The Strategies for Management of Anti-Retroviral Therapy
SNP	Sodium nitroprusside
SOCa²⁺	Store-operated Ca ²⁺ channel
SOD	Superoxide dismutases
SP	Substance P
SQV	Saquinavir
SR	Sarcoplasmic reticulum
SS	Serum starved

Tat	Trans-activator of transcription
TDF	Tenofovir disoproxil fumarate
TP	Thromboxane prostanoid receptor
TXA₂	Thromboxane A
UCT	University of Cape Town
US	University of Stellenbosch
USA	United States of America
VEGF	Vascular endothelial growth factor
VSMC	Vascular smooth muscle cells

List of Figures

CHAPTER 1 – LITRETURE REVIEW

FIGURE 1.1: MORPHOLOGICALLY DISTINCT LAYERS IN A HEALTHY ARTERY	3
FIGURE 1.2: THE FORMATION OF NO FROM L-ARGININE, WITH THE NADPH AND OXYGEN REQUIREMENTS FOR EACH REACTION	5
FIGURE 1.3: ENOS SIGNALING IN CAVEOLAE.....	6
FIGURE 1.4: ENDOTHELIAL NO PRODUCTION AND ITS ACTIONS IN THE VSMCs.....	8
FIGURE 1.5: THE PATHOPHYSIOLOGICAL CHANGES SEEN IN A DYSFUNCTIONAL ENDOTHELIUM	10
FIGURE 1.6: OXIDATIVE AND NITRO-OXIDATIVE STRESS.....	13
FIGURE 1.7: POTENTIAL MECHANISMS BY WHICH CARDIOVASCULAR RISK FACTORS LEAD TO ED THROUGH INCREASED OXIDATIVE STRESS	14
FIGURE 1.8: COUPLED AND UNCOUPLED ENOS	15
FIGURE 1.9: PROGRESSION FROM RISK FACTORS TO ATHEROSCLEROSIS AND CVD MEDIATED BY OXIDATIVE STRESS AND ED.....	17
FIGURE 1.10: THERAPUTIC APPROACHES TO ENDOTHELIAL DYSFUNCTION.....	18
FIGURE 1.11: SUMMARY OF THE GLOBAL HIV EPIDEMIC (2016).....	20
FIGURE 1.12: STRUCTURE OF AN HIV VIRION PARTICLE	21
FIGURE 1.13: A BRIEF SUMMARY OF THE HIV LIFE-CYCLE	22
FIGURE 1.14: STAGES OF THE HIV LIFE CYCLE THAT ARE TARGETED BY ARV DRUGS.....	23
FIGURE 1.15: PATHWAYS OF INDOLIC CATABOLISM INVOLVED IN THE FORMATION OF MELATONIN.	32
FIGURE 1.16: DIRECT AND INDIRECT ACTIONS OF MELATONIN IN AN OXIDATIVE CAPACITY.....	34
FIGURE 1.17: OXIDATIVE STRESS AND SITES OF ACTION OF MELATONIN	38

CHAPTER 2 – MATERIALS AND METHODS: *IN VITRO* STUDIES

FIGURE 2.1: PASSAGING AND ALIQUOT STORAGE PROCEDURES.....	44
FIGURE 2.2: INDIVIDUAL ARV DRUG CONCENTRATIONS THAT WERE COMBINED TO MAKE-UP THE THREE FIXED DOSE COMBINATION ART TREATMENT GROUPS.	48
FIGURE 2.3: EXPERIMENTAL LAYOUT AND SUMMARY OF STEPS FOLLOWED FOR EACH PLATE READER EXPERIMENT.....	50
FIGURE 2.4: A SCHEMATIC REPRESENTATION OF THE PROTOCOL USED FOR TREATMENT WITH DAF-2/DA AND POSITIVE NO CONTROL, DEA/NO.	52
FIGURE 2.5: DEA/NO POSITIVE CONTROL.....	53

FIGURE 2.6: A SCHEMATIC REPRESENTATION OF THE PROTOCOL USED FOR TREATMENT WITH DHR-123 AND POSITIVE CONTROL, AUTHENTIC PEROXYNITRITE.....	54
FIGURE 2.7: PEROXYNITRITE POSITIVE CONTROL	55
FIGURE 2.8: dH ₂ O POSITIVE CONTROL.....	56

CHAPTER 3 – MATERIALS AND METHODS: *EX VIVO* AND *IN VIVO* STUDIES

FIGURE 3.1: A THORACIC AORTA EXCISED AND CLEANED OF CONNECTIVE TISSUE AND PERIVASCULAR FAT.....	65
FIGURE 3.2: ORGAN BATH WITH A 4 MM SEGMENT OF AORTA SUSPENDED BETWEEN TWO STEEL HOOKS	66
FIGURE 3.3: LABCHART RECORDING SHOWING THE AORTIC RING RESPONSES TO THE EXPERIMENTAL PROTOCOL FOLLOWED FOR THE <i>EX VIVO</i> STUDIES	68
FIGURE 3.4: FLOW CHART INDICATING <i>IN VIVO</i> TREATMENT GROUPS	69
FIGURE 3.5: SCHEME INDICATING PROCEDURES PERFORMED ON CLEANED AORTIC TISSUE TO OBTAIN AORTIC RINGS FOR ISOMETRIC TENSION STUDIES	72
FIGURE 3.6: A REPRESENTATIVE LABCHART RECORDING SHOWING THE AORTIC RING RESPONSES TO THE EXPERIMENTAL PROTOCOL FOLLOWED FOR PHE ADMINISTRATION FOLLOWED BY ACH	73
FIGURE 3.7: A REPRESENTATIVE LABCHART RECORDING SHOWING THE AORTIC RING RESPONSES TO THE EXPERIMENTAL PROTOCOL FOLLOWED FOR L-NAME PRE-TREATMENT FOLLOWED BY PHE AND ACH ADMINISTRATION	74
FIGURE 3.8: A REPRESENTATIVE LABCHART RECORDING SHOWING THE AORTIC RING RESPONSES TO THE EXPERIMENTAL PROTOCOL FOLLOWED FOR PHE ADMINISTRATION FOLLOWED BY SNP	75

CHAPTER 4 – RESULTS: *IN VITRO* STUDIES

FIGURE 4.1: THE EFFECTS OF 24H SS FOLLOWED BY 24H MELATONIN TREATMENT ON NO PRODUCTION.....	79
FIGURE 4.2: THE EFFECTS OF 24H SS FOLLOWED BY 24H MELATONIN TREATMENT ON RNS PRODUCTION.....	80

FIGURE 4.3: THE EFFECTS OF 24H SS FOLLOWED BY 24H MELATONIN TREATMENT ON NECROSIS	81
FIGURE 4.4: THE EFFECTS OF 24H SS FOLLOWED BY 1H MELATONIN TREATMENT ON NO PRODUCTION.	82
FIGURE 4.5: THE EFFECTS OF 24H SS FOLLOWED BY 1H MELATONIN TREATMENT ON RNS PRODUCTION.	83
FIGURE 4.6: THE EFFECTS OF 24H SS FOLLOWED BY 1H MELATONIN TREATMENT ON NECROSIS	84
FIGURE 4.7: THE EFFECTS OF 24H SS FOLLOWED BY 24H ART TREATMENT ON NO PRODUCTION	86
FIGURE 4.8: THE EFFECTS OF 24H SS FOLLOWED BY 24H ART TREATMENT ON RNS PRODUCTION	87
FIGURE 4.9: THE EFFECTS OF 24H SS FOLLOWED BY 24H ART TREATMENT ON NECROSIS	88
FIGURE 4.10: THE EFFECTS OF 24H SS FOLLOWED BY 24H MELATONIN AND ART COMBINATION TREATMENT ON NO PRODUCTION MEASURED BY DAF-2/DA FLUORESCENCE.	89
FIGURE 4.11: THE EFFECTS OF 24H SS FOLLOWED BY 24H MELATONIN AND ART COMBINATION TREATMENT ON DHR-123 FLUORESCENCE	90
FIGURE 4.12: THE EFFECTS OF 24H SS FOLLOWED BY 24H MELATONIN AND ART COMBINATION TREATMENT ON PI FLUORESCENCE.	91
FIGURE 4.13: CHANGES IN ENOS PHOSPHORYLATION AND EXPRESSION IN AECs TREATED WITH MELATONIN AND ART	93
FIGURE 4.14: iNOS WESTERN BLOT OF AECs TREATED WITH MELATONIN AND ART	94
FIGURE 4.15: CHANGES IN NITROTYROSINE LEVELS IN AECs TREATED WITH MELATONIN AND ART.	94
FIGURE 4.16: CHANGES IN P22 PHOX EXPRESSION IN AECs TREATED WITH MELATONIN AND ART.	95
FIGURE 4.17: CHANGES IN CLEAVED CASPASE-3 EXPRESSION IN AECs TREATED WITH MELATONIN AND ART.	96
FIGURE 4.18: ANTIOXIDANT CAPACITY OF AECs TREATED WITH MELATONIN AND ART.	97

CHAPTER 5 – RESULTS: *EX VIVO* AND *IN VIVO* STUDIES

FIGURE 5.1: GRAPH INDICATING THE EFFECTS OF <i>EX VIVO</i> MELATONIN AND ART TREATMENT ON PHE INDUCED CONTRACTION AND ACH INDUCED RELAXATION.	99
---	----

FIGURE 5.2: GRAPH INDICATING THE EFFECTS OF <i>IN VIVO</i> MELATONIN AND ART TREATMENT ON PHE INDUCED CONTRACTION AND ACH INDUCED RELAXATION.....	101
FIGURE 5.3: THE EFFECTS OF L-NAME PRE-ADMINISTRATION ON PHE INDUCED CONTRACTION	103
FIGURE 5.4: THE EFFECTS OF L-NAME PRE-ADMINISTRATION ON ACH INDUCED RELAXATION...	105
FIGURE 5.5: GRAPH INDICATING THE EFFECTS OF <i>IN VIVO</i> MELATONIN AND ART TREATMENT ON PHE INDUCED CONTRACTION AND SNP INDUCED RELAXATION	107
FIGURE 5.6: CHANGES IN eNOS PHOSPHORYLATION AND EXPRESSION IN AORTIC TISSUE FROM RATS TREATED WITH MELATONIN AND ART, <i>IN VIVO</i>	109
FIGURE 5.7: CHANGES IN iNOS EXPRESSION IN AORTIC TISSUE FROM RATS TREATED WITH MELATONIN AND ART, <i>IN VIVO</i>	110
FIGURE 5.8: CHANGES IN NITROTYROSINE LEVELS IN AORTIC TISSUE FROM RATS TREATED WITH MELATONIN AND ART, <i>IN VIVO</i>	111
FIGURE 5.9: CHANGES IN p22 PHOX EXPRESSION IN AORTIC TISSUE FROM RATS TREATED WITH MELATONIN AND ART, <i>IN VIVO</i>	112
FIGURE 5.10: CHANGES IN CLEAVED CASPASE-3 EXPRESSION IN AORTIC TISSUE FROM RATS TREATED WITH MELATONIN AND ART, <i>IN VIVO</i>	113
FIGURE 5.11: ANTIOXIDANT CAPACITY OF AORTIC TISSUE FROM RATS TREATED WITH MELATONIN AND ART, <i>IN VIVO</i>	114

CHAPTER 6 – DISCUSSION: *IN VITRO* STUDIES

FIGURE 6.1: SUBSTRATES INVOLVED IN NITROTYROSINE PRODUCTION.	123
---	-----

CHAPTER 7 – DISCUSSION: *EX VIVO* AND *IN VIVO* STUDIES

FIGURE 7.1: THE SPONTANEOUS CONTRACTION OF <i>EX VIVO</i> AORTIC RINGS.	128
--	-----

List of Tables

CHAPTER 1 – LITERATURE REVIEW

TABLE 1.1: A LIST OF FAVOURABLE EFFECTS ENFORCED BY A HEALTH ENDOTHELIUM.	2
TABLE 1.2: ENDOTHELIUM DERIVED VASO-REGULATORY MEDIATORS.....	4
TABLE 1.3: PRESENTLY AVAILABLE ARV DRUGS. DRUGS IN EACH CLASS ARE LISTED IN APPROXIMATE ORDER OF APPROVAL/AVAILABILITY.....	25
TABLE 1.4: SUMMARY OF ARVs USED FOR FIRST LINE FDC THERAPY IN SA	27
TABLE 1.5: MECHANISMS BY WHICH HIV AND ART MAY ADVERSELY AFFECT THE VASCULATURE .	28
TABLE 1.6: EFFECTS OF MELATONIN ON ROS/RNS AND OXIDANT ENZYMES.....	37

CHAPTER 2 – MATERIALS AND METHODS: *IN VITRO* STUDIES

TABLE 2.1: EXCITATION AND EMISSION WAVELENGTHS USED FOR THE VARIOUS PROBES ON THE MICROPLATE READER.....	50
TABLE 2.2: LYSIS BUFFER CONTENTS AND PREPARATION.	59
TABLE 2.3: CONTENTS OF 2X LAEMMLI BUFFER.	59
TABLE 2.4: SPECIFICATIONS FOR EACH ANTIBODY AFTER OPTIMISATION FOR WESTERN BLOTTING	61

CHAPTER 3 – MATERIALS AND METHODS: *EX VIVO* AND *IN VIVO* STUDIES

TABLE 3.1: COMPOSITION OF KREBS HENSELEIT BUFFER	65
--	----

CHAPTER 5 – RESULTS: *EX VIVO* AND *IN VIVO* STUDIES

TABLE 5.1: <i>EX VIVO</i> E_{MAX} VALUES FOR THE VARIOUS TREATMENT GROUPS	100
TABLE 5.2: <i>IN VIVO</i> E_{MAX} VALUES FOR THE VARIOUS TREATMENT GROUPS	102
TABLE 5.3: <i>IN VIVO</i> E_{MAX} VALUES FOR L-NAME PRE-TREATED TREATMENT GROUPS.....	106
TABLE 5.4: <i>IN VIVO</i> E_{MAX} VALUES FOR THE VARIOUS TREATMENT GROUPS	108

1 - Literature Review

1.1 General Introduction

The human immunodeficiency virus (HIV) is a global pandemic affecting 34 million people, with African countries accounting for 70% of all HIV-infected individuals worldwide (Thienemann, Sliwa, & Rockstroh, 2013). In South Africa (SA) alone, there are approximately 7 million people living with HIV (Statistics South Africa, 2015). There is still no cure for HIV infection, however, implementation of antiretroviral therapy (ART) has allowed for the effective management of the virus. Although ART has dramatically reduced HIV-associated morbidity and mortality, non-HIV-related conditions and comorbidities continue to rise (Thienemann et al., 2013). Cardiovascular disease (CVD) has been reported to be the leading comorbidity and cause of death in the HIV-positive population receiving ART (Thienemann et al., 2013), creating a double burden of disease – both communicable and non-communicable – specific to low-and-middle-income countries like SA.

Endothelial dysfunction (ED) is defined as an imbalance between vasodilating and vasoconstricting substances produced by, or acting on the endothelium (Deanfield et al., 2005), and is recognised as a critical initiating factor in CVD. Numerous studies on the effects of ART on the vasculature indicate that ART may impair the function of the vascular endothelium (Jiang et al., 2010). Increased production of reactive oxygen species (ROS) and imbalances between the levels of oxidants and antioxidants in the vasculature are considered important factors in ART-induced ED.

There is need for a therapy with the potential to alleviate the oxidative stress induced by ART. Melatonin is a free radical scavenger and strong antioxidant (Reiter, Tan, Osuna, & Gitto, 2000), giving it the potential to ameliorate damage caused by ART-induced ROS production, which leads to ED.

1.2 The Vascular Endothelium

The vascular endothelium is made up of a monolayer of endothelial cells (ECs), which line the lumen of blood vessels, providing a barrier between the vascular walls and circulating blood (Lerman & Zeiher, 2005; M. S. Park, Ravi, & Araujo, 2010). For many years, the endothelium was thought of as an inert membrane, with the sole purpose of maintaining

vessel wall permeability through the physical separation of the tissue and blood (Cines et al., 1998). Now, it is well established that the endothelium is in fact a dynamic organ that is heterogeneous and involved in the synthesis and secretion of key factors, as well as fulfilling important metabolic and immunological functions (Fishman, 1982). The endothelium plays a vital role in preserving vascular homeostasis by maintaining a delicate balance between vasodilatory and vasoconstrictory factors (Bevilacqua, Nelson, Mannori, & Cecconi, 1994; Versari, Daghini, Viridis, Ghiadoni, & Taddei, 2009). For this reason, maintaining endothelial health is fundamental in sustaining an antithrombotic and antiatherogenic milieu. Table 1.1 summarises the various atheroprotective effects of the healthy endothelium.

Table 1.1: A list of favourable effects enforced by a healthy endothelium (Bonetti, Lerman, & Lerman, 2003).

Favourable and Atheroprotective Effects of the Healthy Endothelium:
Promotion of vasodilation
Antioxidant effects
Anti-inflammatory effects
Inhibition of leukocyte adhesion and migration
Inhibition of smooth muscle cell proliferation and migration
Inhibition of platelet aggregation and adhesion
Anticoagulant effects
Profibrinolytic effects

1.2.1 Localisation and Structure

The vascular endothelium lines the entire circulatory system, from the heart, to the smallest capillaries (Rajendran et al., 2013). Positioned at the interface between the blood and the tissue, the endothelium is in the ideal location to detect and respond to any biological changes in the local environment caused by trauma or inflammation (Cines et al., 1998). The vascular wall is comprised of three layers (Fig 1.1): an inner layer called the intima, a middle layer known as the tunica media, and an outer layer called the tunica adventitia (Sandoo, van Zanten, Metsios, Carroll, & Kitas, 2010). The endothelium

comprises approximately 1.6×10^{13} cells, all of which are in close association with the smooth muscle cells (Limaye & Vadas, 2007), and located on the intima. These cells are highly specialised, with the ability to receive and transmit biochemical and physical information (Cines et al., 1998). This information can be transmitted directly – through active transport or direct permeation through the intercellular spaces between the ECs – or indirectly, whereby the ECs modulate the behaviour of the smooth muscle cells and other components of the vessel wall (Cines et al., 1998).

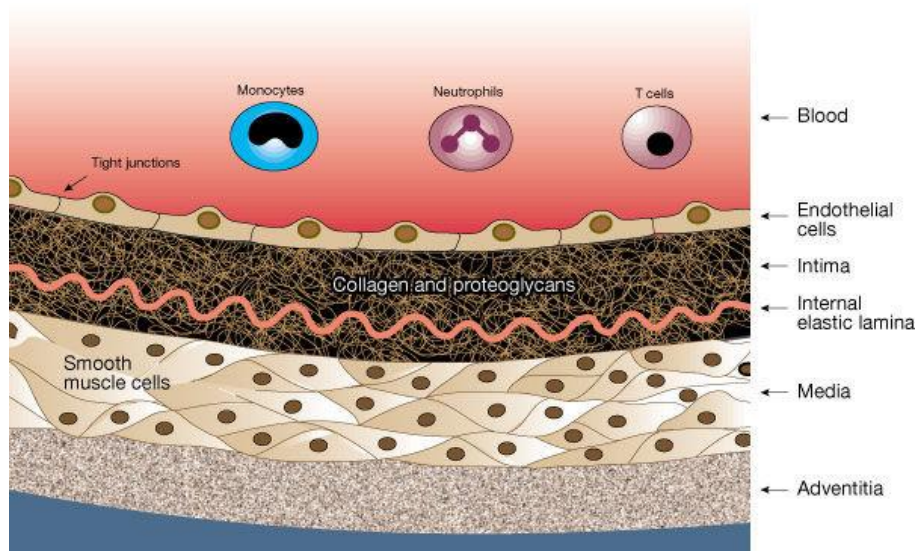


Figure 1.1: Morphologically distinct layers in a healthy artery (Lusis, 2000).

These actions are facilitated via membrane-bound receptors; which convey the signals of numerous molecules, such as proteins, lipid transporting particles, metabolites and hormones (Cines et al., 1998). The ECs also have specialised junctional proteins and receptors, which govern cell-cell and cell-matrix interactions.

1.2.2 Function

It has been established that the endothelium embodies a wide range of homeostatic functions (Durand & Gutterman, 2013). These functions are carried out through the secretion of specific mediators (Table 1.2) that have the ability to influence vascular hemodynamics (Cines et al., 1998). The various mediators controlled by ECs play an important role in the regulation of vascular tone and growth of blood vessels, thrombosis and thrombolysis, as well as platelet and leukocyte interactions with the vessel wall (Verhamme & Hoylaerts, 2006). ECs also contribute to the regulation of blood pressure and blood flow, by releasing vasodilators and vasoconstrictors (Cines et al., 1998).

Table 1.2: Endothelium Derived Vaso-regulatory Mediators (Adapted from (Cines et al., 1998; Mudau, Genis, Lochner, & Strijdom, 2012).

Mediator	Effects	Source and Mechanism of Action
<i>Nitric Oxide (NO)</i>	<ul style="list-style-type: none"> • Potent vasodilator • Inhibits inflammation, VSMC proliferation and migration, platelet activation, aggregation and adhesion, and leukocyte adhesion • Regulates myocardial contractility • Regulates cardiac metabolism • Maintains basal tone of vessels 	<ul style="list-style-type: none"> • Synthesised by enzymes: eNOS; nNOS and iNOS, with eNOS the major endothelial source of NO during physiological conditions • Diffuses from ECs to underlying VSMCs where it binds to sGC, leading to a cascade of events that ultimately result in vascular relaxation
<i>Prostacyclin (PGI₂)</i>	<ul style="list-style-type: none"> • Vasodilator • Inhibits platelet aggregation and deposition 	<ul style="list-style-type: none"> • Derived from arachidonic acid by cyclooxygenase-2 (COX-2)
<i>Endothelium-derived hyperpolarising factor (EDHF)</i>	<ul style="list-style-type: none"> • Vasodilator, particularly in small arteries ($\leq 300 \mu\text{m}$) 	<ul style="list-style-type: none"> • Its identity is still under suspicion with proposed candidates such as potassium ions and hydrogen peroxide
<i>Endothelin-1 (ET-1)</i>	<ul style="list-style-type: none"> • Potent vasoconstrictor • Mitogen for VSMCs 	<ul style="list-style-type: none"> • Synthesised by endothelin-converting enzyme • Exerts its effects via two receptors: ET_A expressed on endothelial cells which promote vasoconstriction and ET_B on VSMCs, which promote NO production and ultimately reduction in ET-1 production
<i>Thromboxane A (TXA₂)</i>	<ul style="list-style-type: none"> • Potent vasoconstrictor 	<ul style="list-style-type: none"> • Derived from arachidonic acid by COX-1
<i>Angiotensin II (Ang II)</i>	<ul style="list-style-type: none"> • Potent vasoconstrictor 	<ul style="list-style-type: none"> • Synthesised by angiotensin converting enzyme • Elicits its effects via two receptors: AT₁ which promotes vasoconstriction and cell proliferation, and AT₂ which antagonises the effects of AT₁

VSMC (vascular smooth muscle cell); eNOS (endothelial nitric oxide synthase); nNOS (neuronal nitric oxide synthase); iNOS (inducible nitric oxide synthase); sGC (soluble guanylyl cyclase).

1.2.2.1 Nitric Oxide and Nitric Oxide Synthase

As previously mentioned on page 3, there are numerous vasoactive substances produced by the ECs. Nitric Oxide (NO) is the most potent endothelium-dependant vasodilator synthesised in the endothelial cell layer (Durand & Gutterman, 2013; Mudau et al., 2012), and causes the relaxation of the underlying vascular smooth muscle cells (VSMCs) (Sandoo et al., 2010). NO is the heterodiatomic free radical product that is formed through the oxidation of the amino acid L-arginine, to L-citrulline (Fig.1.2) (K. Park & Park, 2015; Stamler, Singel, & Loscalzo, 1992). This conversion is facilitated by the enzyme nitric oxide synthase (NOS) (Palmer, Ashton, & Moncada, 1988).

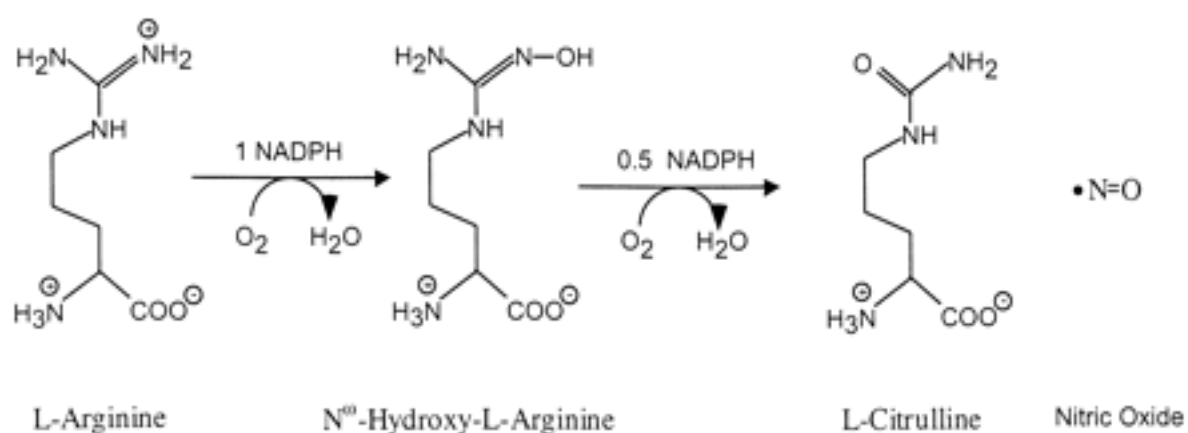


Figure 1.2: The formation of NO from L-Arginine, with the NADPH and oxygen requirements for each reaction shown (Stuehr, 2004). NADPH (Nicotinamide adenine dinucleotide phosphate).

NOS exists in three different isoforms: neuronal NOS (nNOS); inducible NOS (iNOS) and endothelial NOS (eNOS). nNOS produces NO, which plays the role of a neuronal messenger that has the ability to regulate synaptic neurotransmitter release (Prast & Philippu, 2001), while iNOS is only expressed in injured cells that have been exposed to inflammatory mediators that can activate macrophages (Michel & Feron, 1997). eNOS is the most abundant isoform of NOS and is responsible for the NO produced in the vasculature, and therefore vessel dilation (Sandoo et al., 2010). The various isoforms of NOS were originally named and classified according to the cells they were initially observed in, however, it is now evident that the different isoforms also occur in numerous other cells, including cardiac myocytes (Balligand et al., 1995); as well as blood platelets, the hippocampus and skeletal muscle (Arnal, Dinh-Xuan, Pueyo, Darblade, & Rami, 1999).

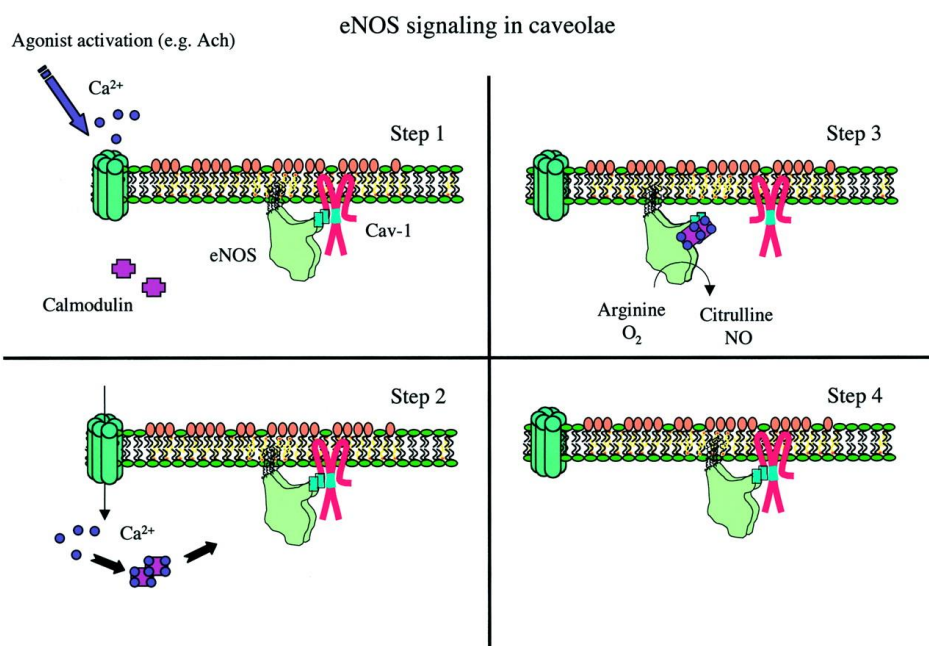


Figure 1.3: eNOS signaling in caveolae. Depicted in the figure is the cycle of eNOS activation and inhibition in caveolae. In step 1, Cav-1 is bound to eNOS, inhibiting eNOS activity. In step 2, agonist activation by Ach initiates an influx of calcium that binds to and activates calmodulin. In step 3, calcium-activated calmodulin binds to eNOS thereby relieving its inhibition by Cav-1 and NO is produced. Finally, in step 4, Cav-1 binds to eNOS again, completing the cycle (**Razani, Woodman, & Lisanti, 2002**). Cav-1 (caveolin); Ca²⁺ (calcium).

In the vascular endothelium, NO production is influenced by the release of chemical agonists acting on specific endothelial chemo-receptors (K. Park & Park, 2015). Such NO agonists include acetylcholine (ACh), bradykinin (BK), adenosine tri-phosphate (ATP), adenosine di-phosphate (ADP), substance P (SP) and thrombin (Moncada & Higgs, 2006)

Inactive eNOS is bound to the protein caveolin and kept within small invaginations in the cell membrane, known as caveolae (Bucci et al., 2000). eNOS is activated by the receptor-dependent NO agonists, which stimulate the release of calcium from the endoplasmic reticulum (ER) (Fig 1.4) (Bae et al., 2003), thereby increasing intracellular calcium levels and causing the detachment of eNOS from caveolin (Fig 1.3) (Sandoo et al., 2010; Venema, Sayegh, Arnal, & Harrison, 1995). When intracellular calcium from the ER is depleted, endothelial membrane receptors receive a signal to open the calcium channels and allow the entry of extracellular calcium into the cell (Schilling, Cabello, & Rajan, 1992), which is known as store operated calcium entry or capacitative calcium entry (Putney, 1986). In order to bind to and activate eNOS, calcium must undergo a structural change, which is achieved through the binding of calcium to calmodulin within the cell cytoplasm (Fleming & Busse, 1999). Active eNOS is then able to catalyse the production

of NO through the conversion of L-arginine (Fig 1.2). This process of NO production in ECs is shown in Figure 1.4.

In this particular pathway, it is important to note that NO production is dependent on the amount of intracellular calcium in the ER, as well as the quantity of extracellular calcium that diffuses into the cell (Sandoo et al., 2010). When calcium levels decrease, the calcium-calmodulin complex dissociates from eNOS. The unbound eNOS is then free to bind with caveolin again, and therefore becomes inactivated (Fleming & Busse, 1999). In this way, short-term increases in NO are dependent on calcium levels, but once intracellular calcium is depleted, alternative mechanisms need to be activated in order to further regulate NO production. In such cases, eNOS can be alternatively activated through phosphorylation (Butt et al., 2000), which occurs through specific protein kinases, like protein kinase A (PKA) (Bae et al., 2003) and cyclic guanosine-3', 5-monophosphate (cGMP) protein kinase dependent II (Butt et al., 2000).

Once eNOS has been activated and NO has been consequently synthesised, NO diffuses across the EC into the adjacent VSMC (Fig 1.4), where it binds to the enzyme soluble guanylyl cyclase (sGC), thereby activating it (Ignarro, Harbison, Wood, & Kadowitz, 1986). Active sGC increases the conversion rate of guanosine triphosphate (GTP) to cGMP, which decreases smooth muscle tension (Jones, Wong, Jankowski, Akao, & Warner, 1999), effectively decreasing the release of calcium from the sarcoplasmic reticulum (SR) in the VSMCs (Collins, Griffith, Henderson, & Lewis, 1986), which overall reduces VSMC contraction. All the mechanisms described above are continuously active, and the resultant production of NO is used to maintain basal vasodilatory tone (Sandoo et al., 2010).

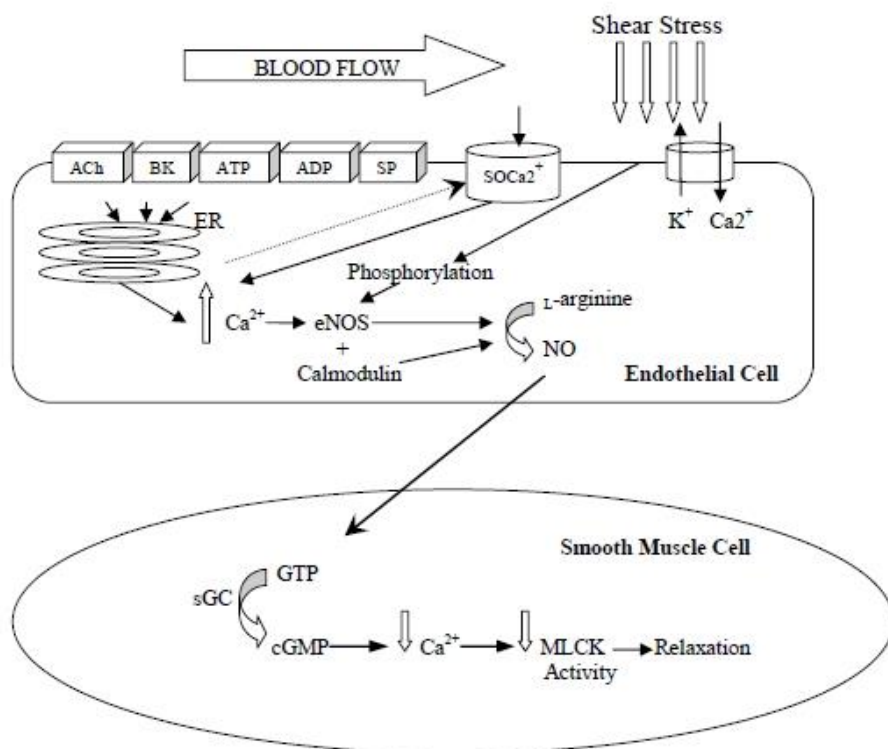


Figure 1.4: Endothelial NO production and its actions in the VSMCs. Agonists such as ACh and BK or mechanical forces, such as shear stress, lead to VSMC relaxation by stimulation of NO production. When ER calcium stores are depleted, the SOCa²⁺ channel allows extracellular calcium into the EC (Durand & Gutterman, 2013; Sandoo et al., 2010). ACh (acetylcholine); BK (bradykinin); ATP (adenosine triphosphate); ADP (adenosine diphosphate); SP (substance P); SOCa²⁺ (store-operated Ca²⁺ channel); ER (endoplasmic reticulum); NO (nitric oxide); sGC (soluble guanylyl cyclase); cGMP (cyclic guanosine-3',5-monophosphate); MLCK (myosin light chain kinase).

Under normal physiological conditions, endothelial NO production is mainly regulated by mechanical forces, particularly shear stress, which act on specific mechano-receptors (Gutiérrez et al., 2013). This mechanical activation of eNOS is the most important regulator of eNOS activity and contributes to the phenomenon of flow-mediated vasodilatation (Fig 1.4), which is a vital autoregulatory mechanism that increases blood flow in response to physical activity or exercise (Loscalzo & Vita, 1994).

NO production and regulation is vital to maintaining vascular homeostasis and healthy endothelial function, and therefore quantifying NO levels in a specific vascular area might be helpful in determining endothelial function. However, NO is a volatile substance with a

short half-life, making its moment-by-moment quantification almost impossible (Versari et al., 2009). For this reason, NO bioavailability is usually evaluated through the measurement of its downstream effects. For example, endothelium-dependent relaxation can be measured through vascular reactivity tests (Deanfield et al., 2005), using either receptor-operated (ACh; BK; SP) stimuli *in vitro* and *ex vivo* or mechanical stimuli such as shear stress *in vivo*, using flow-mediated vasodilation (FMD) as the technique of assessment (John & Schmieder, 2000).

It is clear that NO and NOS play key roles in endothelial function, not only in a vasodilatory capacity, but also through a plethora of other important regulatory functions (Table 1.2). It is essential for the healthy endothelium that these two regulators are present in desirable quantities, since an imbalance in NO and NOS levels can have dire consequences for endothelial health.

1.3 Endothelial Dysfunction

When the endothelium loses its regulatory ability to maintain a balance between endothelial-derived vasodilatory and vasoconstrictory factors, it results in ED (Mudau et al., 2012). ED is characterised by a shift in the actions of the endothelium toward reduced vasodilation, a proinflammatory state, and prothrombotic properties (Rajendran et al., 2013), resulting in progressive pathophysiological changes (Fig 1.5). Mechanisms by which these pathophysiological changes occur appear to be complex and multifactorial. ED is associated with most major cardiovascular risk factors (Versari et al., 2009), and is therefore a key role player in the progression to atherosclerosis and CVD. Perhaps most importantly, ED represents an initial reversible step in the development of various CVDs (Bonetti et al., 2003), making it a promising target for the prevention of such diseases when identified early (Chhabra, 2009).

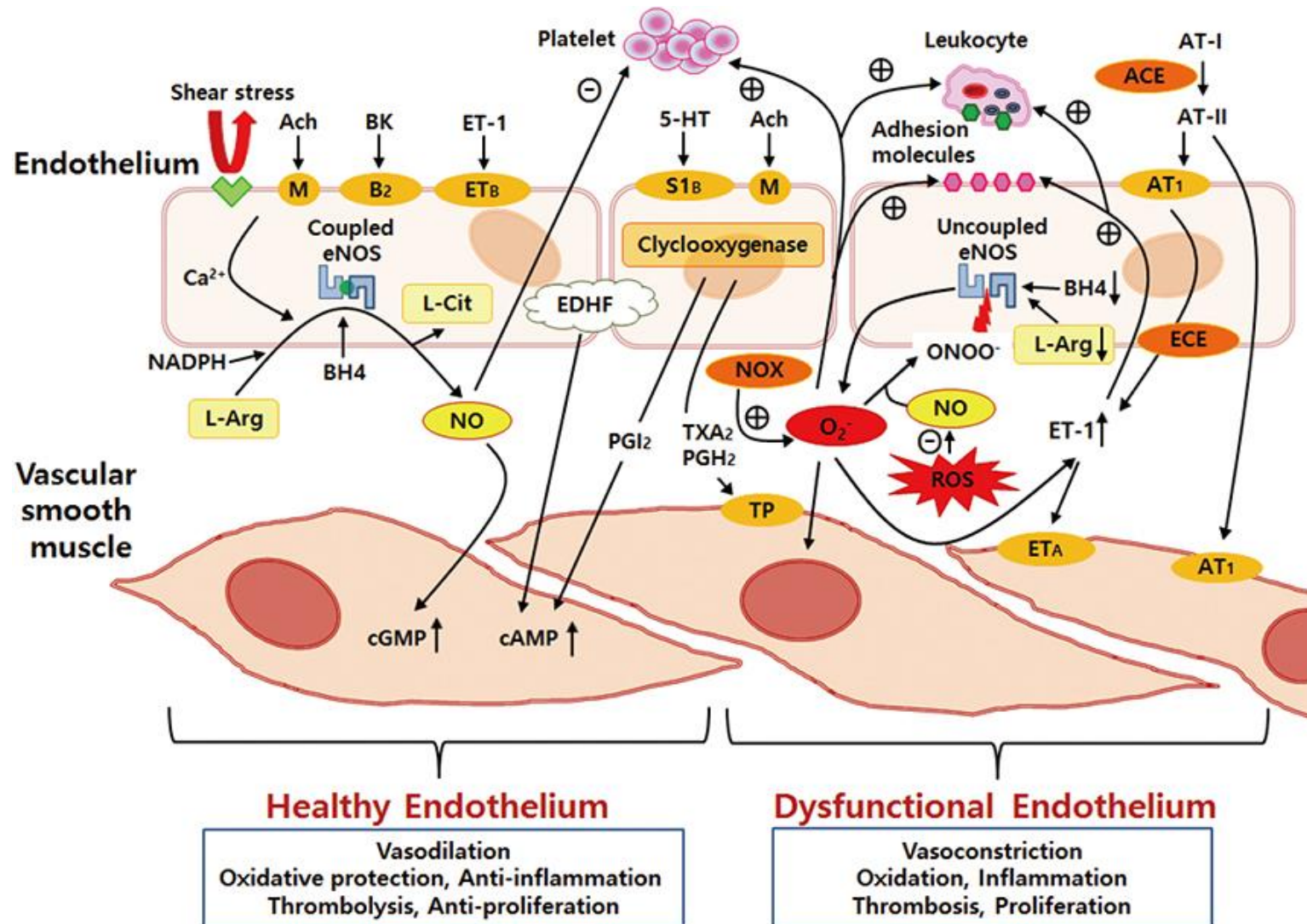


Figure 1.5: The pathophysiological changes seen in a dysfunctional endothelium. In the healthy endothelium, the eNOS is responsible for most of the vascular NO production. However, eNOS becomes a potential ROS generator when in the pathological uncoupled state, due to various oxidative stresses (K. Park & Park, 2015). ACE (angiotensin-converting enzyme); Ach (acetylcholine); AT-I (angiotensin I); AT-II (angiotensin II); AT₁ (angiotensin 1 receptor); BH₄ (tetrahydrobiopterin); BK (bradykinin); cAMP (cyclic adenosine monophosphate); cGMP (cyclic guanosine monophosphate); ECE (endothelin converting enzyme); eNOS (endothelial nitric oxide synthase); EDHF (endothelium derived hyperpolarizing factor); ET_A and ET_B (endothelin A and B receptors); ET-1 (endothelin-1); L-Arg (L-arginine); L-Cit (L-citrulline); M (muscarinic receptor); O₂⁻ (superoxide anion); ONOO⁻ (peroxynitrite); NADPH (nicotinamide adenine dinucleotide phosphate); NO (nitric oxide); NOX (nicotinamide adenine dinucleotide phosphate oxidase); PGH₂ (prostaglandin H₂); PGI₂ (prostaglandin I₂); ROS (reactive oxygen species); S_{1B} (serotonin receptor); TP (thromboxane prostanoid receptor); TXA₂ (thromboxane); 5-HT (serotonin); ⊖ (inhibition); ⊕ (stimulation).

1.3.1 Pathophysiology

The fundamental feature of ED is the impaired or reduced NO bioavailability (Endemann & Schiffrin, 2004; Versari et al., 2009), resulting in the inability of the endothelium to initiate vasodilation in response to vasodilatory stimuli such as acetylcholine or shear stress (Mudau et al., 2012). In the presence of impaired NO bioavailability, the endothelium has to implement alternative physiological pathways in an attempt to compensate for NO deficiency (Versari et al., 2009).

ED comprises of a state of chronic “endothelial activation” (Bonetti et al., 2003), sometimes referred to as the endothelial activation–dysfunction–injury triad (Bijl, 2003). This state is characterised by a proinflammatory, proliferative, and procoagulatory milieu (Anderson, 1999), which is detrimental to the progression of CVDs, specifically all stages of atherogenesis.

Along with NO deficiency, a dysfunctional endothelium can become imbalanced in its release of other substances and mediators that are detrimental to the arterial wall, leading to excessive release of factors including endothelin-1 (ET-1), thromboxane (THA₂), prostaglandin H₂ (PGH₂), and reactive oxygen species (ROS) (Fig 1.5) (Taddei, Ghiadoni, Virdis, Versari, & Salvetti, 2003). As the endothelial function further deteriorates, the ECs exhibit reduced anti-oxidant and anti-inflammatory effects, increased vascular permeability to lipoproteins, and the increased expression of inflammatory cytokines and adhesion molecules (Libby, Ridker, & Maseri, 2002). C-reactive protein (CRP) is an example of a specific compound that moves into the tissue and causes inflammation (Devaraj, Singh, & Jialal, 2009), leading to further aggravation of the faulty endothelium.

1.3.2 Aetiology and Mechanisms of ED

Chronic exposure to cardiovascular risk factors and the harmful circulating stimuli associated with these conditions overwhelms the defence mechanisms of the vascular endothelium, hence compromising its integrity and ultimately initiating ED (Deanfield, Halcox, & Rabelink, 2007). ED has been observed to be associated with major cardiovascular risk factors, such as aging, hyperhomocysteinemia, post-menopause state, smoking, diabetes, hypercholesterolemia, hypertension, and more (Rajendran et al., 2013; Versari et al., 2009).

Most cardiovascular risk factors are associated with the up-regulation of intracellular oxidative stress and ROS (Cai & Harrison, 2000; K. Park & Park, 2015). Among various complex mechanisms, oxidative stress appears to be the most common underlying mechanism for the development of ED (Drexler, 1997; K. Park & Park, 2015). Oxidative stress is caused by an imbalance between the pro-oxidative and anti-oxidative molecules (Cahill & Redmond, 2016; Pennathur & Heinecke, 2007), often resulting in biomolecular damage caused by excess ROS (Halliwell, 2007). ROS is a term that includes oxygen radicals such as superoxide (O_2^-) and the hydroxyl radical (OH^-), as well as non-radical derivatives of oxygen (O_2) including hydrogen peroxide (H_2O_2) (Cahill & Redmond, 2016). In most instances, the human body has an adequate supply of endogenous antioxidants, as well as antioxidants obtained from various foods to neutralise these free radicals. If the body is depleted of these antioxidants, or in the presence of multiple cardiovascular factors, injury to the endothelium and a loss in NO homeostasis can occur (Rajendran et al., 2013).

In the presence of cardiovascular risk factors, NADPH oxidases (NOX) and eNOS are often both dysregulated (Forstermann & Munzel, 2006), as a compensatory mechanism to increase NO levels and therefore all of the athero- and vaso-protective effects associated with it. The upregulation of NOX results in an increased production of ROS – specifically O_2^- - in the vascular wall, with NOX being implicated as the main source for oxidative excess in the vasculature (Hamilton, Brosnan, Al-Benna, Berg, & Dominiczak, 2002). The upregulation of functional eNOS results in increased levels of NO, which is the desired effect. However, in the presence of excess O_2^- , NO cannot be utilised for its pro-dilatory properties, and instead O_2^- combines with NO to form the highly reactive nitrogen species (RNS), peroxynitrite ($ONOO^-$) (Fig 1.6) (Forstermann & Munzel, 2006). Under physiological conditions, the enzyme sodium oxide dismutase (SOD) usually regulates O_2^- levels, but in diseased states, this defensive mechanism is overwhelmed (Landmesser & Harrison, 2001). This is to be expected considering O_2^- combines with NO at a rate that is three times faster than the dismutation of O_2^- by SOD (Heitzer, Schlinzig, Krohn, Meinertz, & Munzel, 2001). Together, this all results in the characteristic pathophysiological reduced NO bioavailability in ED (Tomasian, Keaney Jr, & Vita, 2000). O_2^- , along with $ONOO^-$, also has the ability to directly inhibit the main target of NO, sGC and further enhance oxidative stress by inhibiting SOD (Munzel, Daiber, Ullrich, & Mulsch, 2005).

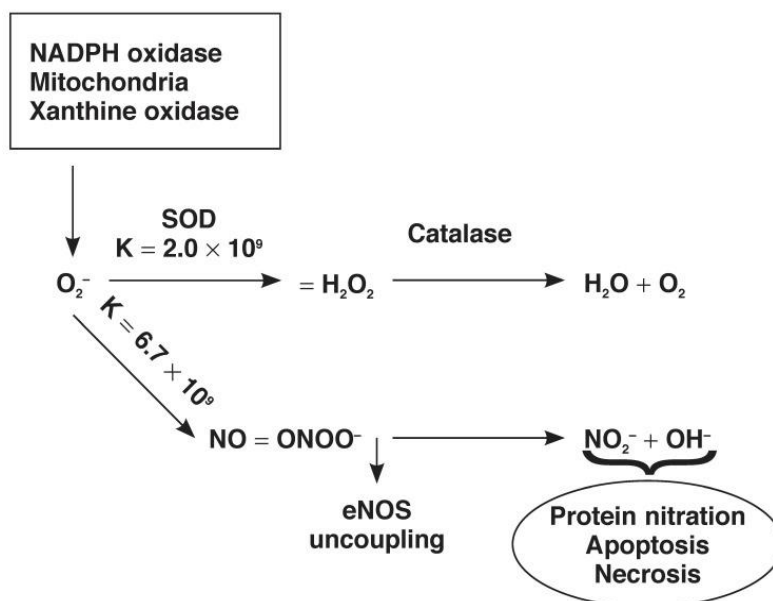


Figure 1.6: Oxidative and nitro-oxidative stress. Superoxide released from sources such as NADPH oxidase, mitochondria and xanthine oxidase is dismutated to hydrogen peroxide by SOD, which is then converted to water and oxygen by catalase. However, superoxide has a higher affinity for NO than SOD, and when in excess, it preferentially combines with NO to produce peroxynitrite with various pathophysiological consequences (**Mudau et al., 2012**). SOD (superoxide dismutase); O_2^- (superoxide); H_2O_2 (hydrogen peroxide); NO (nitrogen oxide); $ONOO^-$ (peroxynitrite); NO_2^- (nitrite); OH^- (hydroxyl); H_2O (water); O_2 (oxygen).

The consequently high levels of $ONOO^-$ are injurious to the cells, since it has the ability to oxidatively damage DNA, lipids and proteins (Mudau et al., 2012). $ONOO^-$ can undergo protonation to form peroxynitrous acid ($ONOOH$), or it can combine with carbon dioxide (CO_2) to form nitroso-peroxocarbonate ($ONOOCO_2^-$), both of which yield tyrosine-nitrating compounds (Hurst, 2002). Via formation of these compounds, $ONOO^-$ causes the nitration of tyrosine residues of proteins, leading to formation of nitrotyrosine (Pacher, Beckman, & Liaudet, 2007), causing cell damage. In addition to being cytotoxic, $ONOO^-$ causes oxidative damage to the zinc-thiolate cluster of eNOS, resulting in the loss of the zinc ion and the formation of disulfide bonds between the enzyme monomers, and thus disruption of the binding site for BH_4 and L-arginine (Forstermann & Munzel, 2006). $ONOO^-$ can also oxidise tetrahydrobiopterin (BH_4) - which is an essential cofactor of eNOS- to the trihydrobiopterin (BH_3^{\cdot}) radical. Both of the above eventually lead to eNOS uncoupling (Fig 1.8) (Forstermann & Munzel, 2006; Kuzkaya, Weissmann, Harrison, & Dikalov, 2003). Figure 1.7 gives an overview of everything discussed above.

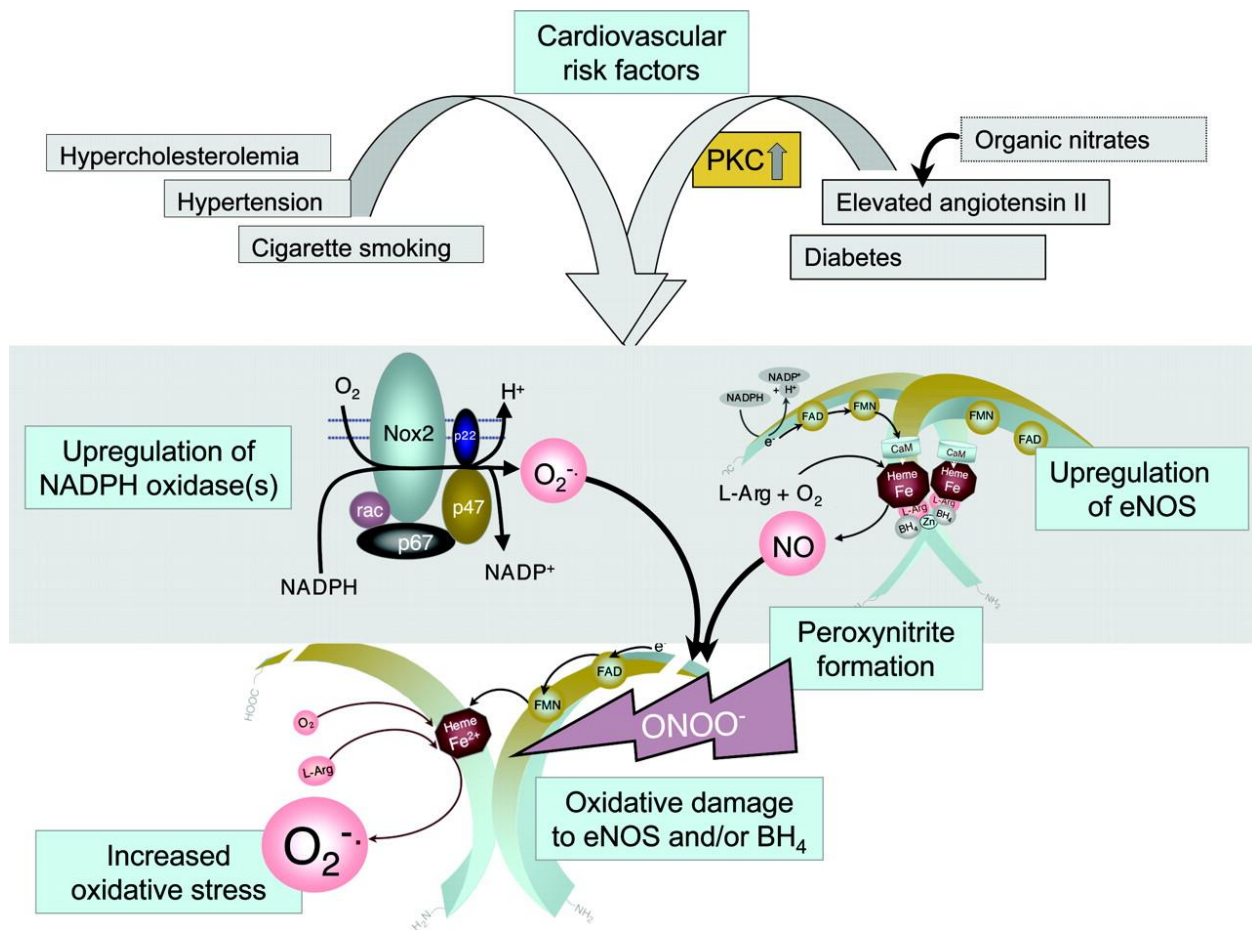


Figure 1.7: Potential mechanisms by which cardiovascular risk factors lead to ED through increased oxidative stress (Forstermann & Munzel, 2006).

eNOS uncoupling involves the dissociation of the ferrous-oxygen complex of eNOS. The resultant faulty eNOS enzyme can now produce $O_2^{\cdot-}$ from the oxygenase domain (Fig 1.8), rather than its natural product, NO (Forstermann & Munzel, 2006). This makes uncoupled eNOS a potential ROS generator (Landmesser & Harrison, 2001; K. Park & Park, 2015). In addition to $ONOO^-$ -induced eNOS uncoupling, other oxidants such as H_2O_2 have also been shown to uncouple the enzyme (Mudau et al., 2012).

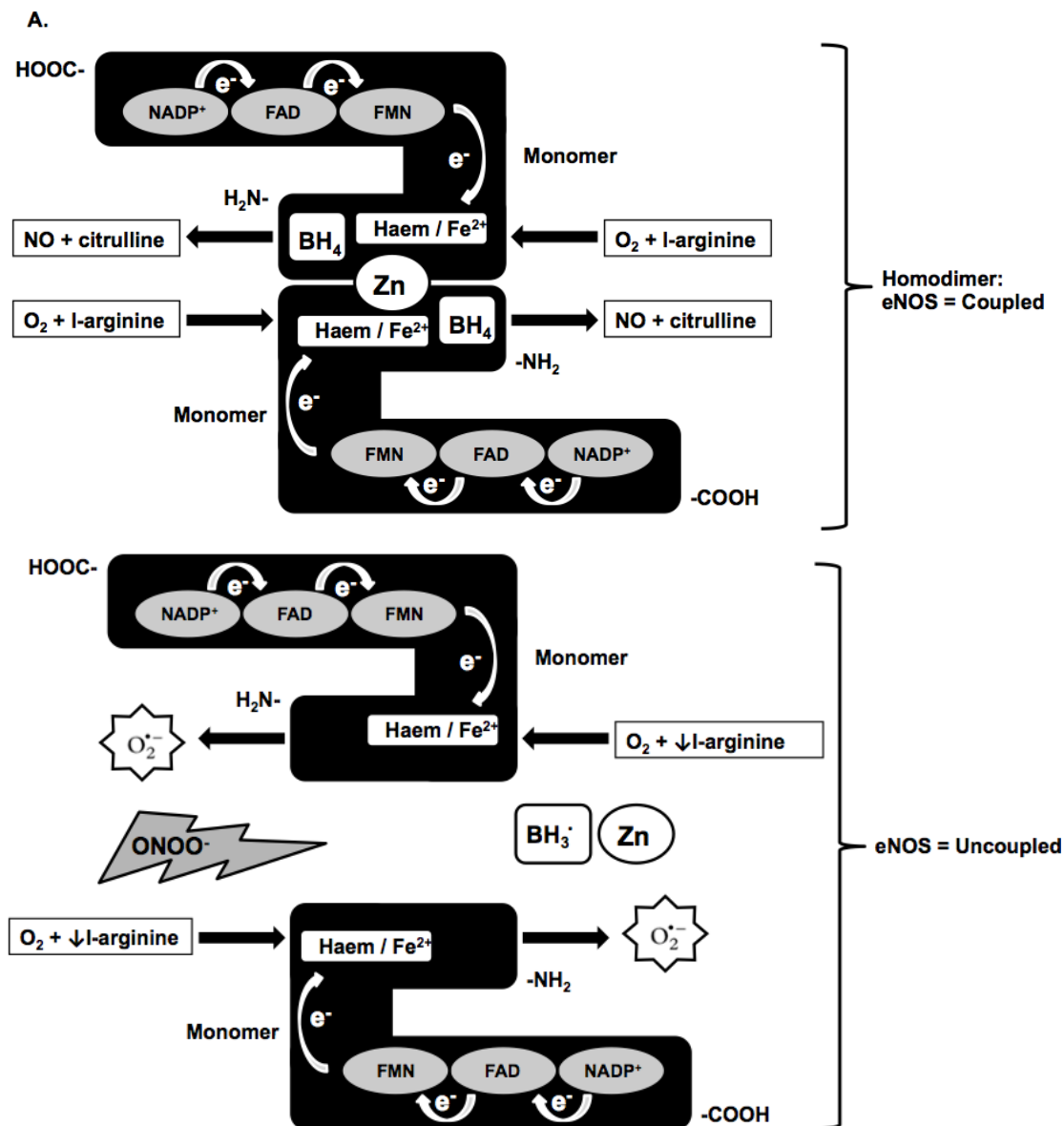


Figure 1.8: Coupled and uncoupled eNOS. (A) In the presence of sufficient levels of substrates and co-factors, and the absence of harmful reactive species, eNOS monomers will form a dimerised, coupled enzyme and produce physiological amounts of NO. (B) Decreased levels of the substrate, L-arginine and/or harmful effects exerted by increased levels of ONOO⁻, cause failure of the enzyme to dimerise, leading to the uncoupling of eNOS and the production of O₂⁻ instead of NO (Mudau et al., 2012).

H₂O₂ is formed as a by-product of the dismutation of O₂⁻ by SOD (Fig 1.6). Excess production of H₂O₂, along with being implicated in eNOS uncoupling, can increase eNOS expression, through transcriptional and post-transcriptional mechanisms (Forstermann & Munzel, 2006). In the presence of antioxidant enzymes such as catalase or glutathione peroxidase, H₂O₂ can be dismutated into water (H₂O) and O₂ (Fig 1.6). However, in the presence of transition metals – such as copper and iron- or O₂⁻, H₂O₂ generates highly reactive hydroxyl radicals, which cause cell damage through the peroxidation of lipids (Feletou & Vanhoutte, 2006). In addition, ROS promote the contraction of VSMCs by

facilitating the mobilization of calcium and increasing the sensibility of the contractile proteins to calcium ions (Feletou & Vanhoutte, 2006). Together, all these contributors further exacerbate the overload of ROS in ED.

Inflammation is another common underlying mechanism of ED, and there seems to be a causal relationship between oxidative stress and inflammation (Karbach, Wenzel, Waisman, Munzel, & Daiber, 2014). Under physiological conditions, appropriate levels of NO, released by the healthy endothelium, control vascular inflammation. However, during ED, excess ROS aggravates vascular inflammation (K. Park & Park, 2015). Oxidative stress may amplify the vascular pro-inflammatory signaling pathways, leading to even higher levels of ROS, since inflammatory cells release $O_2^{\cdot-}$ (Karbach et al., 2014). ROS has been shown to upregulate adhesion and chemotactic molecules (Griendling & FitzGerald, 2003), while inflammatory markers such as C-reactive protein (CRP) have been shown to decrease eNOS activity (Venugopal, Devaraj, Yuhanna, Shaul, & Jialal, 2002). Other than oxidative stress and chronic inflammation, infection, anti-oxidant deficiency and abnormal shear stress are all mechanisms implicated in ED (K. Park & Park, 2015).

1.3.3 Consequences of ED

The presence of ED can be regarded as a clinical syndrome that is associated with, and predicts an increased rate of adverse cardiovascular events (Bonetti et al., 2003). A study by Lerman & Zeiher (2005) showed an analysis of close to 2500 patients, which demonstrated that ED is strongly and independently associated with cardiovascular events (Lerman & Zeiher, 2005).

Most evidence points towards ED as one of the major pathologic changes between exposure to the cardiovascular risk factors, and the development of atherosclerotic CVD (Fig 1.9) (K. Park & Park, 2015).

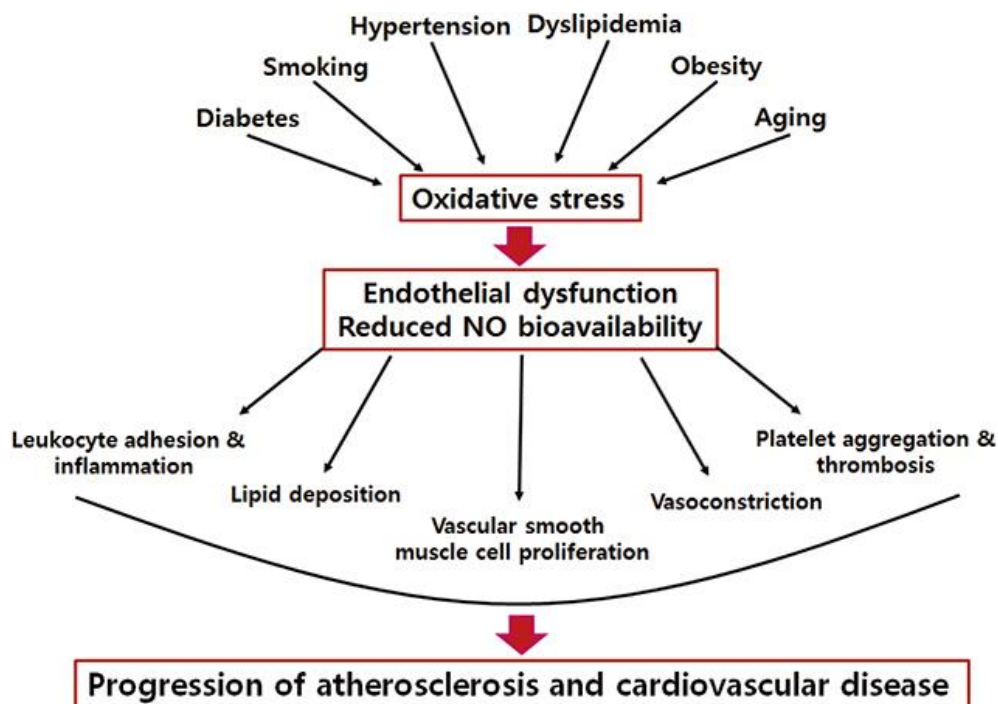


Figure 1.9: Progression from risk factors to atherosclerosis and CVD mediated by oxidative stress and ED (K. Park & Park, 2015).

Figure 1.9 shows that reduced NO bioavailability as a consequence of ED results in pro-atherosclerotic changes to the endothelial milieu (Heitzer et al., 2001). By upregulating platelet aggregation, leukocyte adhesion, and thrombosis, amongst other factors, the dysfunctional endothelium is not only an initiator, but also an important factor in the progression of atherosclerosis and CVD (Barton & Haudenschild, 2001). Thus, ED is not only a consequent feature of risk factors, but also a possible pathogenic mechanism for their onset (Versari et al., 2009).

ED is associated with most CVDs and risk factors for CVD. Amongst others, examples include hypertension, coronary artery disease, chronic heart failure, stroke, peripheral vascular disease, insulin resistance, diabetes and chronic kidney failure (Rajendran et al., 2013).

The oxidative stress associated with ED also has negative effects, independent of the ED as a whole. These include increased VSMC proliferation (resulting in thickening of the vascular wall), endothelial cell apoptosis, and increased expression and activity of matrix metalloproteinases, which are involved in the establishment of an atherosclerotic plaque (Mudau et al., 2012).

1.3.4 Prevention and Treatment of ED

The reversal of ED may be a critical point of in the prevention of atherosclerosis and CVD since ED has been implicated as the initial, reversible step in these conditions (Mudau et al., 2012). Treatment of ED involves the alteration of specific pathogenic pathways, with the goal of preserving or restoring endothelial function (K. Park & Park, 2015).

There are two classes of endothelial therapy (Fig 1.10): primary endothelial therapy involves the preservation and improvement of endothelial function in subjects without CVD, whereby lifestyle changes are made in order to reduce and prevent exposure to cardiovascular risk factors (Barton & Haudenschild, 2001). Secondary endothelial therapy involves the improvement of the dysfunctional endothelium through the treatment of underlying cardiovascular risk factors and established CVDs (Goff et al., 2014), and is applicable to both modifiable (hypertension, obesity, diabetes, dyslipidemia) and non-modifiable conditions (aging, menopause, coronary or peripheral artery disease, heart failure, end-stage renal disease) (K. Park & Park, 2015).

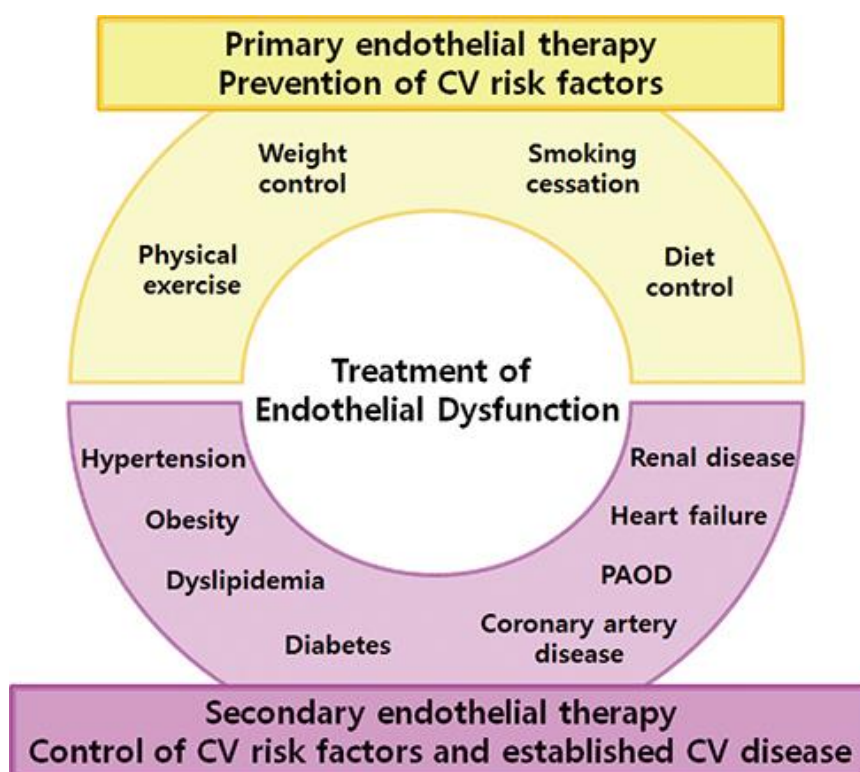


Figure 1.10: Therapeutic approaches to ED (K. Park & Park, 2015). CV (cardiovascular); PAOD (peripheral arterial occlusive disease).

Considering that oxidative stress is regarded by many as the main pathophysiologic mechanism leading to impaired NO bioavailability and ED (Versari et al., 2009), antioxidant substances could potentially play a substantial role in the treatment of ED. Acute studies have shown high-dose antioxidant vitamins are extremely effective in restoring normal endothelial function, however, interventional studies using oral administration of antioxidant substances including vitamin C and E have failed to provide consistent data (Viridis et al., 2004). The reason for the lack of benefit of long-term antioxidant supplementation in the setting of primary and secondary prevention, however, is not clear (Bonetti et al., 2003). Recent evidence suggests that certain antioxidants, including vitamin E, may be inappropriate to reduce oxidative stress *in vivo* or may even be pro-oxidant under certain conditions (Landmesser & Harrison, 2001). These mixed findings may point to the importance of testing new antioxidants or combining different antioxidant compounds in order to observe an adequate reduction of oxidative stress (Bonetti et al., 2003), a specific endpoint which will be addressed in this study (see section 1.8).

1.4 HIV/AIDS & ART

HIV is a retrovirus that was first isolated in 1983 (De Cock, 2011) and was subsequently proven to be the cause of acquired immunodeficiency syndrome (AIDS) a year later (Ruelas & Greene, 2013). Since then, the HIV/AIDS epidemic has evolved to become the greatest challenge in global health (De Cock, Jaffe, & Curran, 2012), and one of the most devastating viral pandemics in history (Freed, 2015). There are two strains of HIV, with HIV-1 being the main cause of AIDS, while HIV-2 is associated with isolated infections in central and western Africa (Sharp & Hahn, 2011). With the prolonged period between HIV infection and symptomatic AIDS – on average 11 years in adults – there was widespread transmission of HIV before recognition of the epidemic and any prevention attempts (De Cock, 2011). In the 1990s, almost 15 years after HIV/AIDS was discovered, ART was developed to combat HIV-1 infection (Laskey & Siliciano, 2014). ART has dramatically improved survival of patients with HIV/AIDS (Thienemann et al., 2013), and patients who are diagnosed and treated with ART early can experience acceptable immune recovery and expect a near-normal lifespan (Laskey & Siliciano, 2014; Thienemann et al., 2013). Although effective at suppressing viral replication, current drugs do not eradicate the virus, making treatment with ART a life-long necessity (Freed, 2015).

Number of people living with HIV in 2016	Total	36.7 million [30.8 million – 42.9 million]
	Adults	34.5 million [28.8 million – 40.2 million]
	Women	17.8 million [15.4 million – 20.3 million]
	Men	16.7 million [14.0 million – 19.5 million]
	Children (<15 years)	2.1 million [1.7 million – 2.6 million]
<hr/>		
People newly infected with HIV in 2016	Total	1.8 million [1.6 million – 2.1 million]
	Adults	1.7 million [1.4 million – 1.9 million]
	Children (<15 years)	160 000 [100 000 – 220 000]
<hr/>		
AIDS deaths in 2016	Total	1.0 million [830 000 – 1.2 million]
	Adults	890 000 [740 000 – 1.1 million]
	Children (<15 years)	120 000 [79 000 – 160 000]

Source: UNAIDS/WHO estimates.



Figure 1.11: Summary of the global HIV epidemic (2016) (WHO, 2016).

1.4.1 Epidemiology

As of 2016, it is estimated that there are 36.7 million people worldwide living with HIV (Fig 1.11), while around 35 million people have died from AIDS-related illnesses since the start of the epidemic (UNAIDS, 2017; WHO, 2016). Southern Africa carries the highest burden, where as few as nine countries - which account for less than 2% of the world's population - represent about one third of global HIV infections (De Cock et al., 2012).

With the rollout of ART and various prevention programmes in middle-and-low-income countries, the most affected populations are now receiving adequate treatment (Delpech, 2013). For this reason, the global prevalence of HIV has begun to plateau, and every year, there is a promising decline in newly infected individuals.

1.4.2 Virus Structure, Targets and Life-cycle

HIV-1 is a retrovirus that belongs to the lentivirus family. Infections with lentiviruses typically show a chronic course of disease, a long period of clinical latency and persistent viral replication (Rubbert, Behrens, & Ostrowski, 2007). The HIV virion has a spherical shape and a diameter of roughly 100–130 nm. The viral envelope is composed of a lipid membrane, which is derived from the host cell and contains cellular proteins, as well as about 7–12 trimeric complexes of viral envelope protein (Kirchhoff, 2013). The core antigen contains two single strands of viral RNA (Fig 1.12) with a length of close to 10,000

nucleotides. The virion contains the enzymatic equipment that is necessary for replication, namely a reverse transcriptase (RT), an integrase and a protease (Rubbert et al., 2007).

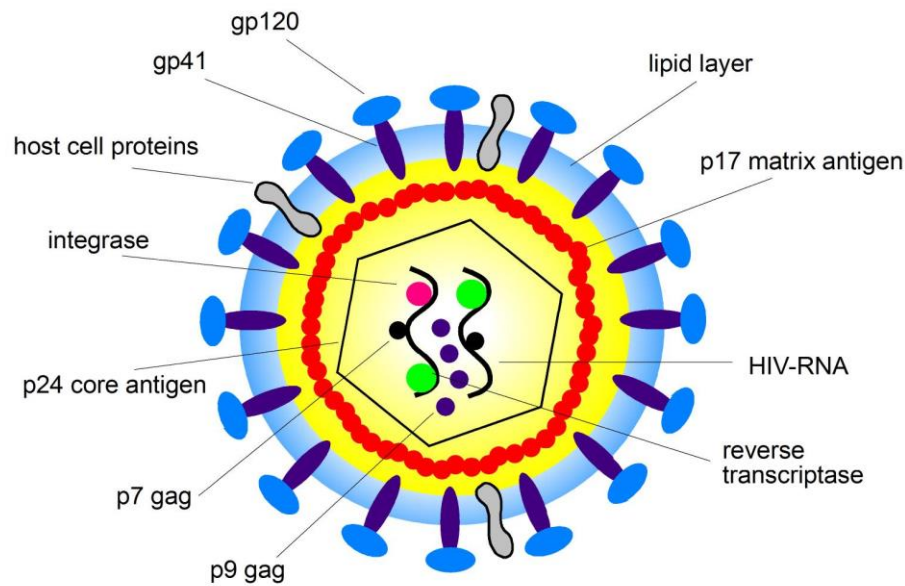


Figure 1.12: Structure of an HIV virion particle (Rubbert et al., 2007). Gp (glycoprotein); gag (group-specific antigen).

The main targets of HIV are CD4⁺ helper T cells, which are key regulators of the humoral and cellular immune responses (Kirchhoff, 2013). The destruction and depletion of these cells renders the body unable to defend itself against opportunistic pathogens, eventually resulting in AIDS (Laskey & Siliciano, 2014). When HIV infects an activated CD4⁺ T cell, it hijacks and manipulates its transcriptional and translational machinery to reproduce itself (Kirchhoff, 2013). HIV also has the ability to infect other immune cells, such as macrophages and immature dendritic cells, which may play a role in harboring the virus in a silent integrated proviral form and thus contribute to the establishment and maintenance of viral reservoirs that prevent the eradication of HIV from the human body, even during ART (Kirchhoff, 2013).

The HIV-1 life cycle is complex and can roughly be divided in an early and a late phase of replication. The early phase begins with the attachment or fusion of the virion at the cell surface, includes reverse transcription of the viral RNA to DNA amongst other steps, and ends with the integration of the proviral DNA into the host genome (Freed, 2015; Kirchhoff, 2013). The late phase of replication starts with the initiation of proviral

transcription and ends with the release of fully infectious progeny virions, which contain activated viral proteases (Kirchhoff, 2013; Laskey & Siliciano, 2014). This process is summarized below in Figure 1.13. The viral life cycle illuminates some of the challenges associated with HIV infection. For example, the HIV life cycle lasts just one to two days and the viral RT has an extremely high mutation rate of roughly 1 error per 10 000 nucleotides (Kirchhoff, 2013). Together, a short generation time, a massive virus production rate of up to 2×10^9 virions per day, and a large error rate (Sharp & Hahn, 2011), allow HIV to rapidly adapt to its host environment and to develop resistance against ART or immune responses (Kirchhoff, 2013).

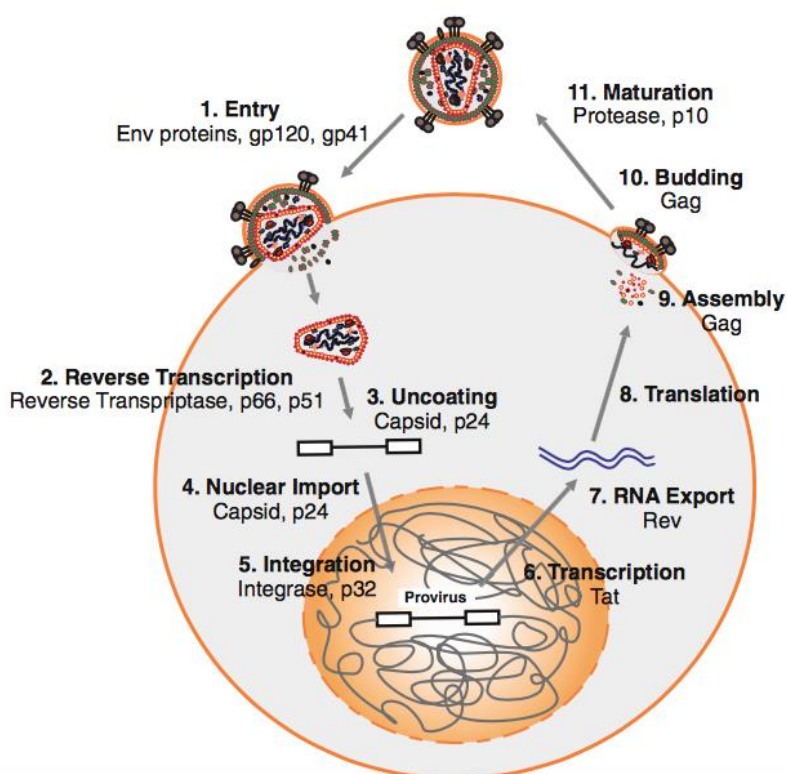


Figure 1.13: A brief summary of the HIV life-cycle (Kirchhoff, 2013). Env (envelope); gp (glycoprotein); p (protein); tat (trans-activator of transcription); Rev (trans-activator involved in protein expression); gag (group-activated antigen).

1.4.4 Antiretroviral therapy (ART)

Although there is no cure for HIV, more than 30 different anti-HIV drugs have now been approved for clinical use targeting different steps in the viral life cycle (Ruelas & Greene, 2013). ART suppresses the viral load by interfering with viral replication (Laskey & Siliciano, 2014). The different classes of antiretroviral (ARV) drugs are broadly classified by the phase of the retrovirus life cycle that the drug inhibits (Fig 1.14).

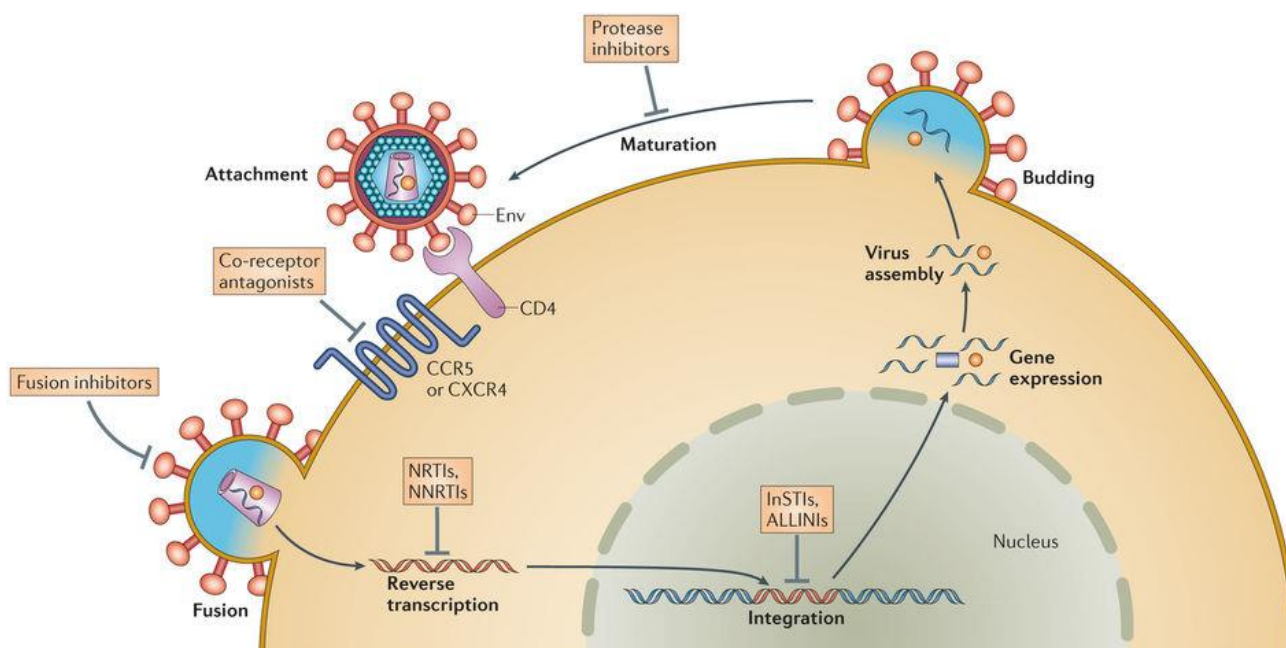


Figure 1.14: Stages of the HIV life cycle that are targeted by ARV drugs (Laskey & Siliciano, 2014). CCR5 (C-C chemokine receptor type 5); CXCR4 (C-X-C chemokine receptor type 4); NRTIs (nucleoside/nucleotide reverse transcriptase inhibitors); NNRTIs (non-nucleoside reverse transcriptase inhibitors); InSTIs (integrase strand transfer inhibitors); ALLINIs (allosteric integrase inhibitors); Env (envelope); CD4 (cluster of differentiation 4).

There are six main classes of ARVs (AIDSinfo, 2013; Arts & Hazuda, 2012): The first and second ARV classes are co-receptor agonists and entry inhibitors/fusion inhibitors respectively. These classes of ARVs compete with specific receptors involved in HIV attachment and therefore block the attachment and subsequent entry of the virus into the host cell. The third and fourth type, are nucleoside or nucleotide reverse transcriptase inhibitors (NRTIs/NtRTIs) and non-nucleoside reverse transcriptase inhibitors (NNRTIs). These two classes of ARVs stop the virus from converting its RNA into DNA. The fifth class of ARVs, are integrase inhibitors, which inhibit the viral enzyme integrase. Integrase is responsible for integration of viral DNA into the DNA of the infected cell. The last type of

ARVs, are Protease Inhibitors (PIs). PIs block the viral protease enzyme, which is necessary to produce mature and infectious virions.

Initially, ARV drugs were given as monotherapy, but the standard of care has since evolved to include the administration of a cocktail or combination of ARV drugs (Arts & Hazuda, 2012), in order to prevent drug resistance (Laskey & Siliciano, 2014). Combination therapy, also known as highly active antiretroviral therapy (HAART), consists of a combination of at least three ARV drugs - drawn from four of the six main ARV classes - where two or more NRTIs typically form the backbone of most regimens (Carr, 2003). In modern day treatment, co-formulations of these individual ARVs have reduced the “pill burden” and improved patient adherence (Thompson et al., 2012). There are now 19 licensed drugs in these four classes (Table 1.3), which can be combined into more than 3,000 potential HAART regimens (Carr, 2003). The firm establishment and implementation of HAART has led to major declines in opportunistic complications, making HIV infection more of a chronic disease than an acute one, and so more drugs are being used in more patients for longer periods (Carr, 2003; Ruelas & Greene, 2013).

Table 1.3: Presently available ARV drugs. Drugs in each class are listed in approximate order of approval/availability (Carr, 2003).

Drug Class	Specific Drug
Nucleoside reverse transcriptase inhibitors (NRTIs)	Zidovudine (AZT), didanosine (ddl)*, zalcitabine (ddC), lamivudine (3TC)*, stavudine (d4T), abacavir (ABC)*, emtricitabine (FTC)
Nucleotide reverse transcriptase inhibitors (NRTIs)	Tenofovir disoproxil fumarate (TDF)*
Non-nucleoside reverse transcriptase inhibitors (NNRTIs)	Nevirapine (NVP), delavirdine (DLV), efavirenz (EFV)*
Protease inhibitors (PIs)	Saquinavir (SQV), indinavir (IDV), ritonavir (RTV), nelfinavir (NFV), amprenavir (APV), lopinavir/ritonavir (rLPV), atazanavir (AZV)*
Fusion inhibitors	Efuvirtide (ENV; T-20)

*Administered once daily.

1.4.5 HIV & ART in a South African Context

SA has the largest HIV-infected population globally, with an estimated 7 million people living with HIV in 2015 (Statistics South Africa, 2015). The reason for this large South African population of HIV-infected people is unclear, but various biological and social factors may play a role (De Cock, 2011). The long-term AIDS-denialism – the view that HIV is not the cause of AIDS- in SA may have also played a pivotal role, since it led to the delayed implementation of ART by the government and resulted in thousands of deaths.

SA has the largest ART programme in the world (South African National AIDS Council, 2015). In April 2014, more than 3 million people were receiving ART, which equates to 47% of people living with HIV in the country (South African National AIDS Council, 2015). This is a monumental increase compared to statistics from 12 years earlier, where only 2% of the HIV positive population in SA was receiving ART (Joint United Nations Programme

on HIV/AIDS, 2010). The extent of the HIV/AIDS epidemic and the need for increased access to ART has had a profound effect on already stretched health care systems in SA (Levitt et al., 2011). In 2013, SA changed the CD4+ cut-off value at which patients could start ART, from 200 to 350 cells/ μ l, making more people eligible for treatment. By the end of 2014, SA increased the level again to 500, expanding eligibility even further (South African National AIDS Council, 2015; UNAIDS, 2016). In 2015, the WHO released guidelines recommending people living with HIV be offered ART immediately following diagnosis, regardless of CD4+ count (Dutta et al., 2015). As of 2016, SA began implementing this recommendation (South African National AIDS Council, 2016). Despite all of these implementations, HIV prevalence still remains as high as 19.2% among the general South African population, although, this varies considerably between regions (UNAIDS, 2014).

1.4.5.1 SA First Line Fixed Dose Combination Therapy

In 2013, a new fixed dose combination (FDC) therapy was implemented in SA, under various trade names, including Odimune®. A single Odimune® tablet consists of two NRTIs - Emtricitabine (FTC): 200 mg / day, and Tenofovir disoproxil fumarate (TDF): 300 mg / day – as well as a NNRTI - Efavirenz (EFV): 600 mg / day (Table 1.4) (Davies, 2013). This combination constitutes the preferred first-line regimen for previously untreated patients (Meintjes et al., 2014). A once daily FDC tablet has substantially simplified the prescription, dispensing and stock management of ART drugs (Davies, 2013), as well as improved treatment adherence and the burden on patients subjected to multiple drug regimens (Meintjes et al., 2014). Table 1.4 summarizes various aspects of the different ARV drugs used in South African first line ART.

Table 1.4: Summary of ARVs used for first line FDC therapy in SA (Arts & Hazuda, 2012; Davies, 2013; Does, Thiel, & Johnson, 2003; Meintjes et al., 2014; Palmisano & Vella, 2011; Sierra-Aragon & Walter, 2012).

Name	Class	Recommended Dose (mg/day)	M _r (g/mol)	Mechanism of action	Common or severe ADR [†]	Alternative drugs
Emtricitabine (FTC)	NRTI	200	247.2	Cellular enzymes phosphorylate FTC to FTC-5'- triphosphate which in turn competes with the natural substrate, deoxycytidine 5'- triphosphate and is subsequently incorporated into the nascent viral DNA and leads to chain termination.	Palmar hyperpigmentation, hyperlactataemia/ steatohepatitis (very low potential).	Lamivudine (3TC).
Tenofovir disoproxil fumarate (TDF)	NtRTI	300	287.2	TDF diphosphate inhibits HIV RT through competition with the natural substance deoxyadenosine 5'- triphosphate and leads to DNA chain termination after incorporation into the viral-DNA.	Renal failure , tubular wasting syndrome, reduced bone mineral density, hyperlactataemia/ steatohepatitis (very low potential).	Abacavir (ABC).
Efavirenz (EFV)	NNRTI	600 (at night) – 400 if < 40kg	315.7	Diffuses into the host cell and binds next to the active site of RT which leads to a conformation change and inhibits the enzyme's function. It is also a non-competitive inhibitor of HIV RT with respect to template, primer or nucleoside triphosphates.	Central nervous system symptoms (vivid dreams, problems with concentration, dizziness, confusion, mood disturbance, psychosis), rash, hepatitis, gynaecomastia.	Rilpivirine (RPV), nevirapine (NVP) – If EFV; RPV and NVP are contraindicated, raltegravir (RAL) or a PI can be substituted.

[†]Life-threatening reactions are included in **bold**. M_r (molecular weight); ADR₇(adverse drug reaction); mg (milligram); g (gram); mol (mole); RT (reverse transcriptase); kg (kilogram).

1.5 HIV, ART and ED/CVD

It has been established that the prevalence of CVD is augmented in HIV positive patients compared with the general population (Masiá et al., 2007), with recent studies showing the relative risk of developing CVD as high as 61% higher in HIV positive populations compared to uninfected people (Islam, Wu, Jansson, & Wilson, 2012). Factors associated with HIV infection and ART have been implicated in the premature development of atherosclerosis and coronary heart disease (CHD) (Masiá et al., 2007). CVD is the leading comorbidity and cause of death in this population (DAD Study Group, 2007; Thienemann et al., 2013), where ED is thought to be the main link between HIV infection, ART and CVD and atherosclerosis (Francisci et al., 2009), amongst other factors (Table 1.5) (de Larrañaga, Petroni, Deluchi, Alonso, & Benetucci, 2003; Wolf et al., 2002). It has been reported that enhanced oxidative stress in HIV infected patients may contribute to ED, while it has also been shown that ART and therapeutic control of HIV replication induces a pro-oxidative state (Day & Lewis, 2004; Hulgan et al., 2003).

Table 1.5: Mechanisms by which HIV and ART may adversely affect the vasculature (Dube et al., 2008).

HIV infection	ART
Endothelial dysfunction	Endothelial dysfunction
Lipid disorders associated with HIV infection	Increased endothelial permeability
Viral protein-related EC activation	Increased oxidative stress
Systemic inflammatory cytokine-chemokine dysregulation	Increased mononuclear cell adhesion
Direct HIV infection of endothelium and VSMCs	Insulin resistance
Enhanced atheroma formation by activated macrophages	Accelerated lipid accumulation in vessel wall
Prothrombotic state	Persistent inflammation and immune activation
	Impaired response to vascular injury

However, it is still debated whether cardiovascular complications are a consequence of the HIV infection itself or due to the long-term use of ART (Francisci et al., 2009). Certain studies have shown that it may be the ART that is responsible for the increased risk for CVD (Obel et al., 2007), with one study in particular showing that the risk of CVD for people living with HIV receiving ART was found to be two times greater than the risk for HIV positive patients who were treatment-naïve (Islam et al., 2012). Other studies contest this evidence, suggesting HIV infection itself and not ART is the pathological initiator (Baker et al., 2011; Francisci et al., 2009). The Strategies for Management of Anti-Retroviral Therapy (SMART) study, showed that persons undergoing episodic ART had an increased risk of cardiovascular events identical to that of patients undergoing continuous therapy (Strategies for Management of Antiretroviral Therapy (SMART) Study Group, 2006). Some studies have even shown that ART actually has a protective role in terms of risk for ED and CVD (Arildsen, Sørensen, Ingerslev, Østergaard, & Laursen, 2013; Francisci et al., 2009; Grubb et al., 2006; Solages et al., 2006; Torriani et al., 2008; Wolf et al., 2002), suggesting rather that viral load, CD4+ cell count and cardiovascular risk factors are responsible for the endothelial function impairment observed in other studies (van Wijk et al., 2006; Wolf et al., 2002). It is important to note however, that most studies showing a cardioprotective role for ART, were performed in treatment-naive patients, initiating short term ART treatment (up to 24 weeks) (Torriani et al., 2008). Therefore it is uncertain if the improvements were due to ART, suppression of viremia, or changes in immune activation (Torriani et al., 2008). Unfortunately, it is still unclear how to distinguish the effects of a chronic HIV infection from those of ART (Skowrya, Zdziechowicz, Mikula, & Wiercińska-Drapało, 2012), making a consensus more difficult to obtain.

1.5.1 ART induced ED/CVD

Although ART has dramatically reduced HIV-associated morbidity and mortality (Jiang et al., 2007), life-long treatment may expose patients to an increased risk for developing CVD (DAD Study Group, 2007; SMART study group, 2006). With recent consensus guidelines recommending the initiation of ART as early as possible in the course of HIV infection, the average duration of exposure to ART is increasing, and therefore complications associated with treatment are also expected to become more common (Choi et al., 2011). Despite all the confounding reports, the vast majority of trials indicate that ART can lead to ED (Skowrya et al., 2012). Cardiovascular complications are considered a new challenge for HIV patients receiving ART with numerous studies investigating the effects of ART on the

vasculature indicating that ART may impair the function of the vascular endothelium (Blanco et al., 2006; Shankar, Dubé, Gorski, Klaunig, & Steinberg, 2005; Stein et al., 2001). The Data Collection on Adverse Events of Anti-HIV Drugs (DAD) study group reported that ART was associated with a 26% increase in the rate of myocardial infarction (MI) per year of exposure to ARV drugs (DAD Study Group, 2007). This finding led to the theory that duration of exposure to ART may be one of the main factors associated with risk of developing CVD, which has been confirmed in other studies (Islam et al., 2012).

The major underlying mechanism is thought to be ART-induced NO serum level reduction, as well as increased ROS and cholesterol (Skowrya et al., 2012). ART-induced ROS production is thought to be of mitochondrial origin, likely resulting from mitochondrial dysfunction and leakage of electrons from a dysfunctional mitochondrial electron transport chain (Jiang et al., 2007). There is controversy however; surrounding which ART class has the highest degree of associated risk of developing CVD.

1.5.1.1 Protease Inhibitors

The majority of studies investigating ART have demonstrated that PI's are associated with increased cardiovascular risk. PIs are thought to directly induce ED by damaging mitochondrial DNA of ECs (Skowrya et al., 2012). An early study documented severe ED in patients who received long-term, PI-based ART (mean duration of ART was 70 months, including 31 months of therapy with a PI) but not in those receiving ART without a PI (Stein et al., 2001). In contrast, another early observational study of hospitalisation rates in Northern California, Klein *et al.* (2002) found that PIs did not tend to increase the rates of hospitalisations for CHD among persons living with HIV. Increased risk of MI in HIV patients receiving PI-based ART has been reported by multiple cohorts (DAD Study Group, 2007; Holmberg et al., 2002; Lang et al., 2010). Yeboah *et al.* (2007) demonstrated that the administration of a PI impaired endothelial function in healthy men, while several other studies have identified cellular or molecular mechanisms of ED associated with the use of PIs (Grubb et al., 2006; Wang, Chai, Yao, & Chen, 2007; Zhong et al., 2002). Clinical and experimental models have shown that PI-induced ED appears to be mediated by reduced NO production (Shankar et al., 2005), due to reduced expression of eNOS (Fu, Chai, Yao, & Chen, 2005) and increased ROS (Dube et al., 2008).

1.5.1.3 Nucleoside Reverse Transcriptase Inhibitors

More recent studies have also implicated NRTI-based ART in playing a damaging role (Carr, 2003; Choi et al., 2011; Gallant, Parish, Keruly, & Moore, 2005; Jiang et al., 2007; Sutliff et al., 2002; Young et al., 2007), with far less literature being available regarding the specific effects of NNRTI-based ART (Hulgan et al., 2003; Stein et al., 2001). This is of particular relevance for South African first line ART, which is composed of two NRTIs and one NNRTI. NRTI-based ART use is also associated with an increased risk of CVD, but not to the same extent as PI-based ART (Islam et al., 2012). Mitochondrial toxicity is recognised as the most common side effect of NRTIs (Sutliff et al., 2002), and is associated with the development of a number of tissue-specific complications (Lewis & Dalakas, 1995). Mitochondrial dysfunction is thought to be the result of two interrelated pathophysiological mechanisms that result from defective oxidative phosphorylation, namely increased production of mitochondrial ROS and reduced energy production (Lewis, Copeland, & Day, 2001). Furthermore, the production of free radicals has been implicated in mitochondrial DNA damage and dysfunction in ECs (Ballinger et al., 2000). A study by Sutliff *et al.* (2002) demonstrated that NRTIs profoundly impaired endothelium-dependent relaxation in murine aortas, with increased O_2^- levels being implicated as the mediator of these adverse effects. This finding has been supported by numerous other studies that have found a link between NRTI toxicity and increased free radical levels (de la Asuncion et al., 1998; Jiang et al., 2007; Jiang, Hebert, Zavec, & Dugas, 2006). Together, these mechanisms are thought to be responsible for the association of NRTI's with accelerated vascular disease such as platelet activation, hyperlipidemia, T-lymphocyte activation, abnormal endothelial function and vascular inflammation (Choi et al., 2011). In contrast, a recent meta-analysis of clinical trial studies found that NRTIs were not associated with a greater risk of MI or major CVD events, despite reports from other cohort studies (Cruciani et al., 2011).

It is important to note that majority of the studies reported in the literature are conducted using one or two specific PIs or NRTIs. Therefore one should be wary when making conclusions, since adverse effects discovered in a particular drug should not generally be considered representative of the entire drug class (Dube et al., 2008). It is thus very important to expand the literature and report findings on all ARV drugs currently in use, and in all the different classes of ART.

1.6 Melatonin

Melatonin is a hormone found in all vertebrates, and almost ubiquitously present in bacteria, protozoa, plants, fungi and invertebrates (Hardeland & Poeggeler, 2003). It is rhythmically secreted by the pineal gland, and involved in regulation of circadian and, sometimes, seasonal rhythms (Reiter, 1993). Melatonin is an indoleamine, which contributes to its amphiphilicity, which means it has the ability to enter any cell, compartment or body fluid (Hardeland, Pandi-Perumal, & Cardinali, 2006). During melatonin synthesis, its precursor tryptophan, is taken up from the blood and converted, via 5-hydroxytryptophan, to serotonin. Serotonin is then acetylated to form *N*-acetylserotonin by arylalkylamine *N*-acetyltransferase (AA-NAT), which, in most cases, represents the rate-limiting enzyme. *N*-acetylserotonin is then converted into melatonin by hydroxyindole *O*-methyltransferase (Fig 1.15) (Pandi-Perumal et al., 2006; Sprenger, Hardeland, Fuhrberg, & Han, 1999).

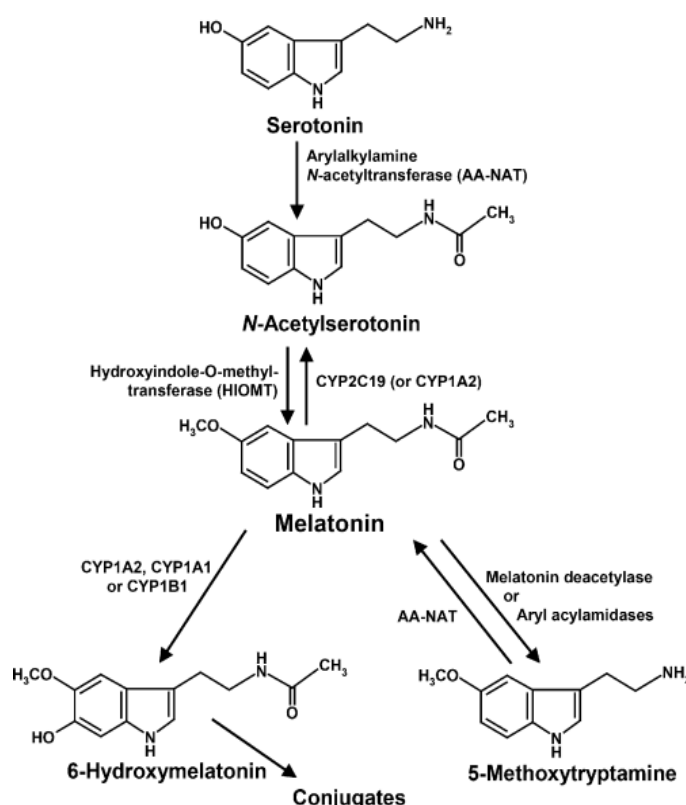


Figure 1.15: Pathways of indolic catabolism involved in the formation of melatonin (Pandi-Perumal et al., 2006).

Pineal melatonin production exhibits a circadian rhythm, with a low level during daytime and high levels during night (Pandi-Perumal et al., 2006). Melatonin is able to retrain the circadian rhythm through its short biological half-life, whereby serum levels of approximately 0.4 nM peak at night (Brzezinski, 1997). This circadian rhythm persists in most vertebrates, irrespective of whether the organisms are active during the day or during the night (Borjigin, Li, & Snyder, 1999; Claustrat, Brun, & Chazot, 2005). Other than regulation of circadian rhythms, melatonin also appears to play a role in immunomodulation, reproduction, tumor growth, and aging (Brzezinski, 1997). Most importantly, melatonin has also been shown to exhibit strong antioxidative properties (Hardeland et al., 2006).

1.6.1 Antioxidant Actions

Melatonin has been reported to have both direct and indirect antioxidant properties (Fig 1.16) (Bonfont-Rousselot & Collin, 2010; Hardeland, 2005; Tan et al., 2002). Direct antioxidant properties of melatonin include the scavenging of ROS (Poeggeler et al., 2002), while indirectly, melatonin upregulates antioxidant enzymes (Hardeland, 2005). The antioxidant activity of melatonin has been reported at both physiological and pharmacological concentrations (Galano, Tan, & Reiter, 2011; Reiter, Tan, & Maldonado, 2005), although pharmacological doses of exogenously administered melatonin typically provide greater protection from large quantities of free radicals (Tan, Manchester, Terron, Flores, & Reiter, 2007). As a whole, the antioxidant properties of melatonin suggest that it could have significant potential in treating chronic diseases associated with oxidative stress (Fig 1.16).

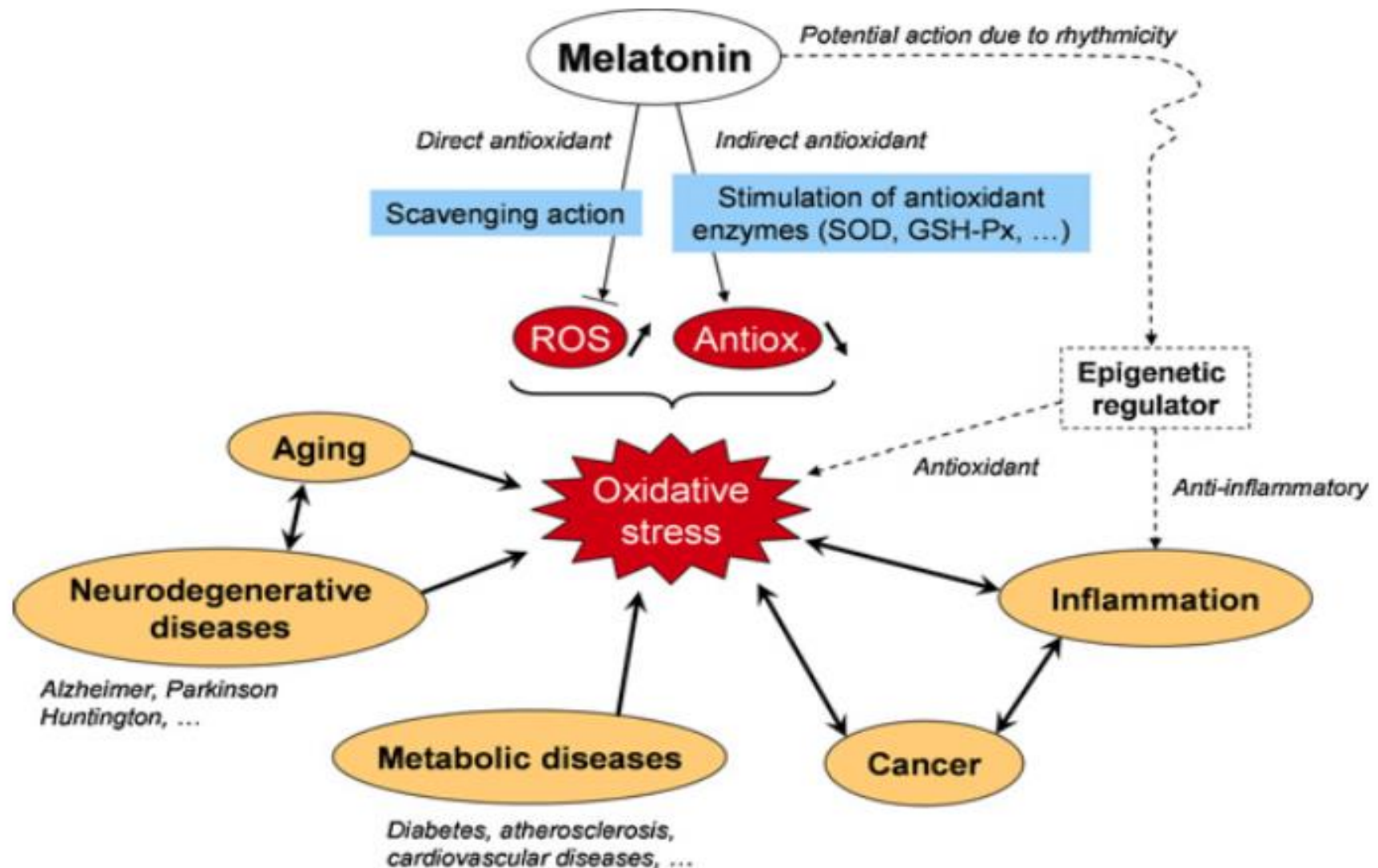


Figure 1.16: Direct and indirect actions of melatonin in an antioxidative capacity (Bonnefont-Rousselot & Collin, 2010). Directly, melatonin acts as an antioxidant, where it has the ability to directly neutralise reactive species. Indirectly, melatonin up-regulates other antioxidant enzymes that in turn, are capable of removing various reactive species. GSH-Px (glutathione peroxidase); ROS (reactive oxygen species); SOD (superoxide dismutase).

1.6.1.1 Free radical Scavenging

There is a vast amount of literature documenting melatonin's ability to directly scavenge both ROS and RNS (Allegra et al., 2003; Poeggeler et al., 2002; Reiter, Tan, Manchester, & Qi, 2001; Tan et al., 2002). Specific species removed by melatonin include OH^\cdot , H_2O_2 , singlet oxygen, O_2^\cdot , NO and ONOO^\cdot .

Melatonin is able to neutralise OH^\cdot by trapping OH^\cdot in one of its indole rings (Tan et al., 2002). H_2O_2 and singlet oxygen - an energy-rich form of O_2 - are thought to be removed through their reaction with melatonin in the presence of the substrate *N*1-acetyl-*N*2-formyl-5-methoxykynuramine (AFMK) (Tan et al., 2000), although this has only been demonstrated in a pure chemical system and whether intracellular melatonin neutralizes H_2O_2 in this manner is unknown (Reiter et al., 2003). Surrounded by more uncertainty, is the efficacy of melatonin in neutralizing the O_2^\cdot , which is poorly defined, and still particularly unclear *in vivo*. Far more is known regarding melatonin's interaction with NO. Blanchard *et al.* (2000) initially showed that melatonin is only capable of interacting with NO in the presence of O_2 , suggesting that melatonin may rather react with a molecule derived from NO, possibly ONOO^\cdot (Reiter et al., 2003). See Table 1.6 for a summary.

1.6.1.2 Antioxidant Upregulation

Antioxidant enzymes represent a first line of defence against toxic oxidant reactants by metabolizing them to innocuous by-products (Rodriguez et al., 2004). The main antioxidant enzymes upregulated by melatonin are superoxide dismutase (SOD), catalase (CAT), glutathione peroxidase (GPx), glutathione reductase (GRd) and tripeptide glutathione (GSH) (Bonfont-Rousselot & Collin, 2010; Hardeland, 2005; Hung et al., 2013; Tengattini et al., 2008).

As previously mentioned on page 13, SOD converts O_2^\cdot to H_2O_2 , thereby decreasing the formation of ONOO^\cdot (Mudau et al., 2012). SOD works in conjunction with other antioxidant enzymes such as CAT and GPx, which are also capable of removing H_2O_2 . (Tengattini et al., 2008). CAT promotes the conversion of H_2O_2 to H_2O and O_2 , while GPx converts peroxides to H_2O using GSH as a substrate (Valko, Rhodes, Moncol, Izakovic, & Mazur, 2006). Melatonin further facilitates this reaction by maintaining high intracellular levels of GSH. Besides upregulating antioxidants, melatonin can also downregulate pro-oxidative enzymes like NOS, which in turn decreases NO production, and decreases the amount of NO available to react with O_2^\cdot , ultimately decreasing ONOO^\cdot levels (Aydogan, Yerer, &

Goktas, 2006; Karbownik & Reiter, 2000). All these effects of melatonin are summarised in Table 1.6 and Figure 1.17 below.

This regulation of antioxidants and oxidants by melatonin is controlled through messenger-ribonucleic acid (mRNA) (Hung et al., 2013). When melatonin binds to its receptor, it stimulates the phospholipase C pathway. The consequent increase in calcium concentration leads to the phosphorylation of protein-kinase C (PKC). PKC activates protein/activation transcription factor cAMP responsive element binding protein and activating transcription factor (CREB-ATF) (Tengattini et al., 2008). This pathway modulates immediate early gene transcription and consequently gene transcription regulation and antioxidant enzyme levels.

The effects of melatonin on the mitochondria has become another recent research focus. It is well established that the opening of the mitochondrial permeability transition pore (mtPTP) causes mitochondrial swelling and rupture of the outer mitochondrial membrane, leading to the release of pro-apoptotic factors such as cytochrome *c* (Petrosillo et al., 2009). Melatonin appears to have the ability to safeguard the respiratory electron flux, reduce oxidant formation by lowering electron leakage, and inhibit the opening of the mtPTP (Hardeland, 2005). A study by Petrosillo *et al.* (2009) showed that melatonin treatment had the ability to completely inhibit mitochondrial cytochrome *c* release in the hearts of male Wistar rats during ischemia-reperfusion. The same study also found that melatonin treated hearts were also less sensitive to mtPTP opening, demonstrating overall the protective effect of melatonin through inhibiting the opening of the mtPTP.

Table 1.6: Effects of melatonin on ROS/RNS and oxidant enzymes (Tengattini et al., 2008). ROS (reactive oxygen species); RNS (reactive nitrogen species); ↓ (decrease); ↑ (increase).

Action	Target		Effect
Scavenging	ROS	Hydrogen peroxide	↓
		Hydroxyl radical	↓
		Singlet oxygen	↓
	RNS	Nitric oxide	↓
		Peroxynitrite anion	↓
Up-regulation	Antioxidant enzymes	Superoxide dismutase	↑
		Catalase	↑
		Glutathione peroxidase	↑
		Glutathione reductase	↑
		Tripeptide glutathione	↑
Down-regulation	Pro-oxidative enzymes	Nitric oxide synthase	↓

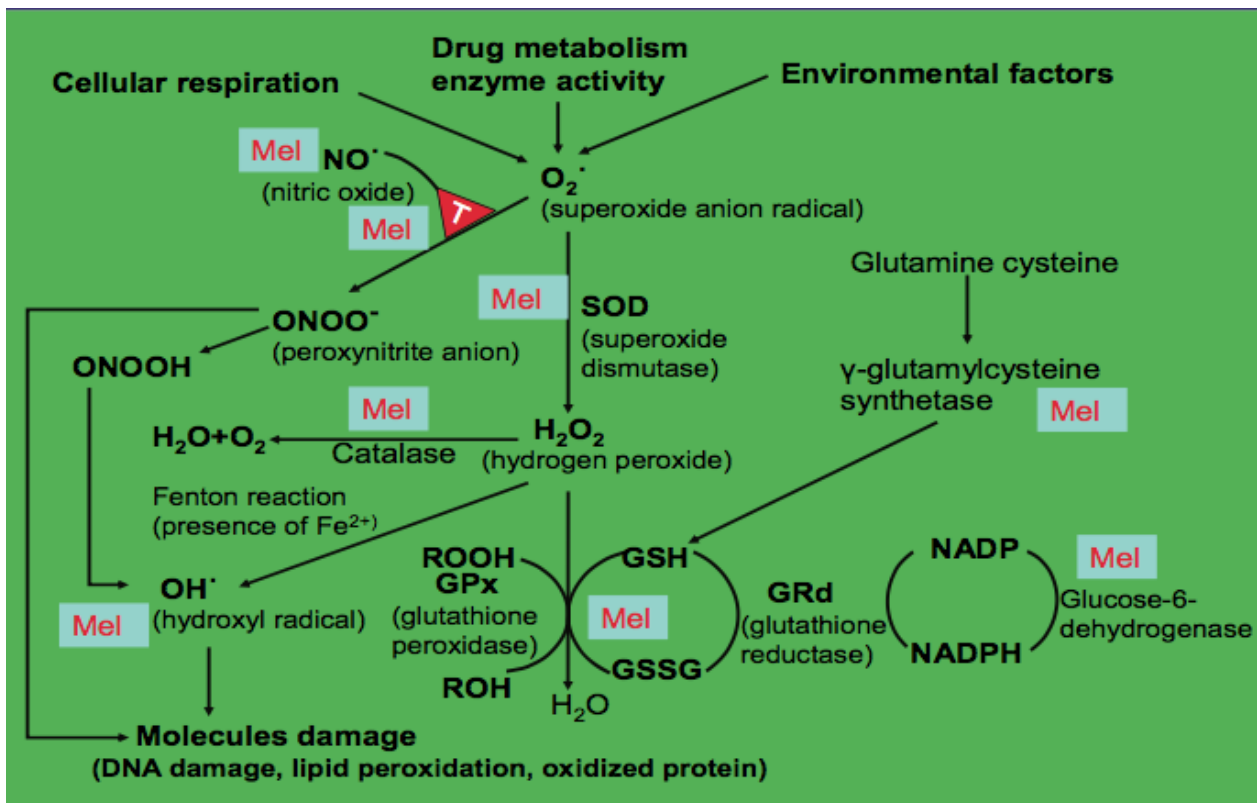


Figure 1.17: Oxidative stress and sites of action of melatonin (Kücükakin, Gögenur, Reiter, & Rosenberg, 2009; Nduhirabandi, 2010). NADP (nicotinamide adenine dinucleotide phosphate); NADPH (the reduced form of NADP); GSH (reduced glutathione); GSSG (glutathione disulfide).

1.6.2 Melatonin in ART induced ED

As discussed earlier, it has been established that the main cause of ART induced ED is oxidative stress due to excessive generation of ROS and RNS, and an imbalance in anti- and pro-oxidative substances. For these reasons, it has been suggested that the treatment or prevention of ART induced ED might be achieved through the use of antioxidants (Dube et al., 2008). A study by De la Asuncion *et al.* (1998) showed that treatment with antioxidant vitamins significantly reduced the development of NRTI-mediated cardiac myopathies, while on the other hand, other studies have shown antioxidant vitamins to have no effect (Sutliff et al., 2002), while the clinical use of antioxidants to ameliorate ED in patients receiving ART is not well documented (Dube et al., 2008). Therefore, more research is needed in order to determine whether antioxidants other than vitamins can be effective in combating ART induced ED.

Melatonin is the optimal antioxidant since it has both the capacity to scavenge radicals as well as upregulate other antioxidants and down-regulate pro-oxidative enzymes (Bonfont-Rousselot & Collin, 2010; Hardeland, 2005; Tan et al., 2002). Melatonin is a

particularly favourable putative therapeutic agent for the treatment of ART induced ED since it has the ability to cross physiological barriers and enter cells, unlike other antioxidants whose actions are limited because of their solubility that limits their partitioning between intra- and extra-cellular compartments (Bonnefont-Rousselot, Collin, Jore, & Gardès-Albert, 2011). Melatonin also offers protection against radical-induced mitochondrial damage, which is an important attribute considering mitochondria have been implicated as one of the main sources of ART-induced ROS generation (Jiang et al., 2007; Lewis et al., 2001). Melatonin has the ability to inhibit the mitochondrial production of superoxide anion and hydrogen peroxide that directly activates the mtPTP - a critical event in mitochondrial-mediated cell death (Bonnefont-Rousselot et al., 2011). The inhibition of the mitochondrial production of O_2^- and H_2O_2 by melatonin has been shown to maintain the efficiency of oxidative phosphorylation and ATP synthesis while increasing the activity of the respiratory complexes (López et al., 2009). Therefore, in theory, melatonin has promising potential as a therapeutic agent, which can be co-administered with ART, however, further research is needed.

1.7 Conclusion

The wide spread use of ART has dramatically reduced HIV/AIDS related morbidity and mortality. With the early commencement of ART, patients are spending longer periods of their lives on these drugs, and due to ART-associated increased life expectancy of these patients, there is a large population of people currently living with HIV, receiving ART. It has been established that long-term or life-long exposure to ART has been associated with increased risk of developing ED. ED is a critical factor in the initiation and of progression CVD, but with early detection and treatment, ED can be reversed. The underlying mechanisms of ART induced ED are still unclear, but the main cause seems to be increased levels of ROS/RNS resulting in oxidative stress and damage. It has been proposed that antioxidant treatment could be a potential solution; with melatonin possessing all the desired properties needed to reduce and potentially reverse ART induced ED. However, literature documenting the specific relationship between melatonin and ART treatment is scarce, and therefore further research is required.

1.8 Problem Identification and Study Aims

1.8.1 Problem Identification

There is a substantial amount of literature documenting the relationship between HIV, ART and ED (Day & Lewis, 2004; Francisci et al., 2009; Masiá et al. 2007). These studies are limited by the inherent difficulty in differentiating between direct drug-based effects and potential HIV effects, secondary host immunological responses, or metabolism-mediated effects on the endothelium (Grubb et al., 2006). There is a lack of studies that investigate the effects of ART alone, with less than a hand-full of studies to date looking at the effects of South African first line FDC ART (EFV + FTC + TDF) on endothelial health (Charania, 2017; Imperial, 2017; Mashele et al., 2016). With the South African health authorities increasing the output and accessibility of ART, and the documented unfavorable effects of NRTI's in particular on the endothelium and cardiovascular system (Choi et al., 2011; Jiamg et al., 2007; Sutliff et al., 2002), it is important to assess this relationship. Since ART is a life-long therapy, it is important to find a potential co-treatment that will not interact with the effects of the ARV drugs themselves, as well as a therapy which can be used long term without any negative side effects. Melatonin meets these criteria, since it has the ability to target all the suggested mechanisms of ROS and RNS production caused by ART. Furthermore, melatonin is a naturally occurring hormone that has shown no toxicity, even at supra-pharmacological levels (Guardiola-Lemaitre, 1997; Tan et al., 2007). All these advantages of melatonin supplementation make the antioxidant hormone a preferential choice over other antioxidative supplements. Therefore, we propose that melatonin may have the potential to ameliorate potential endothelial damage caused by the first line FDC ART drug currently used in SA.

1.8.2 Main Study Aim

To investigate the effects of melatonin supplementation during first line FDC ART: an *in vitro*, *ex vivo* and *in vivo* approach.

1.8.2.1 Specific *in vitro* Study Objectives

- Determine the individual optimum concentrations of both melatonin and first line FDC ART treated aortic endothelial cells (AECs) at which the greatest differences are seen when compared to untreated AECs, with respect to:
 - NO production
 - RNS production

- Cell viability
- Use the optimum concentrations obtained in the dose-response experiments above, to treat AECs with melatonin and ART in combination, in order to analyse any potential synergistic/antagonistic interactions between the two drugs with respect to:
 - NO production
 - RNS production
 - Cell viability
- Examine various protein activation and/or expression levels of important vascular signalling molecules in Melatonin- and/or ART-treated AECs.
- Examine antioxidant capacity exhibited by Melatonin- and/or ART-treated AECs.

1.8.2.2 Specific *ex vivo* and *in vivo* Study Objectives

- Determine the acute effects of melatonin and ART administration on the vascular reactivity of untreated, control male Wistar rat aortas.
- Determine the chronic effects of melatonin and ART administration on the vascular reactivity of male Wistar rats that have been treated for 8 weeks with melatonin and/or ART.
- Examine various protein activation and/or expression levels of important vascular signalling molecules in the aortic tissue of male Wistar rats that were treated for 8 weeks with melatonin and/or ART.
- Examine antioxidant capacity exhibited in the aortic tissue of the rats subjected to the same treatment as above.

2 - Materials and Methods: *In vitro* studies

Chapter 2 contains the materials and methods used for the *in vitro* aortic endothelial cell (AEC) culture experiments. The results for these studies can be found in Chapter 4.

2.1 Aortic Endothelial Cell Culture

For all cell culture experiments, a sample size of 1 was considered as an experiment conducted on a single day with a single batch of cells (biological replicate). The cells of the single experiment ($n = 1$) were divided amongst different plates and randomly subdivided into the various treatment groups (2 - 3 plates per treatment group = technical replicates). The mean value of the technical replicates constitutes the value for a single sample ($n = 1$). This process was then repeated on a different day with a new batch of cells in order to increase the sample size. A sample size of 3 – 4 biological replicates ($n = 3 - 4$) was considered sufficient, since it is the standard sample size optimised and used by our laboratory (Genis, 2014; Mudau; 2012; Strijdom et al., 2008), as well as used in other publications using aortic endothelial cells (Fulton et al., 2002; Mondal et al., 2013).

2.1.1 Materials

- AECs (adult rat): Purchased from *VEC Technologies* (University at Albany Foundation, 1 University PI, Rensselaer, NY 12144, USA).
- Endothelial cell growth medium (EGM-2): *Lonza Ltd* (Clonetics, Cambrex Bio Science, Walkersville, USA) (supplied by Whitehead Scientific locally).
- Attachment factor and trypsin (500 BAEE units' trypsin / 180 μ g EDTA•4Na per ml in Dulbecco's PBS): *Life Technologies* (Carlsbad, California, USA).
- Foetal bovine serum (FBS): *Biochrom-Biotech*.
- Dimethyl sulfoxide (DMSO): *Sigma-Aldrich* (St Louis, Mo, USA).

2.1.2 Passaging

Pure primary adult rat AECs were received from the USA in culture in 75 cm³ flasks and further grown in EGM-2 growth medium in our own laboratory until fully confluent. EGM-2 growth medium was supplemented with 10% FBS; heparin; long chain human insulin-like growth factor (R³-IGF-1); recombinant human epidermal growth factor (rhEGF); antibiotic GA 1000 (contains gentamicin and amphotericin); vascular endothelial growth factor (VEGF); ascorbic acid; recombinant human fibroblastic growth factor B (rhFGF-B) and

hydrocortisone in accordance with the manufacturer's instructions. The cells were grown in a standard tissue culture incubator (Forma Series II, Thermo Electron Corporation, Waltham, MA, USA) at 37 °C in a 40 – 60% humidified, 5% CO₂ atmosphere, and received fresh medium every second day. The primary AECs were grown to various "Parent (P)-generations" (see Figure 2.1) and then suspended in a freezing medium (90 % FBS, 5 % growth medium and 5 % DMSO) and stored in liquid nitrogen for future use. Cultures between the 4th and 7th generation were used for experiments. These parent cells were removed from liquid nitrogen, allowed to thaw and given fresh medium. Once the new cultures reached confluency, the cells were washed with phosphate-buffered saline (PBS) and incubated with pre-warmed (37 °C) trypsin until cells detached from the bottom of gelatin-containing attachment factor-coated 35 mm petri dishes (approximately 3 minutes). Using a 1 ml pipette, the detached cells were then rapidly transferred to a 15 ml conical tube containing fresh growth media, which deactivates the trypsin and prevents the cells from lysing. The tube containing the cells was then centrifuged for 3 minutes at 1000 revolutions per minute (rpm). The supernatant was aspirated and pellet re-suspended in fresh growth medium. The media containing the cells was then split between new 35 mm petri dishes that had been pre-incubated with attachment factor for at least 1 hour prior to the passage. Passaging to the next generation was performed at a 1:2 ratio. A summary of the passaging process can be found in Figure 2.1.

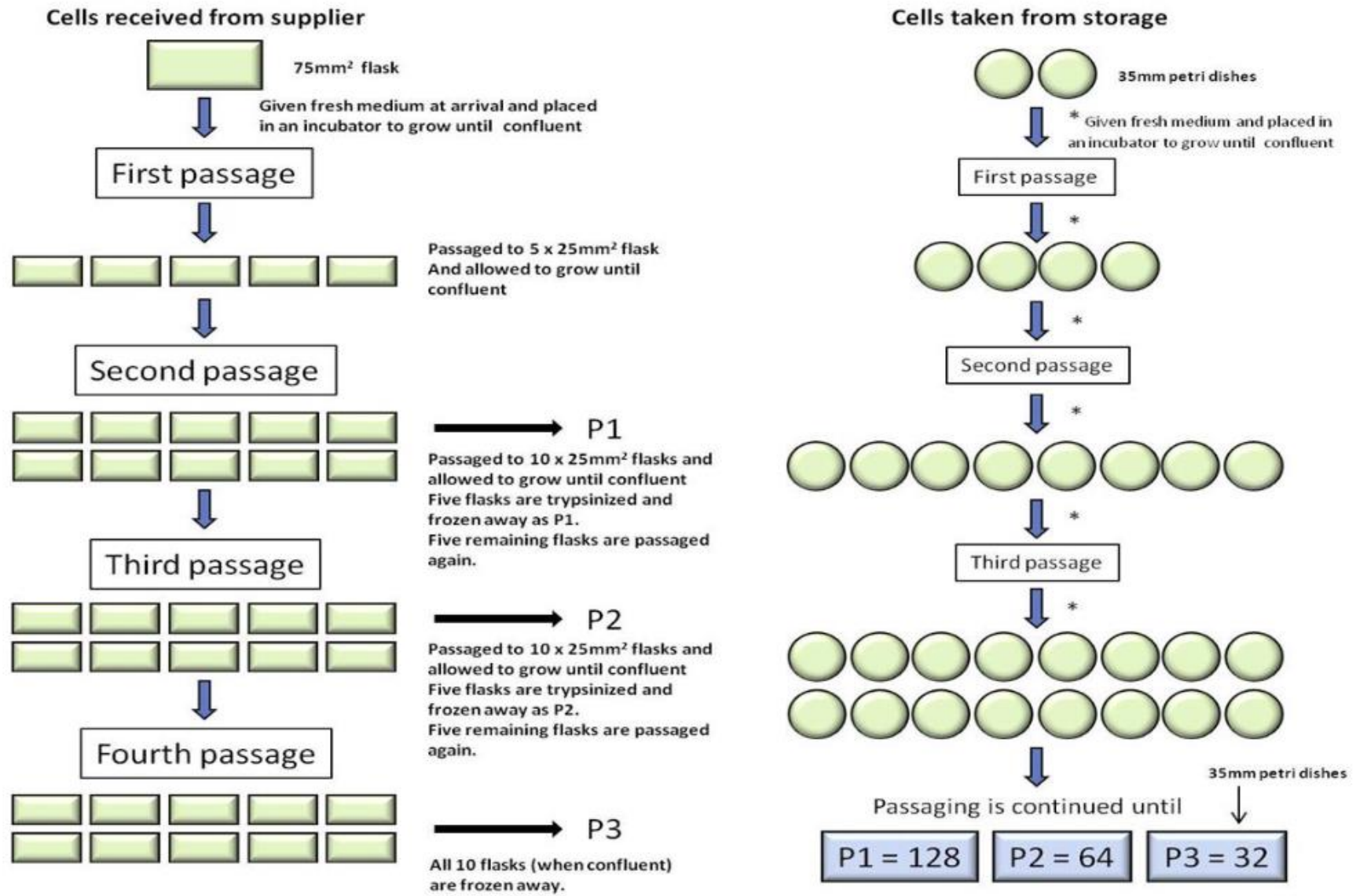


Figure 2.1: Passaging and cell aliquot storage procedures (Genis, 2014).

2.2 Experimental Groups and Protocols

All experiments were performed on confluent cells. The close cell-to-cell contact minimises possible cell cycle variability when evaluating experimental results. The cells remain morphologically and functionally viable, however since they enter cell-cycle arrest, they are no longer proliferative. For all cultures, petri dishes were randomly assigned to respective control and experimental groups. Cells were serum starved before being treated in order to induce cell cycle synchronization, which enhances the cells' responses to experimental treatment (Gerber et al., 1998; Russell & Hamilton, 2014), in otherwise healthy cells. For cells to be serum starved, they were incubated in medium containing 0 % FBS for 24 hours prior to treatment with the various drugs.

2.2.1 Melatonin and Vehicle

For melatonin dose-response experiments, 23.2 mg of melatonin (*Sigma Aldrich*, St Louis, MO, USA) was dissolved in 150 μ l methanol (MeOH) vehicle. This solution was further dissolved in a total volume of 10 ml by adding 9.850 ml of distilled water (dH₂O), thus creating a 10 mM melatonin stock. The 10 mM melatonin stock was further diluted in dH₂O to make various concentrations. Freshly made melatonin stock was used for every experiment, just before treatment. Since melatonin is highly light sensitive, the lights were always turned off during preparation, dilution and treatment with melatonin. All tubes containing melatonin were also covered in tin foil for extra protection from the light. Vehicle preparations followed the same protocol as melatonin preparation, with the omission of melatonin.

Melatonin dose-response experiments consisted of the following groups:

- Absolute Control (AC)
 - The AC group is a control group that does not receive any fluorescent probe and therefore represents the auto-fluorescence of cells.
- Control (C)
 - The C group in an untreated group where normal media is added to the plate, and the plate is kept in the same conditions as the treated plated over the treatment period.
- Positive Control (+C)
 - The +C group is treated with a product that is known to induce the expected effect and therefore validates the experimental procedure.
- 1 nM Melatonin (1 nM Mel)
- 1 nM Vehicle (1 nM Veh)
- 1 μ M Melatonin (1 μ M Mel)
- 1 μ M Vehicle (1 μ M Veh)
- 10 μ M Melatonin (10 μ M Mel)
- 10 μ M Vehicle (10 μ M Veh)

Refer to **Appendix A** for detailed melatonin and vehicle concentration calculations.

2.2.2 ART and Vehicle

South African first line FDC ART consists of three individual ARV drugs, namely efavirenz (EFV), emtricitabine (FTC), and tenofovir (TDF). For experimental purposes, drugs were purchased in their individual ARV form from *SantaCruz Biotechnology* (WhiteHead Scientific in SA). The drugs were received in 10 mg powder form and dissolved in various solvents/vehicles.

For ART dose-response experiments, three concentrations were chosen for each individual ARV component (EFV: 5 μ M; 8 μ M; 12 μ M, FTC: 5 μ M; 7.5 μ M; 10 μ M, TDF: 80 nM; 400 nM; 1 μ M). The various concentrations were chosen based on literature documenting the use of these specific ARV drugs in cells and rats (Bertrand & Toborek, 2015; Borroto-Esoda, Vela, Myrick, Ray, & Miller, 2006; Bousquet, Pruvost, Guyot, Farinotti, & Mabondzo, 2009; De Pablo et al., 2012; Glover et al., 2014; Jamaluddin, Lin, Yao, & Chen, 2010). The average serum concentration found in humans after taking the recommended dose of the relevant individual ARV drug was also taken into consideration when deciding on the final concentrations (Kearney, Flaherty, & Shah,

2004; Luber et al., 2010; Molina et al., 2004; Villani et al., 1999). The three concentrations were either classed as a low, mid or high concentration for the purposes of this study. For experimental treatment, the individual ARV drug components (EFV; FTC and TDF) were combined to form a drug cocktail similar to the first line FDC ART drug regimen. The three drugs were combined in such a way that the low concentration of each individual ARVs were combined to form one low concentration FDC ART regimen. The same was applied for the mid and high concentrations (Fig 2.2). See below for the specific concentrations used in the low, mid and high concentration groups.

ART dose-response experiments consisted of the following groups:

- Absolute Control (AC)
 - The AC group is a control group that does not receive any fluorescent probe and therefore represents the auto-fluorescence of cells.
- Control (C)
 - The C group is an untreated group where normal media is added to the plate, and the plate is kept in the same conditions as the treated plates over the treatment period.
- Positive Control (+C)
 - The +C group is treated with a product that is known to induce the expected effect and therefore validates the experimental procedure.
- Low concentration ART (Low ART)
- Low concentration Vehicle (Low Veh)
- Mid concentration ART (Mid ART)
- Mid concentration Vehicle (Mid Veh)
- High concentration ART (High ART)
- High concentration Vehicle (High Veh)

Refer to **Appendix B** for detailed ARV and vehicle concentration calculations.

		Individual ARV Drugs				
		EFV	FTC	TDF		
Concentration Class	Low	5 μM	5 μM	80 nM	Combined	Low Concentration FDC ART
	Mid	8 μM	7.5 μM	400 nM	Combined	Mid Concentration FDC ART
	High	12 μM	10 μM	1 μM	Combined	High Concentration FDC ART

Figure 2.2: Individual ARV drug concentrations that were combined to make-up the three fixed dose combination ART treatment groups.

2.2.2.1 EFV

The 10 mg EFV powder was dissolved in 1.5 ml of MeOH vehicle to create an EFV stock solution (21.119 mM). This stock was then divided into 40 μl aliquots and frozen away at -20 °C until needed. For experiments, the required amount of aliquot was thawed and added in specific quantities to growth medium to yield the desired final concentration of ART. Vehicle preparations followed the same protocol, with the omission of the actual drug.

2.2.2.2 FTC

The 10 mg FTC powder was dissolved in 4 ml of dH₂O vehicle to create an FTC stock solution (10.111 mM). This stock was then divided into 65 μl aliquots and frozen away at -20 °C until needed. For experiments, the required amount of aliquot was thawed and added in specific quantities to growth medium to yield the desired final concentration of ART. Vehicle preparations followed the same protocol, with the omission of the actual drug.

2.2.2.3 TDF

The 10 mg TDF powder was dissolved in 40 ml of dH₂O vehicle to create TDF stock solution A (0.3934 mM). TDF stock solution A was then divided into 350 μl aliquots and frozen away at -20 °C until needed. For experiments, the required amount of aliquot was thawed, after which a stock solution B (50 μM) was made, in order to obtain the lowest concentration that TDF was used in. 127.1 μl TDF of stock solution A was added to 872.9 μl of dH₂O to create TDF stock solution B. Both stocks were added in specific quantities, where applicable, to growth medium to yield the desired final concentration of ART. Vehicle preparations followed the same protocol, with the omission of the actual drug.

2.2.3 Combined drugs and Vehicles

For the combination studies, one concentration of melatonin and one concentration level for ART was selected, based on dose-response results (See Chapter 4, sections 4.1.1 and 4.1.2). We chose to use 1 nM melatonin along with the high concentration ART, based on the fact that these concentrations resulted in the greatest change in the investigated variable (Fig 4.6; 4.13; 4.14 & 4.15). The same stock and vehicle preparation methods were used in the combination studies as was described above, to achieve the desired concentrations, with the combined vehicle containing a mixture of MeOH (for melatonin and EFV) and dH₂O (for FTC and TDF).

2.3 Plate Reader Analyses

2.3.1 Materials

- 4,5-diaminofluorescein-2/diacetate (DAF-2/DA): *Calbiochem* (San Diego, CA, USA).
- Dihydrorhodamine-1, 2, 3 (DHR-123): *Sigma-Aldrich* (St Louis, Mo, USA).
- Diethylamine NONOate diethylammonium salt (DEA/NO): *Sigma-Aldrich* (St Louis, Mo, USA).
- Propidium iodide (PI) solution: *Biochrom-Biotech* (San Diego, CA, USA).
- Authentic peroxyxynitrite: *Millipore* (Billerica, MA, USA)
- All other chemicals and buffer reagents: *Merck* (Damstadt, Germany).

2.3.2 Methods

At the final passage, AECs were re-seeded onto Vision Plates™ (clear bottom, black-walled 24-well plates) (*4titude*, Surrey, UK) and grown to confluency for experimentation. Upon the establishment of confluence, the cells were serum starved for 24 hours (see section 2.2) and treated with the various drugs. After 1- or 24-hours of drug treatment, the cells were rinsed with pre-warmed (37 °C) PBS and treated with the applicable fluorescent probe (in the dark). The fluorescence intensity was measured using a FLUOstar Optima microplate reader (*BMG Labtech*, Germany). Figure 2.3 A gives an example of an experimental layout of a single sample (n = 1) on a given day, while the general protocol followed for each experiment is summarised in Figure 2.3 B. Table 2.1 shows the specific excitation and emission wavelengths used on the microplate reader for the various

probes. Data generated by the microplate reader was stored and analysed with MARS Omega Data Analysis (software version 1.30; *BMG Labtech*, Germany).

Table 2.1: Excitation and emission wavelengths used for the various probes on the microplate reader

Settings	DAF	DHR	PI
Excitation	485	485	544
Emission	520	520	640

A

Cells are passaged to the appropriate

On the final passage, the cells are passaged

On establishment of confluence, the individual wells are spilt into the various treatment groups and treated. See below for an example of the layout used for treatment groups on a 24-well plate:

TG 1 (Tech. rep. #1)	TG 2 (Tech. rep. #1)	TG 3 (Tech. rep. #1)	VG 1 (Tech. rep. #1)	VG 2 (Tech. rep. #1)	VG 3 (Tech. rep. #1)
TG 1 (Tech. rep. #2)	TG 2 (Tech. rep. #2)	TG 3 (Tech. rep. #2)	VG 1 (Tech. rep. #2)	VG 2 (Tech. rep. #2)	VG 3 (Tech. rep. #2)
TG 1 (Tech. rep. #3)	TG 2 (Tech. rep. #3)	TG 3 (Tech. rep. #3)	VG 1 (Tech. rep. #3)	VG 2 (Tech. rep. #3)	VG 3 (Tech. rep. #3)
Absolute Control	Normal Control	Normal Control	Normal Control	Positive Control	Positive Control

Plate is treated with appropriate fluorescent probe

Plate is taken to the Plate reader for analysis

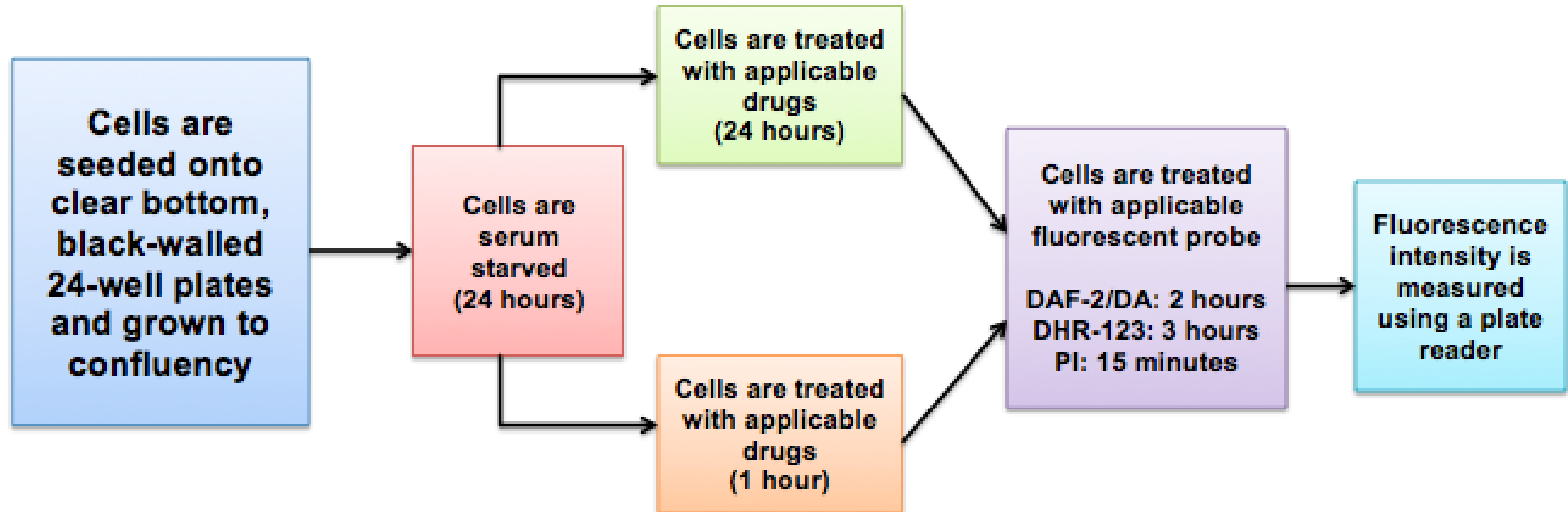
B

Figure 2.3: **A:** (Depicted above on pg 50) Example of an experimental layout used in plate reader studies. **B:** Summary of steps followed for each plate reader experiment.

2.3.2.1 NO Measurements – DAF

DAF-2/DA is a NO-specific fluorescent probe (Strijdom, Muller, & Lochner, 2004), which measures intracellular NO-production. Upon reacting with NO, DAF-2/DA is oxidized and emits a green fluorescence, which can be measured by the microplate reader. For cell treatment, DAF-2/DA was diluted with PBS to a final concentration of 10 μM , and then applied to the cells in the 24-well plate for 2 hours at 37 °C (Fig 2.4). After 2 hours, the DAF-2/DA-PBS supernatant was aspirated and the cells were washed once with PBS, and then covered in 500 μl PBS for microplate reader analysis.

Positive Control: DEA/NO

DEA/NO is a NO donor, and has previously been shown in our laboratory to be a consistent and reliable positive control for intracellular NO measured by DAF-2/DA. Designated positive control (+C) wells were first incubated with DAF-2/DA for 1.5 hours, before 100 μM DEA/NO was added for an additional period of 30 minutes. In other words, DEA/NO was added to the +C wells for the final 30 minutes of the 2-hour DAF-2/DA protocol (Fig 2.4 and 2.5).

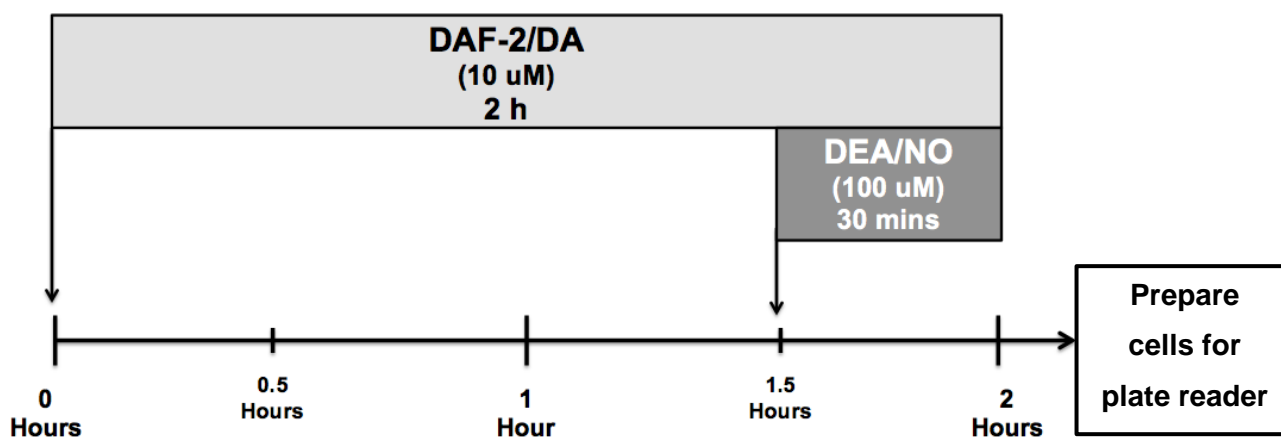
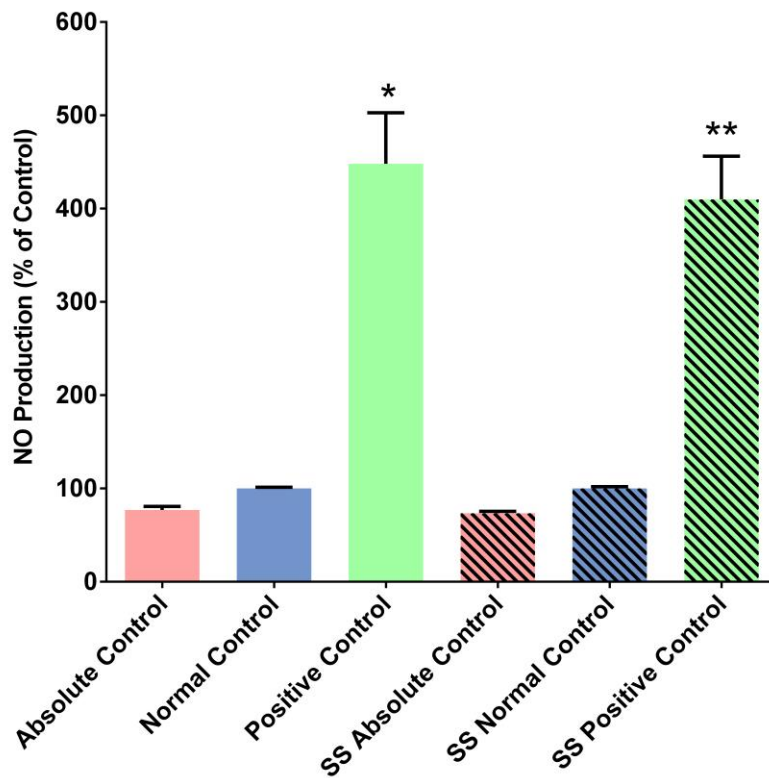


Figure 2.4: A schematic representation of the protocol used for treatment with DAF-2/DA and positive NO control, DEA/NO.



*: $p < 0.0001$ vs absolute control; normal control

** : $p < 0.0001$ vs SS absolute control; SS normal control

Figure 2.5: DEA/NO (100 μ M; 30 minutes) significantly increased mean DAF-2/DA fluorescence intensity compared to the normal control in non-serum starved samples and serum starved (SS) samples. DEA/NO was included as a positive NO control in all experiments ($n = 6$ / group). All values calculated as mean+SEM.

2.3.2.2 RNS Measurements – DHR

DHR-123 is an uncharged and non-fluorescent indicator of RNS (used as a marker of peroxynitrite in this study) (Tiede, Cook, Morsey, & Fox, 2012) that passively diffuse across the membrane, and is oxidized to form cationic rhodamine-123. Rhodamine-123 eventually localizes in the mitochondria and emits a green fluorescence that is detected by the microplate reader. For cell treatment, 2 μM DHR-123 was applied to the cells in the 24-well plate for 3 hours at 37 °C (Fig 2.6). The fluorescent probe was then washed out and further prepared as described in section 2.3.2.1.

Positive Control: Authentic peroxynitrite

Designated +C wells were first incubated with DHR-123 for 1 hour, before 100 μM peroxynitrite was added for an additional period of 2 hours. In other words, peroxynitrite was added to the +C wells for the final 2 hours of the 3-hour DHR-123 protocol (Fig 2.6 and 2.7).

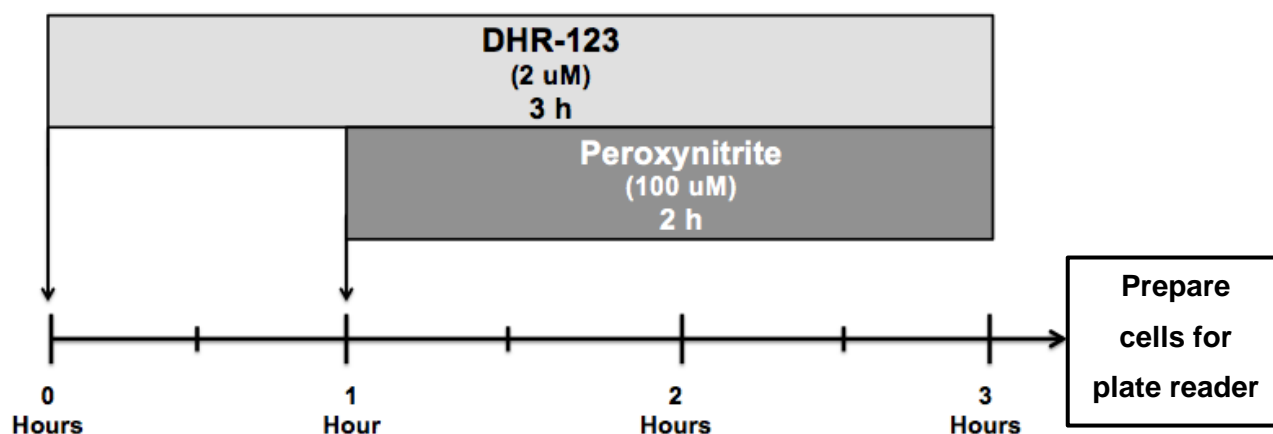
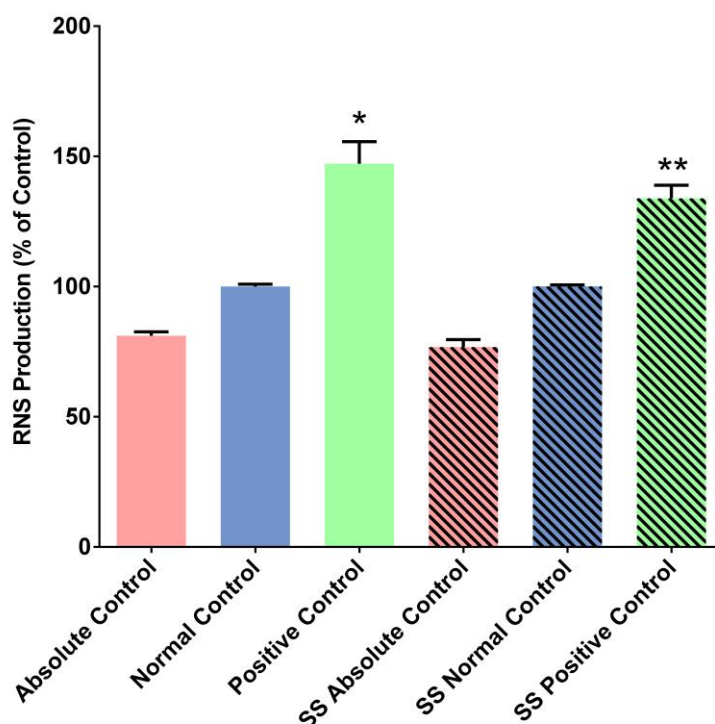


Figure 2.6: A schematic representation of the protocol used for treatment with DHR-123 and positive control, authentic peroxynitrite.



*: $p < 0.0001$ vs absolute control; normal control

** : $p < 0.0001$ vs SS absolute control; SS normal control

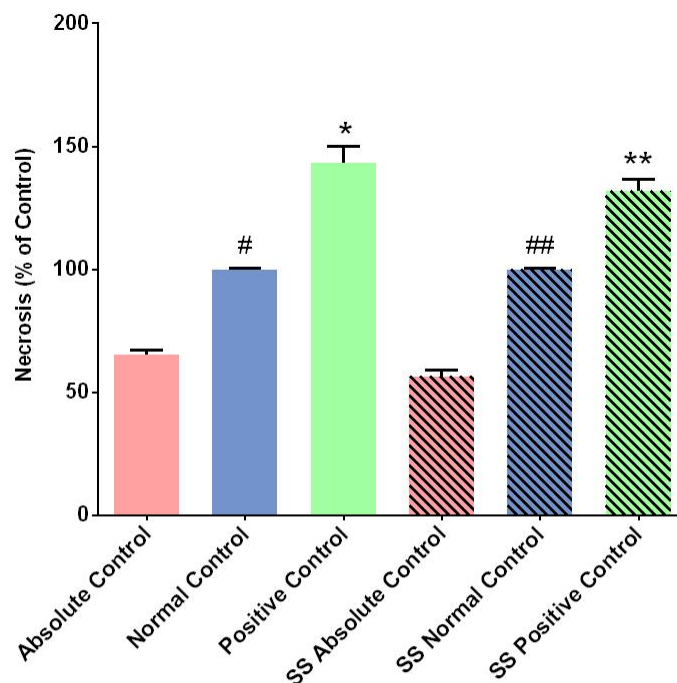
Figure 2.7: Peroxynitrite (100 μM ; 2 hours) significantly increased mean DHR-123 fluorescence intensity compared to the normal control in non-serum starved samples and serum starved (SS) samples. Authentic peroxynitrite was included as a positive control in all experiments ($n = 7$ / group). All values calculated as mean+SEM.

2.3.2.3 Cell Viability Measurements – PI

Cell viability was assessed through the measurement of necrosis. During necrosis, there is a loss in cell membrane integrity. PI is able to enter the nucleus following the cell's loss in membrane integrity and bind to the cell's DNA (Riccardi & Nicoletti, 2006), allowing for the measurement of necrosis (Wilkins, Kutzner, Truong, Sanchez-Dardon, & McLean, 2002). For cell treatment, PI was diluted with PBS to a final concentration of 5 μM , and then applied to the cells in the 24-well plate for 15 minutes at 37 $^{\circ}\text{C}$. After the 15-minute incubation period, PI was left on the plate and the cells were taken to the microplate reader for analysis.

Positive Control: dH₂O

When dH₂O is added to cells, it diffuses across a semi-permeable membrane from an area with low osmolarity (high H₂O concentration) to an area of high osmolarity (low H₂O concentration). Therefore the net result of treating cells with dH₂O is the movement of H₂O molecules over the cell membrane and into the cell. This subjects the cell to osmotic stress, which causes the cell to swell and eventually burst. Rupturing of the cell membrane due to necrosis allows the PI fluorescent probe to enter and stain the nucleus by intercalating with the DNA (Fig 2.8). Designated +C wells were treated with PI that was diluted in dH₂O, while all the other experimental group wells were treated with PI that was diluted in PBS.



*: $p < 0.0001$ vs absolute control; normal control
 **: $p < 0.0001$ vs SS absolute control; SS normal control
 #: $p < 0.0001$ vs absolute control
 ##: $p < 0.0001$ vs SS absolute control

Figure 2.8: dH₂O significantly increased PI staining compared to the normal control in non-serum starved samples and serum starved samples. dH₂O was included as a positive control in all experiments (n = 7/ group). All values calculated as mean+SEM.

2.4 Signalling Investigations – Western Blot Analyses

AEC western blot experiments consisted of the following groups:

- Control (Contains Combined Vehicle Only)
- 1 nM Melatonin + Combined Vehicle
- High concentration ART + Combined Vehicle
- ART + Melatonin + Combined Vehicle

Unlike the microplate reader experimental groups, western blot experimental groups all contained a combined vehicle. This allowed for all groups to be directly compared without considering a vehicle effect. The reason for this alteration was due to the space restrictions associated with western blot sample loading. Limited loading space meant we had to reduce the number of experimental groups in order to cater for an adequate sample size ($n = 5$ / group). The consequence of this alteration was that all melatonin and ART concentrations had to be re-calculated. Refer to **Appendix C** for detailed melatonin, ARV and vehicle concentration calculations. A protein concentration of approximately 4.62 – 7.11 $\mu\text{g}/\mu\text{l}$ was obtained from each petri dish.

2.4.1 Materials

- *Cell Signaling Technologies* (Beverly, MA, USA):
 - eNOS
 - phospho-eNOS (Ser 1177)
 - Cleaved caspase-3
 - Anti-rabbit immunoglobulin G, HRP- conjugated secondary antibody
- *Santa Cruz Biotechnologies* (Santa Cruz, CA, USA)
 - Nitrotyrosine
 - p22 PHOX
 - iNOS
- Clarity™ enhanced chemiluminescence (ECL) detection reagent: *Bio-Rad* (Hercules, CA, USA)
- Primary and secondary SingalBoost™ Immunoreaction Enhancer: *Millipore* (Billerica, MA, USA).
- PageRuler™ Prestained Protein Ladder: *Thermo Scientific* (Lithuania, EU)
- All other chemicals and buffer reagents: *Sigma-Aldrich* (St Louis, Mo, USA) and *Merck* (Darmstadt, Germany).

2.4.2 Methods

The Western blotting procedure requires a high yield of protein. On the third passage, cells were re-seeded from small 35 mm petri dishes to large 100 mm petri dishes. A single large 100 mm petri dish was found to yield a sufficient protein concentration for one lysate.

2.4.2.1 Cell Lysates

After treatment, AECs were covered in 10 ml PBS and a rubber cell-scraper was used to gently lift the cells from the plate. The cell-PBS suspension was then transferred to the relevant tube and centrifuged for 3 minutes at 1000 rpm, after which the cell pellets were transferred to an eppendorff tube. Zirconium oxide beads (0.15 mm) were added to the pellet, along with 650 μ l lysis buffer (Table 2.2) followed by homogenization with a Bullet Blender™ (Next Advance, Inc., NY, USA). 3 cycles of 1 minute were performed on setting 5 of the Bullet Blender. In between cycles, samples were allowed to rest for 5 minutes. Samples were placed on ice for 30 minutes after which they were centrifuged for 20 minutes at 15 000 rpm at 4 °C. Protein content of the supernatant was determined using the Bradford assay (Bradford, 1976). Based on the Bradford assay findings, samples were prepared containing 2X Laemmli buffer (Table 2.3), lysis buffer and protein lysate, where a final protein content of 40 μ g/15 μ l of sample was achieved.

Table 2.2: Lysis buffer contents and preparation.

Reagent	Final concentration in buffer	Amount of 10X stock for 30 ml
Tris-HCl (pH 7.5)	20 mM	3.0 ml
EGTA	1 mM	
EDTA	1.0 mM	300 μ l
NaCl	150 mM	4.5 ml
β -glycerophosphate	1.0 mM	0.006 g
Tetra-sodium pyrophosphate	2.5 mM	0.03 g
NaF	50 nM	0.0639 g
Na ₃ VO ₄	1.0 mM	3.0 ml
Triton-X100 (1ml T in 10ml dH ₂ O)	1.0 %	3.0 ml
Leupeptin	10 μ g / ml	30 μ l
Aprotonin	10 μ g / ml	30 μ l
Sodium dodecyl sulphate (SDS)	0.1 %	30 μ l
PMSF	50 μ g / ml	90 μ l
Distilled water		Fill up to 30 ml

Table 2.3: Contents of 2X Laemmli buffer (Laemmli, 1970).

Reagent	Concentration
SDS	4 %
Glycerol	20 %
2-Mercaptoethanol	10%
Bromophenol blue	0.004 %
Tris HCl	0.125 M

2.4.2.2 Protein Loading and Transfer

Prepared lysates were boiled for 5 minutes before loading. A PageRuler™ ladder was loaded into the first well of every gel (7 µl) followed by 15 µl of lysate for each sample. 26-well (4–15% gradient) Criterion™ TGX Stain-Free™ Protein Gels (*Bio-Rad*, CA, USA) were used for all western blot experiments. Gels were run at 140 V for 10 minutes, followed by a second 40-minute run at 200 V. After running, the gels were activated for 1 minute using the Chemidoc™ MP Imager System with Image Lab™- 5 software (*Bio-Rad*, CA, USA), where the gels could be checked for equal protein loading. Following gel activation, proteins on the gel were transferred to a Trans-Blot® Turbo™ Midi PVDF membrane (*Bio-Rad*, CA, USA), using the Trans-Blot® Turbo™ Transfer System (*Bio-Rad*, CA, USA). The “Standard SD” protocol was used for all transfers and involved a 30 minute transfer at a constant voltage of 25 V and a varying current of up to 1 A. After the transfer the membrane was imaged on the Chemidoc™ again to ensure all proteins transferred correctly and evenly.

2.4.2.3 Immunodetection

Membranes were blocked for non-specific binding for 1.5 hours in 5 % fat-free milk in Tris-buffered saline, 0.1 % tween-20 (TBS-Tween). After blocking, membranes were washed for 30 minutes (3 x 10 minute cycles) with TBS-tween and then incubated overnight at 4 °C with a specific primary antibody (Table 2.4). The next morning, the membranes were washed again for 30 minutes in TBS-tween and then incubated with an anti-rabbit immunoglobulin G, horseradish peroxidase (HRP) - conjugated secondary antibody for 1 hour at room temperature. The specific primary and secondary antibody conditions of each antibody are shown in Table 2.4. After the 1-hour incubation, membranes were rinsed again for 30 minutes, after which protein visualization took place. To visualize the proteins, membranes were incubated in Clarity™ for 5 minutes, after which the stain-free membranes were exposed on the Chemidoc™. Exposure time and the number of images captured were set beforehand and could be visualized throughout the procedure.

Image Lab™- 5 software standardises the visualised protein bands against the total amount of protein per lane transferred to the membrane (the image that was taken following transfer of protein to the membrane). The raw values generated by the software are then used to normalise all values to the control group, where the control is represented by the value 1. See **Appendix D** for the method used to normalise the data.

Some membranes were stripped of their original probe and re-probed for a different antibody. To strip membranes of primary and secondary antibodies, membranes were washed for 14 minutes (2 x 7 minute cycles) with dH₂O, then for 7 minutes with 0.2 M NaOH, followed by 14 minutes with dH₂O again. Membranes were then blocked in 5 % milk for 2 hours and could then be re-probed at a different molecular weight on the membrane than the initial antibody; therefore some proteins shared normalization membrane images.

Table 2.4: Specifications for each antibody after optimisation for Western blotting.

Antibody	Primary Antibody Dilution	Secondary Antibody Dilution
Phospho-eNOS 140 kDa	1:1000 TBS (5µl in 5ml)	1:4000 5% Milk (1.25µl in 5ml)
Total-eNOS 140 kDa	1:1000 TBS (5µl in 5ml)	1:4000 5% Milk (1.25µl in 5ml)
iNOS 131 kDa	1:200 2.5% Milk (25µl in 5ml)	1:4000 5% Milk (1.25µl in 5ml)
Nitrotyrosine 90 kDa	1:5000 TBS (1µl in 5ml)	1:4000 TBS (1.25µl in 5ml)
p22 PHOX 22 kDa	1:500 1% Milk (10µl in 5ml)	1:4000 5% Milk (1.25µl in 5ml)
Cleaved Caspase-3 17/19 kDa	1:500 1° SignalBoost™ (10µl in 5ml)	1:4000 2° SignalBoost™ (1.25µl in 5ml)

2.5 ORAC Assay

The oxygen radical absorbance capacity (ORAC) assay is a method to assess the antioxidant capacity of biological samples (Huang, Ou, Hampsch-Woodill, Flanagan, & Prior, 2002; Prior et al., 2003). ORAC assays were kindly conducted by Dr D Blackhurst (Division of Chemical Pathology, University of Cape Town, SA).

AECs were passaged and maintained with the same method previously described in the section 2.4.2, and treated as previously described under the heading of section 2.4 (See **Appendix C**). After treatment, cells were washed with PBS and then covered with just over 1 ml of PBS. The cells were removed from the petri dish surface using a rubber cell scraper after which exactly 1 ml cell-PBS suspension was transferred to the relevant eppendorff tube. Sample tubes were then frozen and transported to the University of Cape Town (UCT) on dry-ice, for analysis.

For analysis, the cell samples were subjected to sonication using a Virtis VirSonic 100 (*United Scientific* (Pty) Ltd, CPT, SA) with 20 x 1 second bursts at 3 watts. At this stage 25 μ l were removed for protein estimation by the Markwell modification of the Lowry method (Markwell, Haas, Bieber, & Tolbert, 1978), using bovine serum albumin as the standard. Cell samples were then centrifuged at 1000 x g at 4 °C for 15 minutes and the supernatant was used for ORAC measurement, using the method previously described by Maarman *et al.* (2015).

2.6 Statistical Analyses

All microplate reader data was calculated as mean \pm standard error of the mean (SEM), with values expressed as a % of the control (control adjusted to 100%). For Western blot data, controls were adjusted to the value of 1. Total protein expression was calculated as a ratio of the loading control. For the ORAC assays, the antioxidant capacity is expressed in trolox equivalents. Trolox is a vitamin-E analogue that is used as the standard measure of antioxidant capacity.

One-way ANOVA with a Bonferroni post-hoc multiple comparison test were used to determine significance. Differences with a p-value < 0.05 were considered statistically significant. All data was analysed using GraphPad Prism 6 software (*GraphPad Software*, San Diego, CA, USA).

Sample sizes are indicated below each graph in Chapter 4.

3 - Materials and Methods: *Ex vivo* and *In vivo* studies

This chapter contains a description of the materials and methods used for the *ex vivo* and *in vivo* studies. The *ex vivo* studies consisted of investigations into the organ bath-based vascular contraction-relaxation function of aortas obtained from healthy male Wistar rats. In these studies, melatonin and/or ART were administered directly to the aortic rings mounted in the organ bath, and acute vascular and endothelium-dependent responses were measured. The *in vivo* studies comprised of an 8-week period of oral treatment with melatonin and/or ART, followed by organ bath-based investigations into the endothelium-dependent and endothelium-independent vascular contraction-relaxation function of the aortas obtained from the treated animals. The results for these studies can be found in Chapter 5.

3.1 Materials

- Anaesthetic (Sodium pentobarbitone; $C_{11}H_{17}N_2NaO_3$): *Bayer* (Isando, Gauteng, SA).
- *Sigma-Aldrich* (St Louis, Mo, USA):
 - Acetylcholine
 - Phenylephrine
 - *N*_ω-Nitro-L-arginine methyl ester (L-NAME) hydrochloride
 - Sodium Nitroprusside (SNP)
- All other chemicals and buffer reagents: *Sigma-Aldrich* (St Louis, Mo, USA) and *Merck* (Darmstadt, Germany).

3.2 Ethics Clearance and Animal Care

All experiments were conducted in accordance with the accepted standards for the use of animals in research as set out by the South African National Standards document (SANS 10386: 2008) of the South African Bureau of Standards (SABS). Ethics approval was received from The Research Ethics Committee: Animal Care and Use of the University of Stellenbosch (US; Faculty of Medicine and Health Sciences; Protocol Number: SU-ACUD14-00021).

Age matched male Wistar rats with an initial weight range between 180 – 200 g were provided, housed, and cared for by the Animal Housing Unit of the Faculty of Medicine and Health Sciences of US. The animals were housed (2 – 3 rats per cage) in a temperature (22 °C) and humidity (40 %) controlled environment where they were subjected to a normal 12 hour artificial day / night cycle. Animals had free access to a standard rat chow diet as well as drinking water.

3.3 Experimental Protocols and Study Design

For aortic ring experiments, animals were transferred from the Animal Housing Unit to the animal care facility of the Division of Medical Physiology, 1 day prior to sacrifice (usually between 2 – 4 animals). This was to ensure animals had a day to recover from the stress of being transported as well as time to adapt to their new environment.

The animals were anaesthetised through intraperitoneal (IP) injection of 160 mg / kg sodium pentobarbitone in the lower right abdomen. Deep anaesthesia was confirmed by the disappearance of the pedal pain withdrawal reflex and absence of eye reflexes. Euthanasia was achieved by means of a clamshell thoracotomy and eventually exsanguination.

3.3.1 Excision and Mounting of Aortic Rings

Following the establishment of deep anaesthesia, an incision was made through the skin and muscle layers across the ventral side of the rat, just below the thoracic region. The diaphragm and ribcage were cut in a cranial direction as to expose the thoracic cavity. The heart, lungs, trachea and oesophagus were removed. The thoracic aorta (above the diaphragm to distal end of the aortic arch) was excised and immediately placed in ice-cold Krebs Henseleit buffer (KHB) (Table 3.1). Using a magnifying glass, the perivascular fat and connective tissue was removed (Fig 3.1) and the aorta was cut into a 3 - 4 mm ring segment that was subsequently mounted onto two stainless steel hooks (Fig 3.2) in a 25 ml organ bath (*AD Instruments*, Bella Vista, NSW, Australia) containing oxygenated (95% O₂ and 5% CO₂) KHB. Aortic ring tension was recorded with an isometric force transducer (*TRI202PAD*, Panlab, ICornellà, BCN, Spain) and data was analysed with LabChart 7 software (Dunedin, New Zealand) (Westcott, 2015).

Table 3.1: Composition of Krebs Henseleit buffer.

Ingredients	Concentration (mM)
NaCl	119
NaHCO ₃	25
KCL	4.75
KH ₂ PO ₄	1.2
MgSO ₄ .7H ₂ O	0.6
Na ₂ SO ₄	0.6
CaCl ₂ .H ₂ O	1.25
Glucose	10

**Figure 3.1:** A thoracic aorta excised and cleaned of connective tissue and perivascular fat (Loubser, 2014).

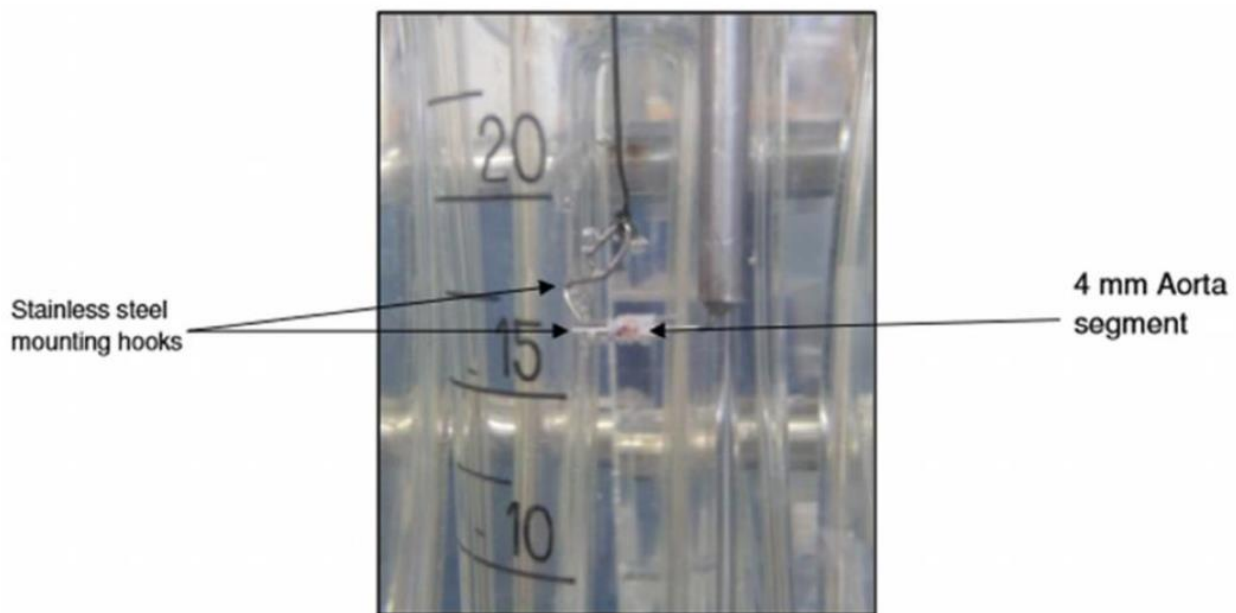


Figure 3.2: Organ bath with a 4 mm segment of aorta suspended between two 2 steel hooks (Loubser, 2014).

3.3.2 Ex Vivo Studies

For all *ex vivo* aortic ring experiments, phenylephrine (Phe) was used to induce contraction, and acetylcholine (Ach) was used to induce relaxation. Phe is an α -adrenergic receptor agonist which acts directly on the VSMCs eventually leading to contraction. Ach binds to endothelial surface receptors (Fig 1.3) resulting in an increase in intracellular calcium and consequently eNOS activation. eNOS activation leads to the release of NO which diffuses to the VSMC layer resulting in VSMC relaxation.

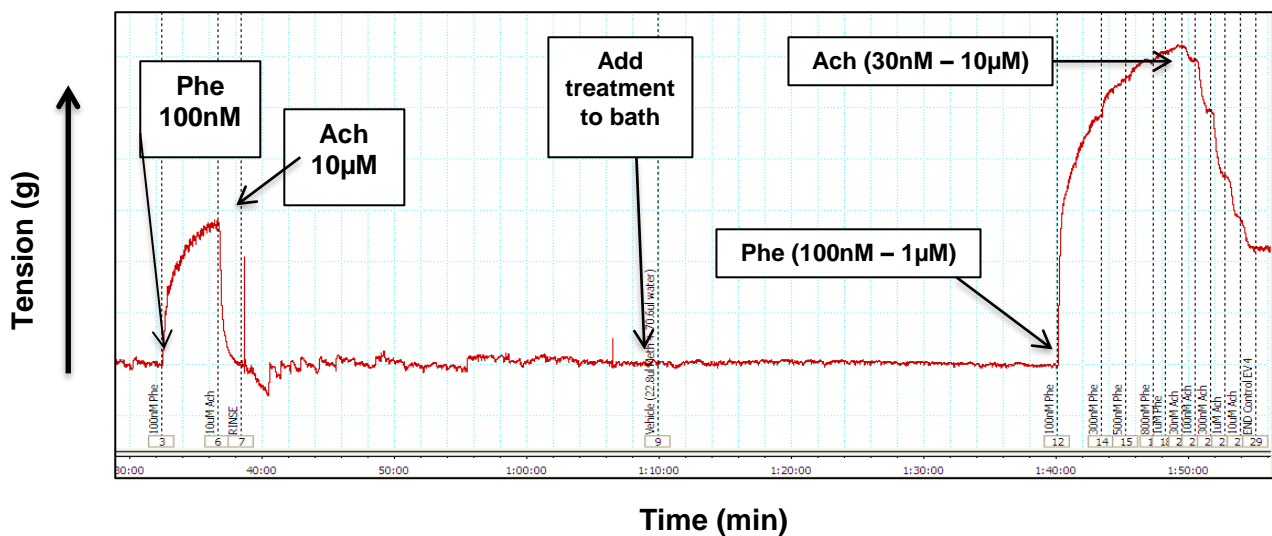
The isometric tension measurement protocol used was a modified version of a technique previously described by Privet *et al.* (2004). The mounted aortic rings were stabilised for 30 minutes at a resting tension of 1.5 g, over which period, the KHB was changed every 10 minutes with fresh, pre-warmed (37 °C) KHB. After the 30-minute stabilisation, an initial functionality test was conducted, whereby 100 nM Phe was added to the organ bath. Once the ring was no longer contracting (a plateau was reached), 10 μ M Ach was added. Rings that showed at least a 70 % relaxation of maximum phenylephrine-induced contraction during the initial functionality test were included for further investigations. Following the functionality test, the organ bath was rinsed 3 times with fresh, warm KHB and the rings were once again stabilised for 30 minutes at a tension of 1.5 g, where the buffer was changed every 10 minutes. After the second 30-minute stabilisation period, the relevant treatment was added to the organ bath, which was followed by a 30-minute incubation

period. Following drug administration and the 30-minutes incubation, aortic ring contraction was induced with the cumulative administration of Phe (100 nM – 1 μ M). Once a plateau was reached, aortic rings were subsequently exposed to cumulative concentrations of Ach (30 nM – 10 μ M). Experiments were terminated once the aortic rings experienced maximum relaxation. Figure 3.3 is a representative LabChart recording showing the aortic ring responses to the experimental protocol followed for the *ex vivo* studies.

Ex vivo aortic ring experiments consisted of the following groups:

- Control (Contains Combined Vehicle Only)
- 10 μ M Melatonin (*Sigma Aldrich*, St Louis, MO, USA) + Combined Vehicle
- High concentration ART (*SantaCruz Biotechnology*, CA, USA) + Combined Vehicle
- ART + Melatonin + Combined Vehicle

Ex vivo treatment groups all contained a combined vehicle. This allowed for all groups to be directly compared without considering a vehicle effect. A very limited number of rats were allocated to the *ex vivo* portion of this study due to the adjusted protocol's novel and experimental nature. A limited number of rats meant we had to reduce the number of experimental groups in order to cater for an adequate sample size ($n = 5 - 6$). For *ex vivo* studies, a melatonin concentration of 10 μ M was used, unlike the 1 nM melatonin concentration, which was used for the *in vitro* studies. The reason for this discrepancy is that the *ex vivo* studies were conducted before the *in vitro* melatonin dose-response experiments were completed, and at that stage, the assumption was made that the higher dose of melatonin would be more effective. It only became evident that the lower dose of melatonin was in fact the more effective concentration to use, once melatonin dose-response experiments were completed. Refer to **Appendix E** for detailed *ex vivo* melatonin, ARV and vehicle concentration calculations.



Stab (30 Min)	Phe (100 nM)	Ach (10 µM)	Stab (30 Min)	Treatment (30 Min)	Phe (100 nM – 1 µM)	Ach (30 nM – 10 µM)
------------------	-----------------	----------------	------------------	-----------------------	------------------------	------------------------

Figure 3.3: LabChart recording showing the aortic ring responses to the experimental protocol followed for the *ex vivo* studies. This graph is from the control experimental group where only vehicles were added at the treatment period.

3.3.3 *In Vivo* Studies

For the *in vivo* studies, 80 male Wistar rats were divided into the following 4 experimental groups (Fig 3.4):

- Control (Untreated)
- Melatonin (*Sigma Aldrich*, St Louis, MO, USA)
- ART/ Odimmune® (*Cipla MedPro*, Bellville, WC, SA)
- ART + Melatonin

One week prior to the start of treatment, rats weighing 180 – 200g were randomly separated into the 4 treatment groups. Between 2 and 3 rats were housed per cage according to the conditions mentioned in section 3.2. During this week, the water-intake of the rats was measured and recorded, but the rats received no other treatment.

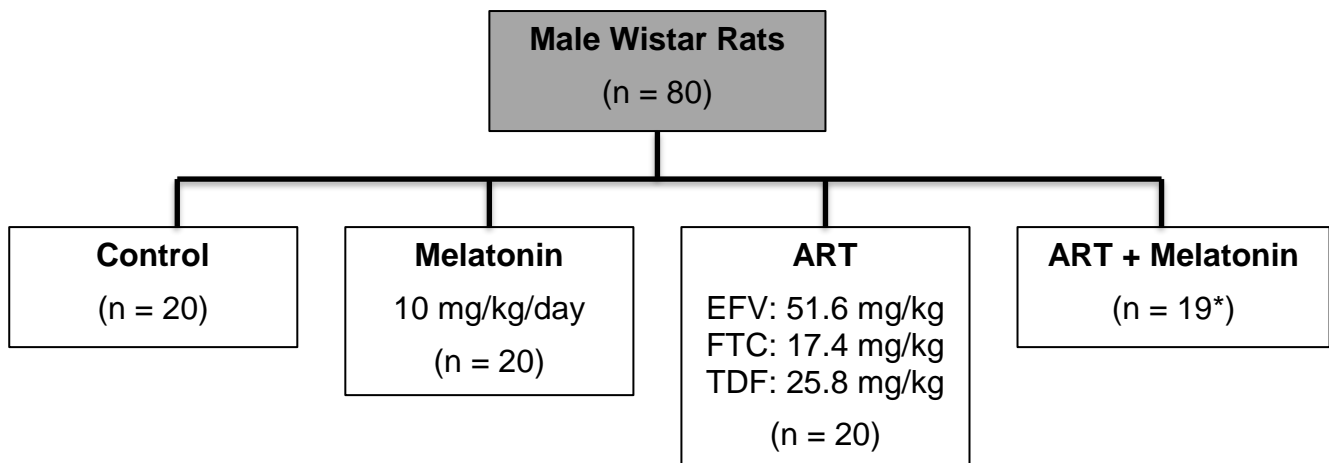


Figure 3.4: Flow chart indicating *in vivo* treatment groups. *1 rat died the week before treatment was initiated.

3.3.3.1 Drug Administration

Following the initial 1-week water-intake monitoring, an 8-week treatment period was initiated. Throughout the 8-week treatment period, rats were weighed once per week (Monday morning) and all fluid intake was monitored and measured on a daily basis. Rats were caged together in groups of 2 or 3, and therefore the amount of fluid drunk per cage was measured, and then divided based on the number of rats per cage.

10 mg/kg melatonin was found to be effective in reducing oxidative damage (Cardinali, Cano, Jimenez-Ortega, & Esquifino, 2011; Favero et al., 2017), and is the current concentration of melatonin used in other studies within our laboratory. This dose of melatonin was administered through the drinking water, where each cage containing a given number of rats was given 200 ml a day, and the melatonin-water was measured the next day at the same time, to assess the amount of water consumed by each cage daily. This amount was then divided by the amount of rats in the given cage in order to calculate the mean water consumed by each rat within a single cage. This information, along with the average weight of the rats in a specific cage allowed for the calculation of the amount of melatonin each cage received for a specific week. This was necessary to ensure the rats were always receiving the prescribed dose of melatonin. For example, in cages that consumed very high quantities of melatonin-water, a lower stock concentration of melatonin was prepared, while cages that drank very little water, needed higher concentrations of melatonin in their drinking water to compensate for their reduced water consumption. Melatonin powder was dissolved in methanol and made up in stocks every

two days, while the drinking water containing melatonin was replaced every day. The amount of methanol used to dissolve the melatonin powder was dependent on the amount of melatonin stock that was made up, where 0.2% of the amount of stock being made was used to determine the quantity of methanol used. For example, if a 500 ml melatonin stock was prepared, 1 ml of methanol (0.2% x 500 ml) was used. All drinking bottles containing melatonin were covered with two layers of aluminium foil and a metal casing to ensure the melatonin was not inactivated by light. For detailed melatonin calculations, stock preparation and administration see **Appendix F**.

For ART treatment, an ART-water drug suspension was administered daily by oral gavaging by a qualified staff member (Mr. Noël Markgraaff; Manager: Care and Use of Laboratory Animals, SU). Groups that did not receive ART were also gavaged, but with water instead of the ART-suspension. The procedure of gavaging involved the insertion of a feeding tube along the roof of the animal's oral cavity towards the animal's left side and down the animal's esophagus and into the stomach of the animal. The ART-suspension or water was therefore injected directly in the stomach of the animal. The rats received 1 ml ART-suspension or water per day. The ART-suspension was made up weekly, according to the average weekly weight of the cage. To make up the ART-suspension, Odimune® tablets were ground into a fine powder using a pestle and mortar. The appropriate amount of Odimune® powder was then weighed and added to dH₂O, after which the mixture was thoroughly mixed and stored in the refrigerator.

Each Odimune® tablet contains the human recommended daily dose of active ingredients (EFV: 600 mg; FTC: 200 mg; TDF: 300 mg) for an average person (70 kg). These values, as well as the weekly rat weights, were used to calculate how much tablet powder needed to be combined with dH₂O in order for the rats to receive the applicable concentrations of the three individual ARVs (EFV: 51.6 mg/kg; FTC: 17.4 mg/kg; TDF: 25.8 mg/kg). See **Appendix G** for the method used to calculate the weekly drug dose.

3.3.3.2 Aortic Ring Investigations

The thoracic aorta was excised, cleaned of connective tissue and suspended in the organ bath as described under section 3.3.1. For *in vivo* experiments, two types of aortic ring investigations were conducted. For the first set of experiments we conducted endothelium-dependent relaxation studies, where Phe was used to induce contraction and Ach was used

to induce relaxation (as previously described in section 3.3.2). As a control for these endothelium-dependent relaxation studies, some of the rings in this section were pre-treated with the NOS inhibitor, L-NAME (100 μ M) 15 minutes prior to the administration of cumulative amounts of Phe and Ach. For these experiments, a single aorta was cut into two rings, which were mounted immediately in separate organ baths (Fig 3.5). The normal Phe-Ach experiments were always conducted in Organ Bath 1, which L-NAME studies were always conducted in Organ Bath 2.

For the second set of experiments we conducted endothelium-independent relaxation studies, where Phe was once again used to induce contraction, however, for these studies sodium nitroprusside (SNP) - an exogenous NO donor - was used to induce relaxation. Since SNP is a NO donor, relaxation observed is independent of the endothelium, as the NO released from SNP diffuses directly into the VSCMs. For SNP investigations, a single aorta was once again cut into two rings (Fig 3.5), and all SNP studies were conducted in Organ Bath 2.

Figure **3.5** shows how aortas were separated and cut for the two different studies.

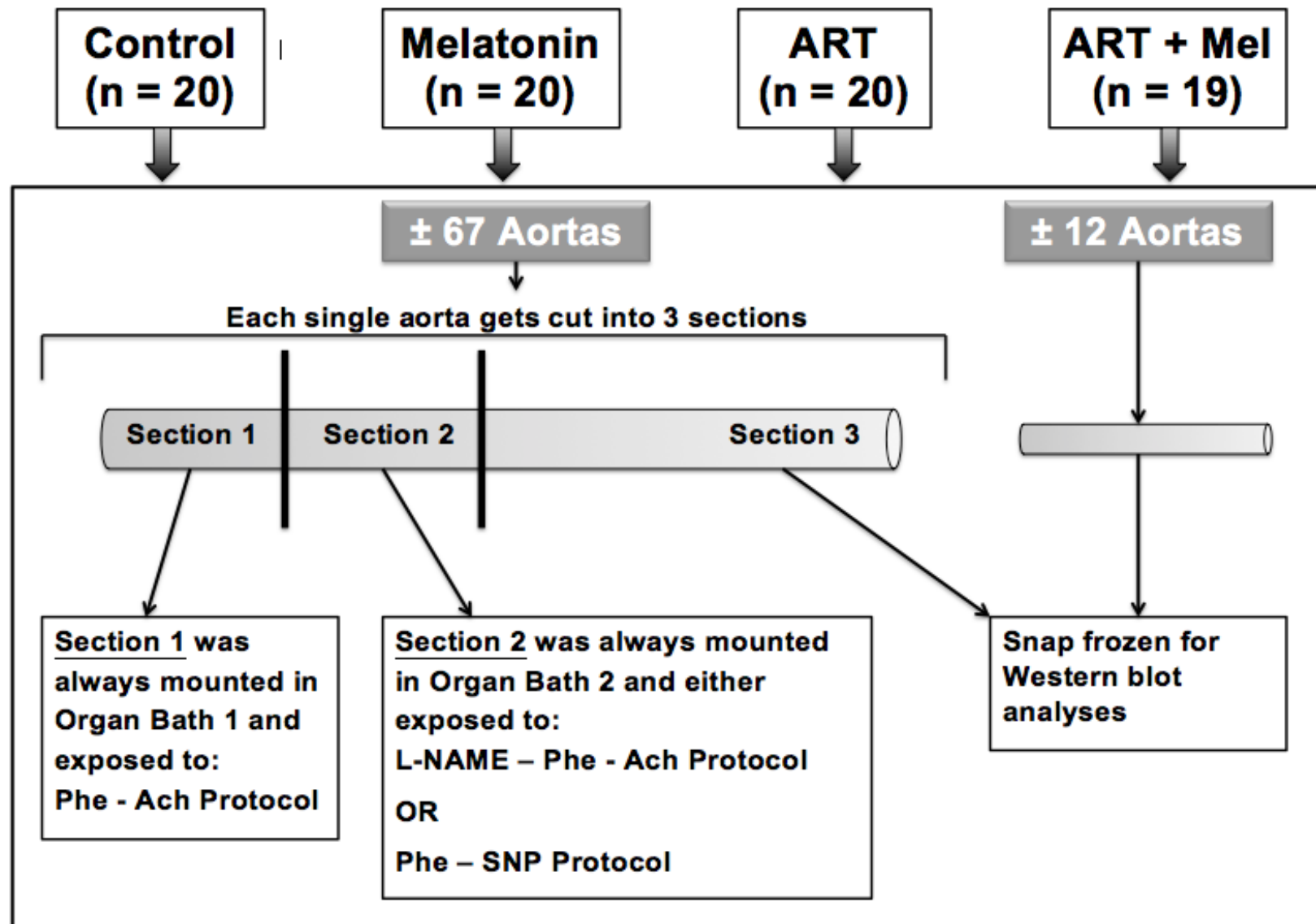
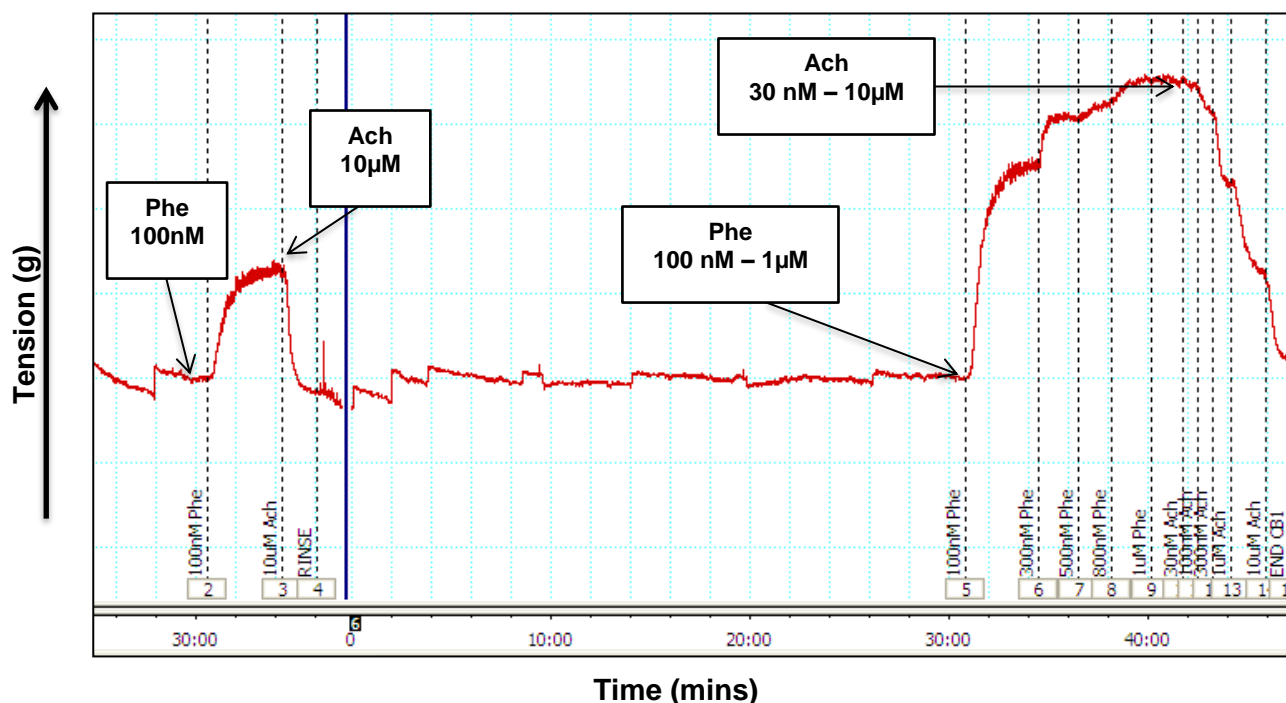


Figure 3.5: Scheme indicating procedures performed on cleaned aortic tissue to obtain aortic rings for isometric tension studies.

Following the initial stabilisation period, functionality test (done with Phe and Ach for all experiments), and the second stabilisation period (as described in section 3.3.2), each group was subjected to the following three isometric tension protocols:

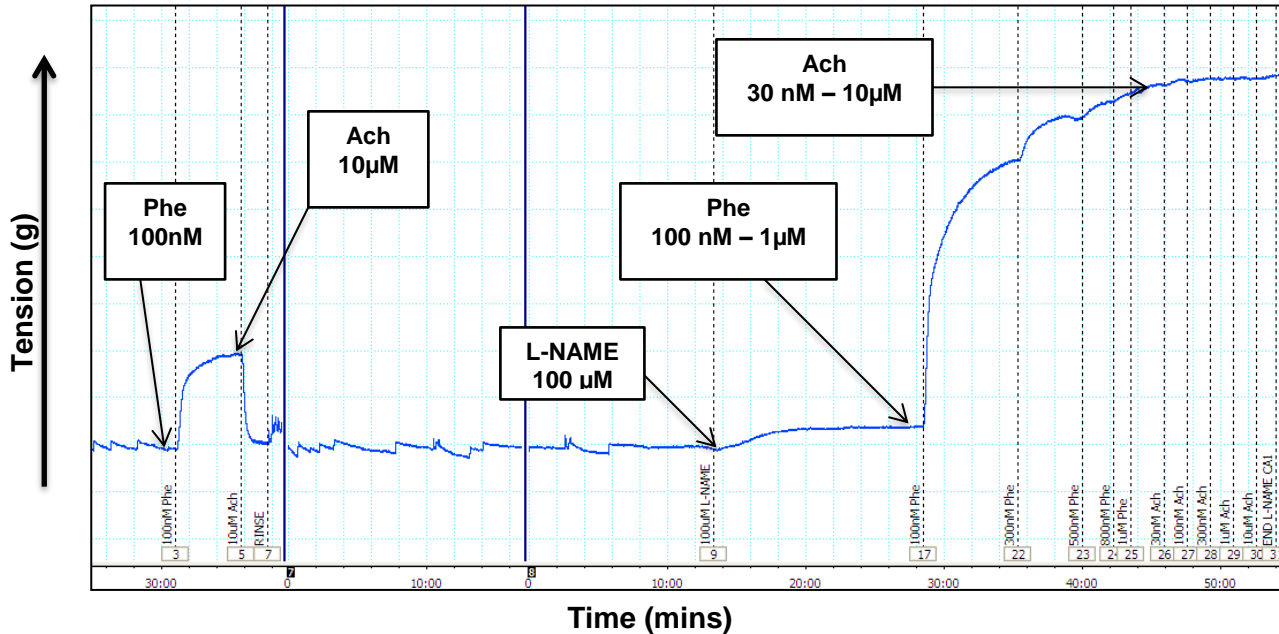
- 1) **Cumulative Phe-induced contraction followed by cumulative Ach-induced relaxation:** Cumulative administration of Phe results in a step-wise increase in the total Phe concentration as follows: 100 nM; 300 nM; 500 nM; 800 nM; 1 μ M. This administration results in cumulative aortic ring contractions. Each dose of Phe was administered directly to the organ bath as soon as maximum contraction was reached with the previous administration. Once the final dose of Phe was administered to produce a final Phe concentration of 1 μ M, maximum contraction was reached and therefore Ach was administered in order to induce endothelium-dependent relaxation. Ach was also administered in a cumulative manner resulting in step-wise increases in Ach concentrations: 30 nM; 100 nM; 300 nM; 1 μ M; 10 μ M. The experimental protocol was terminated once the final Ach administration (final concentration: 10 μ M) resulted in maximum % relaxation of contraction (Fig 3.6).



Stab (30 min)	Phe (100 nM)	Ach (10 μ M)	Stab (30 min)	Phe (100 nM – 1 μ M)	Ach (30 nM – 10 μ M)
------------------	-----------------	---------------------	------------------	-----------------------------	-----------------------------

Figure 3.6: A representative LabChart recording showing the aortic ring responses to the experimental protocol followed for Phe administration followed by Ach. This graph was from an aortic ring in the control group.

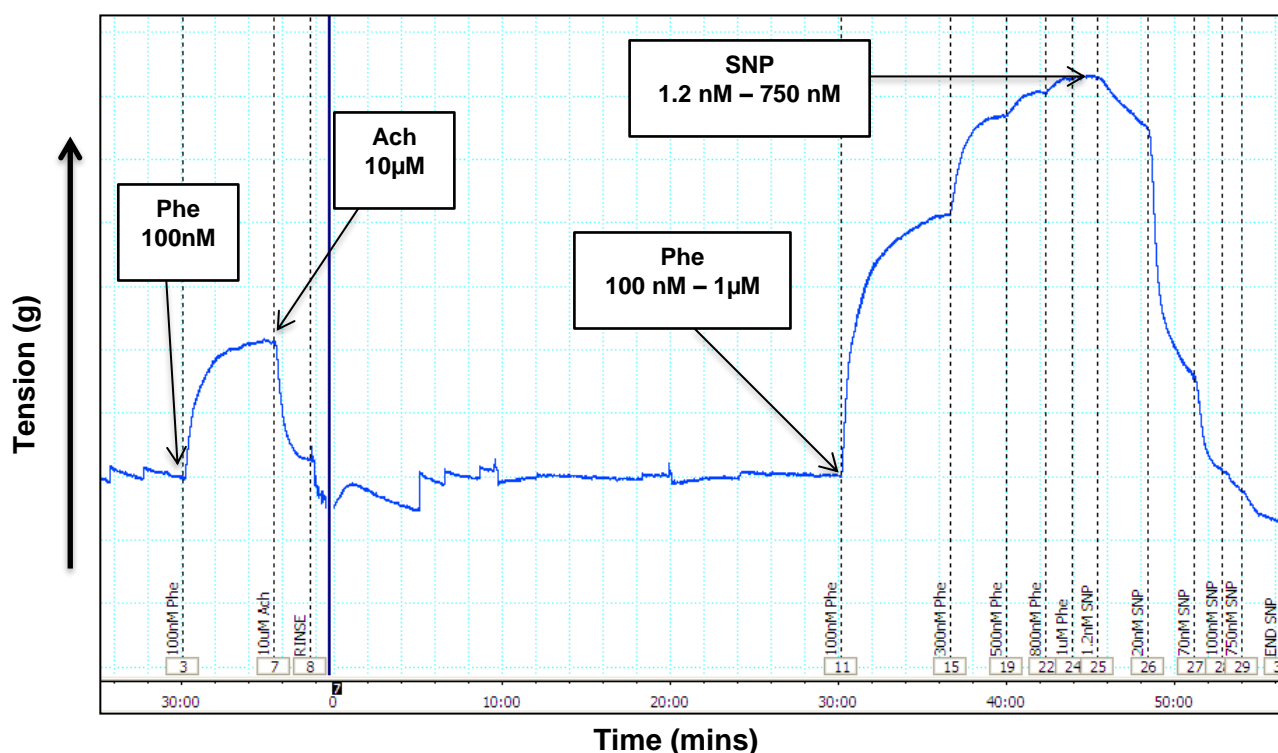
- 2) **L-NAME pre-treatment, followed by cumulative Phe-induced contraction and cumulative Ach-induced relaxation:** In this protocol, the role of NOS-derived NO was manipulated by pre-administration of the NOS-inhibitor, L-NAME (100 μM) 15 minutes prior to the cumulative Phe - Ach protocol (Fig 3.7).



Stab (30 min)	Phe (100 nM)	Ach (10 μM)	Stab (30 min)	L-NAME (100 μM ; 15 min)	Phe (100 nM - 1 μM)	Ach (30 nM - 10 μM)
------------------	-----------------	----------------------------	------------------	--	------------------------------------	------------------------------------

Figure 3.7: A representative LabChart recording showing the aortic ring responses to the experimental protocol followed for L-NAME pre-treatment followed by Phe and Ach administration. This graph is from an aortic ring in the control group.

- 3) **Cumulative Phe-induced contraction followed by cumulative SNP-induced relaxation:** Phe was administered in a cumulative fashion as mentioned in the first protocol. Upon reaching maximum contraction, SNP was administered to induce endothelium-independent relaxation. SNP was also administered in a cumulative manner resulting in step- wise increases in SNP concentrations: 1.2 nM; 20 nM; 70 nM; 100 nM; 750 nM. The experimental protocol was terminated once the final SNP administration (final concentration: 750 nM) resulted in maximum % relaxation of contraction (Fig 3.8). SNP concentrations used were based on various sources in the literature (Ajay & Mustafa, 2006; Ameer, Boyd, Butlin, Avolio, & Phillips, 2015; Banda, Lefer, & Granger, 1997; Bonaventura, Lunardi, Rodrigues, Neto, & Bendhack, 2008; Sutliff et al., 2002). See **Appendix H** for detailed SNP concentration calculations and administration.



Stab (30 min)	Phe (100 nM)	Ach (10 µM)	Stab (30 min)	Phe (100 nM – 1 µM)	SNP (1.2 nM – 750 µM)
------------------	-----------------	----------------	------------------	------------------------	--------------------------

Figure 3.8: A representative LabChart recording showing the aortic ring responses to the experimental protocol followed for Phe administration followed by SNP. This graph is from an aortic ring in the control group.

3.4 Signalling Investigations – Western Blot Analyses

3.4.1 Materials

The same materials were used as described in Chapter 2, section 2.4.1

3.4.2 Methods

Due to the fact that for most samples, only a very small piece of aorta was frozen away, two samples from the same experimental group were combined to make one lysate.

3.4.2.1 Aortic Tissue Lysates

Aortic tissue that had been previously frozen at -80 °C was stored in liquid nitrogen, along with pulverizing equipment and any tools used to scrape or transfer the frozen aortic tissue. All these items were kept cold in liquid nitrogen so that when the tissue was pulverized it formed a fine powder. Following aortic tissue pulverization, 60 – 106 mg of the aortic tissue-powder was placed in an eppendorff tube along with the equivalent mass of 1.6 mm stainless steel beads and 600 µl complete lysis buffer (Table 2.2). Samples were then homogenised in a Bullet Blender™ (*Next Advance*, Inc., NY, USA) with the following protocol:

- 3 minutes at speed 8
- 5 minutes rest
- 2 minutes at speed 10

Samples were placed on ice for 30 minutes after which they were centrifuged for 20 minutes at 15 000 rpm at 4 °C. Protein content was determined by the Bradford assay (Bradford, 1976) as mentioned in Chapter 2, section 2.4.2.1. A final protein content of 60 µg/15 µl of sample was achieved.

3.4.2.2 Protein Loading, Transfer and Measurement

Loading of samples onto the Criterion™ TGX Stain-Free™ Protein Gels, subsequent transfer to membrane as well as antibody conditions and protein band visualization was conducted as described in Chapter 2, sections 2.4.2.2 and 2.4.2.3.

3.5 ORAC Assay

ORAC assays were kindly conducted by Dr D Blackhurst (Division of Chemical Pathology, University of Cape Town, SA).

Aortic tissue for the ORAC assay was prepared through pulverisation in the same manner described above in section 3.4.2.1. Aortic tissue-powder was placed in an empty eppendorf tube where the amount of tissue in mg within each sample tube was recorded. After pulverisation, samples were immediately frozen in liquid nitrogen and then transported to UCT on dry-ice, for analysis.

For analysis, aortic samples were homogenised (using an in-house 'glass-ball') and subjected to the same sonication, protein estimation and ORAC measurement protocols described in chapter 2, section 2.5.

3.6 Statistical Analyses

Data were analysed using GraphPad Prism 6 software (*GraphPad Software*, San Diego, CA, USA). Aortic ring contraction (Phe) studies are expressed as an increase in gram tension from a resting tension of 1.5 g, while relaxation (Ach/SNP) studies are expressed as % relaxation of the maximum contraction. Data were statistically analysed by means of a two-way ANOVA with a Bonferroni post-hoc multiple comparison test. Additionally, E_{max} values were compared using a one-way ANOVA with a Bonferroni post-hoc multiple comparison test. Differences with a p-value < 0.05 were considered statistically significant.

For Western blot data, controls were adjusted to the value of 1. Total protein expression was calculated as a ratio of the loading control.

For the ORAC assays, the antioxidant capacity is expressed in trolox equivalents.

For western blot and ORAC data, one-way ANOVA with a Bonferroni post-hoc multiple comparison test were used to determine statistical significance. Differences with a p-value < 0.05 were considered statistically significant.

Sample sizes are indicated below each graph in Chapter 5.

4 – Results: *In vitro* studies

Chapter 4 describes and reports data collected from the *in vitro* study, the materials and methods for which can be found in Chapter 2.

4.1 Plate Reader Analyses

The initial aim of the *in vitro* study set out to determine the individual optimum concentrations of both melatonin and first line FDC ART treated aortic endothelial cells (AECs) at which the greatest differences were seen when compared to untreated AECs, with respect to NO production, RNS production and cell viability. This was investigated through dose-response studies whereby AECs were treated with various melatonin and ART concentrations for a fixed period.

For the second aim of the *in vitro* study, the optimum concentrations obtained in the dose-response experiments above were used to treat AECs with both melatonin and ART in combination, in order to analyse any potential synergistic/antagonistic interactions between the two with respect to, NO production, RNS production and cell viability. For these studies, a single melatonin and FDC ART concentration was chosen for cell treatment over a period of 24 hours.

Following drug treatment, cells were treated with the applicable fluorescent probes, and the consequent cell fluorescence was measured using a plate reader. All treatment groups were compared to an untreated control group. Individual treatment groups were also compared to their respective vehicles. If no significant difference was seen between a group and its respective vehicle, then any significant changes between that particular treatment group and the control group were considered a vehicle effect. The n value represents the number of individual experiments (biological replicates) that were conducted for each endpoint, where each treatment group within an experiment consisted of 2 to 3 samples (technical replicates) for which the mean value was calculated. All values expressed as a % of the control (control adjusted to 100%). A p-value of < 0.05 was considered statistically significant.

4.1.1 Melatonin Dose-Response Studies

Dose-response experiments comprised of a 24-hour serum starvation (SS) period, followed by a 24-hour melatonin treatment period, followed by probe treatment and plate reader analyses. As previously mentioned in section 2.2, serum starvation (SS) was

introduced to induce cell cycle synchronization, which enhances the cells' responses to experimental treatment (Gerber et al., 1998; Russell & Hamilton, 2014), in otherwise healthy cells. Three treatment groups for melatonin were included: 1 nM; 1 μ M and 10 μ M melatonin. Results from these experiments (24-hour SS followed by 24-hour melatonin treatment) showed few to no changes between treatments groups, we therefore decided to introduce a 1-hour melatonin treatment period following 24-hour SS, to assess the early effects of melatonin on the cells.

4.1.1.1 24h SS + 24h Melatonin Treatment

DAF-2/DA: NO Production

AECs exposed to 24 hours of SS followed by treatment with 1 nM ($103.0 \pm 2.302\%$), 1 μ M ($103.3 \pm 3.432\%$) and 10 μ M ($101.8 \pm 3.544\%$) melatonin for 24 hours, showed no differences in mean DAF-2/DA fluorescence (NO production) compared to the untreated control group ($100.0 \pm 1.662\%$) (Fig 4.1). No changes were observed in any vehicle groups.

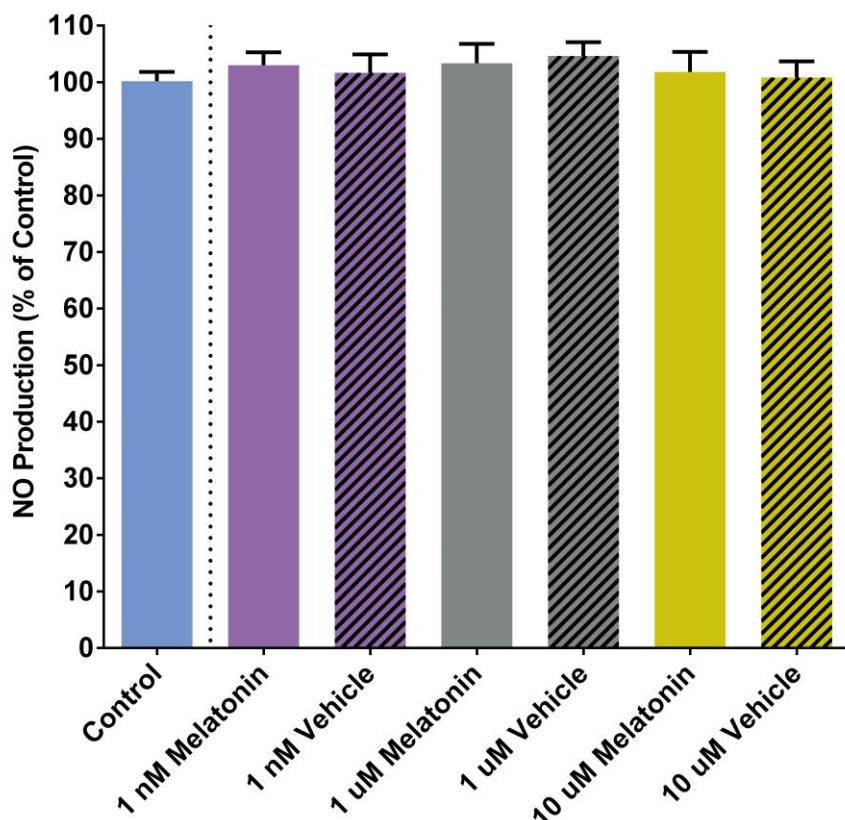


Figure 4.1: The effects of 24h SS followed by 24h melatonin treatment on NO production measured by DAF-2/DA fluorescence. NO production expressed as % DAF-2/DA stained cells (calculated as a percentage of the untreated control group; Control fluorescence adjusted to 100 %), n = 3/ group.

DHR-123: RNS Production

AECs exposed to 24 hours of SS followed by treatment with 1 nM ($109.3 \pm 3.287\%$), 1 μM ($104.6 \pm 3.266\%$) and 10 μM ($105.8 \pm 2.737\%$) melatonin for 24 hours, showed no differences in mean DHR-123 fluorescence (RNS production) compared to the untreated control group ($100.0 \pm 1.080\%$) (Fig 4.2). No changes were observed in any vehicle groups.

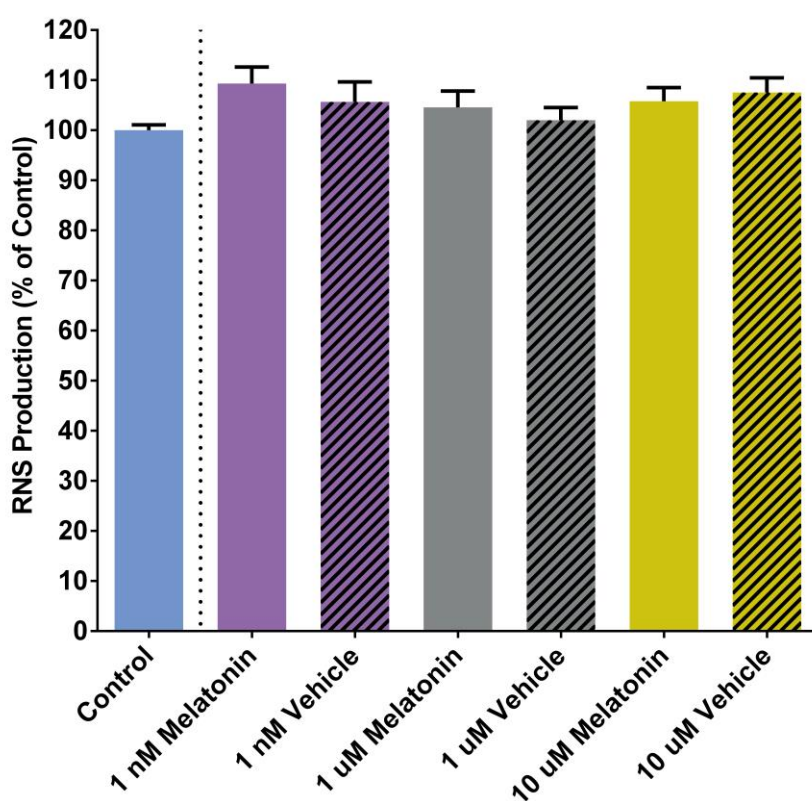
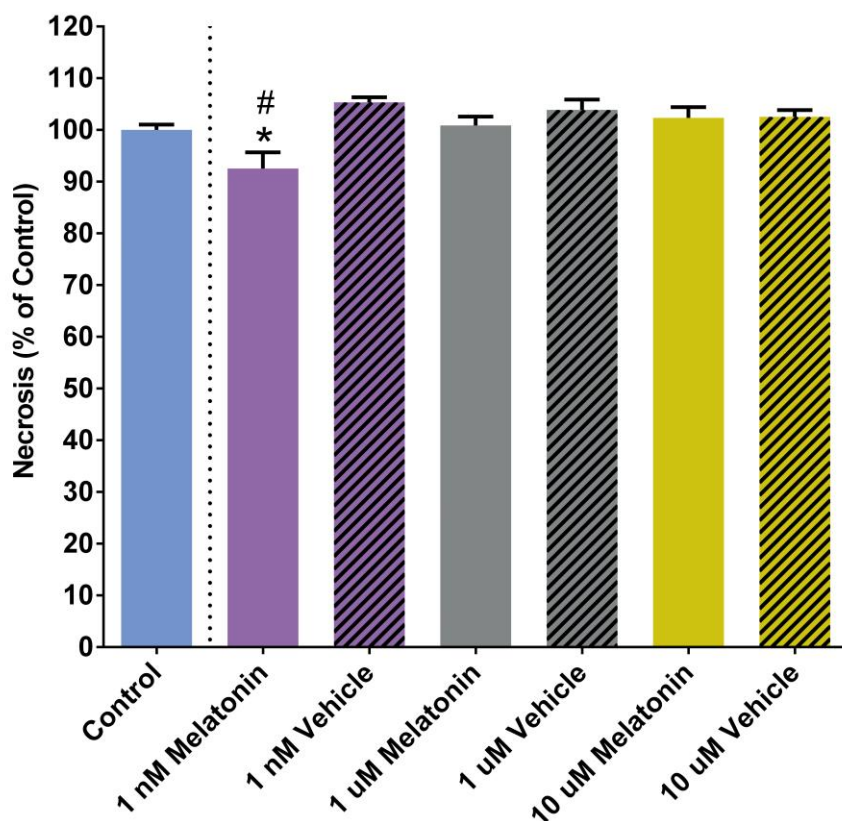


Figure 4.2: The effects of 24h SS followed by 24h melatonin treatment on RNS production measured by DHR-123 fluorescence. RNS production expressed as % DHR-123 stained cells (calculated as a percentage of the untreated control group; Control fluorescence adjusted to 100%), $n = 3/\text{group}$.

PI: Cell Viability (Necrosis)

AECs exposed to 24 hours of SS followed by treatment with 1 nM (92.56 ± 3.114%) melatonin for 24 hours, showed a significant decrease in mean PI fluorescence (necrosis), when compared to the untreated control group (100.0 ± 1.041%), and its own vehicle (105.3 ± 0.9718%) (Fig 4.3). 1 μM (100.9 ± 1.703%) and 10 μM (102.3 ± 2.075%) melatonin treated groups showed no differences in mean PI fluorescence compared to the control group (100.0 ± 1.041%). No changes were observed in 1 μM and 10 μM vehicle groups.



*: p=0.0004 vs control

#: p=0.0004 vs 1nM vehicle

Figure 4.3: The effects of 24h SS followed by 24h melatonin treatment on necrosis measured by PI fluorescence. Necrosis expressed as % PI stained cells (calculated as a percentage of the untreated control group; Control fluorescence adjusted to 100 %), n = 3/ group.

4.1.1.2 24h SS + 1h Melatonin Treatment

DAF-2/DA: NO Production

AECs exposed to 24 hours of SS followed by treatment with 1 nM ($104.0 \pm 1.238\%$), 1 μ M ($100.5 \pm 0.7188\%$) and 10 μ M ($101.5 \pm 0.8466\%$) melatonin for 1 hour, showed no differences in mean DAF-2/DA fluorescence (NO production) compared to the untreated control group ($100.0 \pm 0.9661\%$) (Fig 4.4). No changes were observed in any vehicle groups.

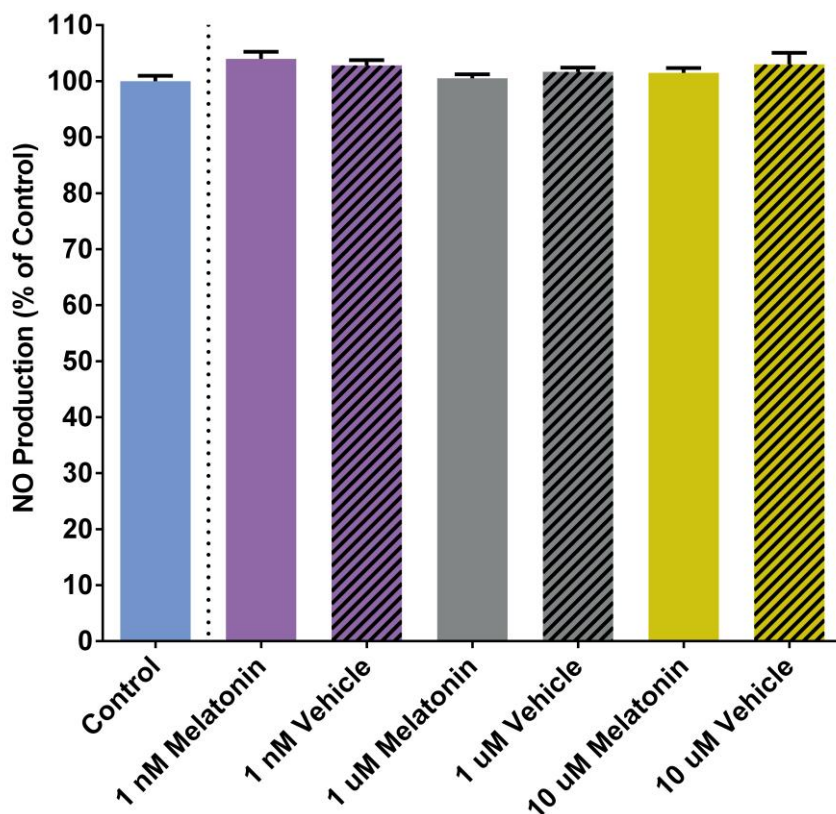


Figure 4.4: The effects of 24h SS followed by 1h melatonin treatment on NO production measured by DAF-2/DA fluorescence. NO production expressed as % DAF-2/DA stained cells (calculated as a percentage of the untreated control group; Control fluorescence adjusted to 100 %), n = 3/ group.

DHR-123: RNS Production

AECs exposed to 24 hours of SS followed by treatment with 1 nM ($101.2 \pm 1.517\%$), 1 μM ($98.5 \pm 1.111\%$) and 10 μM ($98.92 \pm 1.196\%$) melatonin for 1 hour, showed no differences in mean DHR-123 fluorescence (RNS production) compared to the untreated control group ($100.0 \pm 0.9129\%$) (Fig 4.5). No changes were observed in any vehicle groups.

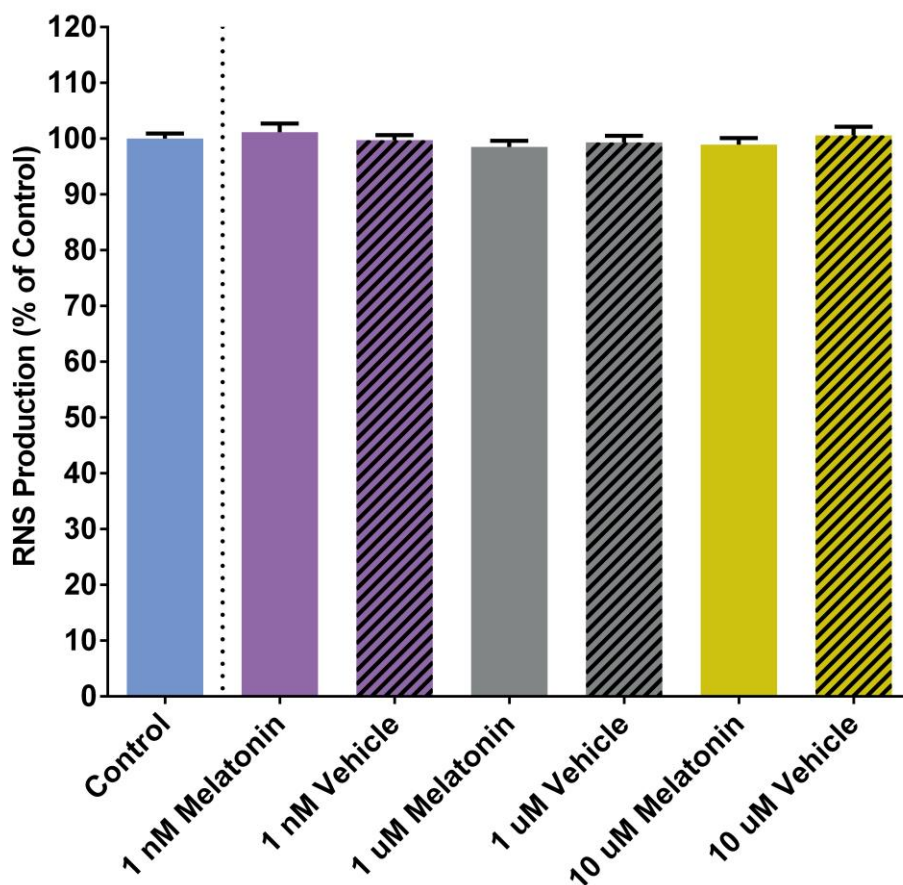
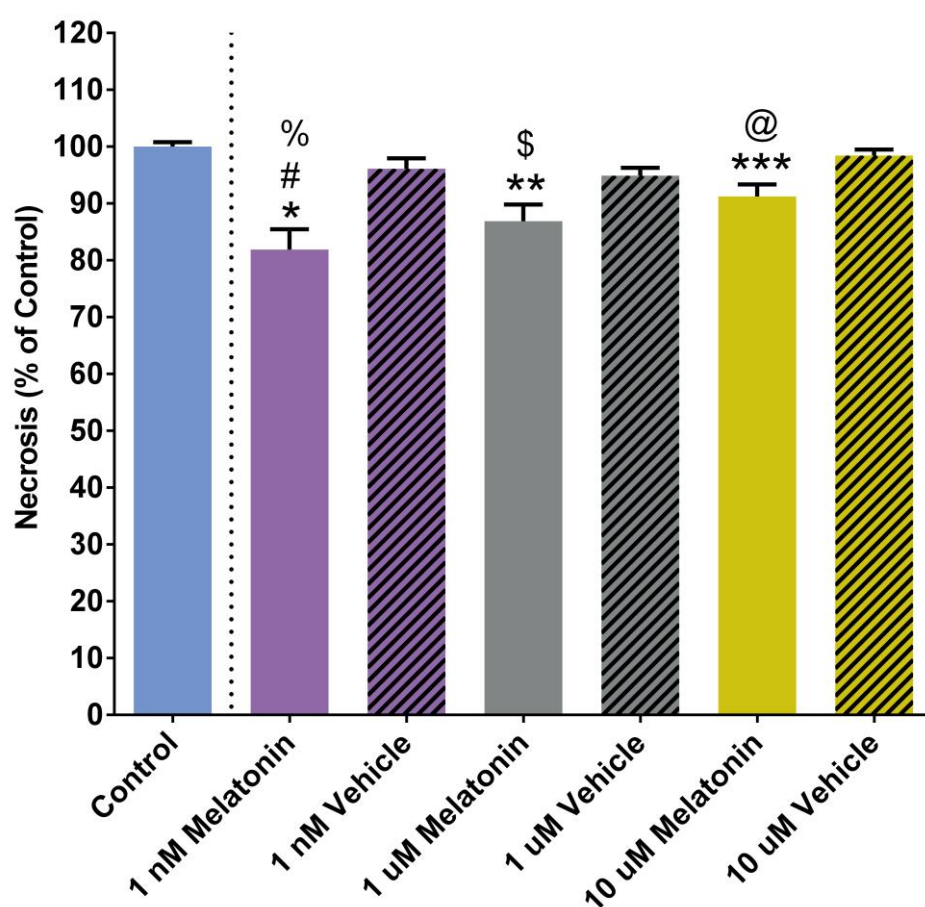


Figure 4.5: The effects of 24h SS followed by 1h melatonin treatment on RNS production measured by DHR-123 fluorescence. RNS production expressed as % DHR-123 stained cells (calculated as a percentage of the untreated control group; Control fluorescence adjusted to 100%), n = 4/ group.

PI: Cell Viability (Necrosis)

AECs exposed to 24 hours of SS followed by treatment with 1 nM ($81.89 \pm 3.572\%$), 1 μM ($86.89 \pm 2.927\%$) and 10 μM ($91.22 \pm 2.133\%$) melatonin for 1 hour, showed a significant decrease in mean PI fluorescence (necrosis) respectively, when compared to the untreated control group ($100.0 \pm 0.7993\%$). All melatonin treatment groups also significantly decreased compared to their respective vehicles (1nM Veh: $96.11 \pm 1.844\%$; 1 μM Veh: $94.89 \pm 1.409\%$; 10 μM Veh: $98.44 \pm 1.042\%$). The 1 nM melatonin treatment group also showed a significant decrease in PI fluorescence compared to the 10 μM melatonin treatment group (Fig 4.6).



*: $p < 0.0001$ vs control

#: $p < 0.0001$ vs 1 nM vehicle

** : $p < 0.0001$ vs control

\$: $p < 0.0001$ vs 1 μM vehicle

***: $p < 0.0001$ vs control

@: $p < 0.0001$ vs 10 μM vehicle

%; $p < 0.0001$ vs 10 μM melatonin

Figure 4.6: The effects of 24h SS followed by 1h melatonin treatment on necrosis measured by PI fluorescence. Necrosis expressed as % PI stained cells (calculated as a percentage of the untreated control group; Control fluorescence adjusted to 100 %), $n = 3/$ group.

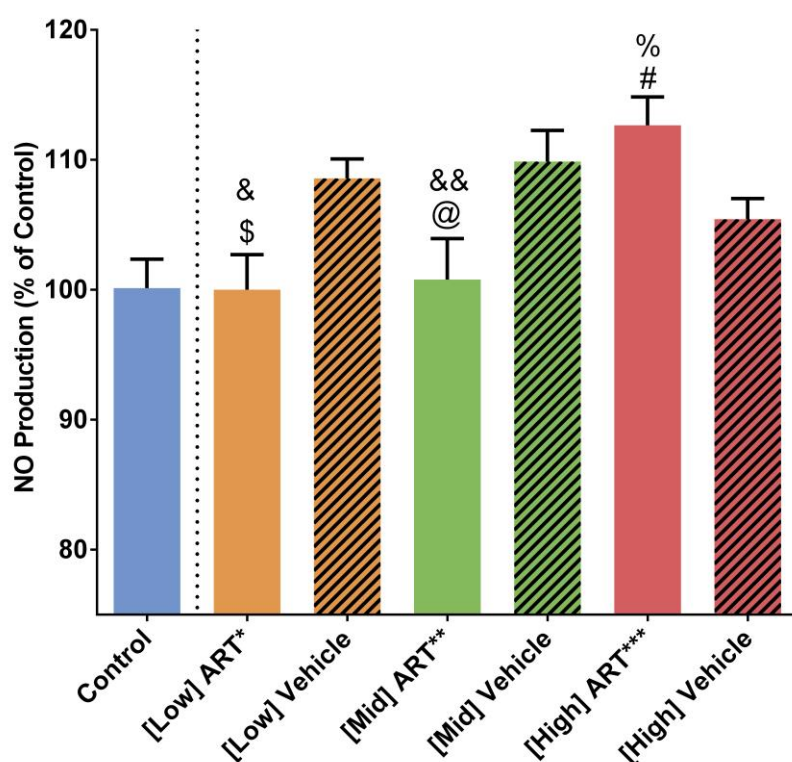
4.1.2 ART Dose-Response Studies

Dose-response experiments comprised of a 24-hour serum starvation (SS) period, followed by a 24-hour ART treatment period, followed by probe treatment and plate reader analyses. Three treatment groups for ART were included: Low concentration ART (EFV: 5 μ M; FTC: 5 μ M; TDF: 80nM); Mid concentration ART (EFV: 8 μ M; FTC: 7.5 μ M; TDF: 400nM) and High concentration ART (EFV: 12 μ M; FTC: 10 μ M; TDF: 1 μ M). In contrast to the melatonin dose-response studies, a 1-hour treatment period was not included for the ART dose-response studies. The shorter 1-hour treatment period was excluded for the ART studies since it would have little clinical relevance.

4.1.2.1 24h SS + 24h ART Treatment

DAF-2/DA: NO Production

AECs exposed to 24 hours of SS followed by treatment with low ($100 \pm 2.703\%$ vs Veh: $108.6 \pm 1.494\%$), mid ($100.8 \pm 3.116\%$ vs Veh: $109.9 \pm 2.394\%$) and high ($112.9 \pm 2.171\%$ vs Veh: $105.4 \pm 1.587\%$) concentration ART for 24 hours, all showed significant differences compared to their relative vehicles. However, only high concentration ART showed a significant increase in mean DAF-2/DA fluorescence (NO production) compared to the untreated control group ($100.1 \pm 2.224\%$). High concentration ART also increased NO production significantly compared to both low and mid concentration ART (Fig 4.7).



* EFV=5uM; FTC = 5uM; TDF= 80nM

** EFV=8uM; FTC = 7.5uM; TDF= 400nM

*** EFV=12uM; FTC = 10uM; TDF= 1uM

#: p=0.0015 vs control

#: p=0.0015 vs [high] vehicle

\$: p=0.0015 vs [low] vehicle

&: p=0.0015 vs [high] ART

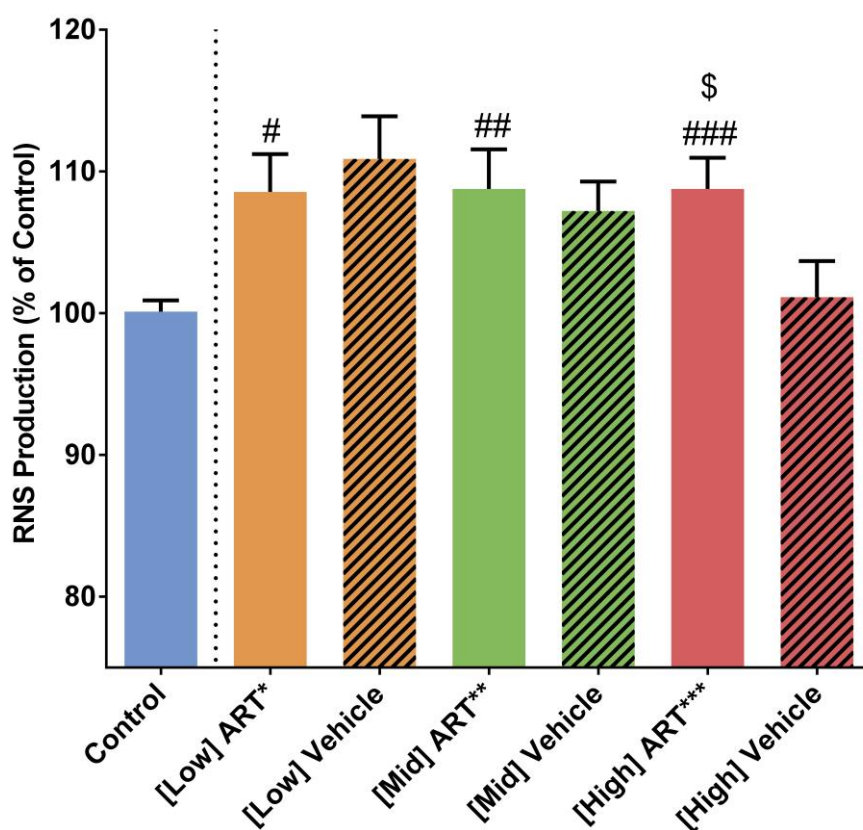
@: p=0.0015 vs [mid] vehicle

&&: p=0.0015 vs [high] ART

Figure 4.7: The effects of 24h SS followed by 24h ART treatment on NO production measured by DAF-2/DA fluorescence. NO production expressed as % DAF-2/DA stained cells (calculated as a percentage of the untreated control group; Control fluorescence adjusted to 100 %), n = 3/ group.

DHR-123: RNS Production

AECs exposed to 24 hours of SS followed by treatment with low ($108.6 \pm 2.667\%$), mid ($108.8 \pm 2.783\%$) and high ($108.8 \pm 2.197\%$) concentration ART for 24 hours, all showed a significant increase in mean DHR-123 fluorescence (RNS production) compared to the untreated control group ($100.0 \pm 0.7896\%$). Only high concentration ART increased significantly compared to its vehicle ($101.1 \pm 2.539\%$) (Fig 4.8), meaning the increase in DHR-123 fluorescence seen in the low and mid concentration ART groups compared to the control were vehicle effects.



* EFV=5uM; FTC = 5uM; TDF= 80nM

** EFV=8uM; FTC = 7.5uM; TDF= 400nM

*** EFV=12uM; FTC = 10uM; TDF= 1uM

#: $p=0.0152$ vs control

##: $p=0.0015$ vs control

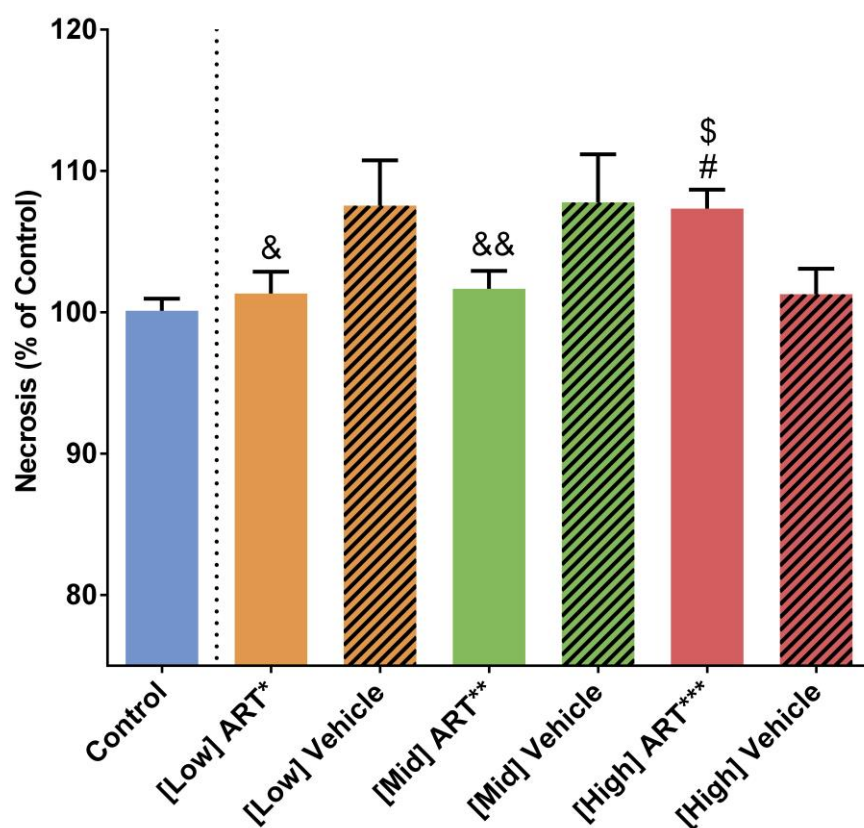
###: $p=0.0015$ vs control

\$: $p=0.0015$ vs [high] vehicle

Figure 4.8: The effects of 24h SS followed by 24h ART treatment on RNS production measured by DHR-123 fluorescence. RNS production expressed as % DHR-123 stained cells (calculated as a percentage of the untreated control group; Control fluorescence adjusted to 100 %), $n = 3/$ group.

PI: Cell Viability (Necrosis)

AECs exposed to 24 hours of SS followed by treatment with high (107.3 ± 1.344%) concentration ART for 24 hours, showed a significant increase in mean PI fluorescence (necrosis) compared to the untreated control group (100.0 ± 0.8571%). Low (101.3 ± 1.537%) and mid (101.7 ± 1.269%) concentration ART showed no differences in mean PI fluorescence when compared to the control. Only high concentration ART increased PI fluorescence significantly compared to its vehicle (101.3 ± 1.796%). High concentration ART also increased necrosis significantly compared to both the low and mid concentration ART groups (Fig 4.9).



* EFV=5uM; FTC = 5uM; TDF= 80nM

** EFV=8uM; FTC = 7.5uM; TDF= 400nM

*** EFV=12uM; FTC = 10uM; TDF= 1uM

#: p=0.0251 vs control

&: p=0.0251 vs [high] ART

\$: p=0.0251 vs [high] vehicle

&&: p=0.0251 vs [high] ART

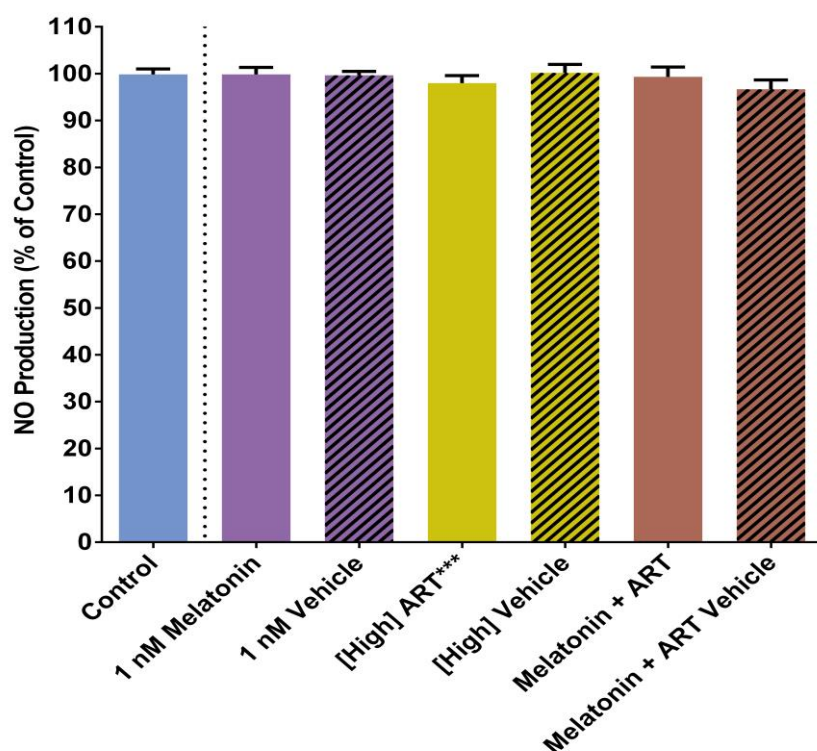
Figure 4.9: The effects of 24h SS followed by 24h ART treatment on necrosis measured by PI fluorescence. Necrosis expressed as % PI stained cells (calculated as a percentage of the untreated control group; Control fluorescence adjusted to 100 %), n = 3/ group.

4.1.3 Combination Studies

As previously mentioned in section 2.2.3, only a single concentration was used for both melatonin and ART in the combination studies. The individual melatonin and ART concentrations were selected based on the results observed in the dose-response experiments. Based on the above data, 1 nM melatonin and high concentration ART (EFV: 12 μ M; FTC: 10 μ M; TDF: 1 μ M) were used in the combination studies. A 24-hour SS period was once again used, followed by a 24-hour treatment period.

DAF-2/DA: NO Production

AECs were exposed to 24 hours of SS followed by treatment with 1 nM melatonin (99.83 \pm 1.515%), high concentration ART (98.00 \pm 1.571%), as well as a combination of 1 nM melatonin + high concentration ART (99.33 \pm 2.060%) for 24 hours. Results showed no differences in mean DAF-2/DA fluorescence (NO production) between the treatment groups and the untreated control group (100.0 \pm 1.124%) (Fig 4.10). No changes were observed in any vehicle groups.

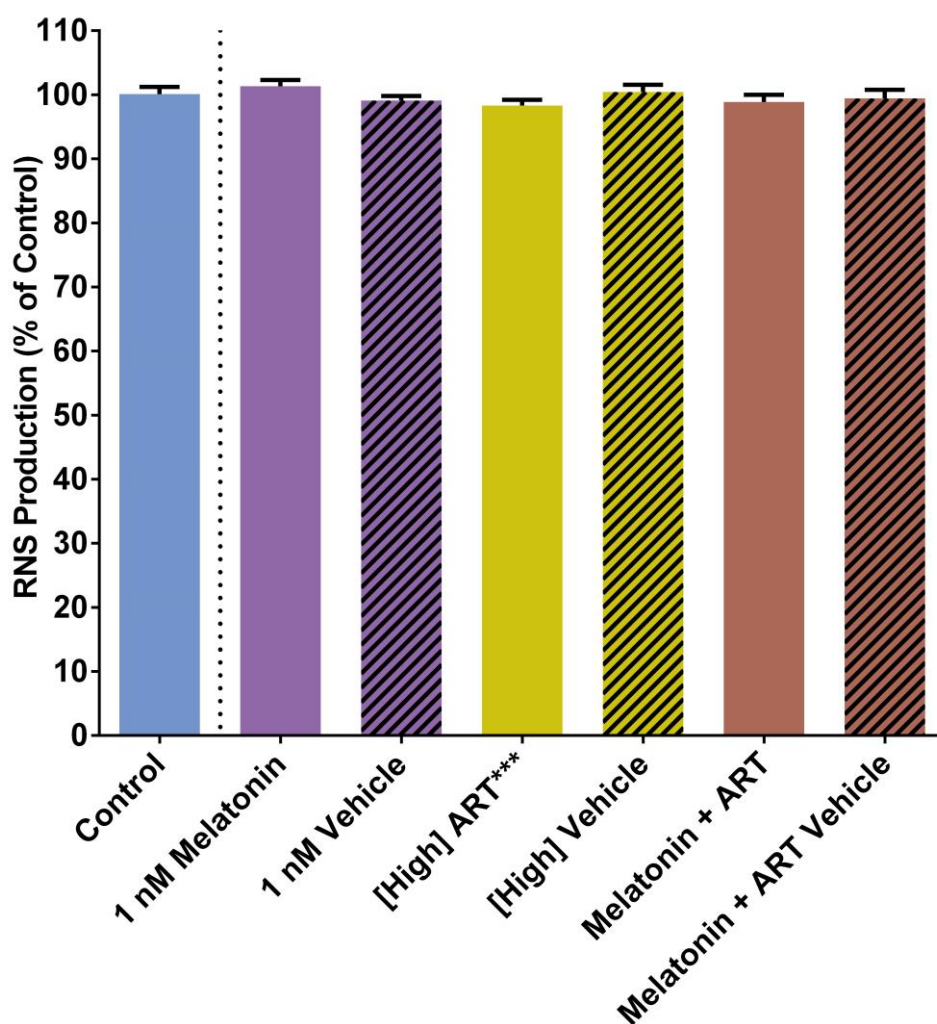


*** EFV=12 μ M; FTC = 10 μ M; TDF= 1 μ M

Figure 4.10: The effects of 24h SS followed by 24h melatonin and ART combination treatment on NO production measured by DAF-2/DA fluorescence. NO production expressed as % DAF-2/DA stained cells (calculated as a percentage of the untreated control group; Control fluorescence adjusted to 100 %), n = 3/ group.

DHR-123: RNS Production

AECs were exposed to 24 hours of SS followed by treatment with 1 nM melatonin ($101.3 \pm 0.9574\%$), high concentration ART ($98.33 \pm 0.8819\%$), as well as a combination of 1 nM melatonin + high concentration ART ($98.89 \pm 1.124\%$) for 24 hours. Results showed no differences in mean DHR-123 fluorescence (RNS production) between the treatment groups and the untreated control group ($100.0 \pm 1.124\%$) (Fig 4.11). No changes were observed in any vehicle groups.

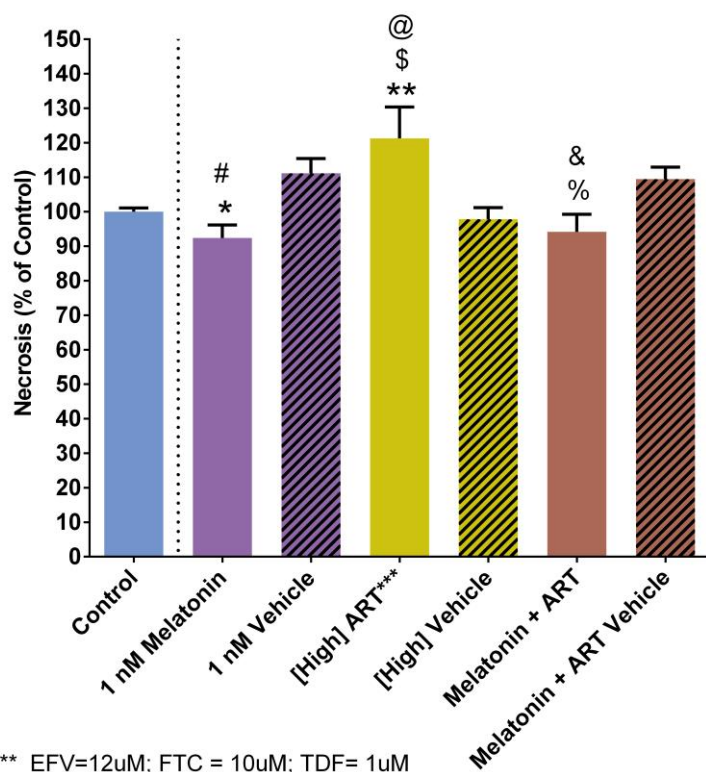


*** EFV=12uM; FTC = 10uM; TDF= 1uM

Figure 4.11: The effects of 24h SS followed by 24h melatonin and ART combination treatment on DHR-123 fluorescence. RNS production expressed as % DHR-123 stained cells (calculated as a percentage of the untreated control group; Control fluorescence adjusted to 100 %), n = 3/ group.

PI: Cell Viability (Necrosis)

AECs were exposed to 24 hours of SS followed by treatment with 1 nM melatonin ($92.43 \pm 3.753\%$), high concentration ART ($121.3 \pm 9.114\%$), as well as a combination of 1 nM melatonin + high concentration ART ($94.17 \pm 5.082\%$) for 24 hours. When compared to the untreated control group ($100.0 \pm 1.067\%$), 1 nM melatonin was seen to significantly decrease mean PI fluorescence (necrosis). In contrast, the high concentration ART treatment group significantly increased mean PI fluorescence compared to the control, as well as compared to the 1 nM melatonin treatment group. When combined, the melatonin + ART treatment group significantly decreased mean PI fluorescence compared to the group treated with only ART. All treatment groups showed significant differences when compared to their relative vehicles (1nM Mel Veh: $111.2 \pm 4.277\%$; High ART Veh: $97.83 \pm 3.381\%$; Mel + ART Veh: $109.5 \pm 3.413\%$) (Fig 4.12).



*** EFV=12uM; FTC = 10uM; TDF= 1uM

*: $p < 0.0001$ vs control #: $p < 0.0001$ vs 1 nM vehicle

** : $p < 0.0001$ vs control \$: $p < 0.0001$ vs [high] vehicle

@: $p < 0.0001$ vs 1 nM melatonin

%; $p < 0.0001$ vs melatonin + ART vehicle

&: $p < 0.0001$ vs [high] ART

Figure 4.12: The effects of 24h SS followed by 24h melatonin and ART combination treatment on PI fluorescence. Necrosis expressed as % PI stained cells (calculated as a percentage of the untreated control group; Control fluorescence adjusted to 100 %), $n = 3/$ group.

4.2 Western Blot Analyses

For *in vitro* cell signaling protein investigations, AECs were serum starved for 24 hours and then treated with a combination of 1 nM melatonin and high concentration ART (EFV: 12 μ M; FTC: 10 μ M; TDF: 1 μ M) for a further 24 hours. The cells were used to make protein lysates as described in section 2.4. All western blot experimental groups contained a combined vehicle, which allowed for all groups to be directly compared without considering a vehicle effect.

For Western blot data, controls were adjusted to the value of 1. Total protein expression was calculated as a ratio of the loading control. A p-value of < 0.05 was considered statistically significant.

4.2.1 NO & RNS Signalling

For NO and reactive nitrogen species (RNS) signalling, total- and phosphorylated eNOS; total iNOS and total nitrotyrosine were examined. eNOS and iNOS are important signaling molecules in the production of NO, while nitrotyrosine is a marker of nitrosative stress.

4.2.1.1 eNOS

eNOS phosphorylation was significantly lower in the melatonin (0.6354 \pm 0.04195), ART (0.4348 \pm 0.05156) and melatonin + ART (0.2535 \pm 0.03983) treatment groups compared to the control (1.000 \pm 0.1068). The melatonin + ART treatment group also showed significantly less levels of eNOS phosphorylation compared to the melatonin treatment group (Fig 4.13 A).

No significant differences were seen in total eNOS expression between any of the treatment groups (Mel: 0.9188 \pm 0.1187; ART: 0.7479 \pm 0.09084; Mel + ART: 0.8895 \pm 0.04375) when compared to the control (1.000 \pm 0.1330) (Fig 4.13 B).

When eNOS phospho/total (P/T) ratios were calculated, the same pattern of significance emerged as was seen for the eNOS phosphorylation levels. All treatment groups showed significantly lower P/T eNOS levels (Mel: 0.5630 \pm 0.01973; ART: 0.4298 \pm 0.02480; Mel + ART: 0.2614 \pm 0.05717) compared to the control (1.000 \pm 0.1207), while the melatonin + ART treatment group had lower P/T eNOS levels when compared to the melatonin treatment group (Fig 4.13 C).

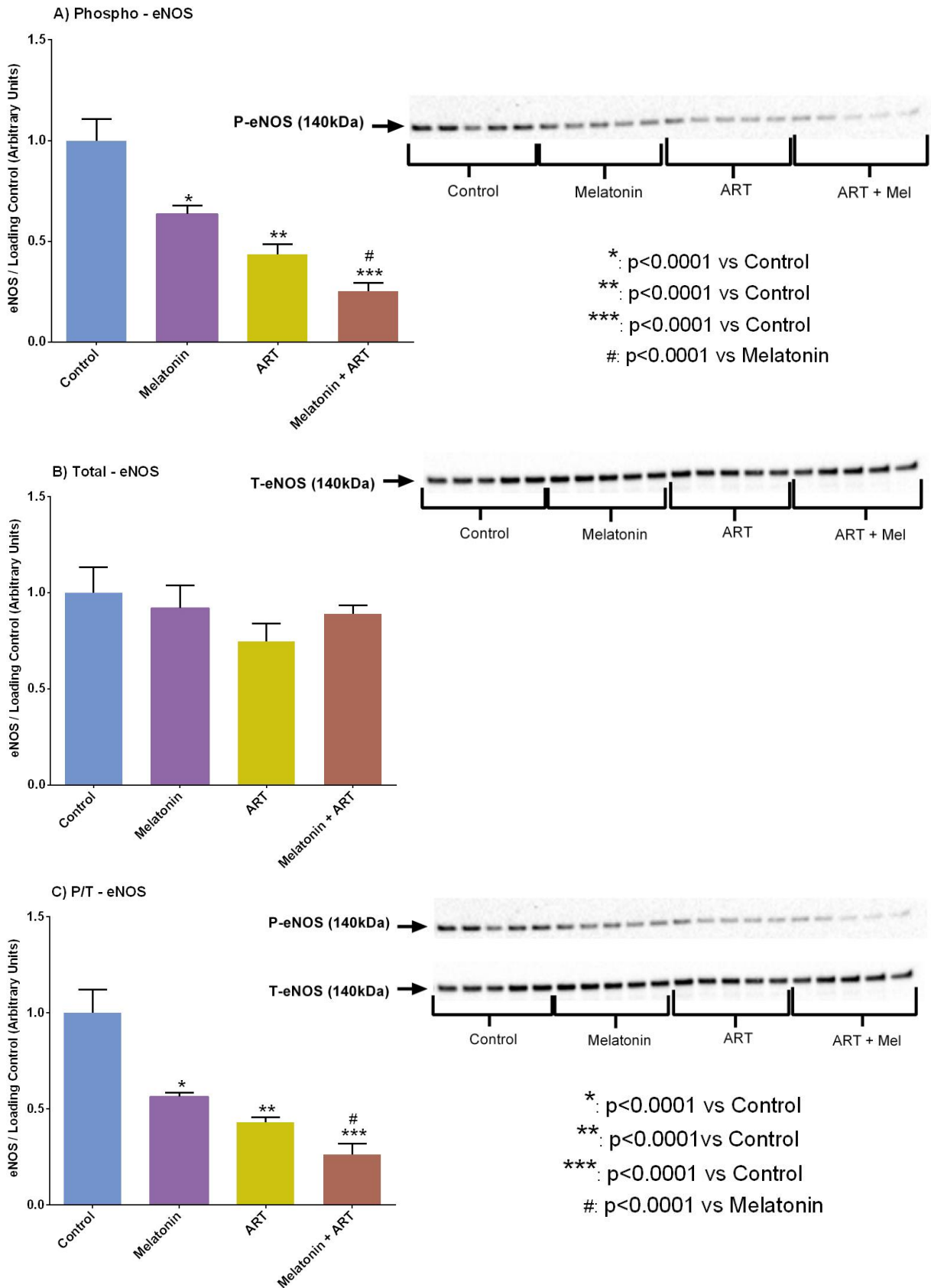


Figure 4.13: Changes in the eNOS phosphorylation and expression (Ser 1177) of AECs treated with melatonin and/or ART, for 24 hours. A) Analysed results and western blot for phospho-eNOS (Ser 1177); B) Analysed results and western blot for total-eNOS; C) Phosphorylated over total (P/T) ratio of eNOS (Ser 1177) (n=5/ group).

4.2.1.2 iNOS

No band was detected for iNOS and therefore no statistical analyses could be conducted (Fig 4.14).

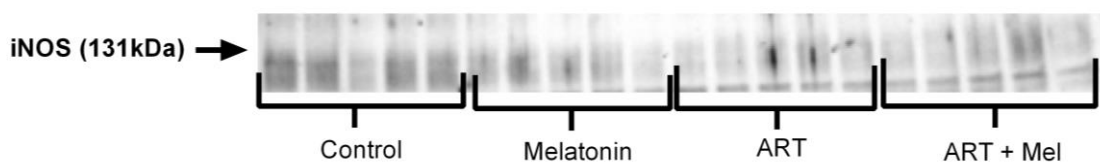


Figure 4.14: No iNOS band was detected in AECs treated with melatonin and/or ART, for 24 hours. Shown is the western blot for iNOS (n=5/ group).

4.2.1.3 Nitrotyrosine

Nitrotyrosine levels in the ART treatment group (2.309 ± 0.3443) was significantly higher compared to the control group (1.000 ± 0.1707). When melatonin and ART were combined (1.266 ± 0.2876), nitrotyrosine levels decreased significantly compared to the group that was treated with ART alone (Fig 4.15). There were no significant differences seen in the melatonin group (2.825 ± 1.564).

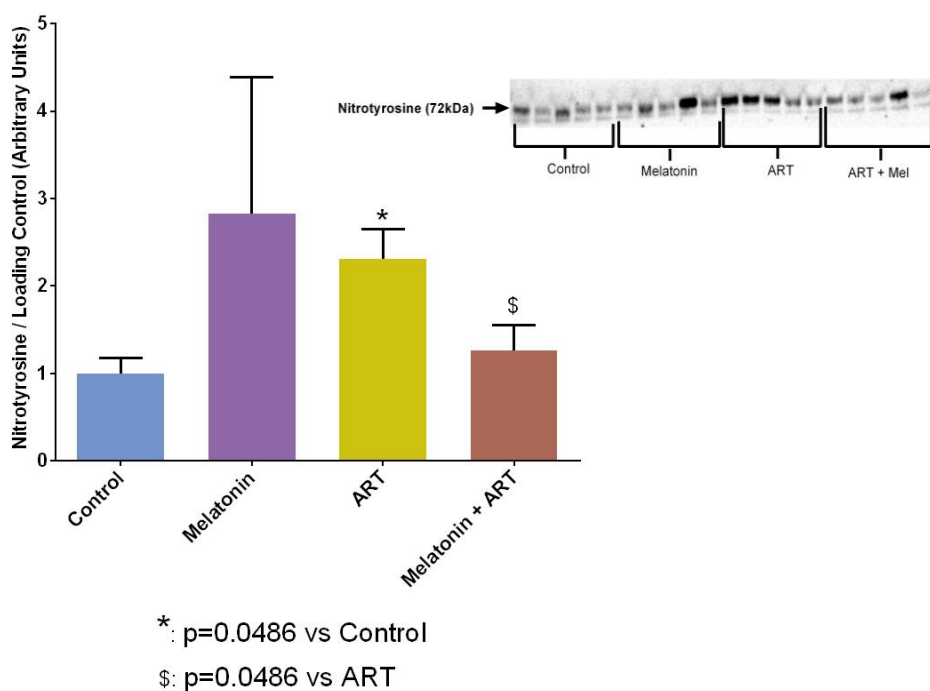


Figure 4.15: Changes in nitrotyrosine levels of AECs treated with melatonin and/or ART, for 24 hours. Shown are the analysed results and western blot for nitrotyrosine (n=5/ group).

4.2.2 ROS Signalling

For reactive oxygen species (ROS) signalling, total- p22 PHOX was examined. p22 PHOX is a marker for NADPH-oxidase derived superoxide (Fukui et al., 1997), a reactive oxygen anion.

4.2.2.1 p22 PHOX

All treatment groups showed decreased p22 PHOX expression compared to the control (1.000 ± 0.1518). Both the ART (0.2039 ± 0.04277) and melatonin + ART (0.2587 ± 0.008877) combination treatment groups also showed significantly decreased p22 PHOX expression compared to the melatonin (0.5217 ± 0.08199) treatment group (Fig 4.16).

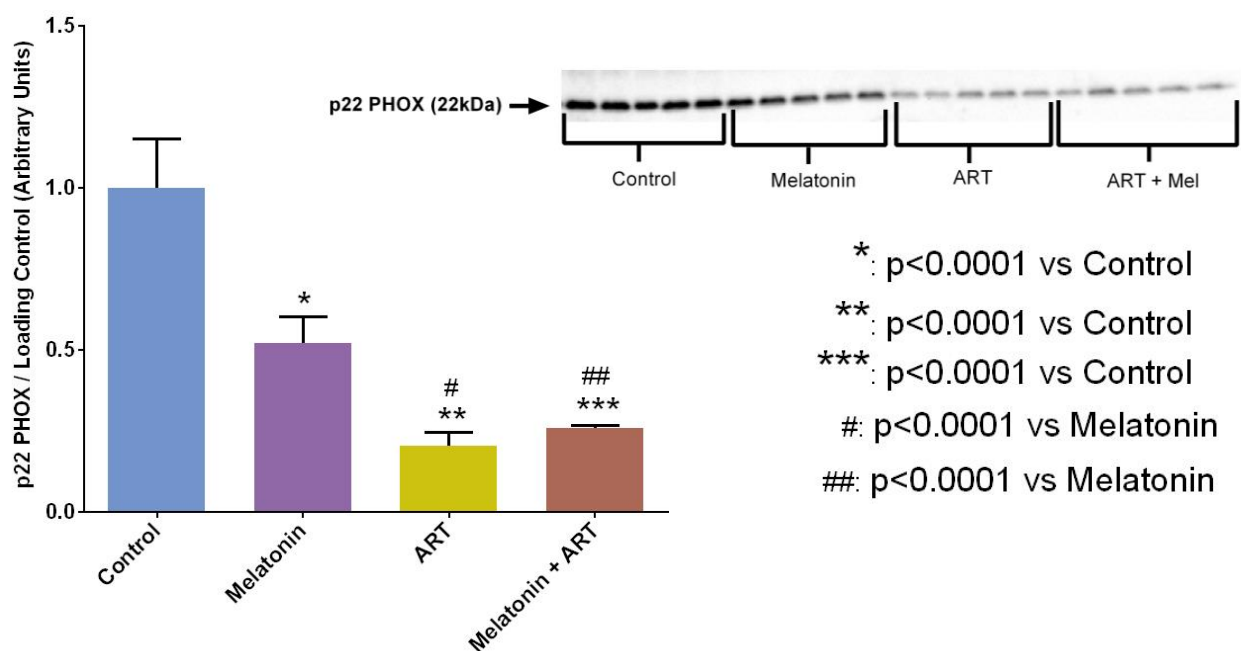


Figure 4.16: Changes in the p22 PHOX expression of AECs treated with melatonin and/or ART, for 24 hours. Shown are the analysed results and western blot for p22 PHOX (n=5/ group).

4.2.3 Cell Viability Signalling

For cell viability signalling, cleaved caspase-3 was examined. Cleaved caspase-3 is a marker of apoptosis (Kuribayashi, Mayes, & El-Deiry, 2006), which is a programmed form of cell death.

4.2.3.1 Cleaved Caspase-3

The ART (0.2519 ± 0.03783) and melatonin + ART (0.3878 ± 0.07965) combination treatment groups showed significantly decreased cleaved Caspase-3 expression compared to the control (1.000 ± 0.1775), as well as compared to the melatonin treatment group (0.7586 ± 0.08004) (Fig 4.17).

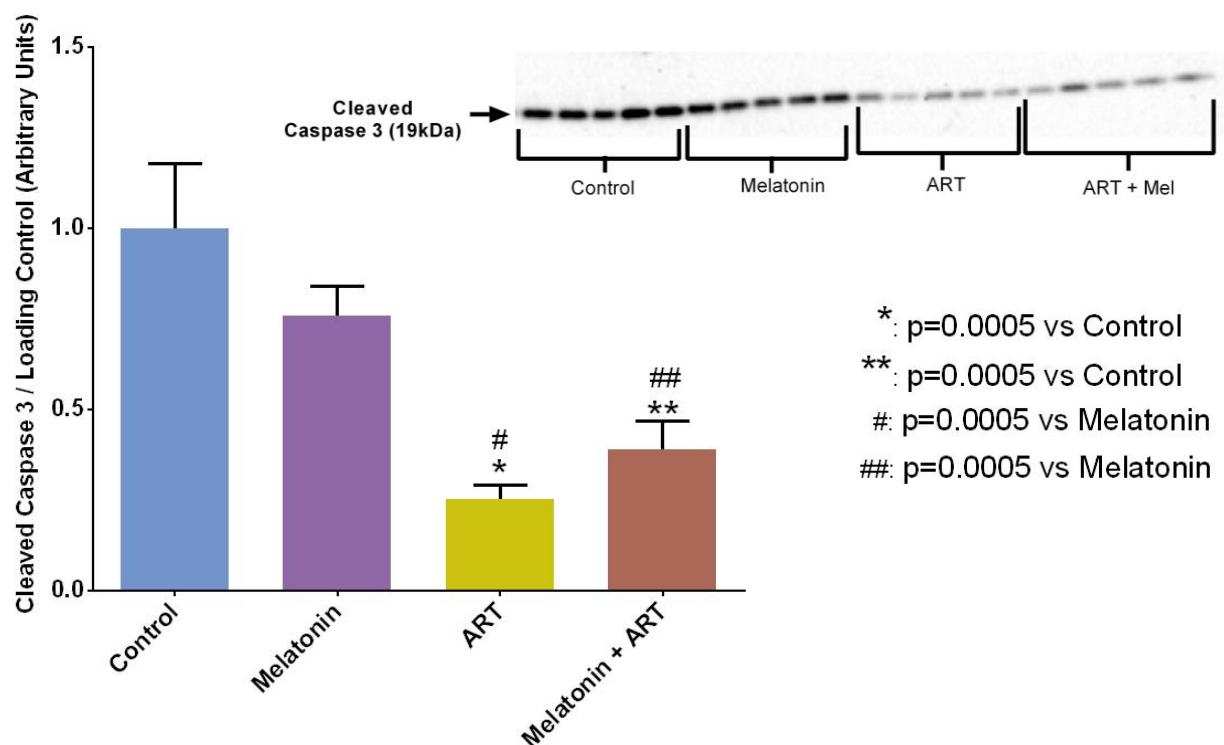


Figure 4.17: Changes in cleaved Caspase-3 expression of AECs treated with melatonin and/or ART, for 24 hours. Shown are the analysed results and western blot for cleaved Caspase-3 (n=5/group).

4.3 Antioxidant Capacity Analyses

For *in vitro* cell antioxidant capacity analyses, AECs were serum starved for 24 hours and then treated with a combination of 1 nM melatonin and high concentration ART (EFV: 12 μ M; FTC: 10 μ M; TDF: 1 μ M) for a further 24 hours. All experimental groups contained a combined vehicle, which allowed for all groups to be directly compared without considering a vehicle effect.

Antioxidant capacity is expressed in trolox equivalents, which is a vitamin-E analogue that is used as the standard measure of antioxidant capacity (Maarman et al., 2015). A p-value of < 0.05 was considered statistically significant.

4.3.1 ORAC Assay

No significant differences were seen between melatonin (0.3324 \pm 0.01852), ART (0.3134 \pm 0.01466) and melatonin + ART (0.3366 \pm 0.01324) treatment groups when compared to the control (0.2710 \pm 0.04975) (Fig 4.18).

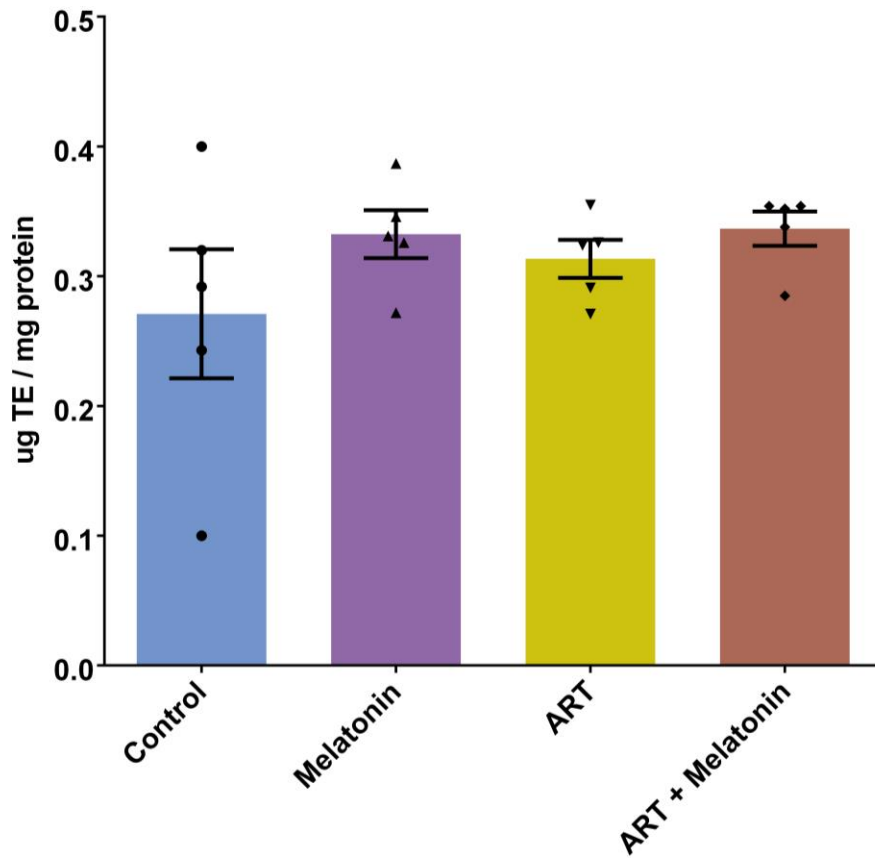


Figure 4.18: Antioxidant capacity of AECs treated with melatonin and ART, as well as a combined vehicle for 24 hours (n = 5/ group).

5 – Results: *Ex vivo* and *In vivo* studies

Chapter 5 describes and reports data collected from the *ex vivo* and *in vivo* studies, the materials and methods for which can be found in Chapter 3. See **Appendix I** for biometric data obtained from the treated rats during the treatment protocol.

5.1 *Ex Vivo* Studies

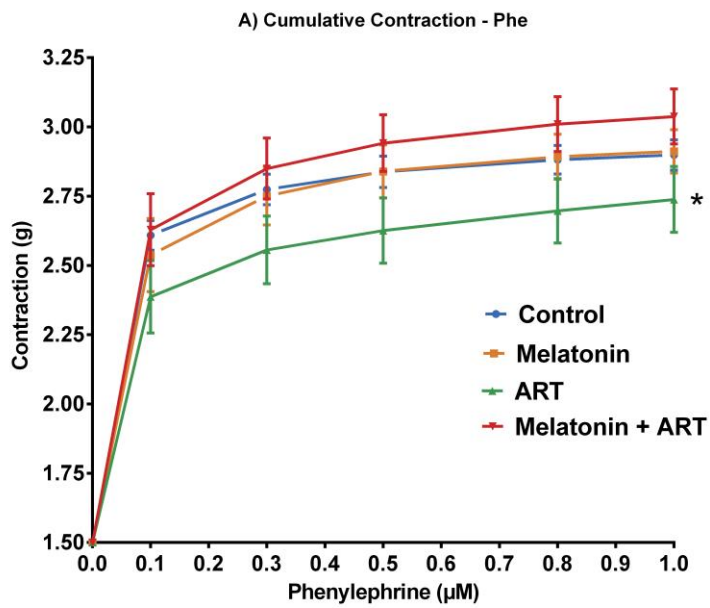
The main aim of the *ex vivo* studies was to determine the acute effects of melatonin and ART administration on the vascular reactivity of untreated, control male Wistar rat aortas. To achieve this, drugs were administered as a pre-treatment, directly to an *ex vivo* organ bath containing a stabilised rat aortic ring. For *ex vivo* studies, 10 μM melatonin was used, along with high concentration ART (EFV: 12 μM ; FTC: 10 μM ; TDF: 1 μM). Following the 30-minute drug pre-treatment, aortic contraction was induced through the cumulative administration of Phe (100 nM – 1 μM). Once maximum contraction was reached, aortic relaxation was induced through the cumulative administration of Ach (30 nM – 10 μM). *Ex vivo* treatment groups all contained a combined vehicle. Only endothelium-dependent *ex vivo* studies were conducted due to limited availability of rats, and well as due to the novel nature of these investigations. No L-NAME control experiments were included for the *ex vivo* studies due to limited equipment availability. For all *ex vivo* isometric tension studies, Phe-contraction results are expressed as an increase in gram tension from a resting tension of 1.5 g, while Ach-relaxation results are expressed as % relaxation of the maximum phenylephrine-pre-contraction. A p-value of < 0.05 was considered statistically significant.

5.1.1 Phe-contraction / Ach-relaxation

Cumulative contraction with Phe, showed that the ART treated aortas contracted (measured by increase in g tension from a stable point of 1.5 g) significantly less when compared to all other treatment groups (Two-way ANOVA Con: p=0.0070; Mel: p=0.0250; Mel + ART: p=0.0001 vs ART) (Fig 5.1 A).

The addition of Ach induced significantly less relaxation (measured by the % decrease in g tension from the point of maximal contraction) in the melatonin + ART group compared to the control group (Two-way ANOVA Con: p=0.0148 vs Mel+ART) (Fig 5.1 B).

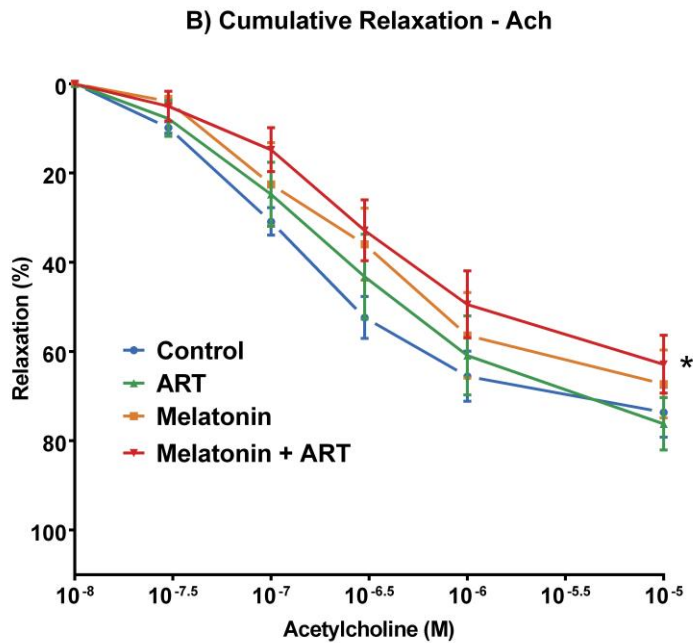
No significant differences were seen in E_{max} values between the different groups (See **Table 5.1**. for E_{max} values). E_{max} is the maximal response of the system.



*: $p \leq 0.0070$ vs control

*: $p = 0.0250$ vs melatonin

*: $p = 0.0001$ vs ART + Mel



*: $p \leq 0.0148$ vs control

Figure 5.1: Graphs indicating the effects of *ex vivo* melatonin and ART treatment on Phe induced contraction and Ach induced relaxation. A) Aortic ring contractions in response to cumulative concentrations of Phe; B) Aortic ring relaxation in response to cumulative concentrations of Ach (n = 5-6/ group).

Table 5.1: *Ex vivo* E_{max} values for the various treatment groups. Phe was used to induce contraction, and Ach was used to induce relaxation.

		Control	Melatonin	ART	Melatonin + ART
Phe (g)	E _{max}	2.998 ±	3.043 ±	2.833 ±	3.171 ±
	± SEM	0.1244	0.1519	0.1369	0.1598
Ach (%)	E _{max}	78.56 ±	67.47 ±	75.50 ±	61.01 ±
	± SEM	4.682	4.275	4.685	4.572

5.2 *In Vivo* Studies

The main aim of the *in vivo* studies was to determine the chronic effects of melatonin and ART administration on the vascular reactivity of male wistar rats that have been treated for 8 weeks with melatonin and/or ART. Additional aims included examining various protein activation and/or expression levels, as well as the antioxidant capacity exhibited in the aortic tissue of these same male Wistar rats.

For these *in vivo* studies, 80 male Wistar rats were randomly divided into four treatment groups: control, melatonin (10 mg/kg/day), ART (EFV: 51.6 mg/kg; FTC: 17.4 mg/kg; TDF: 25.8 mg/kg) and melatonin + ART. The rats received the respective treatments for 8 weeks, after which the animals were sacrificed, the aortas removed and the following data were obtained.

A p-value of < 0.05 was considered statistically significant.

5.2.1 Endothelium-dependent aortic ring investigations

As mentioned in section 3.3.3.2, two types of aortic ring investigations were conducted. The first set of aortic ring investigations conducted, were endothelium-dependent relaxation studies. For these studies, Phe was used to induce contraction and Ach was used to induce relaxation (as previously described above in section 5.1). As a negative control for the endothelium-dependent relaxation studies, some of the rings were pre-treated with the NOS inhibitor, L-NAME (100 µM) 15 minutes prior to the administration of cumulative amounts of Phe and Ach in order to confirm that the relaxation responses were indeed derived from endothelial NOS-NO release.

5.2.1.2 Phe-contraction / Ach-relaxation

Cumulative contraction with Phe, showed that the ART and melatonin + ART treatment groups contracted significantly more overall, when compared to the control group (Two-way ANOVA Con: $p < 0.0001$ vs ART; Mel+ART) (Fig 5.2 A).

Ach induced relaxations were similar for all treatment groups (Fig 5.2 B).

No significant differences were seen in E_{max} values between the different groups (See **Table 5.2.** for E_{max} values).

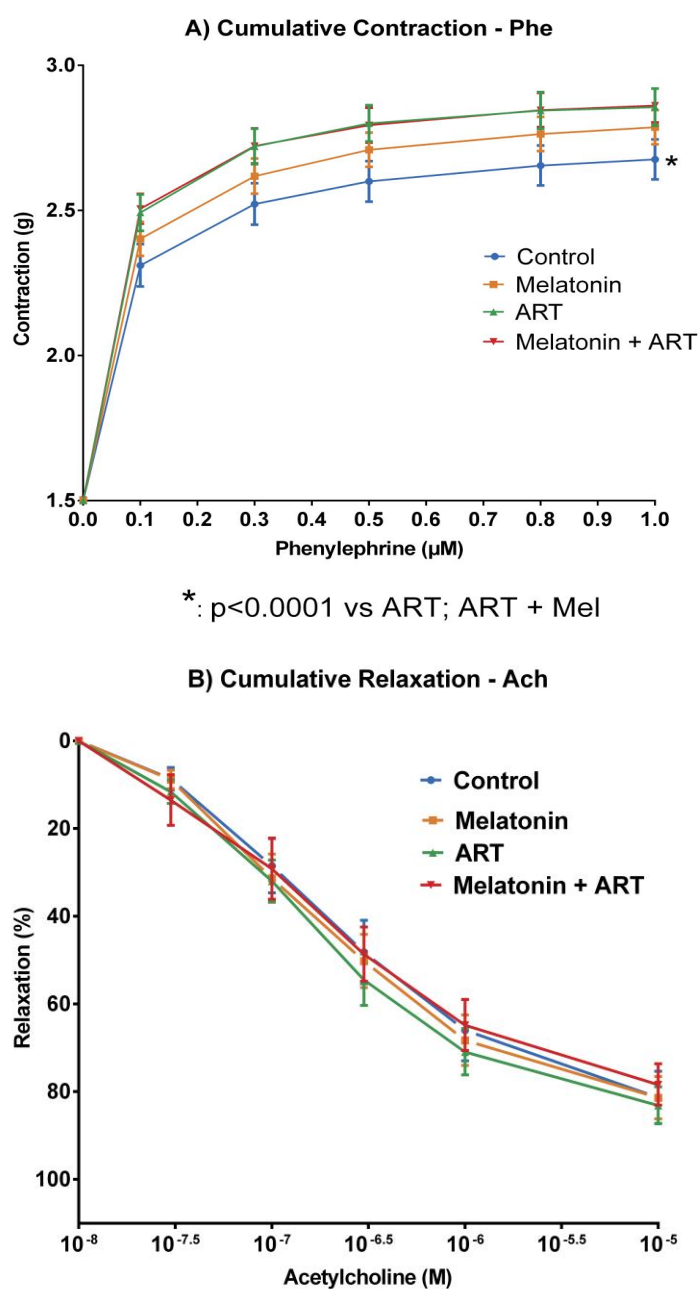


Figure 5.2: Graphs indicating the effects of *in vivo* melatonin and ART treatment on Phe induced contraction and Ach induced relaxation. A) Aortic ring contractions in response to cumulative concentrations of Phe; B) Aortic ring relaxation in response to cumulative concentrations of Ach (n = 12-16/ group).

Table 5.2: *In vivo* E_{max} values for the various treatment groups. Phe was used to induce contraction, and Ach was used to induce relaxation.

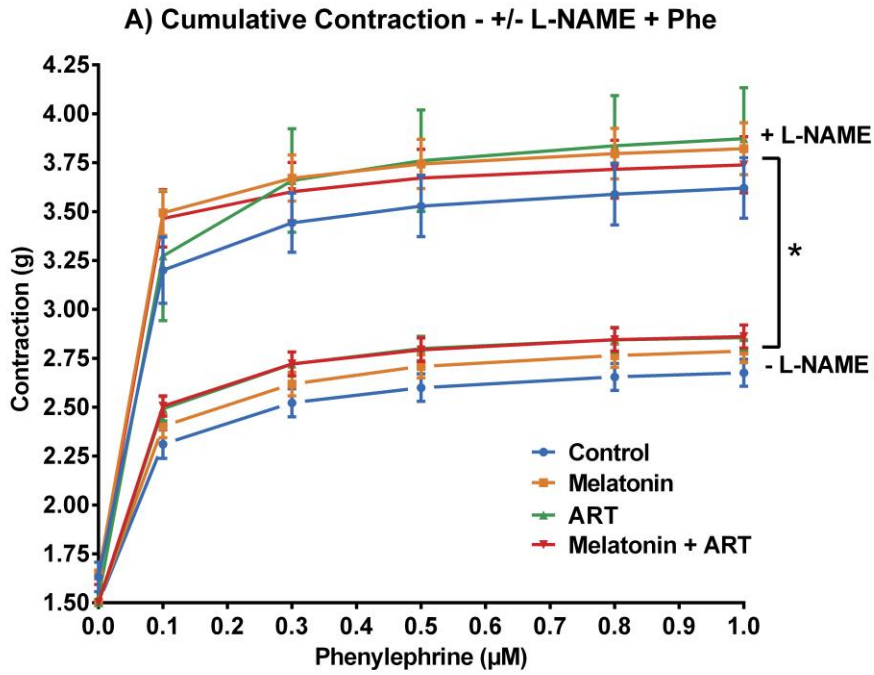
		Control	Melatonin	ART	Melatonin + ART
Phe (g)	E _{max}	2.635 ±	2.862 ±	2.852 ±	2.851 ±
	± SEM	0.07303	0.07496	0.07322	0.07378
Ach (%)	E _{max}	79.80 ±	81.49 ±	84.34 ±	77.72 ±
	± SEM	3.656	3.662	3.568	3.878

5.2.1.3 L-NAME + Phe-contraction / Ach-relaxation

Phe Contraction Studies

Pre-treatment with 100 µM L-NAME caused all treatment groups (Two-way ANOVA $p < 0.0001$ in all groups) to contract significantly more when compared to their respective L-NAME treated group (Fig 5.3 A). The L-NAME+control ($3.714 \pm 0.2148\text{g}$) and L-NAME+melatonin ($3.890 \pm 0.1897\text{g}$) groups experienced a $\pm 35\%$ increase in contraction at the maximum Phe concentration compared to the control ($2.761 \pm 0.07774\text{g}$) and melatonin ($2.876 \pm 0.08195\text{g}$) groups, respectively (Fig 5.3 A). The L-NAME+ART ($4.021 \pm 0.2713\text{g}$) group experienced a similar increase in maximum contraction of $\pm 36\%$ when compared to the ART ($2.953 \pm 0.07830\text{g}$) group. L-NAME+Mel+ART experienced a slightly smaller, but still noteworthy increase in maximum contraction of $\pm 29\%$ when compared to the Mel+ART ($2.950 \pm 0.07860\text{g}$) group (Fig 5.3 A).

However, when L-NAME pre-treated groups were compared with each other, there were no differences seen in Phe induced contraction (Fig 5.3 B), between any of the treatment groups.



* $p < 0.0001$: Control vs L-NAME Control

* $p < 0.0001$: Melatonin vs L-NAME Melatonin

* $p < 0.0001$: ART vs L-NAME ART

* $p < 0.0001$: Mel+ART vs L-NAME Mel+ART

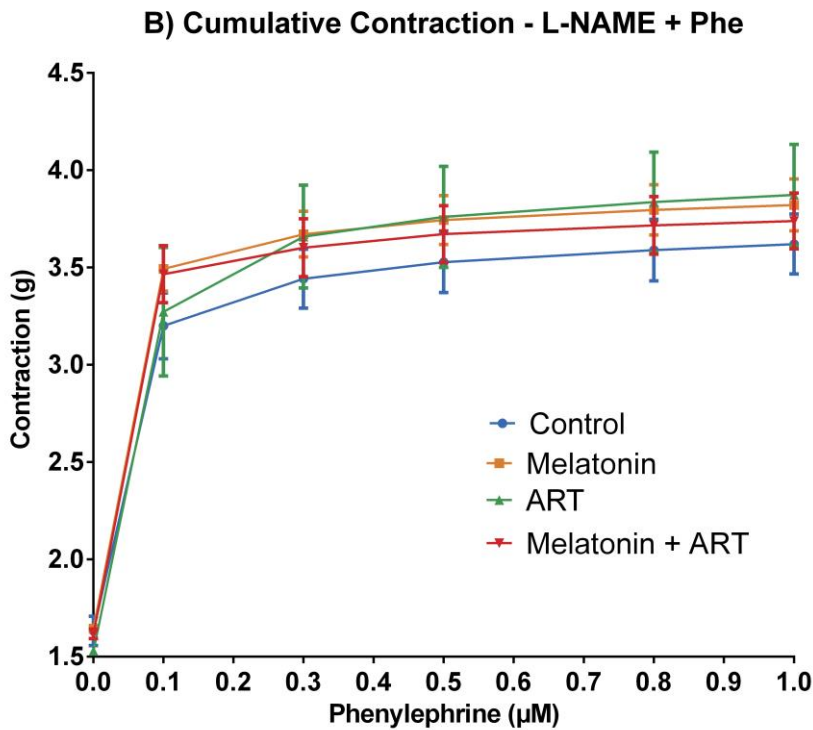


Figure 5.3: The effects of L-NAME pre-administration on Phe-induced contraction. A) The differences in contraction of aortic rings between treatment groups incubated with or without L-NAME. B) The differences in contraction of aortic rings between treatment groups pre-treated with L-NAME (n = 4-5/ group).

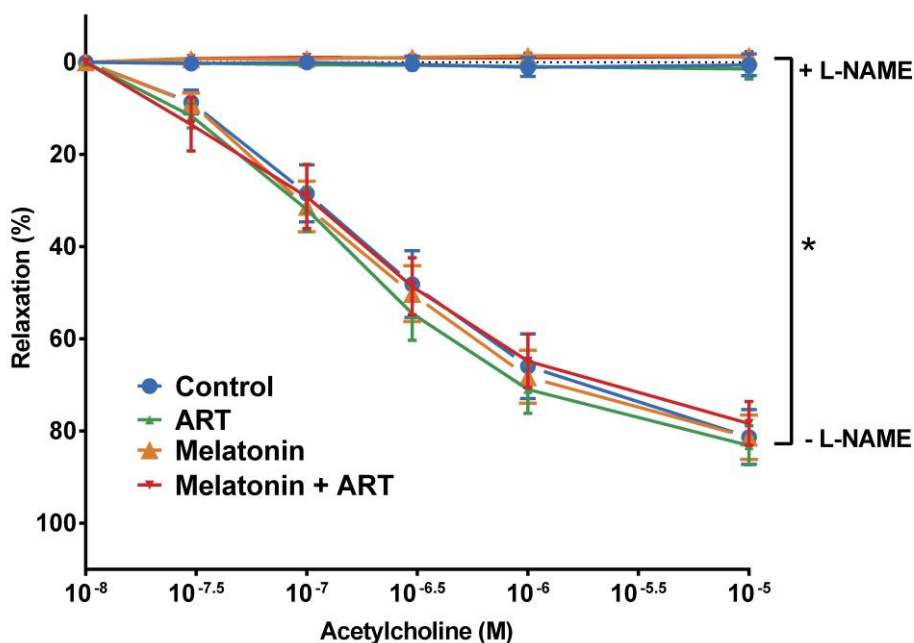
Ach Relaxation Studies

Figure 5.4 A shows that all treatment groups exposed to L-NAME pre-administration relaxed significantly less (Two-way ANOVA $p < 0.0001$ in all groups) when compared to the applicable treatment groups not exposed to L-NAME pre-treatment. The L-NAME+control ($0.7550 \pm 0.7187\%$) and L-NAME+ART ($1.191 \pm 0.6933\%$) groups experienced a $\pm 99\%$ decrease in relaxation capacity at the maximum Phe concentration compared to the control ($79.80 \pm 3.656\%$) and ART ($84.34 \pm 3.568\%$) groups, respectively (Fig 5.4 A). The L-NAME+melatonin ($-1.479 \pm 0.7575\%$) and L-NAME+Mel+ART ($-1.245 \pm 0.7238\%$) groups both continued to contract, even following the addition of the full cumulative dose of Ach (Fig 5.4 A). This meant the final tension (g) after the cumulative addition of Ach in these two groups, was higher when compared to the final tension seen after the accumulative addition of Phe. When the final mean tension values are compared (after the accumulative addition of both Phe and Ach), we see that L-NAME+melatonin had a high ending mean tension of 2.21g, while the melatonin group had a much lower ending mean tension of 0.25g. The same trend was seen in the L-NAME+melatonin+ART group, which had a final mean tension of 2.15g, compared to the much lower final mean tension of 0.31g in the melatonin+ART.

When Ach induced relaxation in L-NAME pre-treated groups were compared with each other, there were once again no differences seen (Fig 5.4 B), between any of the treatment groups. Some aortas continued to contract after the addition of Ach following pre-treatment with L-NAME, which consequently resulted in negative E_{\max} values.

No significant differences were seen in E_{\max} values between the different groups (See **Table 5.3.** for E_{\max} values).

A) Cumulative Relaxation - +/- L-NAME + Ach



- * p<0.0001: Control vs L-NAME Control
- * p<0.0001: Melatonin vs L-NAME Melatonin
- * p<0.0001: ART vs L-NAME ART
- * p<0.0001: Mel+ART vs L-NAME Mel+ART

B) Cumulative Relaxation - L-NAME + Ach

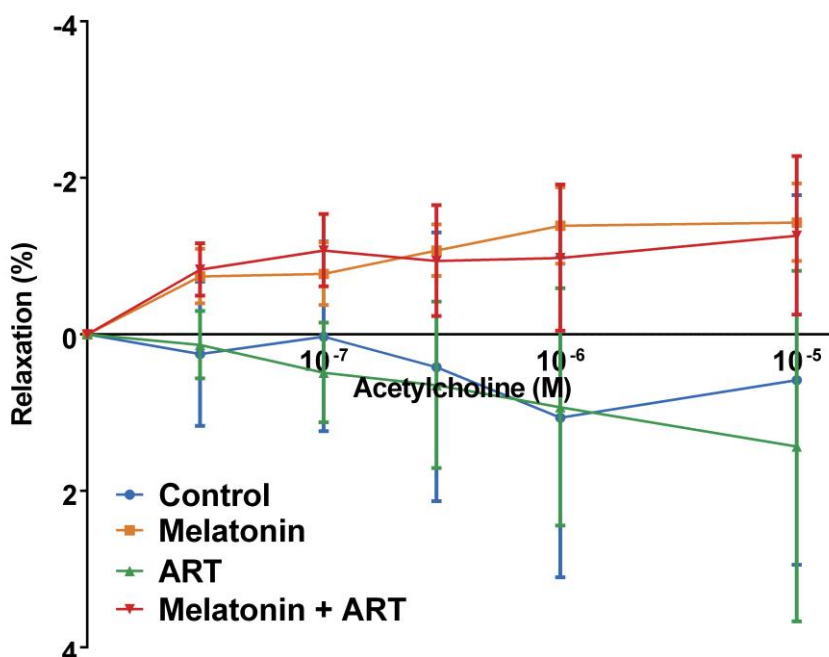


Figure 5.4: The effects of L-NAME pre-administration on Ach-induced relaxation. A) The differences in relaxation of aortic rings between treatment groups incubated with or without L-NAME. B) The differences in relaxation of aortic rings between treatment groups pre-treated with L-NAME (n = 4-5/ group).

Table 5.3: *In vivo* E_{max} values for L-NAME pre-treated treatment groups. Phe was used to induce contraction, and Ach was used to induce relaxation.

		Control	Melatonin	ART	Melatonin + ART
Phe (g)	E _{max}	3.714 ±	3.890 ±	4.021 ±	3.793 ±
	± SEM	0.2148	0.1897	0.2713	0.1767
Ach (%)	E _{max}	0.7550 ±	-1.479 ±	1.191 ±	-1.245 ±
	± SEM	0.7187	0.7575	0.6933	0.7238

5.2.2 Endothelium-independent aortic ring investigations

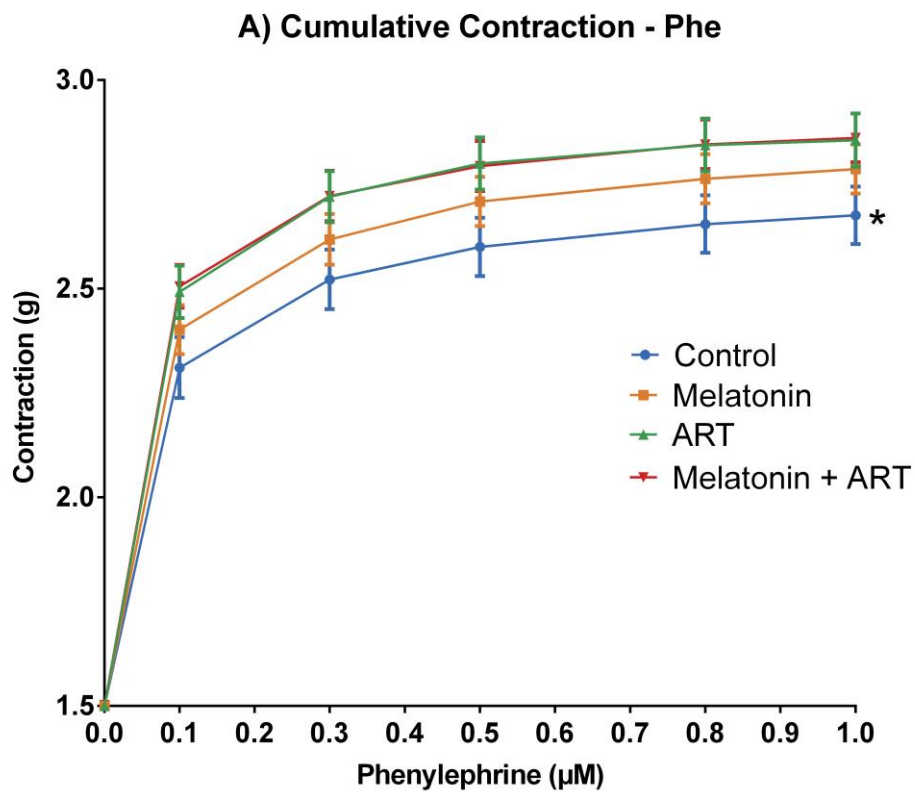
The second set of aortic ring investigations conducted, were endothelium-independent relaxation studies. For these studies, Phe was once again used to induce contraction, however, SNP - an exogenous NO donor - was used to induce relaxation.

5.2.2.1 Phe-contraction / SNP-relaxation

Cumulative contraction with Phe, showed that the ART and melatonin + ART treatment groups exhibited significant pro-contraction properties compared to the control group (Two-way ANOVA Con: $p < 0.0001$ vs ART; Mel+ART) (Fig 5.5 A).

SNP induced relaxations were similar for all treatment groups (Fig 5.5 B).

No significant differences were seen in E_{max} values between the different groups (See **Table 5.4.** for E_{max} values).



*: $p < 0.0001$ vs ART; ART + Mel

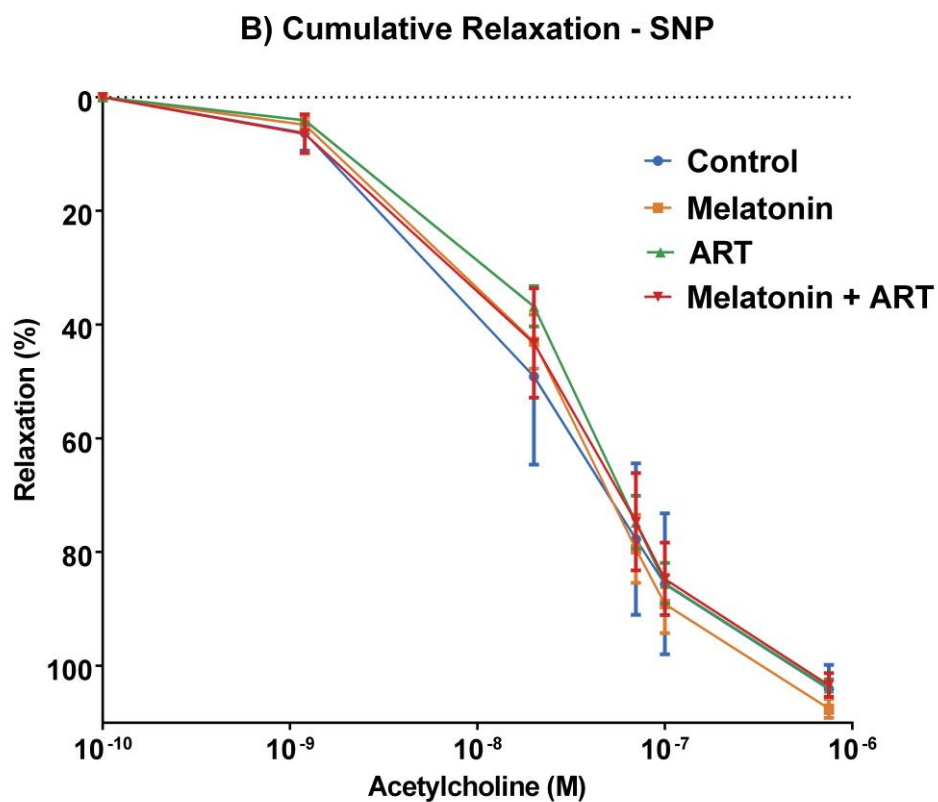


Figure 5.5: Graphs indicating the effects of *in vivo* melatonin and ART treatment on Phe induced contraction and SNP induced relaxation. A) Aortic ring contractions in response to cumulative concentrations of Phe; B) Aortic ring relaxation in response to cumulative concentrations of SNP (n = 5/ group).

Table 5.4: *In vivo* E_{max} values for the various treatment groups. Phe was used to induce contraction, and SNP was used to induce relaxation.

		Control	Melatonin	ART	Melatonin + ART
Phe (g)	E _{max}	3.714 ±	3.890 ±	4.021 ±	3.793 ±
	± SEM	0.2148	0.1897	0.2713	0.1767
Ach (%)	E _{max}	110.3 ±	113.2 ±	108.1 ±	108.0 ±
	± SEM	4.639	3.860	4.153	4.130

5.2.3 Western Blot Analyses

Western blot analyses were performed on snap-frozen aortic tissue of control, melatonin, ART and melatonin + ART treated animals in order to determine whether the functional data of the vascular reactivity investigations could be explained by changes in intracellular signal transduction pathways.

All blots are calculated and expressed as a ratio of the corresponding loading controls. Controls are expressed as 1.

5.2.3.1 NO & RNS Signalling

eNOS

eNOS phosphorylation was significantly lower in the melatonin + ART (0.3292 ± 0.04093) treatment group compared to the control (1.000 ± 0.2814). No significant differences were seen in the phosphorylation levels of the melatonin (0.5541 ± 0.06424) or ART (0.5251 ± 0.1112) treatment groups (Fig 5.6 A)

No significant differences were seen in total eNOS expression between any of the treatment groups (Mel: 0.6192 ± 0.09478; ART: 0.5239 ± 0.07665; Mel + ART: 0.3522 ± 0.07480) when compared to the control (1.000 ± 0.3073) (Fig 5.6 B).

When eNOS P/T ratios were calculated, no significant differences were seen in total eNOS expression between any of the treatment groups (Con: 1.000 ± 0.04927; Mel: 1.081 ± 0.06813; ART 1.156 ± 0.07625; Mel+ART: 1.187 ± 0.1149) (Fig 5.6 C).

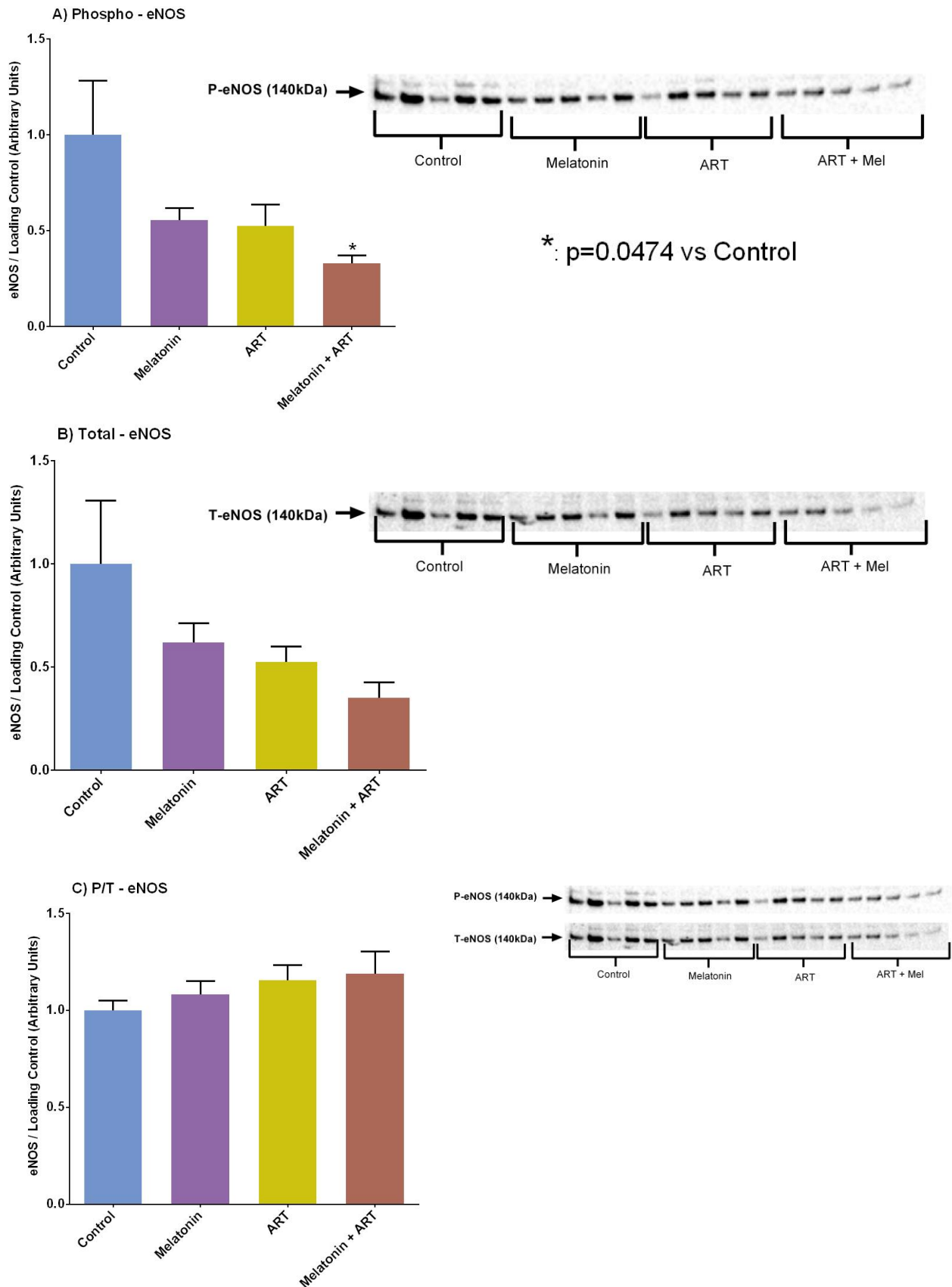


Figure 5.6: Changes in the eNOS phosphorylation and expression (Ser 1177) in aortic tissue from rats treated with melatonin and ART, *in vivo*. A) Analysed results and western blot for phospho-eNOS (Ser 1177); B) Analysed results and western blot for total-eNOS; C) Phosphorylated over total (P/T) ratio of eNOS (Ser 1177) (n=5/ group).

iNOS

No significant differences were seen in total iNOS expression between any of the treatment groups (Fig 5.7)

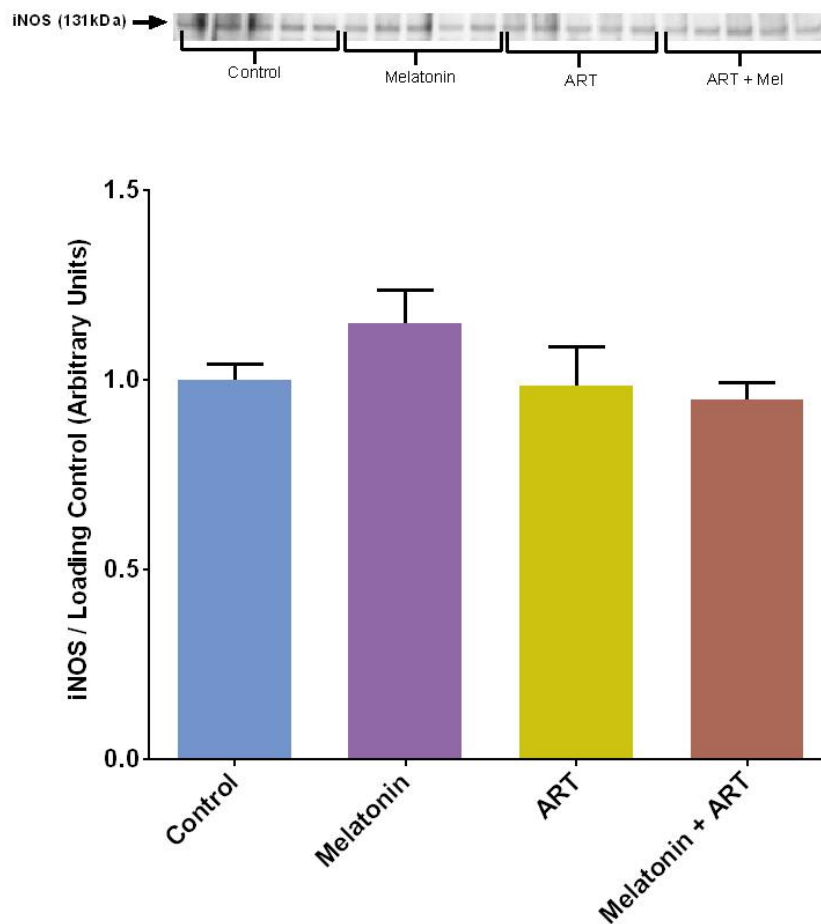


Figure 5.7: Changes in iNOS expression in aortic tissue from rats treated with melatonin and ART, *in vivo*. Shown are the analysed results and western blot for iNOS (n=5/ group).

Nitrotyrosine

No significant differences were seen in nitrotyrosine levels between any of the treatment groups (Fig 5.8)

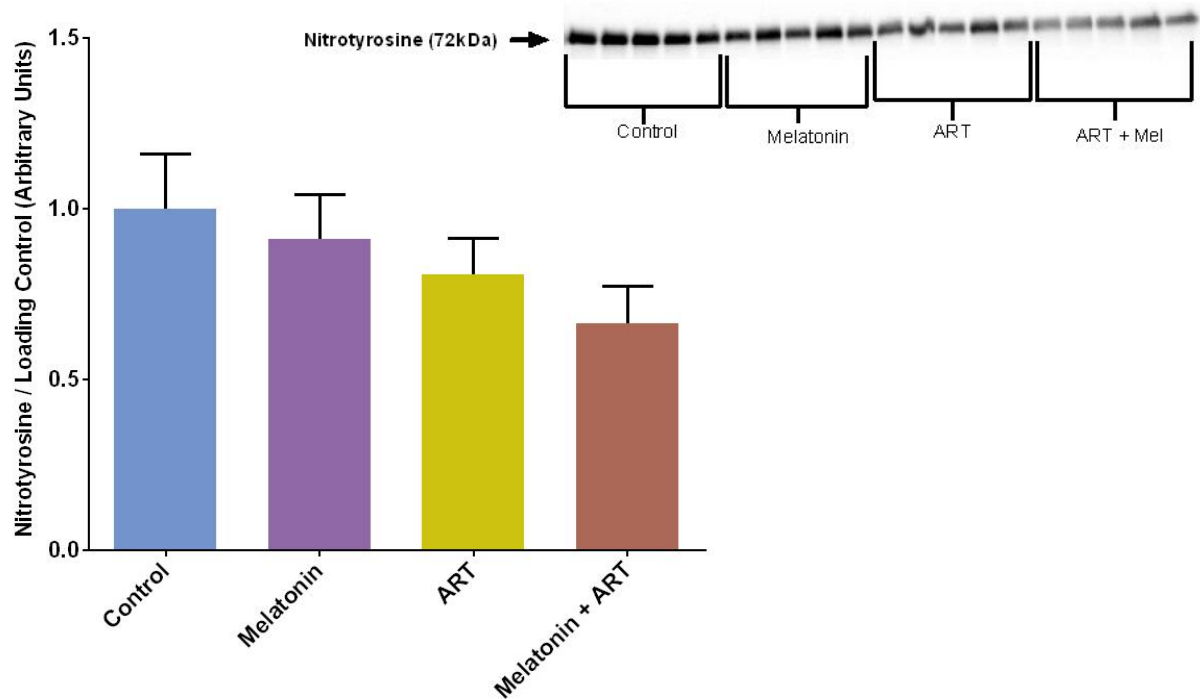


Figure 5.8: Changes in nitrotyrosine expression in aortic tissue from rats treated with melatonin and ART, *in vivo*. Shown are the analysed results and western blot for nitrotyrosine (n=5/ group).

5.2.3.2 ROS Signalling

p22 PHOX

No significant differences were seen in total p22 PHOX expression between any of the treatment groups (Fig 5.9).

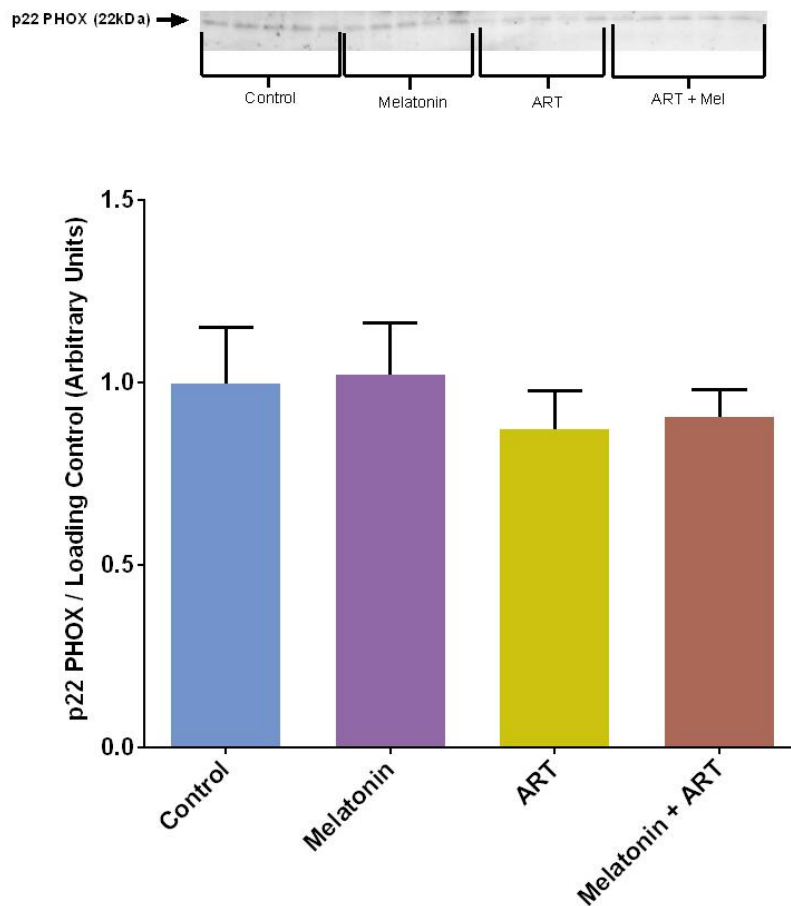
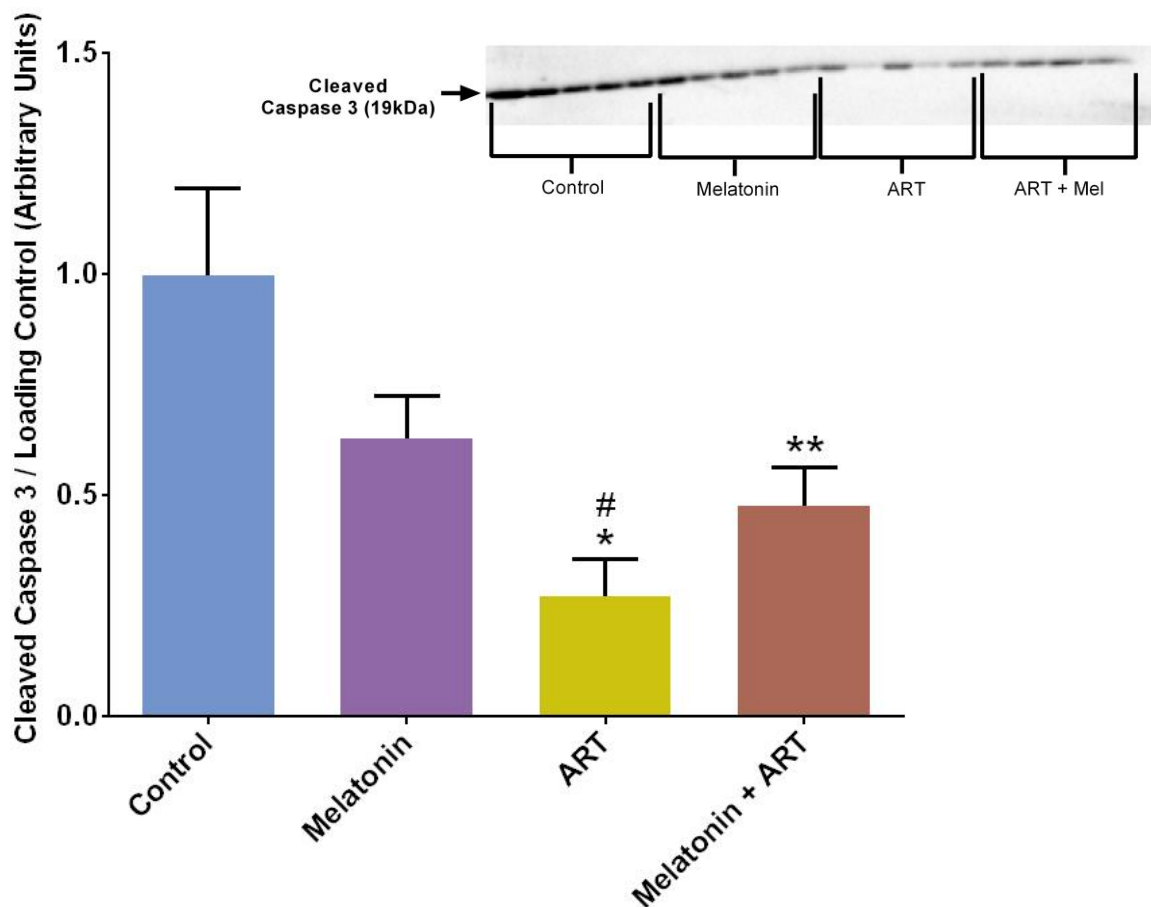


Figure 5.9: Changes in the p22 PHOX expression in aortic tissue from rats treated with melatonin and ART, *in vivo*. Shown are the analysed results and western blot for p22 PHOX (n=5/ group).

5.2.3.3 Cell Viability Signalling

Cleaved Caspase-3

The ART (0.2735 ± 0.08317) and melatonin + ART (0.4757 ± 0.08704) combination treatment groups showed significantly decreased cleaved Caspase-3 expression compared to the control (1.000 ± 0.1945). The ART treatment group also showed significantly decreased cleaved Caspase-3 expression when compared to the melatonin treatment group (0.6309 ± 0.09441) (Fig 5.10).



*: $p=0.0055$ vs Control

** : $p=0.0055$ vs Control

#: $p=0.0055$ vs Melatonin

Figure 5.10: Changes in cleaved Caspase-3 expression in aortic tissue from rats treated with melatonin and ART, *in vivo*. Shown are the analysed results and western blot for cleaved Caspase-3 ($n=5/$ group).

5.2.4 Antioxidant Capacity Studies

Antioxidant capacity studies were performed on snap-frozen aortic tissue of control, melatonin, ART and melatonin + ART treated animals.

Antioxidant capacity is expressed in trolox equivalents, which is a vitamin-E analogue that is used as the standard measure of antioxidant capacity.

5.2.4.1 ORAC Assay

No significant differences were seen between melatonin (0.0564 ± 0.01664), ART (0.0532 ± 0.01131) and melatonin + ART (0.07225 ± 0.006700) treatment groups when compared to the control (0.0430 ± 0.005899) (Fig 5.11).

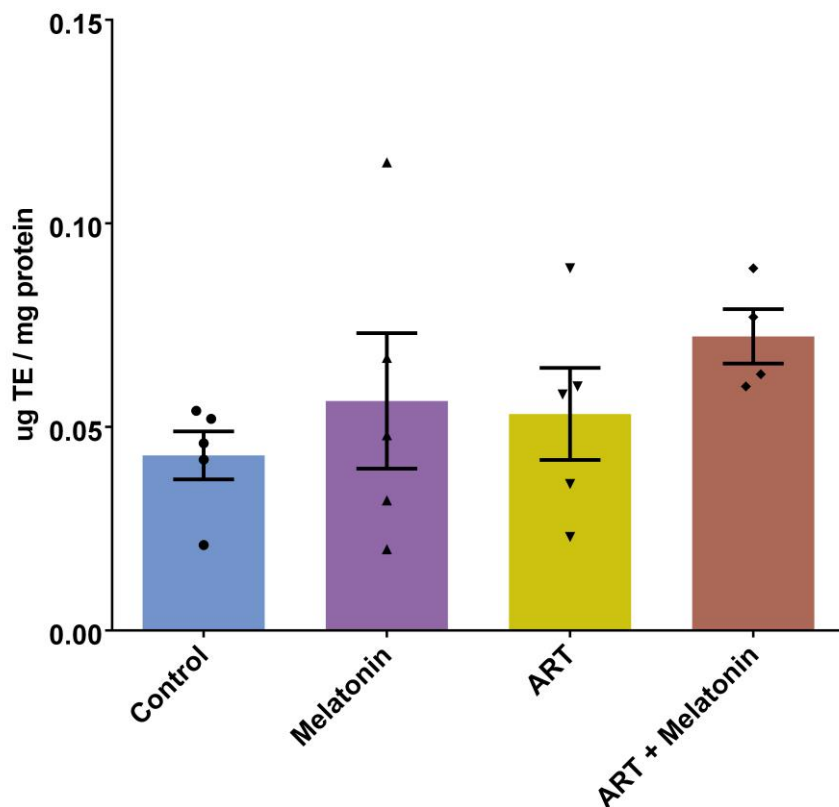


Figure 5.11: Antioxidant capacity of aortic tissue from rats treated with melatonin and ART, *in vivo* (n = 5/ group).

6 – Discussion: *In vitro* studies

Chapter 6 debates the findings of the results obtained from the *in vitro* study. The data discussed in this chapter can be found in Chapter 4, while the materials and methods can be found in Chapter 2.

Throughout the *in vitro* studies, we set out to examine three important variables: NO and RNS levels, ROS levels and cell viability. All three of these factors play important roles in the maintenance of endothelial health and vascular function (Mudau et al. 2012; K. Park & Park, 2015; Versari et al., 2009).

NO is viewed as an endothelial cell survival factor (Dimmeler & Zeiher, 1999), and a reduction in NO bioavailability is considered as a marker for ED (Muniyappa & Sowers, 2013). However, besides its important beneficial activities, in pathophysiological conditions excessive NO production may contribute to oxidative stress and an associated inflammatory state with eventual tissue damage (Pacher et al., 2007). Together, excessive NO or RNS, as well as ROS, can cause a decrease in cell viability and eventually lead to cell death (Circu & Aw, 2010; Fransen et al., 2012; Marín-García, 2016; Murphy, 1999). For cell viability and cell death, we examined both necrosis and apoptosis. Necrosis refers to the pathological or accidental mode of cell death involving irreversible swelling of the cytoplasm and distortion of organelles including mitochondria followed by rupture of the cell membrane and inflammation that damage the cells and its surrounding tissues (Fadeel & Orrenius, 2005). Apoptosis is a sequential process where the dying cell undergoes nuclear and cytoplasmic condensation with blebbing of the plasma membrane leading to formation of apoptotic bodies, which are recognised and removed, *via* phagocytosis by macrophages without damaging the surrounding tissues (Fadeel & Orrenius, 2005).

6.1 Melatonin Dose-Response

The antioxidant activity of melatonin has been reported at both physiological and pharmacological concentrations (Galano et al., 2011; Reiter et al., 2005), although pharmacological dosages of exogenously administered melatonin typically provide greater protection from large quantities of free radicals (Tan et al., 2007). In literature, *in vitro* melatonin supplementation studies conducted on various types of ECs have used a wide

range of melatonin concentrations. Some studies have used dosages as low as 0.1 nM (Tamura, Silva, & Markus, 2006), while others have used concentrations as high as 50 μ M (Pogan, Bissonnette, Parent, & Sauve, 2002). However, most studies used a concentration range between 1 nM and 10 μ M (Silva et al., 2007; Tamura, Cecon, Monteiro, Silva, & Markus, 2009; Urata et al., 1999), and therefore in this study, we decided to use 1 nM; 1 μ M and 10 μ M melatonin in the dose-response studies.

None of the three melatonin dosages tested, elicited any changes in NO (Fig 4.1 & 4.4) or RNS production (Fig 4.2 & 4.5), regardless of the treatment period (1h or 24h). This is contradictory to most *in vitro* findings in literature, where these concentrations of melatonin have been shown to decrease NO and RNS production (Jumnongprakhon, Govitrapong, Tocharus, & Tocharus, 2016; Reiter et al., 2001; Silva et al., 2007; Tamura et al., 2006; Tamura et al., 2009). However, the abovementioned studies were conducted using rat brain microvascular endothelial cells as well as rat microvascular cremaster muscle endothelial cells. Although these are also endothelial cell lines, the function of endothelial cells are specialised depending on their location (Gordon et al., 1991), making a direct comparison difficult. On the other hand, and in line with this investigation, a study by Tamura *et al.* (2006) found that the treatment of rat microvascular endothelial cells with 0.1 nM and 1 nM melatonin had no effect on NO production. However, the observed result in the aforementioned study is most likely due to the very short melatonin incubation period of 1 minute. No studies have been conducted with the specific ECs examined in this study, namely AECs. Therefore further studies would be needed to determine whether the lack of changes in NO and ROS levels observed in AECs, as shown in these results, is a standard response for an AEC, or if these findings are the result of the specific technique used. Various techniques are available to measure NO and RNS production, however, the low levels of NO and RNS produced by cultured vascular ECs *in vitro* exposes the sensitivity limits of many of these assays (Kleinhenz et al., 2003). In this case, a potential more sensitive alternative to fluorometric detection of NO and RNS may be to use a chemiluminescence technique, which has shown to detect these molecules at concentrations as low as 1 p.m., compared to the 2-5 nM detection capacity of the employed fluorometric method (Kleinhenz et al., 2003).

Conversely, the cell viability studies in the present study showed that 1 nM melatonin was the only concentration to decrease necrosis after a 24-hour treatment period (Fig 4.3),

which was in line with findings from other studies (Harms et al., 2000; Song et al., 2014). It was however expected that all melatonin concentrations would decrease necrosis, since the examined melatonin concentration range (1 nM; 1 μ M and 10 μ M) has been shown to increase cell viability over and incubation period of 24h, in multiple other studies (Celik & Maziroglu, 2012; Kim et al., 2011; Osseni et al., 2000). The lack of melatonin activity in the 1 μ M and 10 μ M treatment groups after 24 hours of treatment was therefore very surprising. In contrast, a study conducted on a human liver cell line (HepG2), showed that melatonin treatment at concentrations of 1-10,000 μ M over a longer treatment period (24–96 h) decreased cell viability (Osseni et al., 2000). This finding is line with another study conducted in our laboratory, which found that cardiac microvascular endothelial cells (CMECs) showed decreased cell viability after 6-24 h melatonin treatment (1 nM; 1 μ M and 10 μ M melatonin) (Nduhirabandi, 2014). In the current study, AECs showed no significant loss in cell viability after treatment with higher concentrations of melatonin over 24h (Fig 4.3), which may indicate that AECs are more robust than other previously investigated cell lines. The robustness of this cell line may also be a possible explanation for the lack of significant changes seen in the NO and RNS investigations. A potential solution may be to apply a harmful but not lethal stimulus to the cells before treatment, in order to elicit a protective response by melatonin in otherwise healthy cells.

After the 1-hour treatment period, all concentrations of melatonin showed a significant decrease in necrosis compared to the control, with the addition of 1 nM melatonin decreasing necrosis significantly more compared to 10 μ M melatonin (Fig 4.6). The study by Nduhirabandi (2014) mentioned in the paragraph above, also showed that a melatonin treatment (1 nM; 1 μ M and 10 μ M) period of 1 hour, was the only treatment period where melatonin increased cell viability. The current study's finding that melatonin increases cell viability most effectively at low concentrations over a short treatment period may be explained by a finding that a higher melatonin concentration (10 μ M) induced GSH depletion, that was associated with ROS over-production after only 15 minutes of incubation (Osseni et al., 2000).

Overall, these melatonin dose-response findings led us to conclude that a concentration of 1 nM melatonin would yield the best results in the future combination studies, since it was the only dose where significant differences were observed for the 24 hour treatment period, and the most effective dose over the 1 hour treatment period.

6.2 ART Dose-Response

Despite confounding reports, many trials indicate that ART leads to ED (Skowyra et al., 2012). Cardiovascular complications are considered a new challenge for HIV patients receiving ART with numerous studies on the effects of ART on the vasculature indicating that ART may impair the function of the vascular endothelium (Blanco et al., 2006; Shankar et al., 2005; Stein et al., 2001). ART has been shown to affect NO levels; either through the excessive production of NO (Torre et al., 2015) or through reduced NO production (Shankar et al., 2005), due to reduced expression of eNOS (Fu et al., 2005). Increases in ROS and RNS production (Skowyra et al., 2012) have also been demonstrated in ART, and together, these factors can lead to decreased cell viability.

In this study, high concentration ART (EFV: 12 μ M; FTC: 10 μ M; TDF: 1 μ M) significantly increased NO production compared to both the control and the other two ART concentrations (Fig 4.7). These finding of increased NO production during treatment with ART were surprising. Although it has been reported in literature that ART has the ability to increase excessive production of NO (Torre et al., 2015), the study conducted by was conducted in humans, making it difficult to compare these results with a cell-based study. NO is a cell survival factor (Dimmeler & Zeiher, 1999), and its controlled production plays many important roles in the immune and vascular system (Cines et al., 1998). In the case of cell injury and the release of inflammatory mediators, iNOS is responsible for producing characteristically high concentrations of NO in shorts bursts in order to protect the cells (Matthys & Bult, 1997; Michel & Feron, 1997). Under certain circumstances, this high concentration of NO produced by iNOS can become detrimental, and excessive NO may damage the vascular wall (Matthys & Bult, 1997) or cause cell death through oxidative stress (Murphy, 1999). In the current study, the increase in NO observed between the control group and the highest ART concentration treatment group was as modest as $\pm 13\%$ (Fig 4.7). A study by Speyer *et al.*, (2003) showed that iNOS induced NO production was 20-fold above that found in non-stimulated endothelial cells, where iNOS was inactive. Therefore, it is more likely that the modest increase in NO levels seen in the current study are more likely to be associated with a protective effect on the endothelium, rather than a damaging effect.

Clinical and experimental models have shown that ART-induced ED appears to be mediated by reduced NO production (Shankar et al., 2005). Most these clinical and experimental models make use of protease inhibitors, as opposed to NRTIs and NNRTIs, which comprise first line FDC ART used in the current study. The fact that this study

observed increased NO production after treatment with NRTI and NNRTI based ART may imply that NRTI and NNRTI based therapies may be a safer treatment option with regards to endothelial health and maintaining NO homeostasis. Alternatively, the result of this study may be due to the relatively short incubation time of 24-hours. A longer treatment period is more applicable when treating with ART, since ART-associated ED is usually only observed after many years of treatment (Choi et al., 2011; Islam et al., 2012). Further studies would need to be conducted to determine if NO production would still increase after a longer treatment period.

When RNS production was examined, high concentration ART was the only concentration to significantly increase RNS production (Fig 4.8), with the increase being a slight as $\pm 9\%$ higher than the control group. It is not surprising that there were no significant differences seen in the two lower concentration ART groups, as well as that the high concentration ART group only resulted in a minor increase in RNS production, since no major increase in NO production was observed either. These two findings are related, since excessive levels of NO are associated with increased ONOO⁻ levels (Forstermann & Munzel, 2006), which in turn is associated with the generation of nitrotyrosine (Halliwell, 1997). Therefore, in the absence of excessive NO production, excessive production of RNS is also unlikely. One study examined the effects of ART in a hCMEC/D3 cell line (in vitro model for blood-brain barrier endothelial cells) and found ROS to be highly elevated post ART treatment (Manda, Banerjee, Banks, & Ercal, 2011). However, as is the case with most in vitro studies done on the effects of ART, this study only examined ROS production and not RNS production, as well as used a longer treatment period of 72 hours. Multiple studies have demonstrated increased ART-induced ROS production (Apostolova et al., 2010; Skowryra et al., 2012; Weiß et al., 2016), but no studies have looked at the effects of ART treatment on RNS (specifically peroxynitrite) in vitro. It is therefore important to further investigate the role of RNS in ART-induced ED, by testing different classes of ARV drugs as well as using different techniques to detect specific types of RNS to verify a potential source of RNS.

For the cell viability studies, high concentration ART (EFV: 12 μ M; FTC: 10 μ M; TDF: 1 μ M) increased necrosis in AECs, when compared to the control (Fig 4.9). High concentration ART also showed significantly increased necrosis compared to the other two ART concentrations (Fig 4.9). This result corresponds with the RNS production results (Fig 4.8), where we saw that the high concentration ART group has the largest increase in RNS

production, which could potentially, in part, be responsible for the decreased cell viability observed, since increases in RNS are associated with cell death (Murphy, 1999).

These results are comparable to a study that demonstrated increased necrosis in human umbilical vein endothelial cells (HUVECs) following treatment with EFV (Weiß et al., 2016), one of the components of first line FDC ART. The above-mentioned study treated cells with 30 – 50 μM EFV. The current study has demonstrated a similar increase in necrosis with a much lower concentration of 12 μM EFV. Another study by Zhong *et al.* (2002) showed that protease inhibitor ritonavir directly caused endothelial cell death, mainly through necrosis pathways in human dermal microvascular endothelial cells (HMECs). The only other study conducted on AECs that examined the effect of first line FDC ART treatment on cell viability was conducted in our laboratory. The mentioned study showed that first line FDC ART has no effect on cell viability, at any tested concentration, compared to the untreated control group (Charania, 2017). This finding is inconsistent with the findings of this study, but this discrepancy can most likely be attributed to the lower ART concentration ranges used in the other study (maximum ART concentrations – EFV: 11.2 nM; FTC: 2.6 μM ; TDF: 1 μM).

From our findings, we determined that high concentration ART would be the most effective dosage for the subsequent experiments, since it led to the greatest changes in NO- and RNS production, as well as necrosis.

6.3 Effects of melatonin and ART treatment on NO production, RNS production and cell viability in AECs

As mentioned above in section 6.1 and 6.2, from the dose-response studies, it was determined that 1 nM melatonin along with high concentration ART (EFV: 12 μM ; FTC: 10 μM ; TDF: 1 μM) would be used in the combination studies.

In the NO- and RNS production combination studies, no significant differences were observed between any of the treatment groups (Fig 4.10 and 4.11). This finding was not very surprising with regards to the melatonin groups, since in the dose response studies, melatonin treatment had no effect on NO- and RNS-production. But for the ART treatment groups, we did expect the results from the dose-response studies to be mirrored in the combination treatment investigations. One explanation for these contrasting results may be that new DAF-2/DA and DHR-123 batches had to be purchased and used for the combination experiments. However, it is unlikely that this change should affect the results, since the probes were bought from the same supplier. It is therefore difficult to explain the

discrepancy, as the experimental conditions (other than the different fluorescent probe batches), were identical to the dose-response studies.

Results from the cell viability studies were more in line with the dose-response findings. We found that 1 nM melatonin significantly decreased necrosis compared to the control, while high concentration ART significantly increased necrosis compared to both the control and the 1 nM melatonin treatment group (Fig 4.12). When the two drugs were combined, we saw a significant decrease in necrosis for the combination group compared to the group treated with ART alone (Fig 4.12). In this way, we demonstrated that melatonin was able to ameliorate the harmful effects of ART. This is a novel finding, since to the best of our knowledge, there are no studies that have demonstrated this in AECs using first line FDC ART and melatonin.

These observations may be due to melatonin's antioxidant capabilities, which would allow the cells to remain viable in situations of stress where toxins like ART may lead to a loss in cell membrane viability. However, more specific investigations into the underlying mechanisms are necessary to determine through what means melatonin is able to induce these protective changes.

6.4 Western Blot Analyses

6.4.1 NO & RNS Signalling

It is clear that NO and NOS play key roles in endothelial function, not only in the context of inducing vasodilatation, but also through a plethora of other important regulatory actions (Cines et al., 1998). It is essential for the healthy endothelium that both NOS (as the most important source of vascular NO), and NO are present in desirable quantities, since an imbalance in NO and NOS levels can have dire consequences for endothelial health.

6.4.1.1 eNOS

eNOS is the most abundant isoform of NOS and is responsible for the NO produced in the vasculature, and therefore vessel dilation (Sandoo et al., 2010).

Since no changes in NO production were observed with the fluorescent probe assays, it was expected that eNOS activation (phosphorylation) (Fig 4.13 A) and expression (total protein) levels (Fig 4.13 B) would also remain unchanged. When the phosphorylated eNOS was expressed as a ratio of total, the ratio of all treatment groups decreased compared to the control group, while the melatonin + ART group also decreased significantly compared to the melatonin group (Fig 4.13 C). This ratio was seen to be as a

result of decreased phosphorylated eNOS levels as opposed to increased total eNOS levels. It is well reported that melatonin has the ability to decrease NO levels through its antioxidative capacity (Jumnongprakhon et al., 2016; Reiter et al., 2001; Silva et al., 2007; Tamura et al., 2009). These convincing Western blot results suggest that melatonin treatment could decrease NO levels through decreased eNOS activation. It was interesting, however, that the groups treated with ART also showed decreased eNOS activation, whilst the dose-response studies showed that ART increased NO production. This may imply that ART-induced NO production may be independent of the endothelium and eNOS, although further studies would need to be done for further elucidation on this point.

6.4.1.2 iNOS

While eNOS is associated with the maintenance of basal levels of NO, iNOS has traditionally been associated with high output NO-release in response to inflammatory mediators (Buchwalow et al., 2001; Michel & Feron, 1997) and in many cases is associated with cytotoxic peroxynitrite formation (Strijdom et al., 2009).

iNOS was not detected in the AECs (Fig 4.14). This may imply that iNOS might not have been expressed or that iNOS levels were so low that the antibody was not able to detect iNOS in the cells. Both eNOS and iNOS can therefore be excluded as sources of the increased NO production observed. Therefore this increase in NO production seen in the dose-response studies still has an unknown source that needs investigating. Potential sources of NOS-independent NO include S-nitrosothiols, as well as nitrite and nitrate (Chen, Pittman, & Popel, 2008). Under certain conditions, nitrite and nitrate act as a reservoir, where different enzymes (hemoglobin, myoglobin, xanthine oxidoreductase, mitochondrial cytochrome oxidase, aldehyde dehydrogenase 2, cytochrome P450 reductase and cytochrome P450) can catalyze the reduction of nitrite or nitrate to generate NO (Zhao, Vanhoutte, & Leung, 2015). Various methods exist to measure NOS-independent NO formation (Zweier, Samouilov, & Kuppusamy, 1999), which could be examined in future studies.

6.4.1.3 Nitrotyrosine

Nitrotyrosine is generated when peroxynitrite reacts with a tyrosine or tyrosine containing protein and serves as a marker for nitrosative stress and peroxynitrite damage (Halliwell, 1997). Peroxynitrite is generated as a result of the chemical reaction between NO and superoxide (Forstermann & Munzel, 2006).

Nitrotyrosine levels in the ART treatment group were significantly higher when compared to the control group (Fig 4.15). This finding corresponds to the current literature, which suggests that ART leads to the excess production of ROS, particularly superoxide (Sutliff et al., 2002). Superoxide, along with increased levels of NO production leads to the production of peroxynitrite and eventually nitrotyrosine. The treatment group containing both melatonin and ART showed significantly lower levels of nitrotyrosine compared to the ART group (Fig 4.15). These results may be indicative that melatonin has the ability to decrease the nitrosative stress caused by ART. This protection by melatonin is most likely due to its antioxidative capacities and its ability to scavenge free radicals like superoxide and excess NO (Hardeland, 2005; Poeggeler et al., 2002), thereby decreasing the chance that peroxynitrite and nitrotyrosine will form (Fig 6.1). These results are similar to those seen in the plate reader studies, where ART significantly increased DHR-123 fluorescence compared to the control. Together, these results may suggest that ART induces ED through excess production of RNS like peroxynitrite. Most the literature covers the effects of ART treatment on ROS production. This study establishes that RNS may play an equally important role in the multifactor mechanisms by which ART induces ED. The plate reader studies did not however show similar results with regards to the alleviative effect of melatonin on RNS levels. This may be due to the fact that the nitrotyrosine antibody is a more specific and sensitive probe compared to DHR-123. Further protein and antioxidant capacity studies would be needed to confirm melatonin's specific role in ameliorating nitrosative stress.

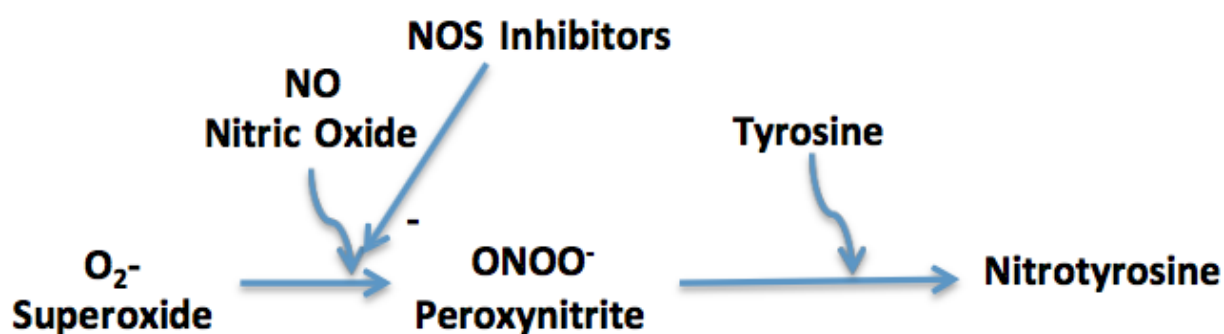


Figure 6.1: Substrates involved in nitrotyrosine production (Everson, 2016).

6.4.2 ROS Signalling

ART has been shown to result in increased ROS-production from various sources (Apostolova et al., 2010; Skowyra et al., 2012; Weiß et al., 2016). Superoxide is of

particular interest since it is essentially a precursor of other harmful radicals and molecules, such as hydrogen peroxide, peroxyxynitrite, the hydroxyl radical and nitrite.

6.4.2.1 P22 PHOX

p22 PHOX is one of multiple subunits of NADPH oxidase, which is responsible for superoxide production. p22 PHOX is therefore regarded as a marker of NADPH-oxidase dependent superoxide production (San Jose, Fortuno, Beloqui, Diez, & Zalba, 2008).

All treatment groups showed lower levels of p22 PHOX expression compared to the control group (Fig 4.16). Both the ART and melatonin + ART groups also showed significantly lower p22 PHOX expression compared to the melatonin group, potentially indicating that ART may be the factor lowering the p22 PHOX expression levels. These results contradict the findings of the DHR-123 investigations where ART increased RNS (peroxyxynitrite) production, as well as opposes many previous reports in literature. This inconsistent finding may be due to the fact p22 PHOX is specific to NADPH-oxidase dependent superoxide, while DHR-123 is reported to be more sensitive to peroxyxynitrite, although some studies have also shown it to be sensitive to mitochondrial ROS (Chan & Miskimins, 2012; Ischiropoulos et al., 1999; Navarro-Antolin et al., 2001). NADPH-oxidase has been implicated as the main source of excess ROS production in the vasculature (Hamilton et al., 2002), however, the main source of ART induced superoxide production is thought to be of mitochondrial origin, likely resulting from leakage of electrons from a dysfunctional mitochondrial electron transport chain (Jiang et al., 2007). The results from the DHR-123 study substantiate this, since the probe is more sensitive to mitochondrial ROS and RNS (peroxyxynitrite), and showed a marked increase in ART treated groups, while the p22 PHOX did not. A marker with greater specificity for mitochondrial superoxide would need to be evaluated. Superoxide dismutase 2 (SOD-2) is involved in the scavenging of superoxide that leaks from the mitochondrial electron transport chain (Zelko, Mariani, & Folz, 2002), and therefore could be an alternative target for further investigation.

6.4.3 Cell Viability Signalling

Previous *in vitro* investigations have examined cell viability through necrosis. However, apoptosis is also an important form of cell death which utilises a different protein transduction pathway to necrosis, and may also be involved in ART induced cell damage.

6.4.3.1 Cleaved Caspase-3

Cleaved caspase-3 is a down-stream target of caspase-8 and indicative of apoptosis (Kuribayashi et al., 2006).

The ART and melatonin + ART treatment groups both showed decreased cleaved caspase-3 expression levels compared to both the control and the melatonin treatment groups (Fig 4.17). In terms of cell viability, these results contradict the findings from the PI-based studies where we saw ART increased necrosis, although apoptosis and necrosis do not necessarily occur simultaneously and therefore cannot be directly compared. These confounding results correlate with evidence from literature, which demonstrates that ART directly induces mitochondrial dysfunction and ROS production that promotes ED without culminating in apoptosis (Jiang et al., 2007).

Another explanation for decreased cleaved caspase-3 expression in groups containing ART may involve ART-induced NO production, which was observed in the dose-response studies. NO has previously been shown to inhibit apoptosis by S-nitrosylation of caspase-3 (Rossig et al., 1999), leading to its inactivation.

ART has been shown to be anti-apoptotic in specific cell types (Badley, 2005; Dieye et al., 2000), although the exact molecular target responsible for this anti-apoptotic effect remains to be defined *in vitro* and *in vivo* (Badley, 2005). The same molecular mechanisms could be at work here, but further protein investigations are needed.

6.5 Antioxidant Capacity Analyses

The oxygen radical absorbance capacity (ORAC) assay was used to assess the antioxidant capacity of the AECs treated with melatonin and ART. Unfortunately, no significant differences were seen between any treatment groups (Fig 4.18). It has been suggested that antioxidant activity should not be concluded based on a single antioxidant test model (Alam, Bristi, & Rafiqzaman, 2013). Therefore, it might be prudent to rather conduct multiple more specialised and specific assays, such as hydrogen peroxide-; nitric oxide- and peroxynitrite radical scavenging assays, as well as thiobarbituric acid reactive substances (TBARS) assays which indicate lipid peroxidation.

6.6 Concluding Remarks

The first main aim for this *in vitro* study was to determine the optimum concentrations of both melatonin and first line FDC ART used to treat AECs at which the greatest differences could be seen when compared to untreated AECs, with respect to NO- and ROS production, as well as cell viability. It was established that 1 nM melatonin and high

concentration ART (EFV: 12 μ M; FTC: 10 μ M; TDF: 1 μ M) showed the greatest differences with regards to examined variables. Unfortunately, the melatonin dose could only be based on results from cell viability studies since no significant differences were seen in the NO- and ROS production studies.

The second main aim was to analyse any potential synergistic/antagonistic interactions between melatonin and ART in AECs treated with the above-determined concentrations, with respect to NO- and ROS production, as well as cell viability. For this aim, the NO- and ROS production studies did not show the same trends previously established in the dose-response studies. However, the changes observed in the dose-response studies were very modest, and would have perhaps been mirrored in the combination studies after an increase in the sample size. Cell viability studies were nevertheless followed the same trends observed in the dose-response studies and showed that melatonin alleviated necrotic damages induced by ART.

Signalling protein investigations established that the observed ART-induced increase in NO production might be independent of the endothelium and eNOS, as well as iNOS, while melatonin was shown to have the capacity to ameliorate nitrosative damage. p22 PHOX signalling eliminated NADPH-oxidase as a potential source of ROS in the ART-induced increase in ROS production and cleaved caspase-3 investigations showed that ART may be pro-necrotic, but it is most likely anti-apoptotic. Antioxidant capacity studies showed no significant changes between treatment groups. Overall, melatonin was shown to be effective in reducing cell necrosis and nitrosative damage, while ART may increase NO- and ROS production, and reduce apoptosis, but the mechanisms behind these changes still need further investigation.

7 - Discussion: *Ex vivo* and *in vivo* studies

Chapter 7 debates the findings of the results obtained from the *ex vivo* and *in vivo* studies. The data discussed in this chapter can be found in Chapter 5, while the materials and methods can be found in Chapter 3.

7.1 *Ex Vivo* Studies

The main aim of the *ex vivo* studies was to determine the acute effects of melatonin and ART administration on the vascular reactivity of untreated, control male Wistar rat aortas. For these studies, Phe was used to induce contraction, while Ach was used to induce relaxation. The relevant treatment was added directly to an *ex vivo* organ bath for 30-minutes before the addition of cumulative concentrations of Ach and Phe.

Cumulative contraction with Phe, showed that the ART treated aortas contracted significantly less, when compared to all other treatment groups (Fig 5.1 A). This finding may be the consequence of an unexpected phenomenon that occurred when ART was administered to the *ex vivo* organ bath (Fig 7.1). Roughly 1 minute after the addition of ART to the organ bath, the aortic ring started to spontaneously contract. On average it took about 5 minutes to reach maximum spontaneous contraction, before the ring began to relax again, eventually relaxing all the way back to a resting tension of 1.5 g before the end of the 30-minute *ex vivo* drug incubation period (Fig 7.1). When the vehicle or melatonin was added to the organ bath, no spontaneous contraction occurred.

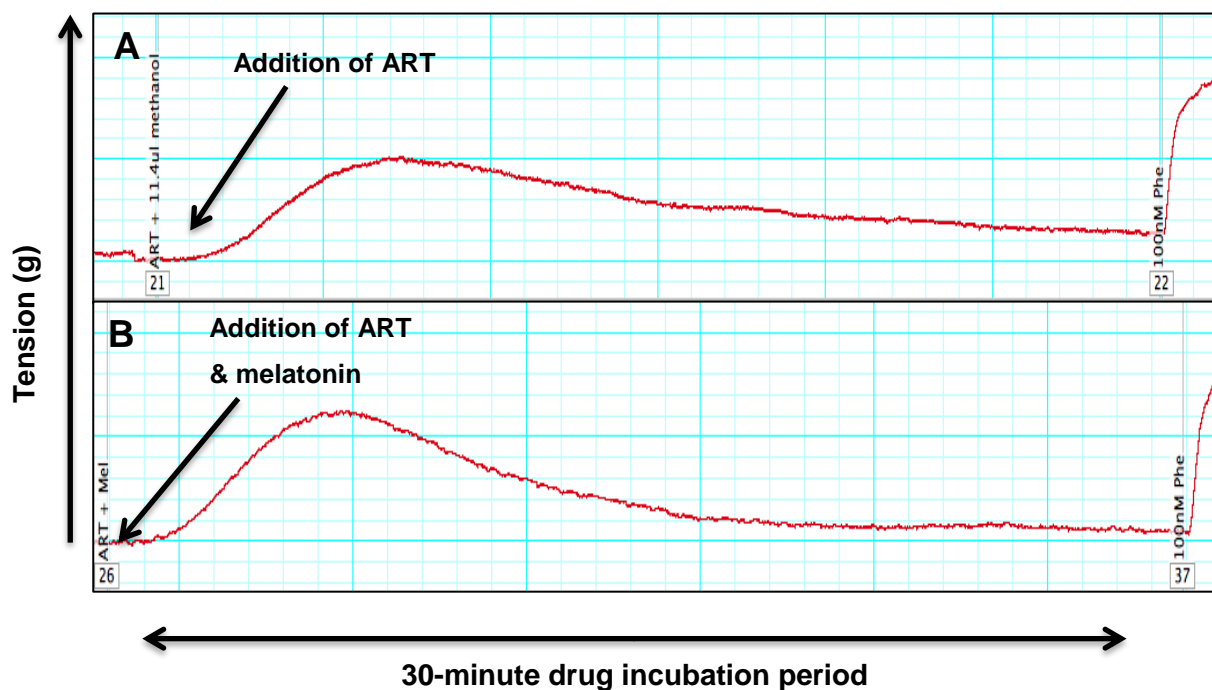


Figure 7.1: The spontaneous contraction of *ex vivo* aortic rings after the addition of A) ART and B) ART and melatonin.

It is possible that this pre-contraction caused by ART may have pre-conditioned the aortic ring to contraction, thereby causing it to contract less intensely when exposed to cumulative concentrations of Phe. Melatonin had the ability to attenuate the pre-conditioning effect of ART, since the melatonin + ART group contracted significantly more than the ART group during the subsequent cumulative Phe protocol, despite also being exposed to a spontaneous pre-contraction following *ex vivo* drug treatment. It is difficult to speculate how melatonin achieves this, since the mechanism of the ART-induced spontaneous pre-contraction is not known either. The spontaneous pre-contraction may be a result of iNOS activation following a bombardment of ROS generated by the *ex vivo* addition of ART. iNOS activation would lead to an excessive release of NO, which in combination with ROS, would be rapidly converted to peroxynitrite and ultimately lead to vascular contraction. Acute ART treatment might also directly stimulate pro-contractile substances such as endothelin-1 (ET-1), thromboxane A (TXA₂) and angiotensin II (Cines et al., 1998; Mudau et al., 2012). This may however be slightly more difficult to examine, although an ELISA assay may be able to detect these substances within the supernatant. Alternatively, the spontaneous contraction may just be a direct drug-induced effect due to an unknown toxicity of one of the components of the FDC ART. Individual components of the ART (EFV; FTC and TDF) could be examined separately to clarify this point. Finally, the acute treatment of ART might stimulate α -adrenergic receptors to release calcium,

thereby inducing the rapid contraction. This rapid stimulation and excessive release of calcium may exhaust calcium supplies, which would explain the decreased contraction experience on administration of Phe.

However, this is all speculative and further investigations are needed to determine the source of this interesting and unexpected phenomenon, as well as the means by which melatonin attenuated the pre-conditioning effect of ART.

Further protein investigations should be conducted, as well as studies conducted with Ca²⁺ channel blockers, to further elucidate the mechanisms at play. The sample sizes should also be expanded to shed more light on these findings.

7.2 *In Vivo* Studies

The main aim of the *in vivo* studies was to determine the chronic effects of melatonin and ART administration on the vascular reactivity of male Wistar rats that have been treated for 8 weeks with melatonin and/or ART. Additional aims included examining various signalling protein activation and/or expression levels, as well as the antioxidant capacity exhibited in the aortic tissue of these same male Wistar rats.

For *in vivo* experiments, two types of aortic ring investigations were conducted. For the first set of experiments we conducted endothelium-dependent relaxation studies, where Phe was used to induce contraction and Ach was used to induce relaxation, and rings were pre-treated with the NOS inhibitor, L-NAME as a control. For the second set of experiments we conducted endothelium-independent relaxation studies, where Phe was once again used to induce contraction, however, for these studies SNP - an exogenous NO donor - was used to induce relaxation.

7.2.1 Endothelium-dependent Aortic Ring Investigations

Cumulative contraction with Phe, showed that the ART and melatonin + ART treatment groups contracted significantly more when compared to the control group (Fig 5.2 A). These results may implicate ART as the factor leading to increased contractility. Two studies by Jiang *et al.* (2006 and 2010) found that ART treatment had no effect on Phe-induced contraction. Both these studies used NRTI, azidothymidine (AZT) and the protease inhibitor, indinavir. Tests were also done on mice aortas rather than rat aortas. Since a different animal model was used, as well as different ART, these two studies cannot be directly compared with the current study, and therefore the contradictory results are not unexpected. However, FTC, one of the components of first line FDC ART, is also a

nucleoside reverse transcriptase inhibitor, like AZT. Perhaps a conclusion that can be drawn from the above-mentioned two studies is that the NRTI (FTC) component of the combination ART is not responsible for the pro-contractile effects seen.

Studies examining the effects of ART treatment on aortic contractility are scarce and it is therefore difficult to determine what might be the cause of ART-induced pro-contractility. Further protein examination would be needed to confirm this mechanism. A potential mechanism for this pro-contractile effect may be ART-induced reduced eNOS expression, and therefore reduced NO release from the endothelium. Since we saw reduced eNOS expression in the ART treated groups *in vitro*, the same might occur *in vivo*.

The fact that the ART groups experienced increased contractility *in vivo* is an expected finding, since ART *in vitro* is thought to lead to impaired function of the vascular endothelium (Blanco et al., 2006; Shankar et al., 2005; Stein et al., 2001). This is however a contradictory result when compared to the observations made in the *ex vivo* studies, where we saw ART treated groups showed anti-contractile properties. The only explanation fathomable for these opposing results is that the duration of exposure to ART plays a significant role in the resultant contractility effect. In other words, the longer the endothelium is exposed to ART for, the greater the risk of developing ED. This theory has been supported by many studies, with the Data Collection on Adverse Events of Anti-HIV Drugs (DAD) study group reporting that ART was associated with a 26% increase in the rate of myocardial infarction (MI) per year of exposure to ARV drugs. Islam *et al.* (2012) also confirmed that the duration of exposure to ART might be one of the main factors associated with risk of developing CVD.

These findings also suggest that melatonin supplementation does not alleviate this pro-contractile effect of ART. This result contradicts results previously obtained in our labs, where melatonin was shown to be a significant pro-relaxant (Smit-van Schalkwyk, 2016). However, these inconsistent findings could be due to multiple factors. This study used a higher dose of 10 mg/kg/day melatonin, where the previous study used a dose of 4 mg/kg/day. This study also used a treatment periods that were 2 weeks longer. Furthermore, the previous study used melatonin to alleviate damage caused by nicotine rather than ART, which may provide an indication that ART does not cause significant enough damage *in vivo* for melatonin to act in a protective, vasodilatory manner. This finding also correctlates with the data obtained from the *in vitro* melatonin dose-response studies, were we found that a shorter treatment period, with a lower melatonin concentration was more protective.

Ach induced relaxations were similar for all treatment groups (Fig 5.2 B), which is surprising considering the few vascular reactivity studies that have been conducted, all showed significant findings in Ach-induced relaxation studies (Jiang et al., 2010; Jiang et al., 2006). Previous studies found that ART had an anti-relaxation effect, but as mentioned above, these studies did not use the same animal model or ART regime. The results found in this study may shed light on the fact that first line ART is less likely to induce ED than other previously studies ART regimes.

Results from pre-treatment with the NOS inhibitor, show that L-NAME elicited a strong pro-contraction effect (Fig 5.3 A) and reduced vasodilatory responses in all the groups (Fig 5.4 A). These experiments not only confirmed that the vascular isometric tension model was functional, but also showed the involvement of NOS and NOS-derived NO in anti-contraction and vasodilatory responses of the vasculature.

7.2.2 Endothelium-independent Aortic Ring Investigations

To determine whether differences in Ach-mediated relaxation were attributable to differential responses of the vascular smooth muscle to NO, relaxation responses to the NO donor SNP were evaluated.

For these endothelium-independent investigations, the Phe contraction studies expectedly followed the same trend as seen for the endothelium-dependent investigations, where cumulative contraction with Phe, showed that the both the ART and melatonin + ART treatment groups exhibited significant pro-contraction properties compared to the control group (Fig 5.5 A).

When SNP was used to induce relaxation, no significant differences were seen between any treatment groups (Fig 5.5 B). This finding indicates that the smooth muscle component of the NO-cGMP pathways remains unchanged during ART treatment (Sutliff et al., 2002). Further protein investigations should be conducted to examine whether this result was simply due to the fact that ART did not cause any oxidative damage, or whether SNP resulted in normal relaxation despite the presence of damaging increased levels of superoxide. This is a phenomenon that many studies have previously demonstrated as possible (Eberhardt et al., 2000; Gunneth, Heistad, & Faraci, 2002), and therefore should be further examined. Mechanisms for the dissociation between elevated superoxide and unaffected relaxation to SNP remain unclear (Sutliff et al., 2002).

Since endothelium-dependent and independent relaxation studies both showed no significant differences between groups, it is difficult to draw any conclusions as to whether

ART-induced damage is limited to the endothelium and endothelium-dependent factors like eNOS.

7.2.3 Western Blot Analyses

Western blot analyses were performed on snap-frozen aortic tissue of control, melatonin, ART and melatonin + ART treated animals from the endothelium-dependent studies, in order to determine whether the functional data of the vascular reactivity investigations could be explained by changes in intracellular signal transduction pathways.

No statistically significant changes were seen between any treatment groups in iNOS (Fig 5.7), nitrotyrosine (Fig 5.8) or p22 PHOX (Fig 5.9) expression, respectively. These results were unsurprising considering no differences were seen when Ach induced relaxation was examined. However, these results indicate that the pro-contractile influence elicited by ART is most likely not due to increased NADPH-dependent superoxide production or due to peroxynitrite-related damage.

7.2.3.1 eNOS

When the phosphorylated eNOS was expressed as a ratio of total, we saw that there were no significant differences between any treatment groups (Fig 5.6 C), despite that fact that eNOS phosphorylation was significantly lower in the melatonin + ART treatment group compared to the control (Fig 5.6 A). The P/T ratio obtained for the treatment groups was most likely due to the fact that the trends seen in eNOS phosphorylation and expression were relatively similar, notwithstanding that no significance was seen between groups for eNOS expression. This result was expected since there were no changes in vasodilatory capacity between groups during relaxation studies. This result does however shed more light on the mechanisms behind the ART-induced pro-contractile responses observed in this study. Previously it was proposed that this effect might be due to decrease NO production from decreased eNOS expression. These results however show that it is unlikely that decreased eNOS expression is the mechanism at work. This might point towards other contractor factors like endothelin-1 (ET-1), thromboxane A (TXA₂) and angotensin II (Cines et al., 1998; Mudau et al., 2012) being upregulated. However, further investigations would need to confirm this.

7.2.3.2 Cleaved Caspase-3

The ART and melatonin + ART combination treatment groups showed significantly decreased cleaved Caspase-3 expression compared to the control, while the ART treatment group also showed significantly decreased cleaved Caspase-3 expression when compared to the melatonin treatment group (Fig 5.10). These findings are very similar to those seen in the cell viability investigations of the *in vitro* study (Fig 4.17). Once again it seems that ART is the factor associated with decreased apoptosis. This finding further cements the anti-apoptotic role of ART, although in these *in vivo* studies, it would appear that this is not influenced by increased NO levels, since there was no increase in vasodilation seen in the ART treated groups. Other studies that looked at cleaved caspase-3 expression during ART have all been in the presences of HIV, and therefore it is difficult to differentiate between the effects of HIV and ART (Cook-Easterwood, Middaugh, Griffin, Khan, & Tyor, 2007; Pitrak et al., 2015).

7.2.4 Antioxidant Capacity Studies

The ORAC assay showed no significant differences in antioxidant capacity between treatment groups (Fig 5.11). As suggested for the *in vitro* studies in section 6.5, perhaps further antioxidant capacity assays should be performed to confirm this result.

7.3 Concluding Remarks

Novel *ex vivo* studies examining the acute effects of melatonin and ART treatment indicated that ART elicited a pro-contractile effect when administered to a healthy rat aorta. This resulted in the ART treatment group being pre-conditioned and consequently contracting less when compared to all other treatment group. It was also established that melatonin does not play a protective role in the presence of ART this situation, since the melatonin + ART treatment group relaxed significantly less than the control group. These findings are very interesting and need further elucidation through protein investigations.

In vivo studies demonstrated that ART has no effect on endothelium-dependent or independent relaxation, as shown by the lack of differences seen between groups in both Ach- and SNP-induced relaxation studies. Both these studies did, however, show that ART seems to have a pro-contractile effect. Further investigations are needed to establish by what mechanism ART elicits a pro-contractile response, yet does not affect vasorelaxation.

Protein investigations were relatively in line with these findings, with cleaved caspase-3 investigations shedding more light on the fact that NO levels are most likely not involved in the anti-apoptotic effects of ART.

8 – Overall Conclusions

This study aimed to investigate the effects of melatonin supplementation during first line FDC ART, through an *in vitro*, *ex vivo* and *in vivo* approach.

The *in vitro* dose-response studies showed that high concentration ART has the ability to induce modest increases in NO and RNS production. Combination studies highlighted that melatonin has the ability to ameliorate necrotic damage caused by ART in AECs. Signalling investigations ruled out endothelium-dependant NOS as a source of the increased NO observed in dose-response studies, as well as excluded NADPH oxidase-dependent super oxide as the likely source of the increase in RNS observed. Finally, ART was shown to have an anti-apoptotic effect, which may have been facilitated by the increase in NO observed in the dose-response studies. Taken together, these results show that first line FDC ART is very mildly damaging to the endothelium, and can even be protective under certain circumstances. Melatonin was shown to be effective in increasing cell viability, but showed no promise of being protective in terms of decreasing excessive NO and RNS production. However, since excessive levels of NO and RNS were not observed or produced in this study, no conclusions can be drawn as to whether melatonin has the ability to decrease excessive levels of NO and RNS *in vitro* from the current findings.

Ex vivo and *in vivo* studies shed light on the fact that there are still many unknowns with regards to the underlying mechanisms involved in the pro-contractile effects of ART. Although ART was shown to definitely elicit contractile responses, the lack of findings in the relaxations studies makes it difficult to draw conclusions on the effects of ART on aortic endothelial health. Since ART was not shown to decrease relaxation capacity in any studies, it could be said that first line FDC ART did not induce endothelial dysfunction, since ART treated aortas showed sufficient vasodilatory responses when compared to untreated aortas. Signalling investigations further established that ART has an anti-apoptotic effect. Whether this finding is specific to the specific regime of ART used in this study, or a general characteristic of ART, would have to be further investigated. In *In vitro* studies, melatonin was also shown to not have a protective effect in contraction and relaxation studies, but this could perhaps just be said for the specific concentration and duration of treatment of melatonin used in this study. *Ex vivo* and *in vivo* studies overall showed that first line FDC ART does not induce reduced relaxation capacity, usually

associated with endothelial dysfunction, while 10 mg/kg/day melatonin treatment over an 8 week period did not provide protective effects.

Taken together, these *in vitro*, *ex vivo* and *in vivo* investigations allowed for a very board overview of the topic and allowed for the examination of vascular endothelial function on a cellular and functional scale. Although it is difficult to fully compare the different models, each aspect of this study allowed for the development and finding of important investigations that still need to be conducted, which could eventually lead to a better understanding behind the mechanisms by which ART potentially causes endothelial damage.

Overall, from these studies, it cannot be explicitly said that South African first line FDC therapy induces damaging endothelial changes, and that melatonin has the ability to alleviate those changes. However, particular findings did indicate that further investigations are need to be conducted, specifically with regards to the necrotic effects of ART and the acute effects of ART.

8.1 Advantages, Limitations and Future Directions

Currently, very few studies exist that investigate the effects of South African first line FDC ART. This study also investigated the effects of ART in isolation from HIV infection, allowing for a more accurate perspective of the effects of ART. This study showed that ART induced necrosis as measured by propidium iodide, can be decreased by conjunctive melatonin treatment. This study also demonstrated that acutely administered ART caused short-term spontaneous contraction, which resulted in an anti-contractile response in ART-treated aortas when exposed to cumulative concentrations of Phe. Both these findings are novel and require further study to clarify the mechanisms by which these actions occur.

Limitations of this study include the use of only three fluorescent probes for the plate reader investigations. In particular, a marker for apoptosis and well as a more specific marker for mitochondrial ROS should be included. Antibodies specific to mitochondrial ROS could also be included to better understand the mechanisms of ART-induced ROS production.

Small sample sizes are a prominent limitation in the *in vitro* western blot analyses. A new method should be developed in order to allow for the combination of multiple parent cell lines when making a single set of lysates, where cells could potentially be treated and then frozen until enough different parent cell lines have been grown.

Another potential limitation of this *in vitro* study might be its potential to translate to clinical relevance, since the long-term effects of ART are the main cause of ART-induced ED, whereas a treatment period of only 24 hours was examined.

Time and equipment-constraints meant that L-NAME studies could not be conducted for the endothelium-independent SNP relaxation investigations. This would be an interesting aspect to add to these studies. Signalling investigations should also be conducted in future studies examining the endothelium-independent chronic effects of ART treatment, as well as the *ex vivo* acute effects of ART treatment.

8.2 Specific roles in the study

- All *in vitro* cell culture experiments were conducted in the Medical Physiology Division on the Faculty of Medicine and Health Science at Stellenbosch University, by the student, with the exception of the ORAC assay which was conducted by Dr D Blackhurst at the University of Cape Town.

- All animal drug treatments were prepared and administered by the student, with the exception of the ART gavaging procedure, which was performed by Mr N Markgraaff and Mr S Smit.
- Animal housing, care, feeding and treatment occurred in the Animal Housing Unit of the Faculty of Medicine and Health Science at Stellenbosch University.
- All *ex vivo* and *in vivo* experiments were conducted in the Medical Physiology Division on the Faculty of Medicine and Health Science at Stellenbosch University, by student, with the exception of the ORAC assay, which was conducted by Dr D Blackhurst at the University of Cape Town.

8.3 Research outputs associated with the study

- **Rawstone, J.**, Strijdom, H., Webster, I., Westcott, C. The effects of melatonin supplementation on vascular tissue during first line ART: an *in vitro* and *in vivo* study. 45th conference of the Physiology Society of Southern Africa, hosted by university of Pretoria, 27- 31 August 2017. (Received an honorary mention for one of the top presentations presented for the Wyndham Competition)

Appendix A: *In vitro* melatonin and vehicle concentration calculations

Melatonin Preparation (1 nM; 1 μ M; 10 μ M):

- Weight off 23.2 mg melatonin and add it to 150 μ l methanol (MeOH).
- Vortex solution well and make up to 10 ml by adding 9.850 ml distilled water (dH₂O) = **10 mM Melatonin Stock**
- To make up 10 μ M melatonin: Add 10 μ l of the **10 mM Melatonin Stock** to 9.990 ml of medium.
- To make up 1 μ M melatonin: Add 2 μ l of the **10 mM Melatonin Stock** to 19.998 ml of medium.
- To make up 1 nM melatonin:
 - Add 1 ml of the **10 mM Melatonin Stock** to 9 ml of dH₂O = STOCK A (1 mM melatonin).
 - Add 1 ml of STOCK A to 9 ml of dH₂O = STOCK B (100 μ M melatonin).
 - Add 1 ml of STOCK B to 9 ml of dH₂O = STOCK C (10 μ M melatonin).
 - Add 2 μ l of STOCK C (10 μ M melatonin) to 19.998 ml of medium.

MeOH Vehicle Preparation (1 nM; 1 μ M; 10 μ M):

- Add 150 μ l MeOH to adding 9.850 ml distilled water (dH₂O) = **10 mM Vehicle Stock**
- To make up 10 μ M vehicle: Add 10 μ l of the **10 mM Vehicle Stock** to 9.990 ml of medium.
- To make up 1 μ M vehicle: Add 2 μ l of the **10 mM Vehicle Stock** to 19.998 ml of medium.
- To make up 1 nM vehicle:
 - Add 1 ml of the **10 mM Vehicle Stock** to 9 ml of dH₂O = STOCK A (1 mM vehicle).
 - Add 1 ml of STOCK A to 9 ml of dH₂O = STOCK B (100 μ M vehicle).
 - Add 1 ml of STOCK B to 9 ml of dH₂O = STOCK C (10 μ M vehicle).
 - Add 2 μ l of STOCK C (10 μ M vehicle) to 19.998 ml of medium.

****All melatonin preparations are done in the dark***

Appendix B: *In vitro* ART and vehicle concentration calculations

Efavirenz (5.0 μ M; 8 μ M; 12 μ M):

MW: 315.67 g/L

Dissolve 10mg in 1.5 ml of Methanol.

$$\begin{aligned}C &= m/MV \\ &= 0.01\text{g}/(315.67 \text{ g/l} \times 0.0015\text{l}) \\ &= 0.010559551 \text{ M} \\ &= 21119 \mu\text{M}\end{aligned}$$

5.0 μ M:

$$C_1V_1 = C_2V_2$$

$$21119 \mu\text{M} \times V_1 = 5.0 \mu\text{M} \times 1000\mu\text{l}$$

$$V_1 = 0.24 \mu\text{L per 1 ml medium}$$

8 μ M:

$$C_1V_1 = C_2V_2$$

$$21119 \mu\text{M} \times V_1 = 8 \mu\text{M} \times 1000\mu\text{l}$$

$$V_1 = 0.38 \mu\text{l per 1 ml medium}$$

12 μ M:

$$C_1V_1 = C_2V_2$$

$$21119 \mu\text{M} \times V_1 = 12 \mu\text{M} \times 1000\mu\text{l}$$

$$V_1 = 0.57 \mu\text{l per 1 ml medium}$$

Emtricitabine (5 µM; 7.5 µM; 10 µM):

MW: 247.25 g/L

Dissolve 10mg in 4 ml of Milipore H₂O.

$$\begin{aligned}
 C &= m/MV \\
 &= 0.01\text{g}/(247.25 \text{ g/l} \times 0.004\text{l}) \\
 &= 0.0101112235 \text{ M} \\
 &= 10111.2 \text{ } \mu\text{M}
 \end{aligned}$$

5 µM:

$$C_1V_1 = C_2V_2$$

$$10111.2 \text{ } \mu\text{M} \times V_1 = 5 \text{ } \mu\text{M} \times 1000\mu\text{l}$$

$$V_1 = 0.5 \text{ ul per 1 ml medium}$$

7.5 µM:

$$C_1V_1 = C_2V_2$$

$$10111.2 \text{ } \mu\text{M} \times V_1 = 7.5 \text{ } \mu\text{M} \times 1000\mu\text{l}$$

$$V_1 = 0.74 \text{ ul per 1 ml medium}$$

10 µM:

$$C_1V_1 = C_2V_2$$

$$10111.2 \text{ } \mu\text{M} \times V_1 = 10 \text{ } \mu\text{M} \times 1000\mu\text{l}$$

$$V_1 = 1.2 \text{ } \mu\text{l per 1 ml medium}$$

Tenofovir (80 nM; 400 nM; 1 µM):

MW: 635.51 g/L

Dissolve 10mg in 40 ml of Millipore H₂O.

$$\begin{aligned}
 C &= m/MV \\
 &= 0.01\text{g}/(635.51 \text{ g/l} \times 0.04\text{l}) \\
 &= 0.0003934 \text{ M} \\
 &= 393.38 \text{ }\mu\text{M} \text{ (Stock A)}
 \end{aligned}$$

80 nM:

Dilute stock of 393.38 µM:

Add **127.1 µl** of **Stock A** to 872.9 µl of Millipore water (**Stock B**) (Now the concentration of Stock B is 50 µM)

$$C_1V_1 = C_2V_2$$

$$50 \text{ }\mu\text{M} \times V_1 = 0.08 \text{ }\mu\text{M} \times 1000\mu\text{l}$$

$$V_1 = 1.6 \text{ }\mu\text{l per 1 ml medium}$$

400 nM (from stock A):

$$C_1V_1 = C_2V_2$$

$$393.38 \text{ }\mu\text{M} \times V_1 = 0.4 \text{ }\mu\text{M} \times 1000\mu\text{l}$$

$$V_1 = 1.02 \text{ }\mu\text{l per 1 ml medium}$$

1 µM (from stock A):

$$C_1V_1 = C_2V_2$$

$$393.38 \text{ }\mu\text{M} \times V_1 = 1 \text{ }\mu\text{M} \times 1000\mu\text{l}$$

$$V_1 = 2.54 \text{ }\mu\text{l per 1 ml medium}$$

Appendix C: Western Blot and ORAC 1 nM melatonin, high concentration ART and vehicle concentration calculations (combined vehicles)

Control Group (Combined Vehicles):

- **1.14 µl MeOH** per 1 ml medium (Melatonin & EFV vehicle)
- **3.74 µl** (1.2 µl + 2.54 µl) **dH₂O** per 1 ml medium (FTC and TDF vehicles)
- 1000 µl medium – 4.88 µl (1.14 µl + 3.74 µl) = **995.1 µl medium**

Melatonin Group (+Combined Vehicles):

- Weigh off 0,002 g melatonin and add to 10 ml MeOH = **Melatonin/MeOH STOCK A**
- Add 10 µl of **STOCK A** to 9.990 ml MeOH = **Melatonin/MeOH STOCK B**
- **1.14 µl Melatonin/MeOH STOCK B** per 1 ml medium (Melatonin & EFV vehicle)
- **3.74 µl** (1.2 µl + 2.54 µl) **dH₂O** per 1 ml medium (FTC and TDF vehicles)
- 1000 µl medium – 4.88 µl (1.14 µl + 3.74 µl) = **995.1 µl medium**

ART Group (+Combined Vehicles):

**The same pre-made ART stocks were used that were mentioned in Appendix B:*

EFV = 21119 µM (0.57 µl per 1 ml medium)

FTC = 10111.2 µM (1.2 µl per 1 ml medium)

TDF = 393.38 µM (2.54 µl per 1 ml medium)

- **0.57 µl EFV/MeOH** per 1 ml medium (EFV vehicle)
- **1.2 µl FTC/dH₂O** per 1 ml medium (FTC vehicle)
- **2.54 µl TDF/dH₂O** per 1 ml medium (TDF vehicle)
- **0.57 µl MeOH** per 1 ml medium (melatonin vehicle)
- 1000 µl medium – 4.11 µl (0.57 µl + 3.54 µl) = **995.9 µl medium**

Melatonin + ART Group (+Combined Vehicles):

- Weigh off 0,004 g melatonin and add to 10 ml MeOH = **Melatonin/MeOH STOCK A**
- Add 10 µl of **STOCK A** to 9.990 ml MeOH = **Melatonin/MeOH STOCK B**
- **0.57 µl Melatonin/MeOH STOCK B** per 1 ml medium (Melatonin vehicle)
- **0.57 µl EFV/MeOH** per 1 ml medium (EFV vehicle)
- **1.2 µl FTC/dH₂O** per 1 ml medium (FTC vehicle)
- **2.54 µl TDF/dH₂O** per 1 ml medium (TDF vehicle)
- 1000 µl medium – 4.88 µl (1.14 µl + 3.74 µl) = **995.1 µl medium**

Appendix D: Western Blot Raw Data Normalisation

1. "Volume Intensity" values are retrieved from Image Lab™- 5 Software for both the loading-control and the specific antibody (eNOS in the example below).
2. For each sample within a treatment group (which represents a single lane on the Western blot gel/membrane), the volume intensity of the specific antibody is divided by the volume intensity of the corresponding lane or sample of the loading-control.
Eg: eNOS "Control group/lane 1" is divided by Loading-control "Control group/lane 1"
3. An average is then determined for each treatment group.
4. The data is then normalised by dividing the antibody/loading-control value of each lane by the average "Control group" antibody/loading-control value (see value highlighted in red).
5. An average value is then determined per treatment group.

EXAMPLE DATA:

Loading-control

Groups	Volume Intensity	Average	Normalisation	Average
Controls	506844		0,7644	
	691977		1,0436	
	517413		0,7803	
	505011		0,7616	
	1094028	<u>663055</u>	1,6500	<u>1,0</u>
Melatonin	648843		0,9786	
	610935		0,9214	
	732069		1,1041	
	884052		1,3333	
	1054911	<u>786162</u>	1,5910	<u>1,2</u>
ART	866268		1,3065	
	1296165		1,9548	
	893295		1,3472	
	528723		0,7974	
	766155	<u>870121</u>	1,1555	<u>1,3</u>
ART + Melatonin	581490		0,8770	
	873522		1,3174	
	678015		1,0226	
	677742		1,0222	
	679848	<u>698123</u>	1,0253	<u>1,1</u>

t-eNOS

Groups	Volume Intensity	t-eNOS/Loading -control	Average	Normalisation	Average
Controls	1412446	2,786747007		1,1035	
	1465338	2,117610845		0,8386	
	1230642	2,37845203		0,9419	
	1848826	3,66096184		1,4497	
	1840748	1,682541946	2,52526	0,6663	1,0
Melatonin	1938342	2,987382156		1,1830	
	1819790	2,978696588		1,1796	
	1705102	2,329154765		0,9223	
	1564416	1,769597264		0,7008	
	1621046	1,536666126	2,32030	0,6085	0,9
ART	1868986	2,157514764		0,8544	
	1551508	1,196998839		0,4740	
	1598114	1,789010349		0,7084	
	1359554	2,571391825		1,0183	
	1324526	1,728796392	1,88874	0,6846	0,7
ART + Melatonin	1276268	2,194823643		0,8691	
	1675758	1,918392439		0,7597	
	1735104	2,559093825		1,0134	
	1633310	2,409928852		0,9543	
	1461328	2,149492239	2,24635	0,8512	0,9

*In the case of eNOS, a P/T ratio also needs to be determined. "P/T ratio" refers to the phospho-eNOS volume intensity divided by the total-eNOS volume intensity for each sample. Se pg 146 for example data.

p-eNOS

Groups	Volume Intensity	Average	Normalisation	Average	P/T ratio	Average	P/T ratio normalisation	Average
Controls	226269		1,218803933		0,160		1,326801227	
	222894		1,200624406		0,152		1,259833713	
	117099		0,63075685		0,095		0,788086909	
	174402		0,93942097		0,094		0,781282472	
	187578	<u>185648</u>	1,010393841	<u>1,0</u>	0,102	<u>0,121</u>	0,84399568	<u>1,0</u>
Melatonin	142893		0,769696911		0,074		0,610566832	
	116856		0,629447924		0,064		0,53184172	
	125280		0,674824022		0,073		0,608532869	
	97344		0,524346022		0,062		0,515358685	
	107388	<u>117952</u>	0,578448293	<u>0,6</u>	0,066	<u>0,068</u>	0,548672351	<u>0,6</u>
ART	118440		0,637980182		0,063		0,524861854	
	71793		0,386714887		0,046		0,383248746	
	77085		0,415220384		0,048		0,399498157	
	68733		0,370232116		0,051		0,418717872	
	67572	<u>80725</u>	0,363978359	<u>0,4</u>	0,051	<u>0,052</u>	0,422531358	<u>0,4</u>
ART + Melatonin	73566		0,396265198		0,058		0,477406055	
	51102		0,27526227		0,030		0,252568541	
	34542		0,186061393		0,020		0,164882525	
	32760		0,176462604		0,020		0,166122299	
	43368	<u>47068</u>	0,233602875	<u>0,3</u>	0,030	<u>0,032</u>	0,245795738	<u>0,3</u>

Appendix E: *Ex vivo* 10 μM melatonin, high concentration ART and vehicle concentration calculations (combined vehicles)

*Calculations made for 20 ml organ bath filled with Krebs Henseleit buffer (KHB)

Control Group (Combined Vehicles):

- **22.8 μl MeOH** in 20 ml organ bath (Melatonin & EFV vehicle)
- **70.6 μl dH₂O** in 20 ml organ bath (FTC and TDF vehicles)

Melatonin Group (+Combined Vehicles):

10 μM melatonin:

**For high concentration EFV (12 μM), 11.4 μl MeOH will be used in 20 ml system since EFV has a set stock concentration that cannot be altered. Therefore 11.4 μl MeOH needs to be used for final 10 μM melatonin when in combination with ART (and EFVs MeOH vehicle). For melatonin alone, 22.8 μl MeOH needs to be used to account for EFV vehicle.*

$$C1V1 = C2V2$$

$$(C1) \times (22.8 \mu\text{l}) = (10 \mu\text{M}) \times (20000\mu\text{l})$$

$$C1 = 0.00877193 \text{ M}$$

MW: 232.278 g/mol

$$m = (0.00877193 \text{ M}) \times (232.278 \times 0.003)$$

$$= 0.006 \text{ g melatonin in 3 ml MeOH}$$

- **22.8 μl Melatonin/MeOH** in 20 ml organ bath (Melatonin & EFV vehicle)
- **70.6 μl dH₂O** in 20 ml organ bath (FTC and TDF vehicles)

ART Group (+Combined Vehicles):

**The same pre-made ART stocks were used that were mentioned in Appendix B & C:*

EFV = 21119 μM (11.4 μl per 20 ml medium)

FTC = 10111.2 μM (19.8 μl per 20 ml medium)

TDF = 393.38 μM (50.8 μl per 20 ml medium)

- **11.4 μl EFV/MeOH** in 20 ml organ bath
- **19.8 μl FTC/dH₂O** in 20 ml organ bath
- **50.8 μl TDF/dH₂O** in 20 ml organ bath
- **11.4 μl MeOH** per 1 ml medium (melatonin vehicle)

Melatonin + ART Group (+Combined Vehicles):

$$C1V1 = C2V2$$

$$(C1) \times (11.4 \mu\text{l}) = (10 \mu\text{M}) \times (20000\mu\text{l})$$

$$\mathbf{C1 = 0.01754386 M}$$

MW: 232.278 g/mol

$$m = (0.01754386 \text{ M}) \times (232.278 \times 0.003)$$

$$= 0.012 \text{ g melatonin in 3 ml MeOH}$$

- **11.4 μl Melatonin/MeOH** in 20 ml organ bath
- **11.4 μl EFV/MeOH** in 20 ml organ bath
- **19.8 μl FTC/dH₂O** in 20 ml organ bath
- **50.8 μl TDF/dH₂O** in 20 ml organ bath

Appendix F: *In vitro* melatonin stock preparation

*Calculations for 1 cage

The rats get 10 mg/kg/day Melatonin which is calculated as follows:

$$10\text{mg/kg/day} = 10\text{mg}/1000\text{g/day} = 0.01\text{mg/g/day}$$

1. Weigh the rats on Monday mornings, and then calculate the average weight per cage

Example:

$$(293.1\text{g} + 283.6\text{g} + 312.4\text{g} + 295.8\text{g})/4 = 296.2\text{g}$$

2. Multiply the average weight by 0.01mg/g/day

Example:

$$296.2\text{g} \times 0.01 = 3\text{mg melatonin per day [A]}$$

3. The week before treatment started, rats were given 200ml of normal water on Monday around 16:30, and the next day at the same time, the left over water was measured to calculate how much water that cage drank in 24 hours. These 7 values are then averaged per cage, and divided by the amount of rats in the cage (usually 4) to get the average amount drank per rat in that cage.

Example (Cage 1):

	<u>Water given (ml)</u>	<u>Water left (ml)</u>	<u>Amount drank (ml)</u>
Monday	200	28	172
Tuesday	200	100	100
Wednesday	200	80	120
Thursday	200	68	132
Friday	200	78	122
Saturday	200	48	152
Sunday	200	22	178

$(172 + 100 + 120 + 132 + 122 + 152 + 178)/7 = 140\text{ml}$ average water drank by cage 1 per day

$140\text{ml}/4 = 35\text{ml}$ average water drank per rat in cage 1 per day [B]

- Calculate grams melatonin needed to ensure each rat is getting 10mg/kg/day when drinking an average of 35ml day. For the stock, 500ml of melatonin stock is prepared on Monday, and give the rats in their bottle (200ml per day). The stock lasts two days. The extra 100ml in the bottle is in case of spillage, and gets thrown away if not used. On Wednesday a fresh 500ml stock is made and on Friday 1 x 250ml stock (For friday) and 1 x 500ml stock (for Sat & Sun) is made.

Example:

$$\begin{aligned} \text{Melatonin (mg) needed in 500ml "stock"} &= [A]/([B]/500\text{ml}) = [0.03\text{mg}]/([35\text{ml}]/500\text{ml}) \\ &= 42.4\text{mg Melatonin} \\ &= 0,042\text{g Melatonin} \end{aligned}$$

- Melatonin is then weighed off and dissolved in 1ml methanol (Melatonin is very insoluble in water, but only 0.2% methanol of the total stock is used - therefore the potential effect of the methanol is considered negligible) and added to 500ml distilled water.

Appendix G: *In vitro* ART stock preparation

The daily dose (mg / kg) of each active ingredient for a human was calculated as follows:

$$A_{ld} = \frac{AI}{m_t}$$

A_{ld} = Daily dose of active ingredient (mg / kg).

AI = Active ingredient (mg).

m_t = Average body mass of a human(kg).

(8.6 mg / kg / day EFV; 2.9 mg / kg / day FTC; 4.3 mg / kg / day TDF)

Daily dosage per animal (mg / kg) was calculated according to the USA FDA guidelines using a conversion factor of X 6 to convert human to rat ratio:

$A_{lrat} = 6(A_{ld})$ A_{lrat} = Daily dose of active ingredient for a rat (mg / kg)

A_{ld} = Daily dose of active ingredient (mg / kg)

(EFV: 51.6 mg / kg / day; FTC: 17.4 mg / kg / day; TDF: 25.8 mg /kg / day).

Thus, for treated groups, the daily dose of active ingredients per animal needed was calculated weekly based on the average TBM of each group as follows:

$A_{ld/r} = A_{lrat}(M_{avg})$ $A_{ld/r}$ = Daily dose of active ingredient per rat (mg / kg).

A_{lrat} = Active ingredient for a rat (mg).

M_{avg} = Average TBM of rats in a group (kg).

The mass of the 3 active ingredients combined in each tablet was 1100 mg (600 mg EFV + 200 mg FTC + 300 mg TDF). The actual % (m / m) of the active ingredients in each tablet was calculated according to the mass of the tablet as follows:

$$AI\% = \frac{AI_T}{m_T} \times 100$$

AI% = % Mass active ingredient in the tablet.

AI_T = Total mass of active ingredient, 1100 g.

m_T = Total mass of the crushed tablet (g).

The amount (mg) of crushed powder of the tablet needed for a treated group with a certain average TBM (350 g per animal for example) was calculated as follow:

$$\text{EFV:Al}_{\text{rat}} = 51.6 \text{ mg/kg/day}$$

$$\text{Al}_{\text{d/r}} = \text{Al}_{\text{rat}}(\text{M}_{\text{avg}})$$

$$= (51.6 \text{ mg / kg})(0.35 \text{ kg})$$

$$= 33.22 \text{ mg}$$

$\text{Al}_{\text{d/r}}$ = Daily dose of active ingredient per rat (mg / kg).

Al_{rat} = Active ingredient for a rat (mg).

M_{avg} = Average TBM of rats in a group (kg).

If the % (m/m) of active ingredient is 68 % (for example), the amount (mg) of tablet powder weighed off was calculated as follow:

$$\text{Al}_w = \text{Al}_{\text{d/r}}(\text{Al}\%)$$

$$= 33.22 \text{ mg (68 \%)}$$

$$= 22.58$$

Al_w = Mass of the tablet powder weighed off per rat (mg).

$\text{Al}_{\text{d/r}}$ = Daily dose of active ingredient per rat (mg / kg).

$\text{Al}\%$ = Mass % active ingredient in the tablet.

To prepare enough of the FDC for 4 rats for 8 days:

$$\text{M}_{\text{TP}} = m_p(\text{N})(\text{d})$$

M_{TP} = Total mass of crushed powder per group per week (g).

m_p = Mass of the crushed tablet needed per rat daily (mg).

N = Number of rats in the group.

d = Number of days

Odimune™ tablets and crushed in a pestle and mortar and weighed according to the above formula. ARVs were made weekly by dissolving the required weight in the appropriate amount of dH₂O is needed.

Appendix H: SNP concentration calculations

- A pestle and mortar was used to crush 1 small SNP crystal.
- 0.001g of SNP powder was weighed off from the crushed crystal and add to 50ml 0.9% saline = **SNP STOCK** (60 μM). The tube was covered in tinfoil.

SNP Dilutions:

1.2nM:

$$C_1V_1 = C_2V_2$$

$$(60 \mu\text{M}) \times V_1 = 0.0012 \mu\text{M} \times 25000 \mu\text{l}$$

$$V_1 = 0.5 \mu\text{l in a 25 ml organ bath}$$

20nM

$$C_1V_1 = C_2V_2$$

$$(60 \mu\text{M}) \times V_1 = 0.0188 \mu\text{M} \times 25000 \mu\text{l}$$

$$V_1 = 7.8 \mu\text{l in a 25 ml organ bath}$$

70nM

$$C_1V_1 = C_2V_2$$

$$(60 \mu\text{M}) \times V_1 = 0.0488 \mu\text{M} \times 25000 \mu\text{l}$$

$$V_1 = 20.3 \mu\text{l in a 25 ml organ bath}$$

100nM

$$C_1V_1 = C_2V_2$$

$$(60 \mu\text{M}) \times V_1 = 0.03 \mu\text{M} \times 25000 \mu\text{l}$$

$$V_1 = 12.5 \mu\text{l in a 25 ml organ bath}$$

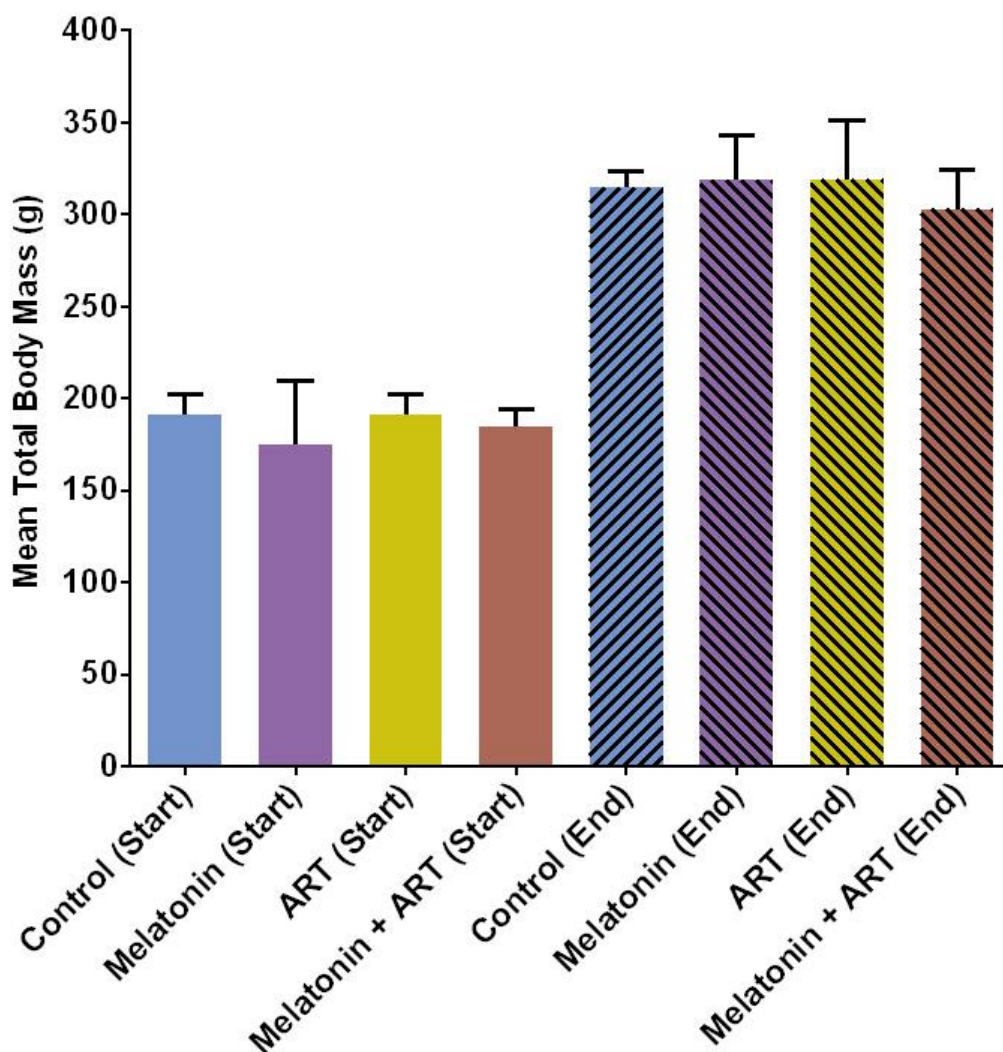
750nM

$$C_1V_1 = C_2V_2$$

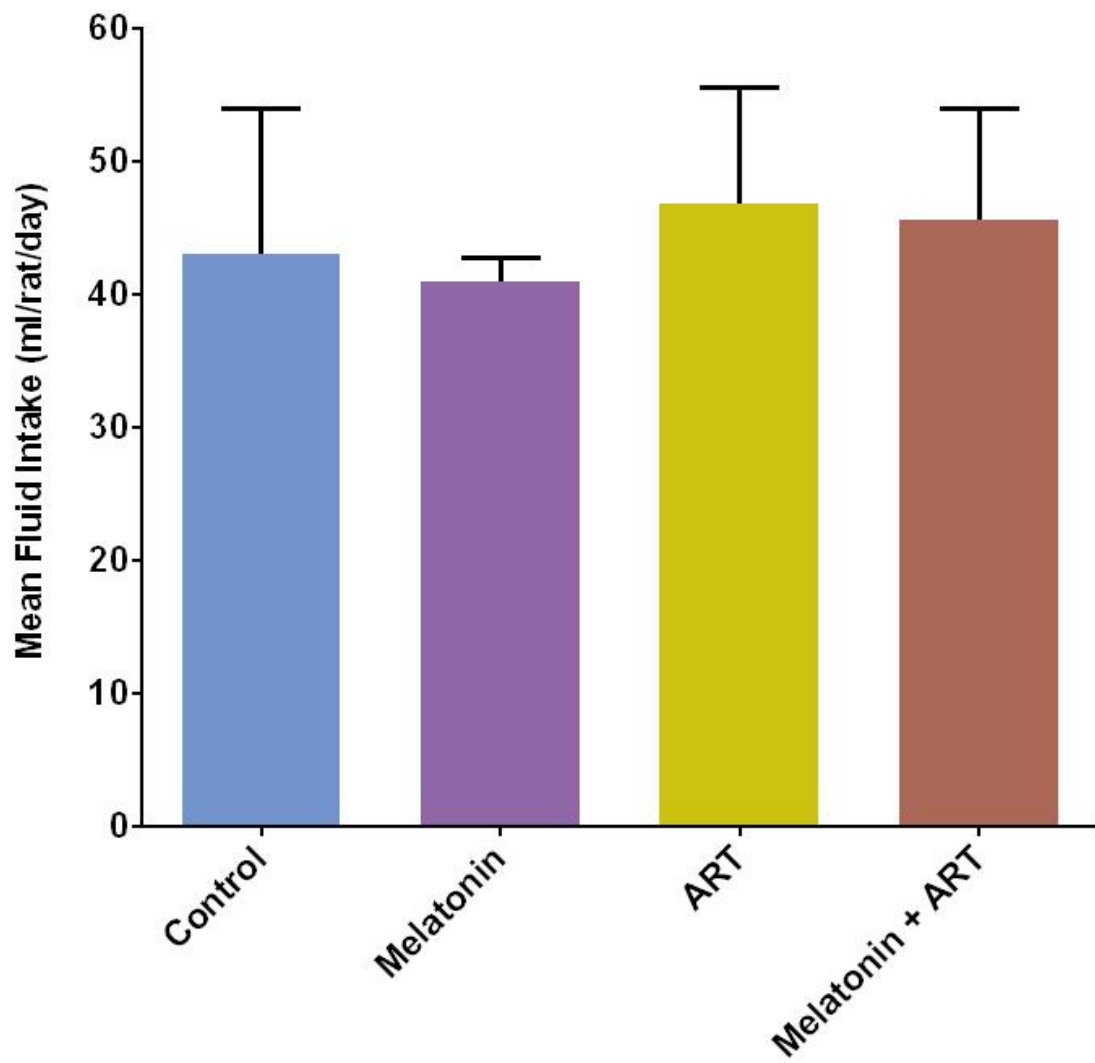
$$(60 \mu\text{M}) \times V_1 = 0.65 \mu\text{M} \times 25000 \mu\text{l}$$

$$V_1 = 270.8 \mu\text{l in a 25 ml organ bath}$$

Appendix I: Male Wistar Rat Biometric Data



Increase in rat body mass (g) over the 8-week treatment period. Starting weights were recorded at week 0, and end weights were recorded before animal sacrifice.



Mean fluid intake (ml/rat/day) over the 8-week treatment period.

References

- AIDSinfo. (2013). Guidelines for the use of antiretroviral agents in HIV-1-infected adults and adolescents.
- Ajay, M., & Mustafa, M. R. (2006). Effects of ascorbic acid on impaired vascular reactivity in aortas isolated from age-matched hypertensive and diabetic rats. *Vascular Pharmacology*, *45*(2), 127-133.
- Alam, M. N., Bristi, N. J., & Rafiquzzaman, M. (2013). Review on in vivo and in vitro methods evaluation of antioxidant activity. *Saudi Pharmaceutical Journal*, *21*(2), 143-152.
- Allegra, M., Reiter, R., Tan, D., Gentile, C., Tesoriere, L., & Livrea, M. (2003). The chemistry of melatonin's interaction with reactive species. *Journal of Pineal Research*, *34*(1), 1-10.
- Ameer, O. Z., Boyd, R., Butlin, M., Avolio, A. P., & Phillips, J. K. (2015). Abnormalities associated with progressive aortic vascular dysfunction in chronic kidney disease. *Frontiers in Physiology*, *6*, 150. doi:10.3389/fphys.2015.00150 [doi]
- Anderson, T. J. (1999). Assessment and treatment of endothelial dysfunction in humans. *Journal of the American College of Cardiology*, *34*(3), 631-638.
- Apostolova, N., Gomez- Sucerquia, L. J., Moran, A., Alvarez, A., Blas- Garcia, A., & Esplugues, J. (2010). Enhanced oxidative stress and increased mitochondrial mass during efavirenz- induced apoptosis in human hepatic cells. *British Journal of Pharmacology*, *160*(8), 2069-2084.
- Arildsen, H., Sørensen, K., Ingerslev, J., Østergaard, L., & Laursen, A. L. (2013). Endothelial dysfunction, increased inflammation, and activated coagulation in HIV-

infected patients improve after initiation of highly active antiretroviral therapy. *HIV Medicine*, 14(1), 1-9.

Arnal, J., Dinh-Xuan, A., Pueyo, M., Darblade, B., & Rami, J. (1999). Endothelium-derived nitric oxide and vascular physiology and pathology. *Cellular and Molecular Life Sciences CMLS*, 55(8-9), 1078-1087.

Arts, E. J., & Hazuda, D. J. (2012). HIV-1 antiretroviral drug therapy. *Cold Spring Harbor Perspectives in Medicine*, 2(4), a007161. doi:10.1101/cshperspect.a007161 [doi]

Aydogan, S., Yerer, M. B., & Goktas, A. (2006). Melatonin and nitric oxide. *Journal of Endocrinological Investigation*, 29(3), 281-287.

Badley, A. D. (2005). In vitro and in vivo effects of HIV protease inhibitors on apoptosis. *Cell Death & Differentiation*, 12, 924-931.

Bae, S. W., Kim, H. S., Cha, Y. N., Park, Y. S., Jo, S. A., & Jo, I. (2003). Rapid increase in endothelial nitric oxide production by bradykinin is mediated by protein kinase A signaling pathway. *Biochemical and Biophysical Research Communications*, 306(4), 981-987.

Baker, J. V., Henry, W. K., Patel, P., Bush, T. J., Conley, L. J., Mack, W. J., . . . Carpenter, C. C. (2011). Progression of carotid intima-media thickness in a contemporary human immunodeficiency virus cohort. *Clinical Infectious Diseases*, 53(8), 826-835.

Balligand, J. L., Kobzik, L., Han, X., Kaye, D. M., Belhassen, L., O'Hara, D. S., . . . Michel, T. (1995). Nitric oxide-dependent parasympathetic signaling is due to activation of constitutive endothelial (type III) nitric oxide synthase in cardiac myocytes. *The Journal of Biological Chemistry*, 270(24), 14582-14586.

Ballinger, S. W., Patterson, C., Yan, C. N., Doan, R., Burow, D. L., Young, C. G., . . . Runge, M. S. (2000). Hydrogen peroxide- and peroxynitrite-induced mitochondrial

DNA damage and dysfunction in vascular endothelial and smooth muscle cells. *Circulation Research*, 86(9), 960-966.

Banda, M. A., Lefer, D. J., & Granger, D. N. (1997). Postischemic endothelium-dependent vascular reactivity is preserved in adhesion molecule-deficient mice. *The American Journal of Physiology*, 273(6 Pt 2), H2721-5.

Barton, M., & Haudenschild, C. C. (2001). Endothelium and atherogenesis: Endothelial therapy revisited. *Journal of Cardiovascular Pharmacology*, 38, S23-S25.

Bertrand, L., & Toborek, M. (2015). Dysregulation of endoplasmic reticulum stress and autophagic responses by the antiretroviral drug efavirenz. *Molecular Pharmacology*, 88(2), 304-315. doi:10.1124/mol.115.098590 [doi]

Bevilacqua, M., Nelson, R., Mannori, G., & Cecconi, O. (1994). Endothelial-leukocyte adhesion molecules in human disease. *Annual Review of Medicine*, 45(1), 361-378.

Bijl, M. (2003). Endothelial activation, endothelial dysfunction and premature atherosclerosis in systemic autoimmune diseases. *Neth J Med*, 61(9), 273-277.

Blanchard, B., Pompon, D., & Ducrocq, C. (2000). Nitrosation of melatonin by nitric oxide and peroxynitrite. *Journal of Pineal Research*, 29(3), 184-192.

Blanco, J. J. R., García, I. S., Cerezo, J. G., de Rivera, José María Peña Sánchez, Anaya, P. M., Raya, P. G., . . . Rodríguez, J. J. V. (2006). Endothelial function in HIV-infected patients with low or mild cardiovascular risk. *Journal of Antimicrobial Chemotherapy*, 58(1), 133-139.

Bonaventura, D., Lunardi, C. N., Rodrigues, G. J., Neto, M. A., & Bendhack, L. M. (2008). A novel mechanism of vascular relaxation induced by sodium nitroprusside in the isolated rat aorta. *Nitric Oxide*, 18(4), 287-295.

- Bonetti, P. O., Lerman, L. O., & Lerman, A. (2003). Endothelial dysfunction: A marker of atherosclerotic risk. *Arteriosclerosis, Thrombosis, and Vascular Biology*, 23(2), 168-175.
- Bonnefont-Rousselot, D., & Collin, F. (2010). Melatonin: Action as antioxidant and potential applications in human disease and aging. *Toxicology*, 278(1), 55-67.
- Bonnefont-Rousselot, D., Collin, F., Jore, D., & Gardès-Albert, M. (2011). Reaction mechanism of melatonin oxidation by reactive oxygen species in vitro. *Journal of Pineal Research*, 50(3), 328-335.
- Borjigin, J., Li, X., & Snyder, S. H. (1999). The pineal gland and melatonin: Molecular and pharmacologic regulation. *Annual Review of Pharmacology and Toxicology*, 39(1), 53-65.
- Borroto-Esoda, K., Vela, J. E., Myrick, F., Ray, A. S., & Miller, M. D. (2006). In vitro evaluation of the anti-HIV activity and metabolic interactions of tenofovir and emtricitabine. *Antiviral Therapy*, 11(3), 377.
- Bousquet, L., Pruvost, A., Guyot, A. C., Farinotti, R., & Mabondzo, A. (2009). Combination of tenofovir and emtricitabine plus efavirenz: In vitro modulation of ABC transporter and intracellular drug accumulation. *Antimicrobial Agents and Chemotherapy*, 53(3), 896-902. doi:10.1128/AAC.00733-08 [doi]
- Bradford, M. M. (1976). A rapid and sensitive method for the quantitation of microgram quantities of protein utilizing the principle of protein-dye binding. *Analytical Biochemistry*, 72(1-2), 248-254.
- Brzezinski, A. (1997). Melatonin in humans. *N Engl J Med*, 1997(336), 186-195.
- Bucci, M., Gratton, J., Rudic, R. D., Acevedo, L., Roviezzo, F., Cirino, G., & Sessa, W. C. (2000). In vivo delivery of the caveolin-1 scaffolding domain inhibits nitric oxide synthesis and reduces inflammation. *Nature Medicine*, 6(12), 1362.

- Buchwalow, I. B., Schulze, W., Karczewski, P., Kostic, M. M., Wallukat, G., Morwinski, R., . . . Slezak, J. (2001). Inducible nitric oxide synthase in the myocardium. *Molecular and Cellular Biochemistry*, 217(1), 73-82.
- Butt, E., Bernhardt, M., Smolenski, A., Kotsonis, P., Frohlich, L. G., Sickmann, A., . . . Schmidt, H. H. (2000). Endothelial nitric-oxide synthase (type III) is activated and becomes calcium independent upon phosphorylation by cyclic nucleotide-dependent protein kinases. *The Journal of Biological Chemistry*, 275(7), 5179-5187.
- Cahill, P. A., & Redmond, E. M. (2016). Vascular endothelium—gatekeeper of vessel health. *Atherosclerosis*, 248, 97-109.
- Cai, H., & Harrison, D. G. (2000). Endothelial dysfunction in cardiovascular diseases: The role of oxidant stress. *Circulation Research*, 87(10), 840-844.
- Cardinali, D. P., Golombek, D. A., Rosenstein, R. E., Brusco, L. I., & Vigo, D. E. (2016). Assessing the efficacy of melatonin to curtail benzodiazepine/Z drug abuse. *Pharmacological Research*, 109, 12-23.
- Cardinali, D. P., Cano, P., Jimenez-Ortega, V., & Esquifino, A. I. (2011). Melatonin and the metabolic syndrome: Physiopathologic and therapeutical implications. *Neuroendocrinology*, 93(3), 133-142. doi:10.1159/000324699 [doi]
- Carr, A. (2003). Toxicity of antiretroviral therapy and implications for drug development. *Nature Reviews Drug Discovery*, 2(8), 624-634.
- Çelik, Ö., & Nazıroğlu, M. (2012). Melatonin modulates apoptosis and TRPM2 channels in transfected cells activated by oxidative stress. *Physiology & behavior*, 107(3), 458-465.

- Chan, D. K., & Miskimins, W. K. (2012). Metformin and phenethyl isothiocyanate combined treatment in vitro is cytotoxic to ovarian cancer cultures. *Journal of Ovarian Research*, 5(1), 19.
- Charania, S. (2017). *Investigating the effects of first line and second line antiretroviral drugs on HIV exposed endothelial function-A clinical study, supported by a mechanistic in-vitro approach* (Masters dissertation, Stellenbosch: Stellenbosch University).
- Chen, K., Pittman, R. N., & Popel, A. S. (2008). Nitric oxide in the vasculature: Where does it come from and where does it go? A quantitative perspective. *Antioxidants & Redox Signaling*, 10(7), 1185-1198.
- Chhabra, N. (2009). Endothelial dysfunction-A predictor of atherosclerosis. *Internet Journal of Medical Update*, 4(1)
- Choi, A. I., Vittinghoff, E., Deeks, S. G., Weekley, C. C., Li, Y., & Shlipak, M. G. (2011). Cardiovascular risks associated with abacavir and tenofovir exposure in HIV-infected persons. *AIDS (London, England)*, 25(10), 1289-1298. doi:10.1097/QAD.0b013e328347fa16 [doi]
- Cines, D. B., Pollak, E. S., Buck, C. A., Loscalzo, J., Zimmerman, G. A., McEver, R. P., . . . Stern, D. M. (1998). Endothelial cells in physiology and in the pathophysiology of vascular disorders. *Blood*, 91(10), 3527-3561.
- Circu, M. L., & Aw, T. Y. (2010). Reactive oxygen species, cellular redox systems, and apoptosis. *Free Radical Biology and Medicine*, 48(6), 749-762.
- Claustrat, B., Brun, J., & Chazot, G. (2005). The basic physiology and pathophysiology of melatonin. *Sleep Medicine Reviews*, 9(1), 11-24.

- Collins, P., Griffith, T., Henderson, A., & Lewis, M. (1986). Endothelium- derived relaxing factor alters calcium fluxes in rabbit aorta: A cyclic guanosine monophosphate-mediated effect. *The Journal of Physiology*, 381(1), 427-437.
- Cook-Easterwood, J., Middaugh, L. D., Griffin, W. C., Khan, I., & Tyor, W. R. (2007). Highly active antiretroviral therapy of cognitive dysfunction and neuronal abnormalities in SCID mice with HIV encephalitis. *Experimental Neurology*, 205(2), 506-512.
- Cruciani, M., Zanichelli, V., Serpelloni, G., Bosco, O., Malena, M., Mazzi, R., . . . Moyle, G. (2011). Abacavir use and cardiovascular disease events: A meta-analysis of published and unpublished data. *AIDS (London, England)*, 25(16), 1993-2004. doi:10.1097/QAD.0b013e328349c6ee [doi]
- DAD Study Group. (2007). Class of antiretroviral drugs and the risk of myocardial infarction. *N Engl J Med*, 2007(356), 1723-1735.
- Davies, N. (2013). Fixed-dose combination for adults accessing antiretroviral therapy: Advice document. *Southern African Journal of HIV Medicine*, 14(1), 41-43.
- Day, B. J., & Lewis, W. (2004). Oxidative stress in NRTI-induced toxicity. *Cardiovascular Toxicology*, 4(3), 207-216.
- De Cock, K. M. (2011). Reflections on 30 years of AIDS-volume 17, number 6—June 2011-emerging infectious disease journal-CDC.
- De Cock, K. M., Jaffe, H. W., & Curran, J. W. (2012). The evolving epidemiology of HIV/AIDS. *AIDS (London, England)*, 26(10), 1205-1213. doi:10.1097/QAD.0b013e328354622a [doi]
- de la Asuncion, J. G., del Olmo, M. L., Sastre, J., Millan, A., Pellin, A., Pallardo, F. V., & Vina, J. (1998). AZT treatment induces molecular and ultrastructural oxidative damage to muscle mitochondria. prevention by antioxidant vitamins. *The Journal of Clinical Investigation*, 102(1), 4-9. doi:10.1172/JCI1418 [doi]

- de Larrañaga, G. F., Petroni, A., Deluchi, G., Alonso, B. S., & Benetucci, J. A. (2003). Viral load and disease progression as responsible for endothelial activation and/or injury in human immunodeficiency virus-1-infected patients. *Blood Coagulation & Fibrinolysis*, *14*(1), 15-18.
- De Pablo, C., Orden, S., Calatayud, S., Martí-Cabrera, M., Esplugues, J. V., & Álvarez, Á. (2012). Short communication differential effects of tenofovir/emtricitabine and abacavir/lamivudine on human leukocyte recruitment. *Antiviral Therapy*, *17*, 1615-1619.
- Deanfield, J., Halcox, J., & Rabelink, T. (2007). Endothelial function and dysfunction: Testing and clinical relevance. *Circulation*, *115*(10), 1285-1295. doi:115/10/1285 [pii]
- Deanfield, J., Donald, A., Ferri, C., Giannattasio, C., Halcox, J., Halligan, S., . . . Pessina, A. C. (2005). Endothelial function and dysfunction. part I: Methodological issues for assessment in the different vascular beds: A statement by the working group on endothelin and endothelial factors of the european society of hypertension. *Journal of Hypertension*, *23*(1), 7-17.
- Delpech, V. (2013). The HIV epidemic: Global and UK trends. *Medicine*, *41*(8), 417-419.
- Devaraj, S., Singh, U., & Jialal, I. (2009). The evolving role of C-reactive protein in atherothrombosis. *Clinical Chemistry*, *55*(2), 229-238. doi:10.1373/clinchem.2008.108886 [doi]
- Dieye, T., Van Vooren, J., Delforge, M., Liesnard, C., Devleeschouwer, M., & Farber, C. (2000). Spontaneous apoptosis and highly active antiretroviral therapy (HAART). *Biomedicine & Pharmacotherapy*, *54*(1), 16-20.
- Dimmeler, S., & Zeiher, A. M. (1999). Nitric oxide-an endothelial cell survival factor. *Cell Death and Differentiation*, *6*(10), 964-968. doi:10.1038/sj.cdd.4400581 [doi]

- Does, A., Thiel, T., & Johnson, N. (2003). Rediscovering biology: Molecular to global perspectives. *Annenberg Learner, Washington*,
- Drexler, H. (1997). Endothelial dysfunction: Clinical implications. *Progress in Cardiovascular Diseases, 39*(4), 287-324.
- Dube, M. P., Lipshultz, S. E., Fichtenbaum, C. J., Greenberg, R., Schechter, A. D., Fisher, S. D., & Working Group 3. (2008). Effects of HIV infection and antiretroviral therapy on the heart and vasculature. *Circulation, 118*(2), e36-40. doi:10.1161/CIRCULATIONAHA.107.189625 [doi]
- Durand, M. J., & Gutterman, D. D. (2013). Diversity in mechanisms of endothelium-dependent vasodilation in health and disease. *Microcirculation, 20*(3), 239-247.
- Dutta, A., Barker, C., & Kallarakal, A. (2015). The HIV treatment gap: estimates of the financial resources needed versus available for scale-up of antiretroviral therapy in 97 countries from 2015 to 2020. *PLoS medicine, 12*(11), e1001907.
- Eberhardt, R. T., Forgione, M. A., Cap, A., Leopold, J. A., Rudd, M. A., Trolliet, M., . . . Loscalzo, J. (2000). Endothelial dysfunction in a murine model of mild hyperhomocyst(e)inemia. *The Journal of Clinical Investigation, 106*(4), 483-491. doi:10.1172/JCI8342 [doi]
- Endemann, D. H., & Schiffrin, E. L. (2004). Endothelial dysfunction. *Journal of the American Society of Nephrology : JASN, 15*(8), 1983-1992. doi:10.1097/01.ASN.0000132474.50966.DA [doi]
- Everson, F. P. (2016). *Investigating the cardiovascular effects of antiretroviral drugs in a lean and high fat/sucrose diet rat model of obesity: An in vivo and ex vivo approach*
- Fadeel, B., & Orrenius, S. (2005). Apoptosis: A basic biological phenomenon with wide-ranging implications in human disease. *Journal of Internal Medicine, 258*(6), 479-517.

- Favero, G., Franceschetti, L., Buffoli, B., Moghadasian, M. H., Reiter, R. J., Rodella, L. F., & Rezzani, R. (2017). Melatonin: Protection against age-related cardiac pathology. *Ageing Research Reviews*, 35, 336-349.
- Feletou, M., & Vanhoutte, P. M. (2006). Endothelial dysfunction: A multifaceted disorder (the wiggers award lecture). *American Journal of Physiology. Heart and Circulatory Physiology*, 291(3), H985-1002. doi:00292.2006 [pii]
- Fishman, A. P. (1982). Endothelium: A distributed organ of diverse capabilities. *Annals of the New York Academy of Sciences*, 401(1), 1-8.
- Fleming, I., & Busse, R. (1999). Signal transduction of eNOS activation. *Cardiovascular Research*, 43(3), 532-541.
- Forstermann, U., & Munzel, T. (2006). Endothelial nitric oxide synthase in vascular disease: From marvel to menace. *Circulation*, 113(13), 1708-1714. doi:113/13/1708 [pii]
- Francisci, D., Giannini, S., Baldelli, F., Leone, M., Belfiori, B., Guglielmini, G., . . . Gresele, P. (2009). HIV type 1 infection, and not short-term HAART, induces endothelial dysfunction. *AIDS (London, England)*, 23(5), 589-596. doi:10.1097/QAD.0b013e328325a87c [doi]
- Fransen, M., Nordgren, M., Wang, B., & Apanasets, O. (2012). Role of peroxisomes in ROS/RNS-metabolism: implications for human disease. *Biochimica et Biophysica Acta (BBA)-Molecular Basis of Disease*, 1822(9), 1363-1373.
- Freed, E. O. (2015). HIV-1 assembly, release and maturation. *Nature Reviews Microbiology*, 13(8), 484-496.
- Fu, W., Chai, H., Yao, Q., & Chen, C. (2005). Effects of HIV protease inhibitor ritonavir on vasomotor function and endothelial nitric oxide synthase expression. *JAIDS Journal of Acquired Immune Deficiency Syndromes*, 39(2), 152-158.

- Fukui, T., Ishizaka, N., Rajagopalan, S., Laursen, J. B., Capers, Q., 4th, Taylor, W. R., . . . Griending, K. K. (1997). p22phox mRNA expression and NADPH oxidase activity are increased in aortas from hypertensive rats. *Circulation Research*, *80*(1), 45-51.
- Fulton, D., Fontana, J., Sowa, G., Gratton, J. P., Lin, M., Li, K. X., & Sessa, W. C. (2002). Localization of endothelial nitric-oxide synthase phosphorylated on serine 1179 and nitric oxide in Golgi and plasma membrane defines the existence of two pools of active enzyme. *Journal of Biological Chemistry*, *277*(6), 4277-4284.
- Galano, A., Tan, D. X., & Reiter, R. J. (2011). Melatonin as a natural ally against oxidative stress: A physicochemical examination. *Journal of Pineal Research*, *51*(1), 1-16.
- Gallant, J. E., Parish, M. A., Keruly, J. C., & Moore, R. D. (2005). Changes in renal function associated with tenofovir disoproxil fumarate treatment, compared with nucleoside reverse-transcriptase inhibitor treatment. *Clinical Infectious Diseases*, *40*(8), 1194-1198.
- Genis, A. (2014). *Exposure of cardiac microvascular endothelial cells to harmful stimuli: A study of the cellular responses and mechanisms* (Doctoral dissertation, Stellenbosch: Stellenbosch University).
- Gerber, H., McMurtrey, A., Kowalski, J., Yan, M., Keyt, B. A., Dixit, V., & Ferrara, N. (1998). Vascular endothelial growth factor regulates endothelial cell survival through the phosphatidylinositol 3'-kinase/akt signal transduction pathway REQUIREMENT FOR flk-1/KDR ACTIVATION. *Journal of Biological Chemistry*, *273*(46), 30336-30343.
- Glover, M., Hebert, V. Y., Nichols, K., Xue, S. Y., Thibeaux, T. M., Zavec, J. A., & Dugas, T. R. (2014). Overexpression of mitochondrial antioxidant manganese superoxide dismutase (MnSOD) provides protection against AZT-or 3TC-induced endothelial dysfunction. *Antiviral Research*, *111*, 136-142.

- Goff, D. C., Jr, Lloyd-Jones, D. M., Bennett, G., Coady, S., D'Agostino, R. B., Gibbons, R., . . . American College of Cardiology/American Heart Association Task Force on Practice Guidelines. (2014). 2013 ACC/AHA guideline on the assessment of cardiovascular risk: A report of the american college of cardiology/american heart association task force on practice guidelines. *Circulation*, *129*(25 Suppl 2), S49-73. doi:10.1161/01.cir.0000437741.48606.98 [doi]
- Gordon, E. L., Danielsson, P. E., Nguyen, T. S., & Winn, H. R. (1991). A comparison of primary cultures of rat cerebral microvascular endothelial cells to rat aortic endothelial cells. *In Vitro Cellular & Developmental Biology-Animal*, *27*(4), 312-326.
- Griendling, K. K., & FitzGerald, G. A. (2003). Oxidative stress and cardiovascular injury: Part II: Animal and human studies. *Circulation*, *108*(17), 2034-2040. doi:10.1161/01.CIR.0000093661.90582.c4 [doi]
- Grubb, J. R., Dejam, A., Voell, J., Blackwelder, W. C., Sklar, P. A., Kovacs, J. A., . . . Gladwin, M. T. (2006). Lopinavir-ritonavir: Effects on endothelial cell function in healthy subjects. *The Journal of Infectious Diseases*, *193*(11), 1516-1519.
- Guardiola-Lemaitre, B. (1997). Toxicology of melatonin. *Journal of biological rhythms*, *12*(6), 697-706.
- Gunnnett, C. A., Heistad, D. D., & Faraci, F. M. (2002). Interleukin-10 protects nitric oxide-dependent relaxation during diabetes: Role of superoxide. *Diabetes*, *51*(6), 1931-1937.
- Gutiérrez, E., Flammer, A. J., Lerman, L. O., Elízaga, J., Lerman, A., & Fernández-Avilés, F. (2013). Endothelial dysfunction over the course of coronary artery disease. *European Heart Journal*, *34*(41), 3175-3181.
- Halliwell, B. (1997). What nitrates tyrosine? is nitrotyrosine specific as a biomarker of peroxynitrite formation in vivo? *FEBS Letters*, *411*(2-3), 157-160.

- Halliwell, B. (2007). Biochemistry of oxidative stress. *Biochemical Society Transactions*, 35(Pt 5), 1147-1150. doi:BST0351147 [pii]
- Hamilton, C. A., Brosnan, M. J., Al-Benna, S., Berg, G., & Dominiczak, A. F. (2002). NAD(P)H oxidase inhibition improves endothelial function in rat and human blood vessels. *Hypertension (Dallas, Tex.: 1979)*, 40(5), 755-762.
- Hardeland, R. (2005). Antioxidative protection by melatonin. *Endocrine*, 27(2), 119-130.
- Hardeland, R., Pandi-Perumal, S., & Cardinali, D. P. (2006). Melatonin. *The International Journal of Biochemistry & Cell Biology*, 38(3), 313-316.
- Hardeland, R., & Poeggeler, B. (2003). Non-vertebrate melatonin. *Journal of Pineal Research*, 34(4), 233-241.
- Harms, C., Lautenschlager, M., Bergk, A., Freyer, D., Weih, M., Dirnagl, U., . . . Hortnagl, H. (2000). Melatonin is protective in necrotic but not in caspase-dependent, free radical-independent apoptotic neuronal cell death in primary neuronal cultures. *FASEB Journal : Official Publication of the Federation of American Societies for Experimental Biology*, 14(12), 1814-1824.
- Heitzer, T., Schlinzig, T., Krohn, K., Meinertz, T., & Munzel, T. (2001). Endothelial dysfunction, oxidative stress, and risk of cardiovascular events in patients with coronary artery disease. *Circulation*, 104(22), 2673-2678.
- Holmberg, S. D., Moorman, A. C., Williamson, J. M., Tong, T. C., Ward, D. J., Wood, K. C., . . . HIV Outpatient Study (HOPS) Investigators. (2002). Protease inhibitors and cardiovascular outcomes in patients with HIV-1. *The Lancet*, 360(9347), 1747-1748.
- Huang, D., Ou, B., Hampsch-Woodill, M., Flanagan, J. A., & Prior, R. L. (2002). High-throughput assay of oxygen radical absorbance capacity (ORAC) using a multichannel liquid handling system coupled with a microplate fluorescence reader in 96-well format. *Journal of Agricultural and Food Chemistry*, 50(16), 4437-4444.

- Hulgan, T., Morrow, J., D'Aquila, R. T., Raffanti, S., Morgan, M., Rebeiro, P., & Haas, D. W. (2003). Oxidant stress is increased during treatment of human immunodeficiency virus infection. *Clinical Infectious Diseases*, 37(12), 1711-1717.
- Hung, M., Kravtsov, G. M., Lau, C., Poon, A. M., Tipoe, G. L., & Fung, M. (2013). Melatonin ameliorates endothelial dysfunction, vascular inflammation, and systemic hypertension in rats with chronic intermittent hypoxia. *Journal of Pineal Research*, 55(3), 247-256.
- Hurst, J. K. (2002). Whence nitrotyrosine? *The Journal of Clinical Investigation*, 109(10), 1287-1289. doi:10.1172/JCI15816 [doi]
- Ignarro, L. J., Harbison, R. G., Wood, K. S., & Kadowitz, P. J. (1986). Activation of purified soluble guanylate cyclase by endothelium-derived relaxing factor from intrapulmonary artery and vein: Stimulation by acetylcholine, bradykinin and arachidonic acid. *The Journal of Pharmacology and Experimental Therapeutics*, 237(3), 893-900.
- Imperial, E. G. (2017). *Effect of Aspalathus linearis supplementation, during anti-retroviral treatment, on the heart and aortas of male Wistar rats and the effects of drinking rooibos on the cardiovascular profile of patients on ART*(Doctoral dissertation, Stellenbosch: Stellenbosch University).
- Ischiropoulos, H., Gow, A., Thom, S. R., Kooy, N. W., Royall, J. A., & Crow, J. P. (1999). [38] detection of reactive nitrogen species using 2, 7-dichlorodihydrofluorescein and dihydrorhodamine 123. *Methods in Enzymology*, 301, 367-373.
- Islam, F., Wu, J., Jansson, J., & Wilson, D. (2012). Relative risk of cardiovascular disease among people living with HIV: A systematic review and meta- analysis. *HIV Medicine*, 13(8), 453-468.

- Jamaluddin, M. S., Lin, P. H., Yao, Q., & Chen, C. (2010). Non-nucleoside reverse transcriptase inhibitor efavirenz increases monolayer permeability of human coronary artery endothelial cells. *Atherosclerosis*, *208*(1), 104-111.
- Jiang, B., Hebert, V. Y., Li, Y., Mathis, J. M., Alexander, J. S., & Dugas, T. R. (2007). HIV antiretroviral drug combination induces endothelial mitochondrial dysfunction and reactive oxygen species production, but not apoptosis. *Toxicology and Applied Pharmacology*, *224*(1), 60-71.
- Jiang, B., Khandelwal, A. R., Rogers, L. K., Hebert, V. Y., Kleinedler, J. J., Zavec, J. H., . . . Dugas, T. R. (2010). Antiretrovirals induce endothelial dysfunction via an oxidant-dependent pathway and promote neointimal hyperplasia. *Toxicological Sciences*, *117*(2), 524-536.
- Jiang, B., Hebert, V. Y., Zavec, J. H., & Dugas, T. R. (2006). Antiretrovirals induce direct endothelial dysfunction in vivo. *Journal of Acquired Immune Deficiency Syndromes (1999)*, *42*(4), 391-395. doi:10.1097/01.qai.0000228790.40235.0c [doi]
- John, S., & Schmieder, R. E. (2000). Impaired endothelial function in arterial hypertension and hypercholesterolemia: Potential mechanisms and differences. *Journal of Hypertension*, *18*(4), 363-374.
- Joint United Nations Programme on HIV/AIDS. (2010). *Global report: UNAIDS report on the global AIDS epidemic 2010* UNAIDS.
- Jones, K. A., Wong, G. Y., Jankowski, C. J., Akao, M., & Warner, D. O. (1999). cGMP modulation of Ca²⁺ sensitivity in airway smooth muscle. *The American Journal of Physiology*, *276*(1 Pt 1), L35-40.
- Jumnongprakhon, P., Govitrapong, P., Tocharus, C., & Tocharus, J. (2016). Inhibitory effect of melatonin on cerebral endothelial cells dysfunction induced by methamphetamine via NADPH oxidase-2. *Brain Research*, *1650*, 84-92.

- Karbach, S., Wenzel, P., Waisman, A., Munzel, T., & Daiber, A. (2014). eNOS uncoupling in cardiovascular diseases-the role of oxidative stress and inflammation. *Current Pharmaceutical Design, 20*(22), 3579-3594.
- Karbownik, M., & Reiter, R. J. (2000). Antioxidative effects of melatonin in protection against cellular damage caused by ionizing radiation. *Proceedings of the Society for Experimental Biology and Medicine, 225*(1), 9-22.
- Kearney, B. P., Flaherty, J. F., & Shah, J. (2004). Tenofovir disoproxil fumarate. *Clinical Pharmacokinetics, 43*(9), 595-612.
- Kim, J. T., Jang, H. Y., Park, C. K., Cheong, H. T., Park, I. C., & Yang, B. K. (2011). Melatonin attenuates nitric oxide induced oxidative stress on viability and gene expression in bovine oviduct epithelial cells, and subsequently increases development of bovine IVM/IVF embryos. *Asian-Australasian Journal of Animal Sciences, 24*(2), 190-197.
- Kirchhoff, F. (2013). HIV life cycle: Overview. *Encyclopedia of AIDS. New York, NY: Springer, , 1-9.*
- Klein, D., Hurley, L. B., Quesenberry, C. P., Jr, & Sidney, S. (2002). Do protease inhibitors increase the risk for coronary heart disease in patients with HIV-1 infection? *Journal of Acquired Immune Deficiency Syndromes (1999), 30*(5), 471-477.
- Kleinhenz, D. J., Fan, X., Rubin, J., & Hart, C. M. (2003). Detection of endothelial nitric oxide release with the 2, 3-diaminonaphthalene assay. *Free Radical Biology and Medicine, 34*(7), 856-861.
- Kücükakin, B., Gögenur, I., Reiter, R. J., & Rosenberg, J. (2009). Oxidative stress in relation to surgery: Is there a role for the antioxidant melatonin? *Journal of Surgical Research, 152*(2), 338-347.

- Kuribayashi, K., Mayes, P. A., & El-Deiry, W. S. (2006). What are caspases 3 and 7 doing upstream of the mitochondria? *Cancer Biology & Therapy*, *5*(7), 763-765.
- Kuzkaya, N., Weissmann, N., Harrison, D. G., & Dikalov, S. (2003). Interactions of peroxynitrite, tetrahydrobiopterin, ascorbic acid, and thiols: Implications for uncoupling endothelial nitric-oxide synthase. *The Journal of Biological Chemistry*, *278*(25), 22546-22554. doi:10.1074/jbc.M302227200 [doi]
- KZN Department of Health. (2014). Publicity material.
- Laemmli, U. K. (1970). Cleavage of structural proteins during the assembly of the head of bacteriophage T4. *Nature*, *227*(5259), 680-685.
- Landmesser, U., & Harrison, D. G. (2001). Oxidant stress as a marker for cardiovascular events: Ox marks the spot. *Circulation*, *104*(22), 2638-2640.
- Lang, S., Mary-Krause, M., Cotte, L., Gilquin, J., Partisani, M., Simon, A., . . . Costagliola, D. (2010). Impact of individual antiretroviral drugs on the risk of myocardial infarction in human immunodeficiency virus–infected patients: A case-control study nested within the french hospital database on HIV ANRS cohort CO4. *Archives of Internal Medicine*, *170*(14), 1228-1238.
- Laskey, S. B., & Siliciano, R. F. (2014). A mechanistic theory to explain the efficacy of antiretroviral therapy. *Nature Reviews Microbiology*, *12*(11), 772-780.
- Lerman, A., & Zeiher, A. M. (2005). Endothelial function: Cardiac events. *Circulation*, *111*(3), 363-368. doi:111/3/363 [pii]
- Levitt, N. S., Steyn, K., Dave, J., & Bradshaw, D. (2011). Chronic noncommunicable diseases and HIV-AIDS on a collision course: Relevance for health care delivery, particularly in low-resource settings--insights from south africa. *The American Journal of Clinical Nutrition*, *94*(6), 1690S-1696S. doi:10.3945/ajcn.111.019075 [doi]

- Lewis, W., Copeland, W. C., & Day, B. J. (2001). Mitochondrial DNA depletion, oxidative stress, and mutation: Mechanisms Of dysfunction from nucleoside reverse transcriptase inhibitors. *Laboratory Investigation*, 81(6), 777.
- Lewis, W., & Dalakas, M. C. (1995). Mitochondrial toxicity of antiviral drugs. *Nature Medicine*, 1(5), 417-422.
- Libby, P., Ridker, P. M., & Maseri, A. (2002). Inflammation and atherosclerosis. *Circulation*, 105(9), 1135-1143.
- Limaye, V., & Vadas, M. (2007). The vascular endothelium: Structure and function. *Mechanisms of Vascular Disease*, , 1-10.
- López, A., García, J. A., Escames, G., Venegas, C., Ortiz, F., López, L. C., & Acuña-Castroviejo, D. (2009). Melatonin protects the mitochondria from oxidative damage reducing oxygen consumption, membrane potential, and superoxide anion production. *Journal of Pineal Research*, 46(2), 188-198.
- Loscalzo, J., & Vita, J. A. (1994). Ischemia, hyperemia, exercise, and nitric oxide. *Circulation*, 90(5), 2556-2559.
- Loubser, D. J. (2014). *Nitric oxide and the endothelium : Characterisation of in vitro nitric oxide detection techniques and an ex vivo method of measuring endothelial function*
- Luber, A., Condoluci, D., Slowinski, P., Andrews, M., Olson, K., Peloquin, C., . . . Pakes, G. (2010). Steady- state amprenavir and tenofovir pharmacokinetics after coadministration of unboosted or ritonavir- boosted fosamprenavir with tenofovir disoproxil fumarate in healthy volunteers. *HIV Medicine*, 11(3), 193-199.
- Lusis, A. J. (2000). Atherosclerosis. *Nature*, 407(6801), 233-241.

- Maarman, G., Blackhurst, D., Thienemann, F., Blauwet, L., Butrous, G., Davies, N., . . . Lecour, S. (2015). Melatonin as a preventive and curative therapy against pulmonary hypertension. *Journal of Pineal Research*, *59*(3), 343-353.
- Manda, K. R., Banerjee, A., Banks, W. A., & Ercal, N. (2011). Highly active antiretroviral therapy drug combination induces oxidative stress and mitochondrial dysfunction in immortalized human blood–brain barrier endothelial cells. *Free Radical Biology and Medicine*, *50*(7), 801-810.
- Marín-García, J. (2016). Cell death in the pathogenesis and progression of heart failure. *Heart failure reviews*, *21*(2), 117-121.
- Markwell, M. A. K., Haas, S. M., Bieber, L., & Tolbert, N. (1978). A modification of the lowry procedure to simplify protein determination in membrane and lipoprotein samples. *Analytical Biochemistry*, *87*(1), 206-210.
- Masiá, M., Padilla, S., Bernal, E., Almenar, M. V., Molina, J., Hernández, I., . . . Gutiérrez, F. (2007). Influence of antiretroviral therapy on oxidative stress and cardiovascular risk: A prospective cross-sectional study in HIV-infected patients. *Clinical Therapeutics*, *29*(7), 1448-1455.
- Mashele, N., Charania, S., Essop, F., Webster, I., Westcott, C., Goswami, N., & Strijdom, H. (2016). The effects of HIV-infection and anti-retroviral treatment on endothelial function in a South African cohort. *Atherosclerosis*, *252*, e162-e163.
- Matthys, K. E., & Bult, H. (1997). Nitric oxide function in atherosclerosis. *Mediators of inflammation*, *6*(1), 3-21.
- Meintjes, G., Conradie, J., Cox, V., Dlamini, S., Fabian, J., Maartens, G., . . . Moorhouse, M. (2014). Adult antiretroviral therapy guidelines 2014. *Southern African Journal of HIV Medicine*, *15*(4), 121-143.

- Michel, T., & Feron, O. (1997). Nitric oxide synthases: Which, where, how, and why? *The Journal of Clinical Investigation*, 100(9), 2146-2152. doi:10.1172/JCI119750 [doi]
- Molina, J., Peytavin, G., Perusat, S., Lascoux- Combes, C., Sereni, D., Rozenbaum, W., & Chene, G. (2004). Pharmacokinetics of emtricitabine, didanosine and efavirenz administered once- daily for the treatment of HIV- infected adults (pharmacokinetic substudy of the ANRS 091 trial). *HIV Medicine*, 5(2), 99-104.
- Moncada, S., & Higgs, E. (2006). The discovery of nitric oxide and its role in vascular biology. *British Journal of Pharmacology*, 147(S1)
- Mondal, D., Liu, K., Hamblin, M., Lasky, J. A., & Agrawal, K. C. (2013). Nelfinavir suppresses insulin signaling and nitric oxide production by human aortic endothelial cells: protective effects of thiazolidinediones. *The Ochsner Journal*, 13(1), 76-90.
- Mudau, M. (2010). *Endothelial dysfunction in cardiac microvascular endothelial cells: an investigation into cellular mechanisms and putative role of oleanolic acid in reversing endothelial dysfunction* (Masters dissertation, Stellenbosch: University of Stellenbosch).
- Mudau, M., Genis, A., Lochner, A., & Strijdom, H. (2012). Endothelial dysfunction: The early predictor of atherosclerosis. *Cardiovascular Journal of Africa*, 23(4), 222-231.
- Muniyappa, R., & Sowers, J. R. (2013). Role of insulin resistance in endothelial dysfunction. *Reviews in Endocrine and Metabolic Disorders*, 14(1), 5-12.
- Munzel, T., Daiber, A., Ullrich, V., & Mulsch, A. (2005). Vascular consequences of endothelial nitric oxide synthase uncoupling for the activity and expression of the soluble guanylyl cyclase and the cGMP-dependent protein kinase. *Arteriosclerosis, Thrombosis, and Vascular Biology*, 25(8), 1551-1557. doi:01.ATV.0000168896.64927.bb [pii]

- Murphy, M. P. (1999). Nitric oxide and cell death. *Biochimica et Biophysica Acta (BBA)-Bioenergetics*, 1411(2-3), 401-414.
- Navarro-Antolin, J., Lopez-Munoz, M. J., Klatt, P., Soria, J., Michel, T., & Lamas, S. (2001). Formation of peroxynitrite in vascular endothelial cells exposed to cyclosporine A. *FASEB Journal : Official Publication of the Federation of American Societies for Experimental Biology*, 15(7), 1291-1293.
- Nduhirabandi, F. (2010). The effects of chronic melatonin treatment on myocardial function and ischaemia and reperfusion injury in A rat model of diet-induced obesity. *The Effects of Chronic Melatonin Treatment on Myocardial Function and Ischaemia and Reperfusion Injury in a Rat Model of Diet-Induced Obesity*,
- Nduhirabandi, F. (2014). *The role of melatonin in cardioprotection: An investigation into the mechanisms involved in glucose homeostasis, microvascular endothelial function and mitochondrial function in normal and insulin resistant states*
- Obel, N., Thomsen, H. F., Kronborg, G., Larsen, C. S., Hildebrandt, P. R., Sørensen, H. T., & Gerstoft, J. (2007). Ischemic heart disease in HIV-infected and HIV-uninfected individuals: A population-based cohort study. *Clinical Infectious Diseases*, 44(12), 1625-1631.
- Osseni, R. A., Rat, P., Bogdan, A., Warnet, J. M., & Touitou, Y. (2000). Evidence of prooxidant and antioxidant action of melatonin on human liver cell line HepG2. *Life sciences*, 68(4), 387-399.
- Pacher, P., Beckman, J. S., & Liaudet, L. (2007). Nitric oxide and peroxynitrite in health and disease. *Physiological Reviews*, 87(1), 315-424. doi:87/1/315 [pii]
- Palmer, R. M., Ashton, D., & Moncada, S. (1988). Vascular endothelial cells synthesize nitric oxide from L-arginine. *Nature*, 333(6174), 664-666.

- Palmisano, L., & Vella, S. (2011). A brief history of antiretroviral therapy of HIV infection: Success and challenges. *Annali Dell'Istituto Superiore Di sanit *, 47(1), 44-48.
- Pandi-Perumal, S. R., Srinivasan, V., Maestroni, G., Cardinali, D., Poeggeler, B., & Hardeland, R. (2006). Melatonin. *The FEBS Journal*, 273(13), 2813-2838.
- Park, K., & Park, W. J. (2015). Endothelial dysfunction: Clinical implications in cardiovascular disease and therapeutic approaches. *Journal of Korean Medical Science*, 30(9), 1213-1225.
- Park, M. S., Ravi, V., & Araujo, D. M. (2010). Inhibiting the VEGF-VEGFR pathway in angiosarcoma, epithelioid hemangioendothelioma, and hemangiopericytoma/solitary fibrous tumor. *Current Opinion in Oncology*, 22(4), 351-355. doi:10.1097/CCO.0b013e32833aaad4 [doi]
- Pennathur, S., & Heinecke, J. W. (2007). Oxidative stress and endothelial dysfunction in vascular disease. *Current Diabetes Reports*, 7(4), 257-264.
- Petrosillo, G., Colantuono, G., Moro, N., Ruggiero, F. M., Tiravanti, E., Di Venosa, N., ... & Paradies, G. (2009). Melatonin protects against heart ischemia-reperfusion injury by inhibiting mitochondrial permeability transition pore opening. *American Journal of Physiology-Heart and Circulatory Physiology*, 297(4), H1487-H1493.
- Pitrak, D. L., Novak, R. M., Estes, R., Tschampa, J., Abaya, C. D., Martinson, J., . . . Landay, A. L. (2015). Apoptosis pathways in HIV-1-infected patients before and after highly active antiretroviral therapy: Relevance to immune recovery. *AIDS Research and Human Retroviruses*, 31(2), 208-216.
- Poeggeler, B., Thuermann, S., Dose, A., Schoenke, M., Burkhardt, S., & Hardeland, R. (2002). Melatonin's unique radical scavenging properties—roles of its functional substituents as revealed by a comparison with its structural analogs. *Journal of Pineal Research*, 33(1), 20-30.

- Pogan, L., Bissonnette, P., Parent, L., & Sauve, R. (2002). The effects of melatonin on Ca²⁺ homeostasis in endothelial cells. *Journal of Pineal Research*, 33(1), 37-47.
- Prast, H., & Philippu, A. (2001). Nitric oxide as modulator of neuronal function. *Progress in Neurobiology*, 64(1), 51-68.
- Prior, R. L., Hoang, H., Gu, L., Wu, X., Bacchiocca, M., Howard, L., . . . Jacob, R. (2003). Assays for hydrophilic and lipophilic antioxidant capacity (oxygen radical absorbance capacity (ORACFL)) of plasma and other biological and food samples. *Journal of Agricultural and Food Chemistry*, 51(11), 3273-3279.
- Privett, K., Kunert, M., & Lombard, J. (2004). Vascular phenotypes: High throughput characterization of vascular reactivity in rats conditioned on 0.4% and 4.0% NaCl diet. *Medical College of Wisconsin*,
- Putney, J. W. (1986). A model for receptor-regulated calcium entry. *Cell Calcium*, 7(1), 1-12.
- Rajendran, P., Rengarajan, T., Thangavel, J., Nishigaki, Y., Sakthisekaran, D., Sethi, G., & Nishigaki, I. (2013). The vascular endothelium and human diseases. *Int J Biol Sci*, 9(10), 1057-1069.
- Razani, B., Woodman, S. E., & Lisanti, M. P. (2002). Caveolae: From cell biology to animal physiology. *Pharmacological Reviews*, 54(3), 431-467.
- Reiter, R. J. (1993). The melatonin rhythm: Both a clock and a calendar. *Experientia*, 49(8), 654-664.
- Reiter, R. J., Tan, D., & Maldonado, M. D. (2005). Melatonin as an antioxidant: Physiology versus pharmacology. *Journal of Pineal Research*, 39(2), 215-216.

- Reiter, R. J., Tan, D., Manchester, L. C., & Qi, W. (2001). Biochemical reactivity of melatonin with reactive oxygen and nitrogen species. *Cell Biochemistry and Biophysics*, 34(2), 237-256.
- Reiter, R. J., Tan, D., Mayo, J. C., Sainz, R. M., Leon, J., & Czarnocki, Z. (2003). Melatonin as an antioxidant: Biochemical mechanisms and pathophysiological implications in humans. *Acta Biochimica Polonica-English Edition*-, 50(4), 1129-1146.
- Reiter, R. J., Tan, D., Osuna, C., & Gitto, E. (2000). Actions of melatonin in the reduction of oxidative stress. *Journal of Biomedical Science*, 7(6), 444-458.
- Riccardi, C., & Nicoletti, I. (2006). Analysis of apoptosis by propidium iodide staining and flow cytometry. *Nature Protocols*, 1(3), 1458-1461.
- Rodriguez, C., Mayo, J. C., Sainz, R. M., Antolin, I., Herrera, F., Martin, V., & Reiter, R. J. (2004). Regulation of antioxidant enzymes: A significant role for melatonin. *Journal of Pineal Research*, 36(1), 1-9.
- Rossig, L., Fichtlscherer, B., Breitschopf, K., Haendeler, J., Zeiher, A. M., Mulsch, A., & Dimmeler, S. (1999). Nitric oxide inhibits caspase-3 by S-nitrosation in vivo. *The Journal of Biological Chemistry*, 274(11), 6823-6826.
- Rubbert, A., Behrens, G., & Ostrowski, M. (2007). Pathogenesis of HIV-1 infection. *HIV Medicine*, 3, 59-63.
- Ruelas, D. S., & Greene, W. C. (2013). An integrated overview of HIV-1 latency. *Cell*, 155(3), 519-529.
- Russell, F. D., & Hamilton, K. D. (2014). Nutrient deprivation increases vulnerability of endothelial cells to proinflammatory insults. *Free Radical Biology and Medicine*, 67, 408-415.

- San Jose, G., Fortuno, A., Beloqui, O., Diez, J., & Zalba, G. (2008). NADPH oxidase CYBA polymorphisms, oxidative stress and cardiovascular diseases. *Clinical Science (London, England : 1979)*, *114*(3), 173-182. doi:10.1042/CS20070130 [doi]
- Sandoo, A., van Zanten, J. J., Metsios, G. S., Carroll, D., & Kitas, G. D. (2010). The endothelium and its role in regulating vascular tone. *The Open Cardiovascular Medicine Journal*, *4*, 302-312. doi:10.2174/1874192401004010302 [doi]
- Schilling, W. P., Cabello, O. A., & Rajan, L. (1992). Depletion of the inositol 1,4,5-trisphosphate-sensitive intracellular Ca²⁺ store in vascular endothelial cells activates the agonist-sensitive ca(2+)-influx pathway. *The Biochemical Journal*, *284* (Pt 2)(Pt 2), 521-530.
- Shankar, S. S., Dubé, M. P., Gorski, J. C., Klaunig, J. E., & Steinberg, H. O. (2005). Indinavir impairs endothelial function in healthy HIV-negative men. *American Heart Journal*, *150*(5), 933. e1-933. e7.
- Sharp, P. M., & Hahn, B. H. (2011). Origins of HIV and the AIDS pandemic. *Cold Spring Harbor Perspectives in Medicine*, *1*(1), a006841. doi:10.1101/cshperspect.a006841 [doi]
- Sierra-Aragon, S., & Walter, H. (2012). Targets for inhibition of HIV replication: Entry, enzyme action, release and maturation. *Intervirology*, *55*(2), 84-97. doi:10.1159/000331995 [doi]
- Silva, C., Tamura, E., Macedo, S., Cecon, E., Bueno- Alves, L., Farsky, S., . . . Markus, R. (2007). Melatonin inhibits nitric oxide production by microvascular endothelial cells in vivo and in vitro. *British Journal of Pharmacology*, *151*(2), 195-205.
- Skowrya, A., Zdziechowicz, I., Mikula, T., & Wiercińska-Drapało, A. (2012). Endothelial dysfunction—An important factor in the progression of atherosclerosis in HIV-infected persons. *HIV & AIDS Review*, *11*(3), 57-60.

- Smit-van Schalkwyk, M. (2016). Rooibos and melatonin: Putative modulation of nicotine-induced effects on vascular function. *Rooibos and Melatonin: Putative Modulation of Nicotine-Induced Effects on Vascular Function*,
- Solages, A., Vita, J. A., Thornton, D. J., Murray, J., Heeren, T., Craven, D. E., & Horsburgh Jr, C. R. (2006). Endothelial function in HIV-infected persons. *Clinical Infectious Diseases*, 42(9), 1325-1332.
- Song, J., Kang, S. M., Lee, W. T., Park, K. A., Lee, K. M., & Lee, J. E. (2014). The beneficial effect of melatonin in brain endothelial cells against oxygen-glucose deprivation followed by reperfusion-induced injury. *Oxidative Medicine and Cellular Longevity*, 2014, 639531. doi:10.1155/2014/639531 [doi]
- South African National AIDS Council. (2015). *Global AIDS response progress report*. ().
- South African National AIDS Council. (2016). Press statement: SANAC applauds health minister's move to treat everyone with HIV.
- Speyer, C. L., Neff, T. A., Warner, R. L., Guo, R. F., Sarma, J. V., Riedemann, N. C., ... & Ward, P. A. (2003). Regulatory effects of iNOS on acute lung inflammatory responses in mice. *The American journal of pathology*, 163(6), 2319-2328.
- Sprenger, J., Hardeland, R., Fuhrberg, B., & Han, S. (1999). Melatonin and other 5-methoxylated indoles in yeast: Presence in high concentrations and dependence on tryptophan availability. *Cytologia*, 64(2), 209-213.
- Stamler, J. S., Singel, D. J., & Loscalzo, J. (1992). Biochemistry of nitric oxide and its redox-activated forms. *Science-New York then Washington-*, 258, 1898-1898.
- Statistics, S. A. (2015). Mid-year population estimates 2015. *Pretoria: Statistics SA*.
- Stein, J. H., Klein, M. A., Bellehumeur, J. L., McBride, P. E., Wiebe, D. A., Otvos, J. D., & Sosman, J. M. (2001). Use of human immunodeficiency virus-1 protease inhibitors is

associated with atherogenic lipoprotein changes and endothelial dysfunction. *Circulation*, 104(3), 257-262.

Strategies for Management of Antiretroviral Therapy (SMART) Study Group. (2006). CD4 count-guided interruption of antiretroviral treatment. *N Engl J Med*, 2006(355), 2283-2296.

Strijdom, H., Friedrich, S. O., Hattingh, S., Chamane, N., & Lochner, A. (2009). Hypoxia-induced regulation of nitric oxide synthase in cardiac endothelial cells and myocytes and the role of the PI3-K/PKB pathway. *Molecular and cellular biochemistry*, 321(1-2), 23-35.

Strijdom, H., & Lochner, A. (2009). Cardiac endothelium: More than just a barrier: Cardiac endothelium. *SA Heart*, 6(3), 174-185.

Strijdom, H., Muller, C., & Lochner, A. (2004). Direct intracellular nitric oxide detection in isolated adult cardiomyocytes: Flow cytometric analysis using the fluorescent probe, diaminofluorescein. *Journal of Molecular and Cellular Cardiology*, 37(4), 897-902.

Stuehr, D. J. (2004). Enzymes of the L-arginine to nitric oxide pathway. *The Journal of Nutrition*, 134(10 Suppl), 2748S-2751S; discussion 2765S-2767S. doi:134/10/2748S [pii]

Sutliff, R. L., Dikalov, S., Weiss, D., Parker, J., Raidel, S., Racine, A. K., . . . Lewis, W. (2002). Nucleoside reverse transcriptase inhibitors impair endothelium-dependent relaxation by increasing superoxide. *American Journal of Physiology. Heart and Circulatory Physiology*, 283(6), H2363-70. doi:10.1152/ajpheart.00151.2002 [doi]

Taddei, S., Ghiadoni, L., Virdis, A., Versari, D., & Salvetti, A. (2003). Mechanisms of endothelial dysfunction: Clinical significance and preventive non-pharmacological therapeutic strategies. *Current Pharmaceutical Design*, 9(29), 2385-2402.

- Tamura, E. K., Silva, C. L., & Markus, R. P. (2006). Melatonin inhibits endothelial nitric oxide production in vitro. *Journal of Pineal Research*, *41*(3), 267-274.
- Tamura, E. K., Cecon, E., Monteiro, A. W. A., Silva, C. L. M., & Markus, R. P. (2009). Melatonin inhibits LPS- induced NO production in rat endothelial cells. *Journal of Pineal Research*, *46*(3), 268-274.
- Tan, D., Manchester, L. C., Terron, M. P., Flores, L. J., & Reiter, R. J. (2007). One molecule, many derivatives: A never- ending interaction of melatonin with reactive oxygen and nitrogen species? *Journal of Pineal Research*, *42*(1), 28-42.
- Tan, D., Manchester, L. C., Reiter, R. J., Plummer, B. F., Limson, J., Weintraub, S. T., & Qi, W. (2000). Melatonin directly scavenges hydrogen peroxide: A potentially new metabolic pathway of melatonin biotransformation. *Free Radical Biology and Medicine*, *29*(11), 1177-1185.
- Tan, D., Reiter, R. J., Manchester, L. C., Yan, M., El-Sawi, M., Sainz, R. M., . . . Hardeland, R. (2002). Chemical and physical properties and potential mechanisms: Melatonin as a broad spectrum antioxidant and free radical scavenger. *Current Topics in Medicinal Chemistry*, *2*(2), 181-197.
- Tengattini, S., Reiter, R. J., Tan, D., Terron, M. P., Rodella, L. F., & Rezzani, R. (2008). Cardiovascular diseases: Protective effects of melatonin. *Journal of Pineal Research*, *44*(1), 16-25.
- Thienemann, F., Sliwa, K., & Rockstroh, J. K. (2013). HIV and the heart: The impact of antiretroviral therapy: A global perspective. *European Heart Journal*, *34*(46), 3538-3546. doi:10.1093/eurheartj/eh388 [doi]
- Thompson, M. A., Aberg, J. A., Hoy, J. F., Telenti, A., Benson, C., Cahn, P., . . . Reiss, P. (2012). Antiretroviral treatment of adult HIV infection: 2012 recommendations of the international antiviral Society–USA panel. *Jama*, *308*(4), 387-402.

- Tiede, L., Cook, E., Morsey, B., & Fox, H. (2012). Oxygen matters: Tissue culture oxygen levels affect mitochondrial function and structure as well as responses to HIV viroproteins. *Cell Death & Disease*, 3(3), e274.
- Tomasian, D., Keaney Jr, J. F., & Vita, J. A. (2000). Antioxidants and the bioactivity of endothelium-derived nitric oxide. *Cardiovascular Research*, 47(3), 426-435.
- Torre, D., Speranza, F., Ghezzi, S., Nozza, S., Tambussi, G., Soldini, L., . . . Poli, G. (2015). Nitric oxide production in HIV-1 infected patients receiving intermittent cycles of interleukin-2 and antiretrovirals. *HIV Clinical Trials*,
- Torriani, F. J., Komarow, L., Parker, R. A., Cotter, B. R., Currier, J. S., Dubé, M. P., . . . Murphy, R. L. (2008). Endothelial function in human immunodeficiency virus-infected antiretroviral-naïve subjects before and after starting potent antiretroviral therapy: The ACTG (AIDS clinical trials group) study 5152s. *Journal of the American College of Cardiology*, 52(7), 569-576.
- UNAIDS. (2014). *The gap report 2014*. ().
- UNAIDS. (2016). Prevention gap report.
- UNAIDS. (2017). HIV statistics factsheet.
- Urata, Y., Honma, S., Goto, S., Todoroki, S., Iida, T., Cho, S., . . . Kondo, T. (1999). Melatonin induces γ -glutamylcysteine synthetase mediated by activator protein-1 in human vascular endothelial cells. *Free Radical Biology and Medicine*, 27(7), 838-847.
- Valko, M., Rhodes, C., Moncol, J., Izakovic, M., & Mazur, M. (2006). Free radicals, metals and antioxidants in oxidative stress-induced cancer. *Chemico-Biological Interactions*, 160(1), 1-40.
- van Wijk, J. P., de Koning, E. J., Cabezas, M. C., Joven, J., op't Roodt, J., Rabelink, T. J., & Hoepelman, A. M. (2006). Functional and structural markers of atherosclerosis in

human immunodeficiency virus-infected patients. *Journal of the American College of Cardiology*, 47(6), 1117-1123.

Venema, R. C., Sayegh, H. S., Arnal, J. F., & Harrison, D. G. (1995). Role of the enzyme calmodulin-binding domain in membrane association and phospholipid inhibition of endothelial nitric oxide synthase. *The Journal of Biological Chemistry*, 270(24), 14705-14711.

Venugopal, S. K., Devaraj, S., Yuhanna, I., Shaul, P., & Jialal, I. (2002). Demonstration that C-reactive protein decreases eNOS expression and bioactivity in human aortic endothelial cells. *Circulation*, 106(12), 1439-1441.

Verhamme, P., & Hoylaerts, M. (2006). The pivotal role of the endothelium in haemostasis and thrombosis. *Acta Clinica Belgica*, 61(5), 213-219.

Versari, D., Daghini, E., Viridis, A., Ghiadoni, L., & Taddei, S. (2009). Endothelial dysfunction as a target for prevention of cardiovascular disease. *Diabetes Care*, 32 Suppl 2, S314-21. doi:10.2337/dc09-S330 [doi]

Villani, P., Regazzi, M. B., Castelli, F., Viale, P., Torti, C., Seminari, E., & Maserati, R. (1999). Pharmacokinetics of efavirenz (EFV) alone and in combination therapy with nelfinavir (NFV) in HIV-1 infected patients. *British Journal of Clinical Pharmacology*, 48(5), 712-715. doi:bcp071 [pii]

Viridis, A., Ghiadoni, L., Salvetti, G., Versari, D., Taddei, S., & Salvetti, A. (2004). Endothelial dysfunction, vascular damage and clinical events. *High Blood Pressure & Cardiovascular Prevention*, 11(1), 15-27.

Wang, X., Chai, H., Yao, Q., & Chen, C. (2007). Molecular mechanisms of HIV protease inhibitor-induced endothelial dysfunction. *Journal of Acquired Immune Deficiency Syndromes (1999)*, 44(5), 493-499. doi:10.1097/QAI.0b013e3180322542 [doi]

- Weiß, M., Kost, B., Renner-Müller, I., Wolf, E., Mylonas, I., & Brüning, A. (2016). Efavirenz causes oxidative stress, endoplasmic reticulum stress, and autophagy in endothelial cells. *Cardiovascular Toxicology*, *16*(1), 90-99.
- Westcott, C. (2015). *Investigating the cholesterol-independent (pleiotropic) effects of selected hypolipidaemic agents in functional and dysfunctional endothelial cells*
- WHO. (2016). HIV/AIDS data and statistics.
- Wilkins, R., Kutzner, B., Truong, M., Sanchez-Dardon, J., & McLean, J. (2002). Analysis of radiation- induced apoptosis in human lymphocytes: Flow cytometry using annexin V and propidium iodide versus the neutral comet assay. *Cytometry Part A*, *48*(1), 14-19.
- Wolf, K., Tsakiris, D. A., Weber, R., Erb, P., Battegay, M., & Swiss HIV Cohort Study. (2002). Antiretroviral therapy reduces markers of endothelial and coagulation activation in patients infected with human immunodeficiency virus type 1. *The Journal of Infectious Diseases*, *185*(4), 456-462.
- Yeboah, J., Crouse, J. R., Hsu, F. C., Burke, G. L., & Herrington, D. M. (2007). Brachial flow-mediated dilation predicts incident cardiovascular events in older adults: The cardiovascular health study. *Circulation*, *115*(18), 2390-2397. doi:CIRCULATIONAHA.106.678276 [pii]
- Young, B., Buchacz, K., Baker, R. K., Moorman, A. C., Wood, K. C., Chmiel, J., . . . HIV Outpatient Study Investigators. (2007). Renal function in tenofovir-exposed and tenofovir-unexposed patients receiving highly active antiretroviral therapy in the HIV outpatient study. *Journal of the International Association of Physicians in AIDS Care*, *6*(3), 178-187.
- Zelko, I. N., Mariani, T. J., & Folz, R. J. (2002). Superoxide dismutase multigene family: A comparison of the CuZn-SOD (SOD1), mn-SOD (SOD2), and EC-SOD (SOD3) gene

structures, evolution, and expression. *Free Radical Biology and Medicine*, 33(3), 337-349.

Zhao, Y., Vanhoutte, P. M., & Leung, S. W. (2015). Vascular nitric oxide: Beyond eNOS. *Journal of Pharmacological Sciences*, 129(2), 83-94.

Zhong, D. S., Lu, X. H., Conklin, B. S., Lin, P. H., Lumsden, A. B., Yao, Q., & Chen, C. (2002). HIV protease inhibitor ritonavir induces cytotoxicity of human endothelial cells. *Arteriosclerosis, Thrombosis, and Vascular Biology*, 22(10), 1560-1566.

Zweier, J. L., Samouilov, A., & Kuppusamy, P. (1999). Non-enzymatic nitric oxide synthesis in biological systems. *Biochimica Et Biophysica Acta (BBA)-Bioenergetics*, 1411(2), 250-262.